Loughborough University

This item was submitted to Loughborough's Institutional Repository (https://dspace.lboro.ac.uk/) by the author and is made available under the following Creative Commons Licence conditions.

creative commons

COMMONS DEED

Attribution-NonCommercial-NoDerivs 2.5

You are free:

- to copy, distribute, display, and perform the work

Under the following conditions:

Attribution. You must attribute the work in the manner specified by the author or licensor.

Noncommercial. You may not use this work for commercial purposes.

No Derivative Works. You may not alter, transform, or build upon this work.

- For any reuse or distribution, you must make clear to others the license terms of this work.
- Any of these conditions can be waived if you get permission from the copyright holder.

Your fair use and other rights are in no way affected by the above.

This is a human-readable summary of the Legal Code (the full license).

Disclaimer

For the full text of this licence, please go to:
http://creativecommons.org/licenses/by-nc-nd/2.5/

Loughborough University

Production of Biodiesel from Used Cooking Oil (UCO) using Ion Exchange Resins as Catalysts

By

Sumaiya Zainal Abidin

A doctoral thesis submitted in partial fulfilment of the requirements for the award of Doctor of Philosophy of Loughborough University

Department of Chemical Engineering

August 2012

Alhamdulillah.....Thank You Allah

Teristimewa buat

Suami yang tercinta, Saipolbarin Ramli
Mama dan Abah yang tersayang, Sadiah Baharom dan Zainal Abidin Bachok
Nenda yang dirindui, Arwahyarhamah Saunah Awang

ACKNOWLEDGEMENT

Bismillahi ar-rahmaan ar-rahim

In the Name of Allah the Most Gracious and Most Merciful

First of all, my praise and thanks to you my Lord Allah, the Most Gracious, Most Merciful for enabling me to complete my PhD successfully. Thank you for blessing, protecting and guiding me throughout this period and for putting so many good people in my PhD journey. I wish to extend my deep thanks gratitude and appreciation to everyone contributed to the successful completion of my thesis.

I offer my sincerest gratitude to my main supervisor, Prof. Basu Saha, London South Bank University for the patient, guidance, encouragement, constructive criticism and advice he has provided throughout my PhD study. I've learned a lot from him, without his help I could not have finished my dissertation successfully. I also owe my sincere gratitude and warm thanks to my supervisor in Loughborough University, Dr. Goran Vladisavljevic, for his supportive co-operation throughout the work. His constructive criticism and valuable advice helped me greatly at all stages.

Special thanks to Sean Creedon, Monica Pietrzak, Dave Smith, Robert Bentham and Graham Moody for being the most dedicated and helpful technicians I've ever met. Honestly, this dissertation would not have been possible without their help and support. I would also like to express my appreciation to all staffs in the Department of Chemical Engineering especially Prof. Zoltan Nagy, Dr. Danish Malik, Mr Tony Eyre, Paul Izzad, Mrs Ann Cage, Miss Yasmin Kosar, Miss Anna Temple, Mrs Liz Attenborough and Ms Janey Briers for the valuable knowledge as well as the administration and technical supports.

I would also like to thank Kathleen Haigh and Dr Dipesh Patel for their valuable suggestions and comments regarding this research work, not forgotten for helping me with the thesis proof reading. Special gratitude also goes to all my friends from all

over UK (Chemical Engineering Department, Masyarakat Melayu Loughborough and UMP colleagues) for their support, trust and friendship.

I would like to thank Universiti Malaysia Pahang and Malaysian Government for sponsoring this PhD study. The research team would also like to express our acknowledgement to Purolite International Ltd (Mr Brian Windsor and late Dr. Jim Dale) for kindly supplying the catalysts for this research work and GreenFuel Oil Company Limited for supplying the used cooking oil.

Most importantly, none of this would have been possible without the love and patience of my family as well as my in-laws. Thank you for the supports, prayers, encouragement and for being by my side through thick and thin.

Lastly, the deepest gratitude goes to my beloved husband for his unconditional support, love and prayers. Thank you for being by my side every step of the way and help me to keep things in perspective. Without you, this journey would not been easy. May this thesis inspire you to achieve the same dream, InsyaAllah.

ABSTRACT

This study focuses on the development of novel two-stage esterification-transesterification synthesis of biodiesel from used cooking oil (UCO) using novel heterogeneous catalysts. The esterification of the UCO was investigated using three types of ion exchange resins catalysts including Purolite D5081, Purolite D5082 and Amberlyst 15. Of all the catalysts investigated, Purolite D5081 resin showed the best catalytic performance and was selected for further optimisation studies. From the optimisation study, it was found that the external and internal mass transfer resistance has negligible effect on the esterification reaction. At the optimum reaction conditions, Purolite D5081 achieved 92% conversion of FFA. During reusability study, the conversion of FFA dropped by 10% after each cycle and it was found that progressive pore blockage and sulphur leaching were dominant factors that decreased the catalytic performance of the Purolite D5081 catalyst. A kinetic modelling for FFA esterification was carried out using Purolite D5081 as a catalyst. Three types of kinetic models were investigated i.e. pseudo homogeneous (PH), Eley-Rideal (ER) and Langmuir-Hinshelwood-Hougen-Watson (LHHW). Experimental data obtained from the batch kinetic studies was successfully represented by the PH model and a good agreement between experimental and calculated values was obtained. The activation energy for esterification and hydrolysis reaction was found to be 53 and 107 kJ mol^{-1}. The transesterification of pre-treated cooking oil (P-UCO) was investigated using various types of heterogeneous catalysts including Purolite CT-122, Purolite CT-169, Purolite CT-175, Purolite CT-275, Purolite D5081, Diaion PA306s and Cs-supported heteropolyacids catalysts. Of all the catalysts investigated, Diaion PA306s catalyst showed the highest conversion of triglycerides and was selected for further optimisation studies. At the optimum reaction conditions, Diaion PA306s achieved ca. 75% of triglycerides conversion. During the reusability study, Diaion PA306s catalyst gave a similar conversion of triglycerides after being reused once. Therefore, it was concluded that the resin can be used several times without losing catalytic activity. Several purification methods have been investigated and dry washing method was chosen as the best alternative for biodiesel purification.

TABLE OF CONTENT

LIST OF FIGURES

LIST OF TABLES

LIST OF ABBREVIATIONS

A, B, C, D	free fatty acids, methanol, fatty acid methyl ester and water, respectively
BET	Brunauer-Emmett-Teller
BSI	British Standard Institution
DVB	Divinylbenzene
EBB	European Biodiesel Board
EIA	Energy Information Administration
ER	Eley-Rideal
EU	European Union
FAAE	Fatty Acid Alkyl Ester
FAEE	Fatty Acid Ethyl Ester
FAME	Fatty Acid Methyl Ester
FEG-SEM	Field Emission Gun-Scanning Electron Microscopy
FFA	Free Fatty Acids
FT-IR	Fourier Transform-Infra Red
GC-MS	Gas Chromatography-Mass Spectrometry
H-NMR	H-Nuclear Magnetic Resonance
HPLC-MS	High Performance Liquid Chromatography-Mass Spectrometry
LC-MS	Liquid Chromatography-Mass Spectrometry
LHHW	Langmuir-Hinshelwood-Hougen-Watson
ML	Modified LHHW
PH	Pseudo Homogeneous
PP	Pöpken
PSD	Particle Size Distribution
P-UCO	Pre-treated Used Cooking Oil
QH	Quasi Homogeneous
RO	Reverse Osmosis
SEC-MS	Size Exclusion Chromatography-Mass Spectrometry
SEM	Scanning Electron Microscopy
SRS	Sum of Residual Squares

TOF	Time-of-Flight
TOF	Turnover Frequency
UCO	Used Cooking Oil
UPLC-MS	Ultra Performance Liquid Chromatography-Mass Spectrometry
US	United States

LIST OF GREEK SYMBOLS

θ	fraction of sites occupied by species *i*
θ_v	fraction of vacant sites
ρ_L	density of liquid sample (kg m^{-3})
ρ_{H_2O}	density of water (kg m^{-3})
ρ_t	true density (g cm^{-3})

LIST OF NOMENCULTURES

A_f	Arrhenius pre-exponential factors for the forward reaction ($kg^2\ kg_{cat}^{-1}\ mol^{-1}\ s^{-1}$)
A_r	Arrhenius pre-exponential factors for the reverse reaction ($kg^2\ kg_{cat}^{-1}\ mol^{-1}\ s^{-1}$)
C_F	concentration of free fatty acids at time '*t*' ($mgKOH\ g^{-1}$)
C_{F0}	initial concentration of free fatty acids ($mgKOH\ g^{-1}$)
C_{HCl}	concentration of HCl (M)
C_{NaOH}	concentration of NaOH (M)
C_T	concentration of triglycerides at time '*t*' ($kmol\ m^{-3}$)
C_{T0}	initial concentration of triglycerides ($kmol\ m^{-3}$)
C_i	concentration of species *i*
E_o	activation energy of the reaction ($kJ\ mol^{-1}$)
K_{eq}	equilibrium constant for the surface reaction
K_i	adsorption equilibrium constant
M_{mix}	mass of reaction mixture (kg)
N_A^{calc}	calculated moles of FFA
N_A^{exp}	experimental moles of FFA
N_{exp}	number of experimental data
N_i	moles of species *i*
V_{HCl}	volume of HCl (ml)
V_{NaOH}	volume of NaOH (ml)
k_a	rate constant for adsorption
k_d	rate constant for desorption
k_f	forward reaction rate constant ($kg^2\ kg_{cat}^{-1}\ mol^{-1}\ s^{-1}$)
k_r	reverse reaction rate constant ($kg^2\ kg_{cat}^{-1}\ mol^{-1}\ s^{-1}$)
m_{H_2O}	mass of water (kg)
m_L	mass of liquid sample (kg)
m_c	mass of catalyst (g)
m_{cat}	mass of catalyst (kg)

q_{NaOH}	sodium capacity (mmol g^{-1})
A	area
K	equilibrium constant for the overall reaction
M	molarity (M)
R	gas constant (8.3144 J mol^{-1} K^{-1})
S	vacant surface site
T	reaction temperature (K)
V	volume
W	weight of sample (g)
r	reaction rate (mol kg_{cat}^{-1} s^{-1})

1 INTRODUCTION

1.1 ECONOMIC OVERVIEW

Human civilisation predominantly depends on the utilisation of energy and it is the most important resources for mankind. Figure 1.1 shows European Union (EU) consumption of energy by sector in 2009 (European Commission, 2011a). Figure 1.1 shows that the transportation sector accounted for the highest consumption of energy (33%), followed by industrial (24.2%), household (26.5%), service (12.6%) and agricultural (2.2%) sectors.

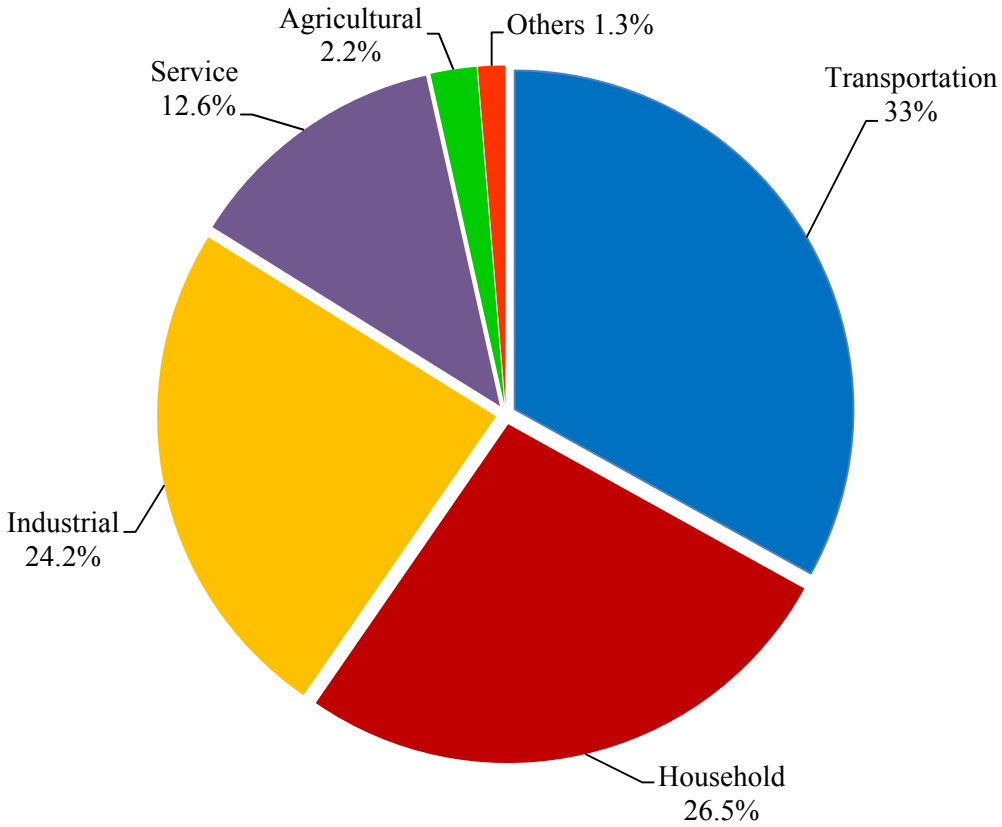

Figure 1.1. European Union (EU) consumption of energy by sector in 2009 (European Commission, 2011a).

Nowadays, the total energy output heavily depends on non-renewable energy resources i.e. oils, natural gases and coals. Figure 1.2 shows a statistical review by the European Commission on EU consumption of energy by sources in 2009 and Figure 1.3 shows a trend of energy consumption from 1999 to 2009

(European Commision, 2011a). In 2009 (see Figure 1.2), the fossil fuel sources i.e. crude oil and petroleum products, natural gases and solid fuels were the dominating resources of energy, comprises nearly 76.8% out of the total energy consumption. It was predicted that by 2035, global energy consumption will increase by 49%, with an increase of 1.4% every year (US Energy Information Administration (EIA), 2011). Within the EU, the demand for diesel fuel was forecasted to grow by 51% from 2000 to 2030 (European Commision, 2011b). Fossil fuels usually take hundreds millions of years to form and as the transport sector is largely dependent on fossil fuels, this is extremely vulnerable to disturbance in oil supply and oil prices (European Commission, 2010). Therefore, diligent efforts are being made to develop an alternative renewable fuel to fulfil the needs of ever increasing high energy demands.

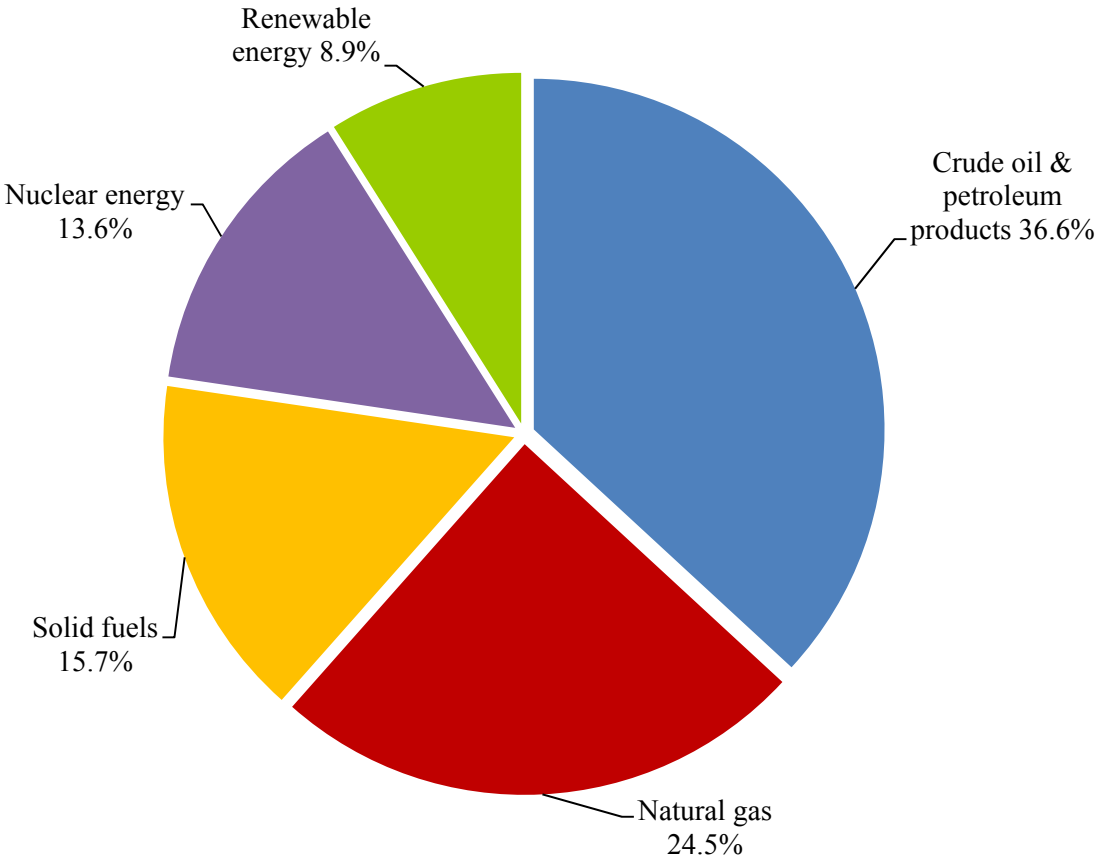

Figure 1.2. European Union (EU) consumption of energy by sources in year 2009 (European Commision, 2011a).

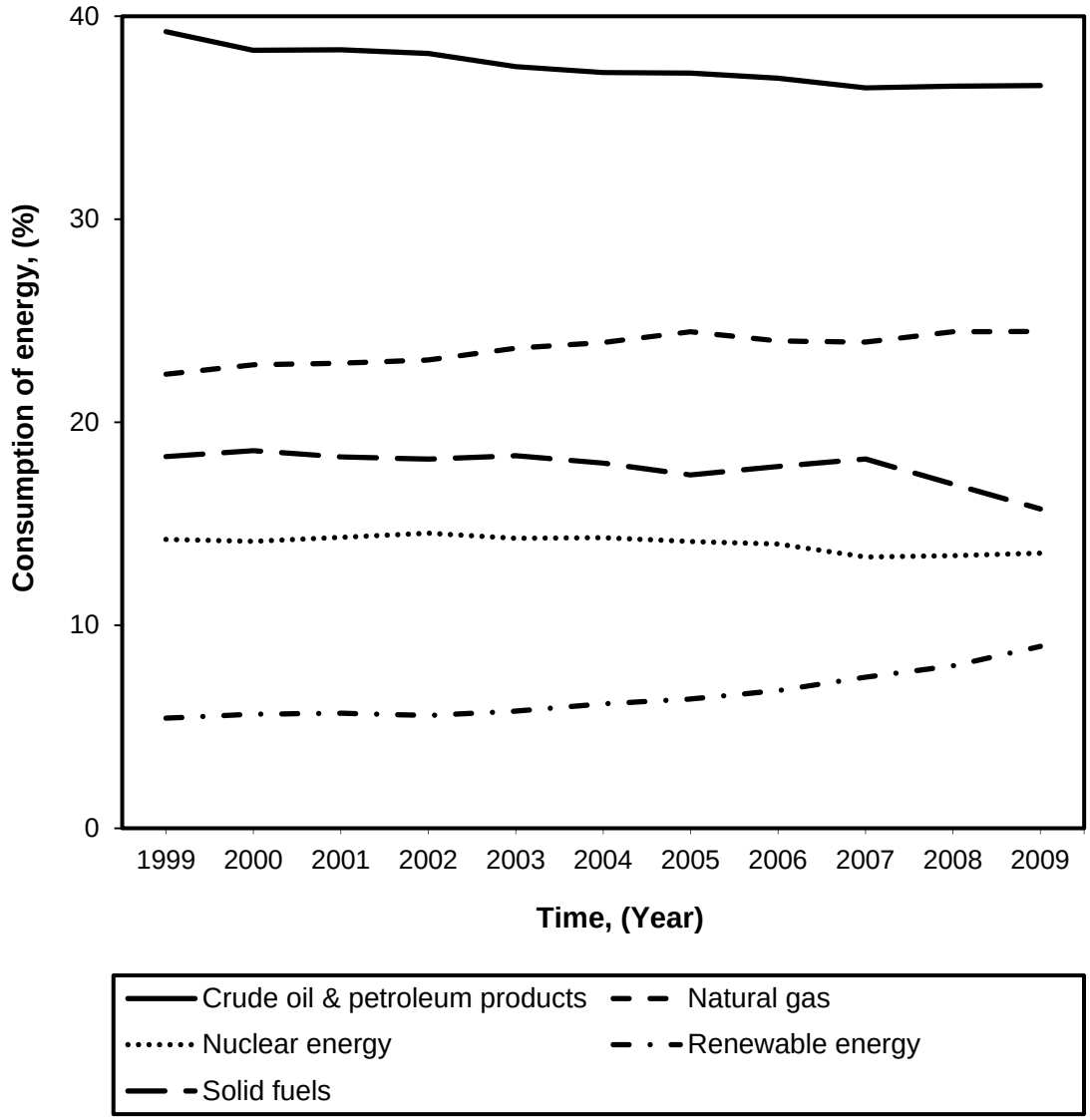

Figure 1.3. A decade trend of total energy consumption in European Union (EU) (European Commision, 2011a).

Renewable energy has become an important alternative for the sustainability of the environment and economic growth. In particular, renewable energy in the form of biodiesel is considered to be one of the best available energy resources (Atabani *et al.*, 2012; Liu *et al.*, 2012). The reason is that biodiesel, an environmentally benign fuel, shows a good combustion emission profile, produces less particulates i.e. unburned hydrocarbon and hazardous gases (i.e. carbon monoxide, sulphur dioxide) than petroleum based diesel fuels (Chen *et al.*, 2009; Guerreiro *et al.*, 2010). Biodiesel has also been found to have a

higher cetane number, higher flash point and a higher lubricity (Lin *et al.*, 2011) as compared to conventional diesel. Table 1.1 (European Biodiesel Board, 2012) shows biodiesel production statistics in the EU countries from 2005 to 2011 and Figure 1.4 (Garofalo, 2011) shows the main consumers of biodiesel in the European Union (EU) in 2011.

Table 1.1. Biodiesel production statistics in European Union (EU) countries (European Biodiesel Board, 2012).

Country	Production Capacity, thousand metric tonnes						
	2005	**2006**	**2007**	**2008**	**2009**	**2010**	**2011**
Austria	85	123	267	213	310	289	560
Belgium	1	25	166	277	416	435	710
Bulgaria	0	4	9	11	25	30	348
Cyprus	1	1	1	9	9	6	20
Czech Republic	133	107	61	104	164	181	427
Denmark & Sweden	72	93	148	231	233	246	527
Estonia	7	1	0	0	24	3	135
Finland*	0	0	39	85	220	288	340
France	492	743	872	1815	1959	1910	2505
Germany	1669	2662	2890	2819	2539	2861	4932
Greece	3	42	100	107	77	33	802
Hungary	0	0	7	105	133	149	158
Ireland*	0	4	3	24	17	28	76
Italy*	396	447	363	595	737	706	2265
Latvia	5	7	9	30	44	43	156
Lithuania	7	10	26	66	98	85	147
Luxemburg	0	0	0	0	0	0	0
Malta	2	2	1	1	1	0	5
Netherlands	0	18	85	101	323	368	1452
Poland	100	116	80	275	332	370	864
Portugal	1	91	175	268	250	289	468
Romania	0	10	36	65	29	70	277
Slovakia	78	82	46	146	101	88	156
Slovenia	8	11	11	9	9	22	113
Spain	73	99	168	207	859	925	4410
United Kingdom	51	192	150	192	137	145	404
Total	3184	4890	5713	7755	9046	9570	22117

*Data include hydro-diesel production
Calculation based on 330 working days per year, per plant, subject to a ±5% margin of error

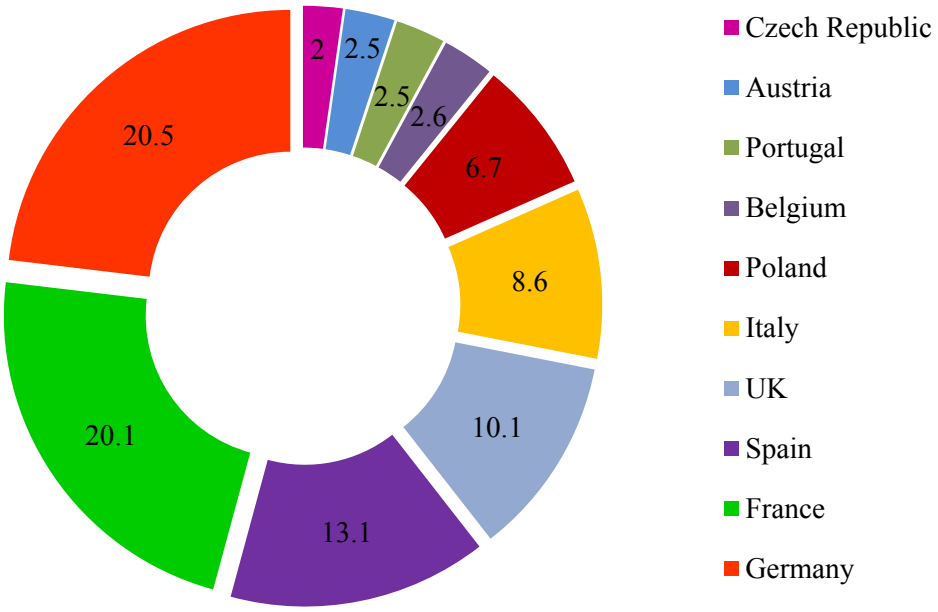

Figure 1.4. The main biodiesel consumers in the European Union (EU) in 2011. The values are in percentage of total EU consumption, based on the 27th National Action Plan (Garofalo, 2011).

1.2 SELECTION OF FEEDSTOCK

Biodiesel also known as fatty acid methyl ester (FAME) is derived from renewable lipid feedstock. Atabani *et al.* (2012) and Salvi and Panwar (2012) reported that more than 350 oil-bearing plants have been identified as potential sources for biodiesel production. Different types of fats and oils have been used in different countries as the raw material for biodiesel production, depending on availability, regional climate, geographical location and local soil conditions (Sharma and Singh, 2008 and Murugesan *et al.*, 2009). These feedstocks are divided into four categories i.e. edible oil, non-edible oil, animal fats and waste oil. Table 1.2 shows the potential biodiesel feedstocks in selected countries around the world (Atabani *et al.*, 2012). According to Atabani *et al.* (2012), these feedstocks should fulfil two main requirements; low production cost and large production scale. Table 1.3 shows the general breakdown cost for the production of biodiesel (Ahmad *et al.*, 2011; Lin *et al.*, 2011; Ragit *et al.*, 2011; Silitonga *et al.*, 2011; Atabani *et al.*, 2012). Table 1.3 highlights that the cost of feedstock alone comprises 75% of the overall cost of biodiesel production.

The major obstacle to commercialise biodiesel from vegetable oil is the high cost of raw feedstock. Cheap, non-edible used cooking oil (UCO) has been found to be an effective feedstock to reduce the cost of biodiesel (Supple *et al.*, 2002; Tomasevic and Silver-Marinkovic, 2003; Canakci, 2005; Ramadhas *et al.*, 2005; Behzadi and Farid, 2007; Stamenković *et al.*, 2011). According to Balat (2011), UCO is 2.5 - 3.5 times cheaper than virgin vegetable oils and thus can significantly reduce the total production cost of biodiesel. As these feedstocks contain high amount of FFA and water, a more efficient and effective technology need to be developed to utilise the potential of low quality feedstock to the fullest, i.e. biodiesel production.

Table 1.2. Current potential feedstocks for biodiesel worldwide (Atabani *et al.*, 2012).

Feedstock	Countries
Animal Fats	Canada, Ireland, Mexico, New Zealand
Castor Oil	Brazil
Coconut Oil	Indonesia, Philippines, Thailand
Cottonseed Oil	Brazil, Greece
Jathropha Oil	China, India, Indonesia, Philippines, Thailand
Karanja Oil	India
Linseed Oil	Canada, Spain
Palm Oil	Brazil, Indonesia, Malaysia, Singapore, Thailand
Peanut Oil	India, United States
Rapeseed Oil	Canada, China, France, Germany, India, Italy, Sweden, United Kingdom
Soybean Oil	Argentina, Brazil, Canada, India, United States
Sunflower Oil	France, India, Italy, Spain
Waste Cooking Oil	China, Ireland, Japan, Mexico, New Zealand, United Kingdom, United States
Yellow Grease	Canada

Table 1.3. General breakdown of biodiesel production cost (Supple *et al.*, 2002; Tomasevic and Silver-Marinkovic, 2003; Canakci, 2005; Ramadhas *et al.*, 2005; Behzadi and Farid, 2007; Stamenković *et al.*, 2011).

Breakdown Cost	Percentage, %
Oil Feedstock	75
Chemical feedstocks	12
Depreciation	7
Direct Labour	3
Energy	2
General Overhead	1

1.3 SELECTION OF PROCESS

There are four major biodiesel production processes that have been studied extensively, i.e. dilution, micro-emulsification, pyrolysis and transesterification techniques. Of all these processes, transesterification is the most popular. In transesterification, three consecutive reversible reactions convert triglycerides into a mixture of esters and glycerol, in the presence of a suitable catalyst and alcohol. The selection of biodiesel production method also depends on the level of free fatty acids (FFA) present in the feedstock (Canakci, 2007). UCO normally has higher acid value than refined vegetable oil due to the presence of high FFA content. Oils and fats with high FFA content (i.e. > 1%) cannot be directly used in a base catalysed transesterification reaction. FFA can react with a base catalyst (neutralisation reaction) and accelerates the base catalyst consumption. The high FFA content also causes saponification during base catalysed transesterification and lowers the yield of biodiesel. The saponification process leads to difficulties in process separation and reutilisation of catalyst because of the formation of stable emulsions and thus it creates a significant amount of toxic wastewater through a neutralisation process. Recently, it was found that a high yield could be achieved using a two-step synthesis of biodiesel (Sharma and Singh, 2008; Zhang and Jiang, 2008). A pre-treatment stage (esterification process) is used to reduce the amount of FFA in the feedstock before base-catalysed transesterification.

1.4 SELECTION OF CATALYST

Most biodiesel processes use homogeneous catalysts because of their simplicity. Homogeneous catalysts are favorable due to their capability to produce a high yield of biodiesel under mild reaction conditions and short reaction times. However, homogeneous catalysts suffer from a number of drawbacks including corrosion of equipment, side reactions, generation of a substantial amount of wastewater, a high production cost due to additional equipment/reagents for separation/neutralisation processes and difficulties in catalyst recovery (Chai *et al.*, 2007; Yan *et al.*, 2010). The use of heterogeneous catalysts simplifies the production and purification processes because they can be easily separated from the reaction mixture. Heterogeneous catalysts allow multiple usage of the catalyst through regeneration,

resulting in a reduction in waste and therefore reduce the impact on environment. In addition, neutralisation process is not needed and less unit operations are required when using heterogeneous catalysts for biodiesel production. There are two types of heterogeneous catalysts for biodiesel i.e. solid acid and solid base catalysts. Solid acid catalysts are found to successfully catalyse both esterification and transesterification reactions simultaneously and are tolerant to FFA and water (Sharma *et al.*, 2010). On the other hand, solid base catalysts are proved to be effective for transesterification of feedstocks with low FFA content (Lee *et al.*, 2009). However, heterogeneously catalysed reactions still have a number of drawbacks. Solid acid catalysts were found to have slower reaction rates, loss in catalytic activity, occurrence of unfavourable side reactions and the requirement of extreme conditions such as higher reaction temperature and longer reaction time (Endalew *et al.*, 2011). On the other hand, the major drawbacks for solid base catalysts were the leaching of active species, poisoning and loss of surface area during the transesterification process (Yan *et al.*, 2010). These solid base catalysts were also found to have high sensitivity towards water, carbon dioxide and FFA (Endalew *et al.*, 2011). The issue of stability for longer catalyst life was also found to be the main problem in most of the heterogeneous catalysts. Therefore, with all the problems associated with the heterogeneous catalysts, only a few researchers have reported the commercial level production of biodiesel using heterogeneous catalysts. One of the commercialised biodiesel processes was the Esterfip-H process using zinc/aluminium (Zn/Al) mixed oxide as a catalyst and operated at high temperature (473-523 K) to produce an equal performance with the homogeneous catalysts.

1.5 MOTIVATION OF RESEARCH WORK

The overview of the four important issues in biodiesel production has been briefly explained in section 1.1 - 1.4. These four issues i.e. economic analysis of current and future sources of energy, selection of a reliable feedstock as a raw material, selection of a suitable process depending on the source of the feedstock and selection of a suitable catalyst for the biodiesel production should be carefully considered to improve the performance of biodiesel synthesis.

The main focus of this research work is to create a green and environmentally benign process for biodiesel production and to reduce the dependency on food supplement materials i.e. vegetable oils as the feedstocks. The study will focus on the usage of a low quality feedstock i.e. UCO due to the following reasons: (i) to reduce the production cost of biodiesel, (ii) to avoid the competition between the food and fuel industry, (iii) to have a sustainable green environment by converting waste oil into a useful product i.e. biodiesel and (iv) to increase the awareness among the citizens on the importance of waste recycling. Furthermore, the usage of low quality feedstocks i.e. non-edible oil, animal fats and waste oil has gained more interest in recent years as the physicochemical properties of these feedstocks are found to be compatible for biodiesel production.

Although the biodiesel esterification and transesterification reactions using acid and base catalysts are well known and practiced on a commercial scale, there is still plenty of scope for improvement, especially on the development of suitable and sustainable catalysts for low quality biodiesel feedstocks. Future development of heterogeneous catalysts for biodiesel production should be focused on several aspects, i.e. to be able to withstand the presence of water and FFA in low quality feedstocks, low temperature activity, low usage of methanol and catalyst, longer catalyst life, catalyst recyclability and cost of catalyst because these aspects have a significant impact on the quality of biodiesel and overall cost of biodiesel process. Additional work is also required to find ways to re-generate or re-activate the spent catalyst that usually deactivated through leaching, poisoning or loss of surface area. In addition, the problems associated with FFA and water content need to be resolved using a pre-treatment process i.e. esterification before the low quality feedstocks can be introduced to the transesterification reaction. Thus, this research will concentrate on the development of esterification - transesterification catalytic reactions using heterogeneous catalysts. This work is conducted in collaboration with Purolite International Limited for possible commercialisation of novel Purolite ion exchange resins as potential biodiesel production catalysts.

1.6 OBJECTIVES OF THE RESEARCH WORK

The objectives of this research work are:

- To characterise various types of heterogeneous catalysts including Amberlyst 15, Purolite CT-122, Purolite CT-169, Purolite CT-175, Purolite CT-275, Purolite D5081, Purolite D5082, Diaion PA306s and heteropolyacids supported salt catalysts [i.e. $Cs_{2.5}H_{0.5}PW_{12}O_{40}$ and $Cs_{2.5}H_{0.5}PW_{12}O_{40}$ (calcined)] via physical and chemical characterisation methods such as field emission gun-scanning electron microscopy (FEG-SEM) analysis, elemental analysis, Fourier transform-infra red (FT-IR) spectroscopy analysis, surface area measurement, true density measurement and particle size distribution (PSD) measurement.
- To develop the analytical technique for the determination of fatty acid methyl ester (FAME) using gas chromatography-mass spectrometry (GC-MS).
- To determine the components in and compositions of UCO using the developed GC-MS method and to characterise the UCO via chemical and physical characterisation methods including acid value, FFA content, moisture content, triglycerides, diglycerides and monoglycerides analysis and bulk density.
- To study batch kinetics for FFA esterification over a wide range of operating conditions such as elimination of mass transfer limitations, catalyst loading, reaction temperature, methanol to UCO feed mole ratio and reusability of the catalyst at the optimum condition.
- To develop a kinetic model for FFA esterification and to determine the activation energy and rate constants (forward and reverse) of the esterification reaction. To correlate experimental data obtained from the esterification reaction with three kinetic models i.e. pseudo homogeneous (PH), Eley-Rideal (ER) and Langmuir-Hinshelwood-Hougen-Watson (LHHW).

- To conduct batch kinetic studies for transesterification over a wide range of operating conditions such as elimination of mass transfer limitations, catalyst loading, reaction temperature, methanol to pre-treated UCO (P-UCO) feed mole ratio and reusability of the catalyst at the optimum condition, followed by the separation and purification process for biodiesel production.

1.7 STUCTURE OF THE THESIS

A brief description of each chapter within the thesis is summarised as follows:

Chapter 2: Literature Review

This chapter presents a detailed background study covering all aspects of biodiesel including the selection of feedstock, route of biodiesel production, reaction mechanism of acid and base catalysis, effect of process parameters on the biodiesel production and the separation and purification of biodiesel. Information obtained from this literature review helps with the decision on selecting the suitable feedstock, process and catalyst for biodiesel production.

Chapter 3: Materials and Methods

This chapter represents the materials and methods used throughout this research work. There are six main sections in this chapter: materials, catalyst preparation and characterisation, development of analytical techniques, physical and chemical analysis of used cooking oil (UCO), esterification reaction, transesterification reaction and separation and purification of biodiesel.

Chapter 4: Catalysts Characterisation

This chapter presents the characterisation of biodiesel catalysts. The information on catalyst characterisation is very important since it provides fundamental knowledge of the chemical and physical properties of the catalysts. The characterisation of the catalysts was performed using field emission gun-scanning electron microscopy (FEG-SEM) analysis, elemental analysis, Fourier transform-infra red (FT-IR) spectroscopy analysis, surface area measurement, true density measurement and particle size distribution (PSD) measurement.

Chapter 5: Development of Analytical Techniques and Physical and Chemical Characterisation of Used Cooking Oil (UCO)

This chapter focuses on the development of gas chromatography-mass spectrometry (GC-MS) analytical technique for fatty acid methyl ester (FAME) determination. This technique was further used to determine the components in and composition of UCO. The characterisation of UCO using chemical and physical characterisation method including determination of acid value and free fatty acids (FFA) content, moisture content analysis, triglycerides, diglycerides and monoglycerides analysis and bulk density measurement were carried out and all developed analytical methods can further be used for biodiesel analysis.

Chapter 6: Esterification of Free Fatty Acids (FFA) in Used Cooking Oil (UCO) using Ion Exchange Resins as Catalysts

In this chapter, the esterification of the UCO using various types of ion exchange resin catalysts is highlighted. All the catalysts were subjected to batch kinetic studies and the catalyst that resulted in the highest conversion of FFA was selected for further optimisation of batch kinetic studies. Elimination of mass transfer resistances and the effect of catalyst loading, reaction temperature and methanol to UCO feed mole ratio on the conversion of FFA were investigated. The experiment was conducted in a jacketed stirred batch reactor to determine the optimum condition for the esterification process prior to transesterification. Reusability of the catalyst was studied at the optimum conditions obtained from the batch kinetic studies.

Chapter 7: Kinetic Modelling of Free Fatty Acids (FFA) Esterification

Batch kinetic modelling of FFA esterification over an ion exchange resin is presented in this chapter. Three types of kinetic models were investigated, i.e. PH, ER and LHHW. These models were used to correlate the experimental data obtained from the esterification reaction. MATLAB 7.0 with built-in ODE45 solver was used to solve the differential equations numerically. The optimum condition was achieved by minimising the sum of residual square (SRS) between the experimental and calculated number of moles of all species involved. The best fitted model was further

investigated to determine the rate constants (forward and reverse) and activation energy of the esterification reaction.

Chapter 8: Transesterification of Pre-Treated Used Cooking Oil (P-UCO) to Biodiesel using Heterogeneous Catalysts

In this chapter, transesterification of pre-treated used cooking oil (P-UCO) to biodiesel using different types of heterogeneous catalysts is discussed in detail. All the heterogeneous catalysts were subjected to batch kinetic studies and the catalyst with the highest conversion of triglycerides was selected for further optimisation of batch kinetic studies. Elimination of mass transfer resistances and the effect of catalyst loading, reaction temperature and methanol to P-UCO feed mole ratio on the conversion of triglycerides were studied. All experiments were conducted in a jacketed stirred batch reactor to determine the optimum condition for the transesterification process. A study of the reusability of the catalyst was performed under optimum condition, followed by the separation and purification processes for biodiesel production. Characterisation of the biodiesel product was carried out and is summarised in Chapter 7.

Chapter 9: Conclusions and Recommendations of Future Work

This chapter provides a summary of the research work presented in the thesis. Recommendations of future work in this field are also presented in this chapter.

2 LITERATURE REVIEW

2.1 INTRODUCTION

Energy is often known as the success factor for a country's development. It is often used as an indicator to measure the level of economic growth in a particular country. Concentrated efforts are being undertaken to ensure the sustainability of energy resources, both depletable and renewable. The majority of the world's energy is supplied through petrochemical sources, coal and natural gases. The demand for petroleum-based fuels also increases with the increase in the industrialisation and motorisation of the world. Among all of the petroleum-based fuels, diesel oils are the more important. Diesel oils are used in city buses, locomotives, electric generators, industrial sectors and they have an essential function in the industrial economy of a country. However, various factors such as the high energy demand from various sectors, global warming, the unstable price and availability of petroleum-based oil as well as the environmental pollution due to the widespread use of fossil fuels all causes petroleum-based diesel supply chain to become unreliable. The world energy forum also predicted that, in less than ten decades, fossil-based fuels, including coal and natural gases will become depleted (Sharma and Singh, 2008). Therefore, it is increasingly necessary to develop renewable diesel resources to replace the traditional ones. The alternatives to diesel fuel must be technically feasible, techno-economically competitive, environmentally acceptable, and readily available (Srivastiva and Prasad, 2000). Many of these requisites are satisfied by vegetable oils or, in general, by triglycerides. Vegetable oils became one of the most popular feedstocks for renewable fuel and are widely available from a variety of sources. In previous years, vegetable oil was not a preferred choice for alternative diesel fuels due to its high cost when compared to conventional diesel. There are also many problems associated with vegetable oil being used directly in a diesel engine, i.e. higher viscosity, incomplete combustion, higher flash point, lube oil dilution, high carbon deposits, ring sticking, scuffing of the engine liner, injection nozzle failure and both higher cloud and pour points (Murugesan *et al.*, 2009). According to Knothe (2005) the viscosity of vegetable oils is 10-20 times higher than the petroleum fuel, therefore directly using vegetable oils as a fuel can cause engine

problems like injector fouling and particle agglomeration. Table 2.1 shows the summarisation made by Harwood (1984) of the known problems and probable causes for direct usage of vegetable oil in a diesel engine.

Table 2.1. Known problems and probable causes for direct usage of vegetable oil in diesel engine (Harwood, 1984).

Problem	Probable Cause
Short-term	
Cold weather starting	High viscosity, low cetane, and low flash point of vegetable oils.
Plugging and gumming of filters, lines and injectors	Natural gums (phosphatides) in vegetable oil.
Engine knocking	Very low cetane of some oils. Improper injection timing.
Long term	
Coking of injectors on piston and head of engine	High viscosity of vegetable oil, incomplete combustion fuel. Poor combustion at part loads with vegetable oils.
Carbon deposits on piston and head of engine	High viscosity of vegetable oil, incomplete combustion fuel. Poor combustion at part loads with vegetable oils.
Excessive engine wear	High viscosity of vegetable oil, incomplete combustion fuel. Poor combustion at part loads with vegetable oils. Possibly free fatty acids (FFA) in vegetable oil. Dilution of engine lubricating oil due to blow-by of vegetable oil.
Failure of engine lubricating oil due to polymerization	Collection of polyunsaturated vegetable oil blow-by in crankcase to the point where polymerization occurs.

However, with the current situation where the fluctuation of diesel prices is unavoidable, it has renewed interest in the usage of vegetable oils in diesel engines. To overcome the engine-unsuitability problems, a slight chemical modification is needed to ensure the usage of vegetable oils in diesel engines is viable and feasible. Several procedures have been established and these include transesterification, blending, cracking, micro-emulsification and pyrolysis. The transesterification process was found to be the key and foremost route to produce the cleaner and more environmentally safe fuel from vegetable oils. Transesterification is a three-step reversible reaction that converts the initial triglycerides into a mixture of esters and glycerine, in the presence of a catalyst and alcohol. Boehman (2005) indicated that vegetable oil and animal fat-based biodiesel fuels have the following advantages over the diesel fuel: they produce less smoke and particulates, they produce lower carbon monoxide and hydrocarbon emissions, they are biodegradable and non-toxic. It has a higher cetane number than diesel fuel, creates a pleasant smell and contains 10-11%

oxygen by weight (Chhetri *et al.*, 2008). Biodiesel also offers safety benefits over diesel fuel because it is less combustible with a higher flash point of 423 K compared to 350 K for conventional diesel (Demirbas and Balat, 2006). Conversely, depending on the sources of feedstock, they present other technical challenges such as low volatility, high pour points, high cloud points and cold filter plugging temperatures, elevated NOx emissions and incomplete combustion (Lotero *et al.*, 2005; Gui *et al.*, 2008; Demirbas, 2009). The world also has a major concern about the unfavourable cold flow properties of biodiesel as it tends to gel (freeze) at a lower temperature. The freezing point of biodiesel is near 0°C and this situation commonly affects the driveability of biodiesel vehicles in countries with extreme cold climate (Gui *et al.*, 2008).

2.2 FEEDSTOCKS FOR BIODIESEL PRODUCTION

Biodiesel can be produced by transesterification of any triglyceride feedstock, which includes any oil-bearing crops, animal fats and algal lipids. However, most current research is focusing considerably on the production of biodiesel from vegetable oil (Balat, 2011; Hoekman *et al.*, 2012). The use of vegetable oils as an alternative fuel has been around for 100 years, ever since the invention of the compression ignition engine by Rudolph Diesel using peanut oil (Shay, 1993).

Generally, the raw material contributes the biggest portion of the overall biodiesel production cost. Zhang *et al.* (2003a), Haas *et al.* (2006) and Demirbas (2007) reviewed that the use of refined or high quality feedstock constitutes 80-88% of the overall production or manufacturing cost. Nowadays, with the current economic situation, the increment of refined oil prices is unavoidable and thus contributes to an even higher fraction of the feedstock cost in the total production expenditure. The properties of feedstocks also cause a significant impact on the quality of the product. Brito *et al.* (2007a & 2007b) revealed that the reduction of feedstock viscosities positively influences the rate of reaction and shortens the reaction time. Furthermore, the suitability of the feedstock also depends on the amount of oil generated from the crop. Crops with a higher oil yield are more preferable because they can reduce the production cost (Gui *et al.*, 2008). The feedstocks employed in biodiesel production

are generally classified into vegetable oil (edible oil and non-edible oil), animal oil and fats, and waste oil (Lang *et al.*, 2001; Dorado *et al.*, 2003; Mittelbach and Remschmidt, 2004).

2.2.1 Edible Oil

At present, the dominant feedstock for biodiesel production is edible vegetable oil, with different countries using different types of vegetable oils, depending upon the climate and soil conditions (Sharma *et al.*, 2008). For example, soybean oil is commonly used in the United States, rapeseed and sunflower oil are used in many European countries, coconut oil is used in the Philippines and palm oils are used in Malaysia for biodiesel production (Ghadge and Raheman, 2005; Demirbas, 2006; Meher *et al.*, 2006a; Sarin *et al.*, 2007). These four crops, soybean (Xie *et al.*, 2006a; Xie *et al.*, 2006b), rapeseed (Cvengros and Povazanec, 1996), palm (Kalam and Masjuki, 2002) and sunflower (Antolìn *et al.*, 2002; Vicente *et al.*, 2005) noticeably dominate the feedstock sources used for worldwide biodiesel production. However, there are no limitations for employing other types of vegetable oils. Other types of oils that are currently being investigated are peanut seed oil (Davis *et al.*, 2009; Kaya *et al.*, 2009), melon seed oils (Mabaleha *et al.*, 2007) and safflower oil (Rashid and Anwar, 2008), Apart from these, other edible vegetable oils like canola, linseed and corn have also been used for biodiesel production and are found to be good as a diesel substitute (Freedman *et al.*, 1986; Lang *et al.*, 2001). However, the increasing world population increases the demand for both food and fuels, and significantly contributes to the food versus fuel issues (Balat, 2011). Therefore, the non-edible feedstocks are found to be the most promising alternative to replace edible feedstocks.

2.2.2 Non-edible Oil

Nowadays, the major obstacle to commercialising biodiesel from vegetable oil is the high cost of the raw feedstock. Zhang *et al.* (2003b) reviewed that approximately 70-95% of biodiesel cost comes from the price of raw feedstock. Therefore, the cheap non-edible vegetable oil, animal fats and waste oils are found to be an effective feedstocks replacement to reduce the cost of biodiesel. Examples of

non-edible oils used in the production of biodiesel are rubber (Ficus elastica), mahua (Mahua indica), Jatropha (J. curcas), karanja (Pongamia pinnatta), polanga (Calophyllum inophyllum) and tobacco (Nicotina tabacum). Most of the non-edible oils contain significant amounts of free fatty acids (FFA); for example, crude mahua oils contain about 13-20% FFA (Shashikant and Hifjur, 2006 and Jena *et al.*, 2010), crude jatropha oils contain about 12-14% FFA (Srivastava and Prasad, 2000; Worapun *et al*., 2012), tobacco seeds oils contain about 17% FFA (Veljković *et al.*, 2006) and Zanthoxylum bungeanum seed oil contains about 25% FFA (Zhang and Jiang, 2008). Asian countries like India and Indonesia have started to use Jatropha curcas (Jatropha) and Pongamia pinnata (karanja) oil as the raw materials for biodiesel fuels. Oils from both plants contains toxin and hence are non-edible. Karanja oils contain furanoflavones, furanoflavonols, chromenoflavones, flavones and furanodiketones as toxins, whereas jatropha oils contain phorbol esters and curcin as toxins (Tewari, 2007). Several studies have been conducted to investigate the performance of these non-edible oils as alternative feedstock sources. Hawash *et al.* (2009) studied the transesterification of jatropha oil using supercritical methanol in the absence of a catalyst under different temperature condition. They revealed that a 100% yield is achieved within 4 min only, at a temperature of 593 K, a pressure of 8.4 MPa and a 43:1 oil to methanol molar ratio. Naik *et al.* (2008) discussed the mechanism of the dual step process adopted for the production of biodiesel from Karanja oil with high FFA content. This dual step process successfully resulted in a 96.6-97% yield of biodiesel. Meher *et al.* (2006b) conducted a study on the optimisation of the transesterification process, employing karanja oils as the raw material. They successfully achieved a 97-98% methyl ester yield under the optimal conditions. Another potential non-edible feedstock for biodiesel production is Mahua (Madhuca indica) oil. As this oil contains a high amount of FFA, Ghadge and Raheman (2006) conducted a two-stage reaction process to optimise the reduction of the FFA content in mahua oil, and successfully obtained a 98% biodiesel yield. The property of mahua biodiesel was found to be comparable with the conventional diesel fuels.

2.2.3 Animal Fats and Oils

Animals fats have also been used as the raw materials for biodiesel production. Chung *et al.* (2009) studied the production of biodiesel using duck tallow as the feedstock and the experiment successfully achieved a 97% fatty acid methyl ester (FAME) conversion. However, animal fats faced certain disadvantages, particularly in terms of quality. Biodiesel derived from animal fats has a higher level of saturated fatty acid and thus due to its poor cold temperature properties it causes problems in winter operation. According to several researchers (Kang and Kim, 2001; Lang *et al.*, 2001; Mittelbach and Remschmidt, 2004; Yang *et al.*, 2007), the degree of saturation also prohibits the biodiesel's excellent fuel properties, specifically towards the level of cetane numbers and heating value. El-mashad *et al.* (2008) studied the production of biodiesel from salmon oil and found that the process was unfeasible as the production cost was almost twice that of biodiesel produced from soybean oil.

2.2.4 Waste Oil

The use of cheap low quality feedstocks such as waste cooking oils, greases and soapstocks (a by-product of vegetable oil refinery) significantly helps to improve the economic feasibility of biodiesel (Supple *et al.*, 2002; Tomasevic and Silver-Marinkovic, 2003; Zhang *et al.*, 2003b; Canakci, 2005; Ramadhas *et al.*, 2005; Behzadi and Farid, 2007). Used cooking oil (UCO) is generally in the liquid state at room temperature, whereas greases and soapstocks are in solid state at room temperature.

UCO was found to be 2.5 - 3.5 times cheaper than virgin vegetable oils, depending on the sources and availability (Balat, 2011). The amount of UCO generated each year in every country is quite massive, depending on the use of vegetable oil. The collection of UCO is estimated to be approximately 0.7-1.0 metric ton per year in the European Union (EU) and 350,000 tons per year in Turkey (Nas and Berktey, 2007). In the United Kingdom, approximately 65,000 tons of the 80,000 tons of UCO collected comes from commercial and industrial sources, originating in commercial catering establishments and the food processing industry (Upham *et al.*, 2009). In

China, the potential amount of waste cooking oils and soapstock is about 2.5 and 1.0 million tonnes per year, respectively.

Grease, on the other hand, was classified into two categories, yellow and brown grease depending on its FFA composition (Canakci, 2007). For yellow grease, it was reported by Kulkarni and Dalai (2006) that on average, every person in United States and Canada produced approximately 8 - 9 pounds of it each day. Zhang *et al.* (2003a) reported that production of yellow grease in Canada is approximately 120,000 tons per year. These low quality feedstocks are usually disposed of directly into the environment, resulting in problems for waste water treatment plants and energy loss, or integrated into the food chain by animal feeding and finally causing human health problems (Felizardo *et al.*, 2006).

However, these waste oils i.e. UCO was reported to have a lower yield as compared to the virgin oil (Dias *et al.*, 2008). Fröhlich and Rice (2009) investigated the sources of yield loss during methanolysis of UCO. They found that it was due to triglycerides and methyl ester hydrolysis and the dissolution of methyl esters in the glycerine phase. The level of FFA and water content also greatly influenced the quality of the biodiesel. Canakci (2007) identified that the level of FFA varied from 0.7% to 41.8% and water from 0.01% to 55.38% for feedstock from waste cooking oils, restaurant grease and animal fats. These wide ranges indicate that an efficient process is needed to tolerate the high level of FFA and water content. To overcome the problem, several studies on the utilisation of waste oils and grease as raw material have been conducted by a few researchers (Canacki, 2007; Longlong *et al.*, 2008 and Ngo *et al.*, 2008) and they found that high yields were achieved using the two-step synthesis of biodiesel. The first stage, the pre-treatment step is needed to reduce the amount of the FFA content in the feedstock, which is normally around 12-40 wt% of FFA before being subjected to the base catalysed transesterification reaction.

2.2.5 Algae

A few studies have also showed that algae could also be a possible raw material for biodiesel production (Nagel and Lemke, 1990; Chisti, 2007). Algae, in the presence

of sunlight, convert carbon dioxide into sugars and protein, but when they are starved of nitrogen, they mainly produce oil. Microalgae are reported to give a higher photosynthetic efficiency, higher biomass production and faster growth as compared to other energy crops (Milne *et al.*, 1990; Ginzburg, 1993; Dote *et al.*, 1994; Minowa *et al.*, 1995). However, despite tremendous interest in algae feedstocks for biodiesel production, there were only a few studies conducted in this area. Many researchers were unable to compare the algal-based feedstock to vegetable-based feedstock due to the lack of compositional profiles of the triglycerides fractions in algal lipids. The fatty acids composition of each algae strain is unique as it is highly influenced by the specific growth conditions such as nutrient levels, temperature and light intensities (Hu *et al.*, 2008). Although there were a number of studies conducted to determine the fatty acid composition of algal lipid, the exact species is often unknown, or a mixed species is used (Hoekman *et al.*, 2012).

2.3 TRIGLYCERIDES COMPOSITION IN BIODIESEL FUELS

The properties of the triglycerides and the biodiesel product are determined by the chemical structure of the fatty acids and their chemical mixtures. The numbers of double bonds and the chain length are the two factors that determine the physical characteristic of both triglycerides and fatty acids (Mittelbach and Remschmidt, 2004). The transesterification process does not alter the fatty acid structure and composition of the feedstock, hence making these structure and composition significantly important with respect to several biodiesel parameters, such as the cetane number, the pour point and the cold flow properties. Fatty acid chemical structure and compositions for different types of vegetable oils are shown in Table 2.2 and Table 2.3.

Table 2.2. Fatty acids and the chemical structures

Fatty Acid	Chemical Structure	Carbon:Double Bonds
Lauric	$CH_3(CH_2)_{10}COOH$	C12:0
Myristic	$CH_3(CH_2)_{12}COOH$	C14:0
Palmitic	$CH_3(CH_2)_{14}COOH$	C16:0
Palmitoleic	$CH_3(CH_2)_5CH=CH(CH_2)_7COOH$	C16:1
Stearic	$CH_3(CH_2)_{16}COOH$	C18:0
Oleic	$CH_3(CH_2)_7CH=CH(CH2)_7COOH$	C18:1
Linoleic	$CH_3(CH_2)_4CH=CHCH_2CH=CH(CH_2)_7COOH$	C18:2
Linolenic	$C_2H_5CH=CHCH_2CH=CHCH_2CH=CH(CH_2)_7COOH$	C18:3
Arachidic	$CH_3(CH_2)_{18}COOH$	C20:0
Gadoleic	$CH_3(CH_2)_9CH=CH(CH2)_7COOH$	C20:1
Behenic	$CH_3(CH_2)_{20}COOH$	C22:0
Erucic	$CH_3(CH_2)_7CH=CH(CH_2)_{11}COOH$	C22:1
Lignoceric	$CH_3(CH_2)_{22}COOH$	C24:0
Nervonic	$CH_3(CH_2)_7CH=CH(CH_2)_{13}COOH$	C24:1

Table 2.3. Fatty acid compositions (wt%) of vegetable oils (Ramos *et al.*, 2009).

Fatty Acid	Palm	Olive	Peanut	Rape	Soybean	Sunflower	Almond	Corn
Lauric	0.1	0.0	0.0	0.0	0.0	0.0	0.0	0.0
Myristic	0.7	0.0	0.1	0.0	0.0	0.0	0.0	0.0
Palmitic	36.7	11.6	8.0	4.9	11.3	6.2	10.4	6.5
Palmitoleic	0.1	1.0	0.0	0.0	0.1	0.1	0.5	0.6
Stearic	6.6	3.1	1.8	1.6	3.6	3.7	2.9	1.4
Oleic	46.1	75.0	53.3	33.0	24.9	25.2	77.1	65.6
Linoleic	8.6	7.8	28.4	20.4	53.0	63.1	7.6	25.2
Linolenic	0.3	0.6	0.3	7.9	6.1	0.2	0.8	0.1
Arachidic	0.4	0.3	0.9	0.0	0.3	0.3	0.3	0.1
Gadoleic	0.2	0.0	2.4	9.3	0.3	0.2	0.0	0.1
Behenic	0.1	0.1	3.0	0.0	0.0	0.7	0.1	0.0
Erucic	0.0	0.0	0.0	23.0	0.3	0.1	0.0	0.1
Lignoceric	0.1	0.5	1.8	0.0	0.1	0.2	0.2	0.1
Nervonic	0.0	0.0	0.0	0.0	0.0	0.0	0.4	0.0

A number of studies have been conducted to investigate the influence of the triglycerides composition in biodiesel fuels. Muniyappa *et al.* (1996) studied the properties of biodiesel synthesised from two different sources, soybean and beef tallow oil. They discovered that the high cloud point of the methyl ester from beef

tallow oil was the indication of a high concentration of saturated fatty esters. Lang *et al.* (2001) conducted a study on biodiesel fuels from several sources (rapeseed, sunflower, canola and linseed oil) and compared their properties with the conventional diesel fuels. They discovered that biodiesels are considerably less volatile than conventional diesel fuels. Dmytryshyn *et al.* (2004) also carried out a similar comparative study on different feedstock and they monitored the performance of the biodiesel by evaluating four parameters, namely the density, viscosity, cloud point and pour point. From their analysis, it was determined that the most potential substitute for diesel fuel is the canola methyl ester because it shows a close similarity when compared to diesel fuel. Ramos *et al.* (2009) reported the influence of raw material composition on biodiesel quality using the transesterification reaction. They revealed that low cetane numbers have been associated with more highly unsaturated components (C18:2 and C18:3). Furthermore, the oxidation stability decreased with the increase of the content of polyunsaturated methyl esters. Feedstocks with a higher monosaturate content result in better fuel properties compared to feedstock with a lower monosaturate content.

2.4 PROCESS FOR BIODIESEL PRODUCTION

Transesterification is a three steps reversible reaction that converts the initial triglycerides into a mixture of fatty acid alkyl ester (FAAE) and glycerine, in the presence of a catalyst and alcohol. This FAAE is known as biodiesel. Figure 2.1 shows the overall transesterification reaction and Figure 2.2 shows the step-by-step conversion of triglycerides to FAAE and glycerine. The stoichiometry between the alcohol and the oil is a 3:1 molar ratio. However, because the reaction is reversible, excess alcohol is needed for maximum FAAE production depending on the process parameters involved (e.g. temperature, amount of catalyst, type of feedstock).

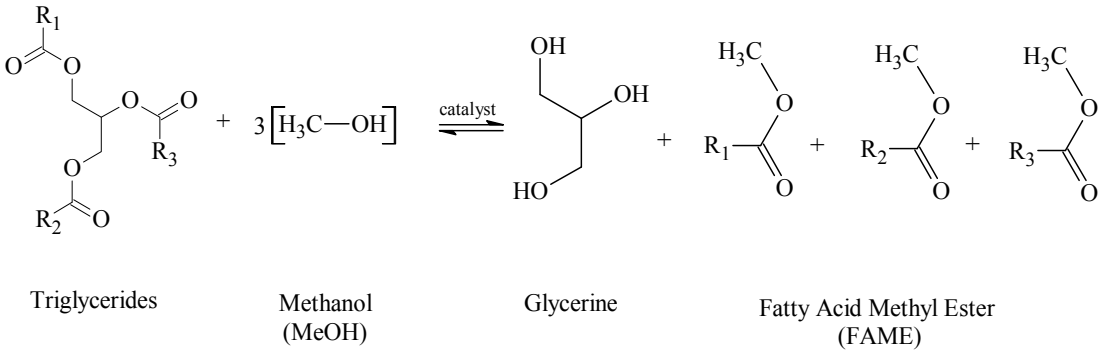

Figure 2.1. A general reaction scheme for the biodiesel production. R_1, R_2 and R_3 represent the fatty acids group attached to the backbone of triglycerides.

$$\text{Triglyceride} + \text{ROH} \rightleftarrows \text{Diglyceride} + \text{RCOOR}_1$$

$$\text{Diglyceride} + \text{ROH} \rightleftarrows \text{Monoglyceride} + \text{RCOOR}_2$$

$$\text{Monoglyceride} + \text{ROH} \rightleftarrows \text{Glycerine} + \text{RCOOR}_3$$

Figure 2.2. Step-by-step conversion of triglycerides to fatty acid alkyl ester (FAME) and glycerine. R refers to alkyl group of the alcohol.

2.4.1 Acid Catalysed Transesterification

Acid catalysed transesterification is a chemical reaction involving fatty acid and alcohol which yields FAAE, glycerine and water. Figure 2.3 shows the acid catalysed mechanism for triglycerides. It can be extended to diglycerides and monoglycerides.

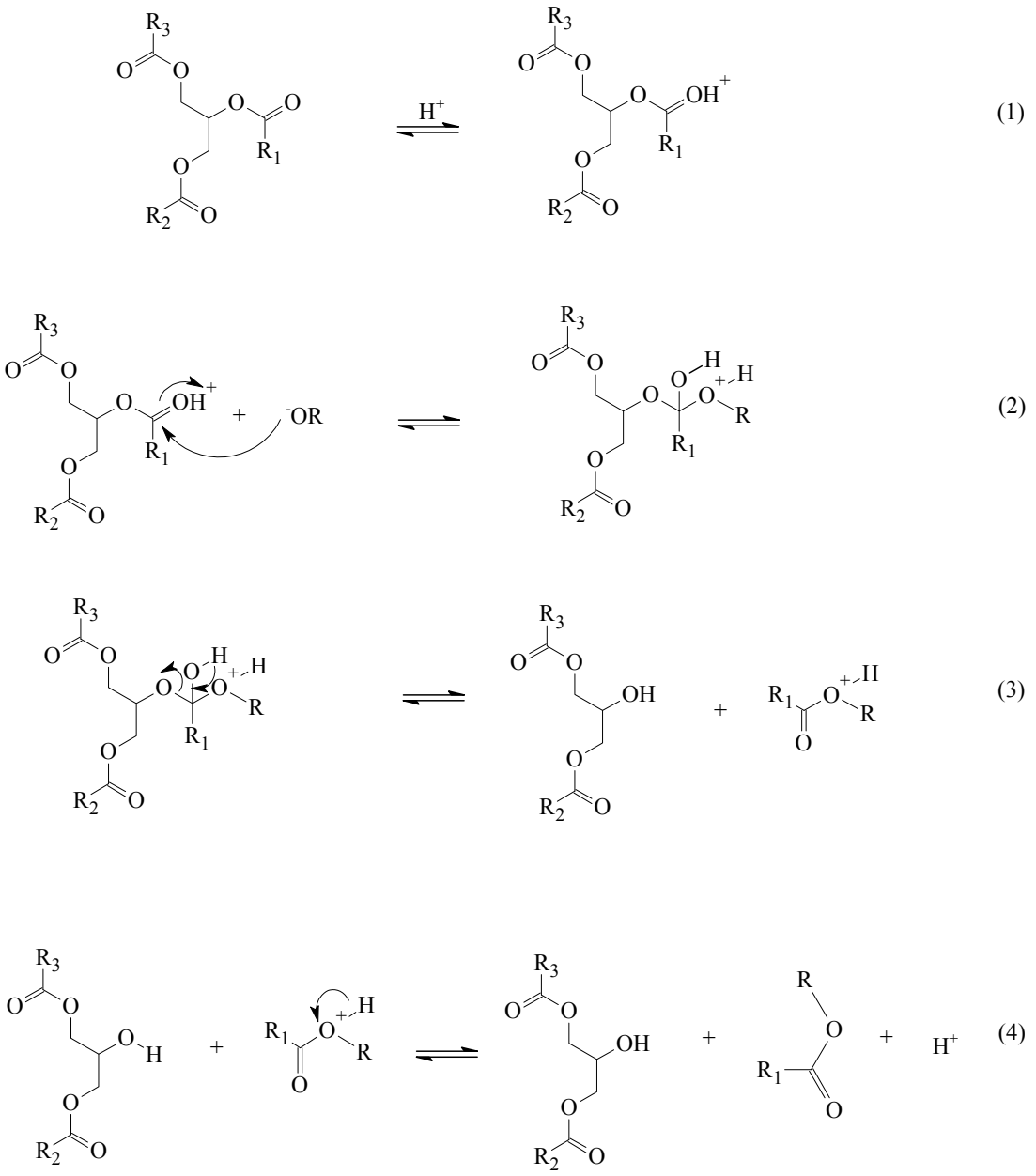

Figure 2.3. Mechanism of acid catalysed transesterification of triglycerides with alcohol. (1) Protonation of the carbonyl group by the acid catalyst, (2) nucleophilic attack of the alcohol, forming a tetrahedral intermediate, (3 and 4) proton migration and the breakdown of the intermediate. R_1, R_2 and R_3 refers to carbon chain of the fatty acid whereas R refers to alkyl group of the alcohol (Lotero *et al.*, 2005).

In the acid catalysed process, the protonation of the carbonyl group of the FAAE leads to the carbocation, and after the nucleophilic attack of the alcohol takes place, the tetrahedral intermediates are formed. Finally, the rearrangement of the tetrahedral intermediate gives rise to an FAAE and a diglyceride. The reaction can be extended

to diglycerides and monoglycerides. The main concern when acid catalysed transesterification is employed as the reaction method is the formation of carboxylic acid as the by-product when water is present in the reaction mixture.

Acid catalysed transesterification is always preferable as a pre-treatment step to reduce the large amount of FFA in the feedstock. Several researchers (Al-Widyan and Al-Shyoukh, 2002; Zhang *et al.*, 2003b) found that for commercialisation purposes, feedstocks with more than a 10% FFA content need to be pre-treated with acid catalysed esterification before they go to the transesterification process. This type of process gives a high yield in FAAE but the reaction is time consuming. Acid catalytic transesterification of fats and oils has been carried out in several studies, including the batch and continuous process. Further explanations and examples can be found in section 2.5.1.

2.4.2 Base Catalysed Transesterification

Base catalysed transesterification is the most adoptable technology for biodiesel production. The researchers found that base transesterification can achieve a high purity and yield of biodiesel product in a short time, approximately 30-60 min (Muniyappa *et al.*, 1996; Antolìn *et al.*, 2002). The base catalysed process is reported to be 4000 times faster than using the acid catalysed process (Ma and Hanna, 1999). However, it is very sensitive to the quality of the feedstock, requiring vegetable oil, animal fats or other sources of raw material with a very low amount of FFA and water content. The reaction mechanism for the base catalysed transesterification process, formulated in three sequential steps, is shown in Figure 2.3.

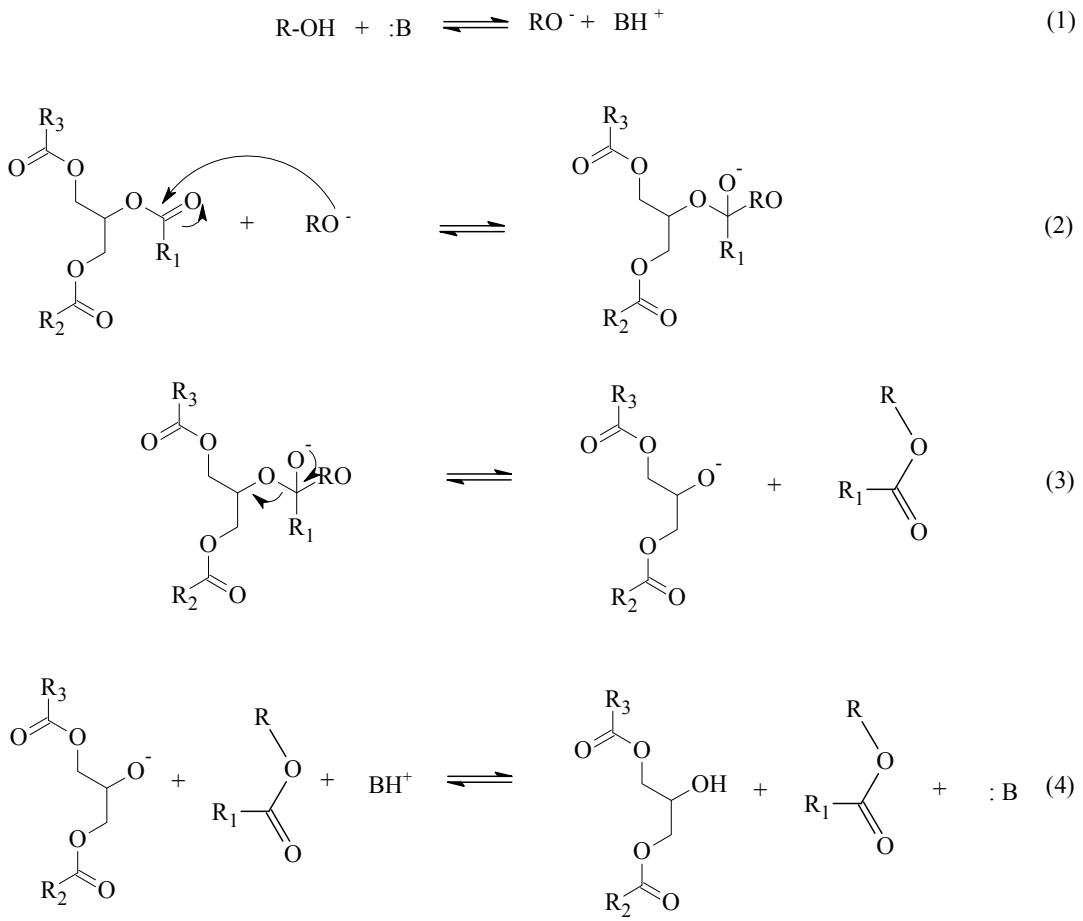

Figure 2.4. The mechanism of base catalysed transesterification of triglycerides with alcohol. (1) Production of active species, RO^-, (2) nucleophilic attack, (3) intermediate breakdown, (4) regeneration of active species.R_1, R_2 and R_3 refers to carbon chain of the fatty acid whereas R refers to alkyl group of the alcohol (Lotero *et al.*, 2005).

The first step is the reaction between the base catalyst with the alcohol, forming the alkolide and the protonated catalyst. The carboxyl group of the triglycerides has a slight positive charge whereas the carbonyl oxygen of the alcohol has a slight negative charge. In the second step, nucleophilic attack takes place when the C=O bond of the triglycerides molecules is attacked by the anion of the alcohol, RO^-, forming the tetrahedral intermediate. This intermediate has a slight negative charge which eventually falls back to the carbon bond, forming FAAE and the anion of diglycerides. The regeneration of active species takes places by the deprotonation of the catalyst using the latter species (anion of diglycerides). Diglycerides and

monoglycerides were converted by the same mechanism as triglycerides. At the end of the process, three moles of FAAE and one mole of glycerine were formed.

The main difference between the acid catalysed transesterification and the base catalysed transesterification is their proton donation. Acid catalyses the reaction by donating a proton to the carboxyl group, thus creating an active species for the group while the base catalyses the reaction by removing the proton from the alcohol, thus making it more reactive. This main difference between acid and base catalysts gives definitive variation to their catalytic activity.

2.4.3 Combination of Esterification – Transesterification Process

Alternative low value feedstocks (e.g. waste cooking oil, non-edible vegetable oil or animal fats) have gained much interest nowadays due to their potential for lowering the production cost of biodiesel. However, the high amount of FFA and water content in the low value feedstocks makes the reactant unsuitable for a direct base catalysed transesterification. FFA can react with the base catalyst (neutralisation reaction) and accelerates the base catalyst consumption. Furthermore, the reaction between FFA and the base catalyst also leads to the formation of soap and as a result, it reduces the conversion and yield of biodiesel. The soap produced by this reaction increases the viscosity of the reaction mixture leading to the formation of a stable emulsion. It makes the purification process difficult and the removal of the catalyst even more challenging. On the other hand, the reaction between FAAE and water contributes to the hydrolysis of FAAE. This situation also results in a low yield and conversion of biodiesel. The esterification step is required to prevent the neutralisation and saponification reactions caused by the high FFA and water content in the feedstocks. However, as mentioned previously, homogeneous acid catalysed transesterification is a time consuming process, especially for a complete conversion reaction. Therefore, a combined homogeneous acid-base catalytic reaction is developed to improve the yield of biodiesel when a feedstock with high FFA content is employed. Table 2.4 summarises some of the research works done on the combination process of the homogeneous esterification-transesterification reaction.

Table 2.4. Summary of research work on two-stage esterification-transesterification processes.

Feedstock	Methanol to Oil Molar Ratio	Catalyst (wt%)	Reaction Temp. (K)	Duration	Conversion	Authors
Madhuca indica	Acid: 0.30-0.35v/v Base: 0.25 v/v	H_2SO_4 (1) KOH (0.7)	333 -	1 h 1 h	98%	Ghadge and Raheman (2006)
Rubber seed oil	Acid: 6:1 Base: 9:1	H_2SO_4 (0.5 vol%) NaOH (0.5 vol%)	318 318	20-30 min 30 min	99%	Ramadhas *et al.* (2005)
Rapseed oil	(4.5:1) & (1:1)	KOH (1wt%) KOH (0.2wt%)	333 333	30 min 30 min	98.5%	Jeong and Park (2006)
Nicotiana tabacum L. (tobacco)	Acid: 18:1 Base: 6:1	H_2SO_4 (1-2) KOH (1)	333 -	25 min 30 min	91%	Veljkovic *et al.* (2006)
Waste cooking oil	Acid: 10:1 Base: 6:1	Fe_2SO_4 KOH	368 338	4 h 1 h	97.02%	Wang *et al.* (2007)
Karanja	Acid: 8:1 Base: 9:1	H_2SO_4 NaOH/KOH	318 -	30 min 30 min	89.5%-mechanical 85%-magnetic	Sharma and Singh (2008)
Zanthoxylum bungeanum seed oil	Methanol Acid: 24:1 Base: 6.5:1	H_2SO_4 (2) NaOH (0.9)	333 333	80 min 90 min	98%	Zhang and Jiang (2008)

2.5 PROCESS VARIABLES EFFECTING ESTERIFICATION AND TRANSESTERIFICATION

2.5.1 Catalyst

A catalyst is the key to chemical transformation. According to Ma and Hanna (1999), the catalyst for biodiesel production falls into three categories, namely the homogeneous catalyst, the heterogeneous catalyst and the enzyme catalyst.

2.5.1.1 Homogeneous Catalyst

Homogeneous catalysis is a chemical term which describes a catalysis reaction where the catalyst is in the same phase as the reactant. The homogeneous catalyst for biodiesel process is divided into two categories, which are the acid and the base catalysts.

a) Homogeneous Acid Catalyst

The most common acid catalysts being used in biodiesel production are sulphuric acid, phosphoric acid, hydrochloric acid or organic sulfonic acid (Goff *et al.*, 2004). The most popular acid catalyst is sulphuric acid (Ghadge and Raheman, 2005; Ramadhas *et al.*, 2005; Veljkovic *et al.*, 2006). One percent (v/v) of 100% H_2SO_4 is commonly the preferable amount of catalyst selected by most of the researchers.

Several studies reported the usage of sulphuric acid when waste oil was used as a feedstock (Al-Widyan and Al-Shyoukh, 2002; Zhang *et al.*, 2003a). In these studies, the reported FAAE conversions were quite low, at only around 82% and the requirement of alcohol was relatively high. The main challenge faced by researchers when low grade feedstock was used as the raw material was the production of water along with FAAE during the methanolysis reaction, which inhibited the transesterification of glycerides. (Canakci, 2007). Nevertheless, an acid catalyst is believed to be more tolerant to water content and a high FFA level compared to a base catalyst (Freedman *et al.*, 1984; Fukuda *et al.*, 2001; Lotero *et al.*, 2005).

A study by Canakci and Van Gerpen (2001) reported the effects of different amounts of sulphuric acid in the transesterification of grease with methanol. An increase in conversion was observed with increased catalyst loading, and the yield improved from 72.7% to 95% as the amount of catalyst increased from 1 to 5 wt%. However, a higher concentration of acid catalyst could lead to formation of ether from the alcohol dehydration process (Keyes, 1932). A high temperature and a high concentration of sulphuric acid as catalyst could also burn some of the oil which will cause a low yield of biodiesel product.

b) Homogeneous Base Catalyst

According to Ma and Hanna (1999), the most effective base catalysts are potassium hydroxide, potassium methoxide, sodium hydroxide and sodium methoxide. There are many contradictory findings between these homogeneous base catalysts. Sodium methoxide (CH_3ONa) and potassium methoxide (CH_3OK) were claimed to perform better compared to sodium hydroxide (NaOH) and potassium hydroxide (KOH)

(Felizardo *et al.*, 2006). They found that the methoxide salts have higher reaction activities compared to the hydroxides since there is negligible formation of the by-product water during the reaction (Marris, 2006). Nevertheless, these methoxide salts were relatively more expensive than the hydroxides and required high quality oils and water-free methanol. Rashid and Anwar (2008) also revealed similar results when 1% (w/w) of sodium methoxide was found to be the optimum catalyst concentration to produce biodiesel from safflower oil. However, a contradictory finding was reported by Encinar *et al.* (2007) when they investigated the transesterification of used frying oil using sodium hydroxide, potassium hydroxide, sodium methoxide and potassium methoxide as catalysts. They found that potassium hydroxide gives the highest yield when ethanol was employed as a solvent. This is due to the formation of potassium ethoxide which is a stronger base than potassium methoxide. A similar comparison study between potassium hydroxide and sodium hydroxide was reported by Vicente *et al.* (2004) and potassium hydroxide was found to have a higher yield (91.67%) as compared to sodium hydroxide (85.9%) but the purity of FAME obtained was similar. However, results from Dias *et al.* (2008) showed that potassium hydroxide was less effective than the sodium based catalyst in terms of its purity.

The amount of catalyst also causes a significant impact on the conversion of FAAE. Leung and Gou (2006) investigated different catalyst amounts for three types of catalysts, namely sodium hydroxide, sodium methoxide and potassium hydroxide. The maximum conversion of FAME was achieved when 1.1, 1.3 and 1.5% of sodium hydroxide, sodium methoxide and potassium hydroxide were employed. A two-stage base catalysed transesterification was also found to be more efficient for biodiesel synthesis. Jeong and Park (2006) reported by having 1% (w/w) potassium hydroxide in the first stage, followed by the addition of 0.2% (w/w) in the second stage, which led to the biodiesel yield increasing from 71% to 98%. Sharma *et al.* (2008) discovered that a lower amount of catalyst resulted in an incomplete reaction whereas too much catalyst could lead to the saponification process. The suitable amount of catalyst varies from 0.7% to 1.5% by weight, depending on the behaviour of the feedstock.

Most of the biodiesel production plants nowadays use homogeneous base catalysts because they are very effective and soluble in methanol. A homogeneous base catalyst was also preferred over a homogeneous acid catalyst because it gave a higher reaction rate, was less corrosive and required a shorter reaction time (Meher *et al.*, 2006a). However, these homogeneous catalysts i.e. homogeneous base and acid catalysts have some drawbacks. Biodiesel produced from a homogeneous catalysed reaction must be neutralised with water and thus this contributes to the generation of wastewater. The homogeneous catalyst cannot be reutilised, and furthermore, with the presence of a high FFA content and water, it will initiate the hydrolysis and saponification process, which leads to difficulty in the separation process.

2.5.1.2 Heterogeneous Catalyst

Heterogeneous catalysis is a chemical term which describes a catalysis reaction where the catalyst is in a different phase to the reactants. Similar to homogeneous catalysts, the heterogeneous catalyst is also divided into two categories, i.e. the solid base and the solid acid catalyst. The popularity of heterogeneous catalysts nowadays is due to the limitations caused by homogeneous catalysts. The conventional homogeneous catalyst is recommended to be replaced by environmentally friendly heterogeneous catalyst as this type of catalyst is proven to simplify the production and purification processes, reduced the amount of wastewater and cut off the number of process equipment. Therefore, the mentioned benefits will lead to a reduction in the biodiesel production cost. These catalysts were also easily separated from the reaction mixture, thus allowing multiple usage of the catalyst through a regeneration process and simultaneously this creates an environmentally friendly condition. The main obstacle faced by many researchers is the development of a suitable heterogeneous catalyst so that the transesterification process can be carried out under mild reaction conditions, within a short period of time and obtain the highest percentage of biodiesel conversion.

a) Heterogeneous Acid Catalyst

The heterogeneous acid catalyst became one of the most potential solid catalysts for esterification and transesterification reactions. According to Lotero *et al.* (2005), an ideal solid acid catalyst should have high stability, numerous strong acid sites, large pores, a hydrophobic surface and a low cost. By having a suitable solid acid catalyst, it can be easily integrated into a continuous flow system, simplify the product separation and purification as well as reduce waste generation.

In general, solid acid catalysts are found to possess low catalytic activity but have a higher stability. Thus, they are commonly used when feedstock with high FFA is used as a raw material (Lotero *et al.*, 2005). Good progress has been made by several researchers on biodiesel production using a heterogeneous acid catalyst. The catalysts are sub-divided into several categories, namely the heteropolyacids, zeolites, sulphated metal oxides, ion exchange resins and other solid acid catalysts.

Heteropolyacids

Heteropolyacids (HPA) have been extensively studied worldwide as solid acid catalysts for different application of reactions. It is a typical strong Brønsted acid and the acidity level of this type of catalyst is much higher compared to conventional acids such as sulphuric acid, Al_2O_3-SiO_2, zeolites and acidic resins. The pH value for HPA can be varies according to the designed processes and systems. HPA can catalyse a wide range of reaction processes, including esterification and transesterification in both the homogeneous and heterogeneous phases (Okuhara, 2002). The majority of catalytic reaction used the most stable and easily available Keggin-type HPA catalysts, namely tungstophosphoric acid ($H_3PW_{12}O_{40}$), tungstosilicic acid ($H_4SiW_{12}O_{40}$), molybdophosphoric acid ($H_3PMo_{12}O_{40}$) and molybdosilicic acid ($H_4SiMo_{12}O_{40}$) (Di Serio *et al.*, 2008). Tungstophosphoric acid (HPW) is amongst the most used heteropolyacids in biodiesel production.

In general, HPA is soluble in a polar solvent, leading to homogeneous catalysed esterification reactions. Mizuno and Misono (1998) found that the use of pure HPA was not favourable due to its low surface area and high solubility in polar solvents.

Several studies have also reported on the catalytic activity of different solid heteropolyacids, particularly in the transesterification of virgin and waste oils. Kulkarni *et al.* (2006) found that the catalytic activity of the HPA catalyst was highly dependent on the reactor temperature rather than the methanol to oil molar ratio or the FFA content. Cao *et al.* (2008) investigated the production of biodiesel from waste frying oil and they found that the tungstophosphoric acid (HPW) catalyst shows higher activity under the optimised reaction conditions compared with the conventional homogeneous catalyst sulphuric acid. The final conversion was nearly 90% however, the reaction required a high methanol to oil molar ratio and a long reaction time i.e. 70:1 and 14 h, respectively.

HPA as a homogeneous catalyst was known to have several disadvantages, such as low surface area and low thermal stability. In order to overcome these limitations, HPA is now used together with a support material, such as hydrous zirconia (Kulkarni *et al.*, 2006), activated carbon (Izumi and Urabe, 1981; Chu *et al.*, 1996), MCM-41 (Nowinska and Kaleta, 2000; Kozhevnikov *et al.*, 1995), silica (Vazquez *et al.*, 1999), niobia (Srilatha el *al.*, 2009), clays (Yadav and Kirthivasan, 1997) and alumina powders (Concellon *et al.*, 1998; Kulkarni *et al.*, 2006). These support materials usually create a high surface area and simultaneously increase the catalytic performance. Most of the supported HPA catalysts are in the range of super acid catalysts and their properties vary with different porous structure and water solubility.

Studies from several authors (Nakato *et al.*, 1998; Okuhara and Nakato, 1998) showed that a salt of HPA with large monovalents ions (e.g. Cs^+, NH_4^+ and Ag^+) has gained more interest nowadays in biodiesel research due to its excellent performance as a water tolerant catalyst with a large surface area. This combination of HPA with monovalent ions creates a microporous solid acid catalyst that is highly effective in most of the catalytic reactions including isomerisation, hydration, alkylation, hydrolysis and esterification (Izumi *et al.*, 1995; Corma *et al.*, 1996; Nakato *et al.*, 1998; Okuhara, 2003; Narasimharao *et al.*, 2007). Chai *et al.* (2007) and Hamad *et al.* (2008) found that the $Cs_{2.5}H_{0.5}PW_{12}O_{40}$ and $Cs_2HPW_{12}O_{40}$ catalysts

perform effectively in the transesterification of Eruca sativa Gars oil (ESG oil) and rapeseed oil respectively. The catalysts were found to be less affected by the presence of high FFA and water content. It is also reported to have high activity, yielding 99% biodiesel at a low catalyst concentration (0.00185:1 weight of catalyst to oil), low methanol to oil ratio (5.3:1), low reaction temperature (338 K) and relatively short reaction time i.e. 45 min (Chai *et al.*, 2007). The regeneration of the catalyst was also feasible and its capability of being re-used was reported to be a minimum of 6 times (Chai *et al.*, 2007). A study on catalytic efficiency was also conducted for caesium salts $Cs_xH_{3-x}PW_{12}O_{40}$ at various Cs content in the methanolysis of tributyrin, a model compound of natural triglycerides and it was found that the activity increased as the Cs content increased, by up to x = 2.0-2.3 (Narasimharao *et al.*, 2007). A further increase in the Cs content makes the catalytic activity drop rapidly (Narasimharao *et al.*, 2007). A comparison study between the potassium and caesium salt of $H_3PW_{12}O_{40}$ in the transesterification of castor oil was also investigated. In spite of experiencing the formation of a colloidal dispersion during the reaction process, it was found that pottasium salts resulted in higher activity compared to caesium salts (Zieba *et al.*, 2009).

NH_4^+, K^+ and Cs^+ salts of $H_3PW_{12}O_{40}$ were also found to be very effective catalysts in the esterification of palmitic acid (Pesaresi *et al.*, 2009; Giri *et al.*, 2005; Pizzio and Blanco, 2003). A transesterification of triacetin using silver salts doped in $H_3PW_{12}O_{40}$ as a catalyst was carried out by Zieba *et al.* (2010). The reaction process experienced a leaching of parent $H_3PW_{12}O_{40}$, particularly when a low level of silver content was employed. The same research work resulted in a remarkable difference when castor oil was employed as the raw material. For castor oil, the catalytic activity dropped and the crystalline particle of Ag-salts turned into 'gel-type' material, making the separation process more difficult. Zhang *et al.* (2010) studied the microwave-assisted transesterification of yellow horn oil using $Cs_{2.5}H_{0.5}PW_{12}O_{40}$ as a catalyst. They achieved 96.22% of FAME yield under optimum conditions: 333 K reaction temperature, 10 min reaction time, 12:1 methanol to oil molar ratio, 1% (w/w of oil) catalyst concentration with the minimum reusability of 9 times.

The reaction involving the supported HPA catalyst was found to contribute to a leaching problem as a result of the weak bonding between HPA and the support surface, especially for reactions involving a polar solvent (Moffat and Kasztelan, 1988). Oliveira *et al.* (2010) discovered a minor leaching of the zirconia-supported HPW catalyst (8 wt% relative to the initial mass of catalyst loading) during their investigation of oleic acid esterification with methanol, and thus decreased the reaction catalytic activity. Xu *et al.* (2008) tried to overcome the leaching problems by conducting a study on the tungsten HPA catalyst supported by mesostructured tantalum oxide. The combination of tantalum oxide and tunsgsten was claimed to create a strong affinity and this could potentially reduce the active species from leaching. However, the outcome showed only a moderate catalytic activity in the transesterification of tripalmitin and the catalyst was easily poisoned by other species over the active sites. On the other hand, Zhang *et al.* (2009) found that a zirconiumdodecatungstophosphate ($Zr_{0.7}H_{0.2}PW_{12}O_{40}$) catalyst with a nanotube structure exhibited higher water tolerance and acid properties compared to $Cs_{2.5}H_{0.5}PW_{12}O_{40}$ and $H_3PW_{12}O_{40}$ in the transesterification of waste cooking oil.

Zeolites

Zeolites are amongst the most popular inorganic catalysts for esterification and transesterification reactions. The ability of zeolites to permit tailoring at different crystal structures, pore sizes, framework Si/Al ratios, surface hydrophobicities and proton-exchange levels contributes to the excellent properties of the catalyst, thus making it one of the more favourable solid catalysts for FAAE production. The acidity level in zeolites is one of the contributing factors that determines their catalytic activity. Too high an acidity level will lead to the deactivation of the catalyst and the occurrence of undesirable by-products, which result in additional costs for process separation. On the other hand, the reaction may not proceed at a reasonable rate by having too low an acidity level. Jothiramalingam and Wang (2009) claimed that the conversion of FFA increases with the increase of Si/Al ratio, indicating that the reactions are majorly influenced by surface hydrophobicity and acid site strength. In contrast, a study by Carmo *et al.* (2009) found that the lowest Si/Al ratio gives the highest conversion of FFA, and methanol was found to be the

best solvent when esterification of palmitic acid using Al-MCM 41 was conducted using different types of solvent such as methanol, ethanol and isopropanol at different Si/Al ratios.

However, the critical issue when zeolites are used as catalyst is the mass transfer limitation due to their microporous nature. Their small pore size limits the diffusion of the large fatty acid molecules, and thus it may not be suitable for biodiesel production (Harmer *et al.*, 1998; Van Rhijn *et al.*, 1998). Zeolites were also found to have low densities of effective acid sites and were capable of losing their activity under harsh conditions. It was concluded that the pore size, the dimensionality of the channel system, and the Si/Al content of the zeolites framework were some of the important variables that contributed to the effectiveness of zeolite catalytic activity.

Sulphated Metal Oxides

Studies on the transesterification of vegetables oils using sulphated metal oxides have been carried out progressively. The structure of the sulphated metal oxide catalyst is a combination of sulphate group with the metal oxide centres. These catalysts were found to have excellence performance in the esterification and transesterification of triglyceride-containing feedstocks. Catalysts such as sulphated zirconia (SO_4^{2-}/ZrO_2), sulphated tin oxide (SO_4^{2-}/SnO_2) and sulphated titanium dioxide (SO_4^{2-}/TiO_2) were found to demonstrate good catalytic activities during the esterification process of FFA (Furuta *et al.*, 2004; Kiss *et al.*, 2006). Jitputti *et al.* (2006) reported the use of sulphated zirconia in the transesterification of crude palm oil and coconut oil with methanol. It was found that sulphated zirconia produced 90.3 and 86.3 wt% of FAME from crude palm kernel oil and crude coconut oil, respectively. However, this catalyst deactivated after its first run due to catalytic site poisoning and the leaching of sulphated ions from the porous support, resulting from the hydrolysis process. The sulphate group can leached out as H_2SO_4 or HSO_4^- (Chen *et al*., 2007), which leads to a homogeneous reaction, interfering with the heterogeneous activity. The same findings, i.e. deactivation and leaching of sulphated zirconia catalyst, were reported by Garcia *et al.* (2008) and López *et al.* (2008). Sulphated zirconia was also not preferred because the raw

material for this catalyst, zirconium is expensive and high temperatures are needed for both calcinations and reactivation of the sulphated zirconia catalyst (Yadav and Nair, 1999; Kiss *et al.*, 2006).

The preparation method for the sulphated zirconia catalyst was reported to have a significant effect on the catalytic performance (Garcia *et al.*, 2008). In this study, conventional sulphated zirconia displayed a very low catalytic activity for the transesterification of soybean oil, whereas sulphated zirconia that was synthesised using a free-solvent method achieved approximately a 99.8% conversion after a 1 h reaction. However, the catalyst deactivated rapidly with only a 59% conversion after being re-used once which dropped to a 39% conversion after being re-used twice. Several studies also focus on the improvements of the catalyst preparation method to overcome the leaching problem. Yadav and Murkute (2004) found a new route to prepare SO_4/ZrO_2 catalyst with a higher sulphate loading and resistance to leaching. It was done by dissolving a chlorosulphonic acid precursor in an organic solvent, instead of the conventional impregnation of sulphuric acid. This novel catalyst showed better catalytic activity than the conventional prepared SO_4/ZrO_2; no leaching was observed and it was able to retain its activity for further reutilisation. Similar work done by Fu and co-workers (2009), observed the stability of sulphated zirconia in the transesterification of waste cooking oil and yellow grease with methanol. They evidenced negligible loss of acid sites by analysing the remaining sulphur content in the used catalyst. Thus, they concluded that there was no sulphate group leached from the support throughout the process.

Another superacidic sulphated metal oxide that has been used in the transesterification reaction is sulphated titania. Although it was claimed to be less active than sulphated zirconia, the catalytic activity increased as the surface area increased. An improvement has also been made for sulphated titania in the catalyst preparation method, by formulating a novel silica supported sulphated titania (Peng *et al.*, 2008). It was made by the impregnation of silica with titanium isopropoxide and consequent calcination, followed by impregnation with sulphuric acid and re-calcination. This material was used in the simultaneous esterification and

transesterification of an oleic acid-refined cotton seed oil mixture with methanol. The improvised catalyst achieved a very high catalytic activity, yielding over 90% of FAME at the optimum condition: 473 K, 3 wt% catalyst loading and 9:1 methanol to oil molar ratio. Only small catalyst decay was found after conducting four consecutive reutilisation runs with the used catalysts. Melero *et al.*, 2009 found that the sulphated titania was proven to have higher stability compared to sulphated zirconia, due to several possible reasons: 1) a stronger interaction between the titania and the sulphate groups, 2) the presence of silica as the stabilising agent.

Other potential sulphated metal oxide that has been investigated was sulphated tin oxide (Lam *et al.*, 2009). A study of the biodiesel reaction using sulphated tin oxide was found to have a higher acid surface compared to sulphated zirconia. The transesterification process of waste cooking oil was conducted by Lam *et al.* (2009) who found that the mixture of alumina/silica with sulphated tin oxide increases the catalytic activity and contributes to 92.3% of FAME yield. Nevertheless, because of the high cost and difficulties posed during the catalyst separation process, the sulphated tin oxide catalysts become less favourable in industrial scale production.

Ion Exchange Resins

Ion exchange resins are becoming more popular nowadays because this type of catalyst can catalyse the esterification and transesterification reactions under mild reaction conditions due to their high concentration of acid sites (López *et al.*, 2007). It is an attractive alternative because it is easy to separate and recover from the product mixture.

Currently, sulphonated cation exchange resin has been found to be the one of most effective resins for esterification of FFA (Tesser *et al.*, 2005; Özbay *et al.*, 2008; Russhueldt and Hoelderich, 2009; Talukder *et al.*, 2009; Tesser *et al.*, 2010a). Cation exchange resins are classified into two types of matrix structure: gelular and macro-reticular. Kouzu *et al.* (2011) conducted a study on the performance of gelular (Amberlyst 31) and macroeticular (Amberlyst 15) matrices in the esterification of soybean oil. It was found that the gelular resin has a higher catalytic activity

compared to macroeticular resin. The uniqueness of these gelular resins lies in their textural properties, i.e. the swelling behaviour. This swelling capacity controls the accessibility of acid sites in the catalyst and it simultaneously affects the overall reactivity. Once the small pores become macropores, they create more accessible sites for the acid functionalities group. Furthermore, the accessibility of long hydrocarbon chains of fatty acids molecules into the acid sites becomes easier and hence improves the catalytic activity. However, the internal mass transfer of gelular resins was much slower compared to macroeticular resins. A similar result was obtained by Russhueldt and Hoelderich (2009) who reported that the catalytic performance of the gelular sulfonic resin was superior to the macroporous catalysts investigated.

Study of the different matrix types of cation exchange resin was also conducted by Feng *et al.* (2010). Three types of resin were employed in this study, namely the NKC-9 (macroeticular), 001 x 7 (gelular) and D61 (macroeticular). In contrast, the highest FFA conversion was obtained using NKC-9 and this resin also showed a good conversion in the reusability study. A similar result was reported by Özbay *et al.* (2008) when they investigated on the esterification of waste cooking oil using Amberlyst 15, Amberlyst 35, Amberlyst 16 (macroeticular) and Dowex HCR-W2 (gelular) as catalysts, and Amberlyst 15 was found to give the highest FFA conversion.

There were also a few studies of the esterification process that focused on the macroeticular strongly acidic cation exchange resin as catalysts. Bianchi *et al.* (2009) studied the de-acidification of animal fats using several types of macroeticular cation exchange resins as catalysts i.e. Amberlyst 15Dry, Amberlyst 36Dry, Amberlyst 39Wet, Amberlyst 40Wet, Amberlyst 46Wet and Amberlyst 70Wet. From this study, more than 90% of the FFA conversion was successfully achieved when Amberlyst 70Wet was used as the catalyst. This catalyst also showed a good conversion rate in the reusability study and performed well even in less severe operating condition (303 K with 1.25 wt% catalyst). Park *et al.* (2008) studied the performance of two different macroeticular cation exchange catalysts, the Amberlyst-15 and

Amberlyst BD20. They found that the amount of pores of the catalyst played an important role, not only in increasing the catalytic activity, but also in reducing the inhibition by water in the esterification process. A few groups of authors (Liu *et al.*, 2009; Shibasaki-Kitakawa *et al.*, 2010) conducted a study to investigate the performance of FFA esterification in a packed bed reactor using cation exchange resins as catalysts. The PK208LH (Shibasaki-Kitakawa *et al.*, 2007) and D002 (Liu *et al.*, 2009) was found to produce the optimum conversions of FFA of 81.4% and 96%, respectively.

The composition of fatty acids in vegetable oil has an impact on the catalytic activity of the ion exchange resin, where a higher content of shorter-chain fatty acid in the oil composition is preferred when an ion exchange resin is used (dos Reis, 2005). However, thermal stability is the main concern when ion exchange resins are used at higher temperatures. In esterification and transesterification reactions, a high temperature is usually required for higher reaction rate and catalyst regeneration.

b) Heterogeneous base catalyst

Detailed investigation of different types of base heterogeneous catalysts such as rare earth oxides, various base metal compounds supported on alumina or zeolite, hydroxides, alkoxides, hydrotalcites and ion exchange resin have been carried out by several researchers (Watkins *et al.*, 2004; Kim *et al.*, 2004; Reddy *et al.*, 2006; Granados *et al.*, 2007; Reddy *et al.*, 2007; Shibasaki-Kitakawa *et al.*, 2007). Solid base catalysts are reported to have high catalytic activities but low stability (Lotero *et al.*, 2005). Heterogeneous base catalysts are classified into 6 different categories: single metal oxide, mixed metal oxide, supported alkali/alkaline earth metal, zeolites, hydrotalcites and ion exchange resins.

Single Metal Oxides

Metal oxides are one of the potential choices for base catalysed transesterification particularly in biodiesel production. Calcium oxide (CaO), magnesium oxide (MgO) and strontium oxide (SrO) are among the popular alkali earth metal and are widely used nowadays. Among all the alkaline single metal oxide catalysts, calcium-derived

oxides are claimed to be the most promising catalysts in biodiesel transesterification because they are cheap, easily available, have a long catalyst lifetime and are less toxic. Gryglewicz (1999) investigated the transesterification of rapeseed oil with methanol using homogeneous catalysts i.e. sodium hydroxide and heterogeneous catalysts i.e. calcium oxide (CaO), calcium methoxide ($Ca(OCH_3)_2$) and barium hydroxide ($Ba(OH)_2$). Calcium catalysts were found to effectively reduce the number of technological stages and the amount of waste product. However, the conversion of FAME using calcium catalysts was much lower compared to sodium hydroxide.

The appropriate water level in the reaction process was found to be one of the factors that could increase the activity of CaO (Liu *et al.*, 2008). This is due to the presence of O^{2-} ions on the surface of the catalyst that attracts H^+ from the water molecules. It leads to the formation of OH^- that eventually combines with H^+ from the methanol to produce methoxide anions, which are among the most favourable catalysts for the transesterification process. Nevertheless, too much water (more than 2.8% of the oil's weight) could result in saponification due to the hydrolysis of fatty acids. Contradictory results were found by Granados *et al.* (2007) during their investigation of the effect of water and carbon dioxide on the catalytic activity of CaO in the methanolysis of sunflower oil. The study showed that CaO was easily contaminated by the presence of water and carbon dioxide from the atmosphere. Therefore, they introduced a thermal treatment method for this catalyst to solve the contamination problem. The catalyst was calcined at high temperature (more than 973 K) and strictly forbidden from being exposed to the atmosphere, prior to use.

Several studies have also been conducted to improve the catalytic properties of CaO. Studies on the improvement of CaO activity have been carried out by modifying the surface basicity (Zhu *et al.*, 2006). In their study, CaO was immersed in an ammonium carbonate solution, which was followed by the calcination of the catalyst at 1173 K. The yield of FAME was 94% at 9:1 molar ratio, 1.5 wt% catalyst loading and 343 K reaction temperature. The hydration-dehyration approach has also been used by Yoosuk *et al.* (2010) to create a simple and flexible calcined catalyst. This new catalyst was found to have a higher surface area and a higher amount of basic

sites. The FAME yield increased from 75.5 to 93.9% using conventionally calcined and novel improvised CaO, respectively. Research by Bai *et al.* (2009) focused on the improvement of catalyst morphology by developing the highly porous microsphere of CaO to increase the catalytic performance. This study successfully reached nearly 99% of FAME conversion. The main problem when CaO was used as the catalyst was the leaching of the active sites from the surface of the catalyst. This condition resulted in the formation of homogeneous $Ca(OCH_3)_2$ catalysts and simultaneously contributed to a semi-homogeneous reaction.

MgO also has shown a good catalytic activity for biodiesel synthesis. Veljkovic *et al.* (2009) obtained approximately 98% of biodiesel yield using MgO as catalyst. For this catalyst, the FAME yield is largely dependent on the methanol to oil molar ratio and the reaction temperature. The previous statement was proven by research conducted by Tateno and Sasaki (1998) into the transesterification of soybean oil with methanol. The optimum FAME yield (ca. 97%) was obtained at 573 K, 0.58 wt% of catalyst and a large amount of methanol (39.3:1 methanol to oil molar ratio). Several studies have also been conducted using other types of metal oxides. An ultrasonic-assisted transesterification with different types of alkali oxide catalyst (CaO, SrO and BaO) has been conducted by Mootabadi *et al.* (2010). They found that BaO gives the highest (95%) yield within an hour. However, the catalytic activity dropped during the subsequent reusability study, resulting from catalyst dissolution during the reaction process.

The capability of transition metal oxides i.e. zirconium oxide (ZrO_2) and zinc oxide (ZnO) as biodiesel catalyst also sparks an interest for the catalyst developer, due to their acidic properties. Jitputti *et al.* (2006) examined the performance of the zinc oxide and zirconium oxide during the methanolysis of palm oil under supercritical conditions (pressure at 50 bar under nitrogen atmosphere, temperature at 473 K). The FAME yield was found to be 86.1% for zinc oxide and 64.5% for zirconium oxide after 1 h of reaction using 3 wt% of catalyst and 6:1 methanol to oil molar ratio.

Mixed Metal Oxide, Supported Alkali and Alkali Earth Metal Oxides

A mixed metal oxide catalyst is also known as a one-step improvement over the single metal oxide. The introduction of the third lattice within the original structure of the single metal oxide increase the catalyst's durability and stability. Kawashima *et al.* (2008) studied the combination of A-B-O type metal oxides, where A is an alkaline-earth metal, alkaline metal, or rare earth metal i.e. calcium (Ca), barium (Ba), magnesium (Mg), lanthanum (La) and B is a transition metal i.e. titanium (Ti), manganese (Mn), ferum (Fe), zirconium (Zr) and cerium (Ce). Thirteen kinds of catalyst were developed and tested in the transesterification of rapeseed oil with methanol. The transesterification was carried out at 333 K reaction temperature with a 6:1 molar ratio of methanol to oil. The calcium-containing catalysts i.e. $CaTiO_3$, $CaMnO_3$, $Ca_2Fe_2O_5$, $CaZrO_3$, and $CaO\text{-}CeO_2$ showed high activities and approximately 90% yields of FAME.

Supported materials have been widely used in transesterification and esterification catalysis due to their availability to enhance the performance of the catalyst (e.g. larger surface area and higher stability/durability). Sodium, pottasium, lithium, barium and magnesium were frequently used either in the ionic form of halide, hydroxide, carbonate, nitrate or in the metallic form. These ionic and metallic metals were impregnated in various metal supports such as aluminium oxide (AlO_3), ZnO, MgO and CaO to develop various types of metal supported catalysts. As mentioned in the previous section (i.e. single metal oxides), CaO possess moderate catalytic activity during the reaction process and therefore, Yan and co-workers (2008) tried to overcome the limitation by impregnating the CaO on several types of metal oxide support such as manganese (MgO), silica (SiO_2), alumina (AlO_3) and zeolites HY. The best condition obtained with the combination of CaO/MgO and the optimum conversion was ca. 92% at 337.5 K. However, the catalyst activity dropped after the fourth run of reutilisation due to the blockage of the active sites by the product and by-product of the reaction. The activity of the catalyst could be restored to the initial condition using a thermal treatment method, together with the addition of extra calcium precursor. Macedo *et al.* (2006) examined the alcoholysis of soybean oil with Al_2O_3-SnO and Al_2O_3-ZnO as catalysts. Under the optimum conditions,

80% yield of FAME was achieved after 4 h of reaction time with 5 wt% catalyst and 333 K reaction temperature.

A summary of the activity of metal oxides, mixed metal oxides supported alkali and alkali earth metal oxides catalyst is presented in Table 2.5. The main difficulty faced by researchers with this type of catalyst is the dissolution problem. In most cases, catalysts will eventually leach out from their support, turning themselves into liquid phases, which eventually complicates the separation process due to the occurrence of the semi-homogeneous reaction.

Table 2.5. Production of biodiesel using metal oxide and their supported catalyst as heterogeneous base catalyst.

Catalyst	Operating Condition	Conversion/ Yield	Authors
Na/NaOH/ γ-Al_2O_3	Feedstock: Soybean oil, Temp (K):333, Time (h): 2, Solvent: methanol, Solvent/Oil: 9:1, Catalyst loading: 1g. Stirring: 300 rpm, Co-solvent/oil: 1:5 (n-hexane)	Conversion: 94%	Kim *et al.* (2004)
KNO_3/Al_2O_3	Feedstock: Soybean oil, Temp (K): -, Time (h): 7, Solvent : methanol (reflux), Solvent/Oil: 15:1, Catalyst loading (wt%): 6.5	Conversion: 87%	Xie *et al.* (2006a)
KI/Al_2O_3	Feedstock: Soybean oil, Time (h): 8, Solvent: methanol (reflux), Solvent/Oil: 15:1, Catalyst loading (wt%): 2.5	Conversion: 96%	Xie and Li (2006)
KF/γ-Al_2O_3	Feedstock: Cottonseed oil, Temp (K):338 Time (h):, Solvent: methanol, Solvent/Oil: 12:1, Catalyst loading (wt%): -	Conversion: 95%	Lingfeng *et al.* (2007)
Ba/ZnO	Feedstock: Soybean oil, Temp (K):338, Time (h): 1, Solvent : methanol, Solvent/Oil: 12:1, Catalyst loading (wt%): 6	Conversion: 95%	Xie and Yang (2007)
Li/ZnO	Feedstock: Soybean oil, Time (h): 3, Solvent: methanol (reflux), Solvent/Oil: 12:1, Catalyst loading (wt%): 5	Conversion: 96.3%	Xie *et al.* (2007a)
$Sr(NO_3)_2$/ZnO	Feedstock: Soybean oil, Temp (K):338, Time (h): 5, Solvent: methanol, Solvent/Oil: 12:1, Catalyst loading (wt%): 5	Conversion: 94.7%	Yang and Xie (2007)
KF/MgO	Feedstock: rapeseed oil, Time (h): 3, Solvent: methanol (reflux), Solvent/Oil: 15:1	Conversion: 79.82%	Wan *et al.* (2008)
KNO_3/Al_2O_3	Feedstock: Jatropha oil, Temp (K):343 Time (h): 6, Solvent: methanol, , Solvent/Oil: 12:1, Catalyst loading (wt%): 6	Conversion: 84%	Vyas *et al.* (2009)
CaO/ZnO	Feedstock: Sunflower oil, Temp (K):333, Time (h): 2, Solvent: methanol, Solvent/Oil: 12:1, Catalyst loading (wt%): 1.3	Yield: > 90%	Alba-Rubio *et al.* (2010)
CaO/MgO	Feedstock: Jatropha curcas oil, Temp (K):393, Time (min): 180, Solvent: methanol, Solvent/Oil: 25:1, Catalyst loading (wt%): 3	Yield: 90%	Taufiq-Yap *et al.* (2011)

Zeolites

Zeolites are known as amongst the most versatile catalyst where they permit tailoring of many different aspects: the chemical composition, the pore size distribution and ion exchange capabilities. The basicity and acidity of zeolites can be controlled by selecting a suitable type and amount of ion exchange cation to be introduced into the zeolite's structure, as well as the Si/Al ratio of the main zeolite's framework (Lee *et al.*, 2009). Hattori (1995) suggested two approaches to control the basicity of zeolites; the first one is by exchange of ions with the alkali metal ions, and the second one is the impregnation of the basic components on the inner surface of the zeolite's pores. The first approach was claimed to produce relatively weak basic sites while the second one appeared to create a stronger basic catalyst.

The commonly used zeolites in biodiesel synthesis are zeolite-X and titanosilicate (ETS-4 and EST-10). Zeolite-X is considered to be the most basic zeolite catalyst. The basicity of this catalyst can be manipulated by having different level of electropositive metal ions such as pottasium (K) and caesium (Cs) (Barthomeuf, 1996). Suppes *et al.* (2004) reported that zeolites with K^+ ions performed better compared to zeolites with Cs^+ ions. The main reason for this is that the large size of Cs^+ limits the exchange capacity compared to the small size of K^+ and this factor caused a significant effect on the basicity and transesterification activity of biodiesel synthesis. The same group of authors also tested the incorporation of the NaO_x species in the zeolite-X framework, and the result was compared with K-X zeolite catalyst. The K-X zeolite catalyst resulted in a higher FAME conversion, where the conversion value increased from 22.7% to 94.2%. On the other hand, Xie *et al.* (2007b) investigated the impregnation of KOH on the Na-X zeolite catalyst. The best result was obtained with Na-X zeolite loaded with 10% KOH, followed by heating at 393 K for 3 h. The FAME yield reached up to 85% conversion after 8 h of reaction with 8:1 methanol to oil molar ratio and 338 K reaction temperature.

Engelhard titanosilicate structure (ETS) zeolites have also gained much attention due to their unique capabilities i.e. strong basic sites, large pore structure and high cation

exchange capacity (Anderson *et al.*, 1994; Das *et al.*, 1996; Leclercq *et al.*, 2001; Suppes *et al.*, 2004; Xie *et al.*, 2007b). ETS-10 are known as microporous inorganic titanium containing zeolites that have a three dimensional 12-ring pore structure consisting of interlocking chains of octahedral titanium (TiO_6^{8-}) and tetrahedral silicon ($SiO4^{4-}$) atoms (Philippou *et al.*, 1999). This catalyst was reported to have four times the basicity compared to NaX (Philippou *et al.*, 1999). However, ETS-10 has to go through several chemical treatment steps in order to reach this level of activity. Beynese *et al.* (1996) studied on the transesterification of soybean oil with methanol using EST-4 and EST-10. The reaction produced 86% and 53% of FAME when EST-4 and EST-10 were used as catalysts, with 493K reaction temperature and 1.5 h reaction time. A transesterification of triacetin using ETS-10 as catalyst was carried out by López and co-workers (2005) and they found that this type of catalyst suffered the internal mass transfer limitation because of its microporous structure. Most of the liquid transesterification studies benefits from the presence of large pore structures but not by the large surface area created by zeolite's inner pore structure (Suppes *et al.*, 2004).

The improvement of ETS-10 was motivated by the development of mesoporous zeolites such as SBA-15 and MCM-41 (Barrault *et al.*, 2004; Gaudino *et al.*, 2005; Li and Rudolph, 2008). SBA-15, a mesoporous silicate with uniform pore size, was claimed to be more stable than MCM-41, in terms of its hydrothermal stability. Other compounds such as MgO (Li and Rudolph, 2008) and CaO (Albuquerque *et al.*, 2008) have been introduced to the structure of SBA-15 to enhance the catalytic performance. The impregnation of MgO into the SBA-15 structure leads to better catalytic activities with 96% of fatty acid ethyl ester (FAEE) conversion when the reaction was carried out at 220°C for 5 h (Li and Rudolph, 2008). However, it was not based on individual performance factors (e.g basicity, surface area, porosity and surface MgO concentration) but rather resulted from the combined effect of all the factors. A study of the transesterification of vegetable oil using CaO/SBA-15 as catalyst was carried out by Albuquerque *et al.* (2008). They found that strong interaction between SBA-15 and CaO could prevent leakage of active sites from the catalyst structures and the

performance was claimed to be better when compared to homogeneous NaOH transesterification.

Hydrotalcites

Hydrotalcites are a class of anionic and basic clays known as layered double hydoxides. The general formula for a hydrotalcite is $[M_{1-x}^{2}+M_x^{3+}(OH)_2]^{x+}[(A^{n-})_{x/n}]\cdot m$H2O where M^{2+}, M^{3+} and A^{n-} are monvalent or divalent ions (e.g. Mg, Fe, Co, Cu, Ni, or Zn), with trivalent ions (e.g. Al, Cr, Ga, Mn or Fe) and an anion (e.g. CO_3^{2-}) where the value of *x* is equal to the molar ratio of $M^{2+}/(M^{2+} + M^{3+})$, respectively. Hydrotalcites have gained more interest for the transesterification process due to their capability to be modified, producing catalysts with different basicity and surface area. The modification process can be done in two ways, either by varying the chemical composition of the hydrotalcites or by having different catalyst preparation methods.

The most well-known hydrotalcites catalyst combination is the calcined Mg-Al hydrotalcites as they appear to have consistent activities during the transesterification process (Xie *et al.*, 2006b; Liu *et al.*, 2007). The calcination temperature and the Mg/Al ratio were found to be the most crucial factors in the development of base hydrotalcites catalysts. The change in the Mg/Al ratio was claimed to give more variation to the basicity of the catalyst (Díez *et al.*, 2003). Few studies has been conducted to investigate the best Mg/Al molar ratio for biodiesel application, and a ratio of 3 is claimed to be the best in terms of its basic activity (Fishel and Davis, 1994; Cantrell *et al.*, 2005; Xie *et al.*, 2006b; Zeng *et al.*, 2008). Modification of the calcination temperature also leads to better thermal stability as well as higher catalyst basicity (Di Cosimo *et al.*, 1998; Liu *et al.*, 2007). 773 K and 823 K were claimed to be the best calcination temperatures when the molar ratios of Mg/Al hydrotalcites were 2.93 and 2.3 (Xie *et al.*, 2006b; Liu *et al.*, 2007). Liu *et al.* (2007) studied the transesterification of poultry fat with methanol using Mg/Al hydrotalcite derived catalysts and they achieved 67% conversion of FAME after 9 h of reaction, with 15:1 methanol oil molar ratio, 333 K reaction temperature, 7.5 wt% catalyst and the three molar ratios of Mg/Al hydrotalcites.

Apart from this, hydrotalcites catalysts also spark more interest for many biodiesel catalyst manufacturers due to their availability to withstand feedstock with high FFA and water content. Mg-Al hydrotalcites showed good results when the transesterifications of cottonseed oil (9.5 wt% of FFA) and animal fat oil (45 wt% of water) with methanol were conducted (Barakos *et al.*, 2008). After 3 h of reaction, both feedstocks resulted in 99% of triglycerides conversion using 1 wt% catalyst, 6:1 methanol to oil molar ratio, 473 K reaction temperature and with FFA content decreased to 1 wt%. Georgogianni *et al.* (2009) have investigated the transesterification of rapeseed oil using homogeneous and heterogeneous catalysts and Mg-Al hydrotalcite shows the highest catalytic activity with 97% of FAME conversion. The performance of the catalyst was found to be related to the basic strength of the hydrotalcites catalyst. Advanced studies of the impregnation of additional metal catalysts to Mg-Al hydrotalcites have also been carried out and tested in transesterification systems. Gao *et al.* (2008) conducted a comparison study on the methanolysis of palm oil using KF/Mg-Al and parent Mg-Al hydrotalcites as catalyst. At this optimum condition; 12:1 methanol to oil molar ratio, 338 K reaction temperature, 3 wt% catalyst and 5 h reaction time, the conversion of triglycerides using KF/Mg-Al hydrotalcites reached up to 88.7% while the parent Mg-Al hydrotalcites gave much a lower conversion, at only around 44.7 wt%.

Apart from the impregnation of additional metal on the hydrotalcites structure, substitution of the Al^{3+} ion with another type of metal ion has also been investigated. Macala *et al.* (2008) found that by doping Fe^{3+} ions into the Mg-Al structure, they could increase the catalytic activity of the hydrotalcites. 10% Fe doped Mg-Al hydrotalcites resulted in 100% conversion of triacetin after 40 min reaction time with 6:1 methanol to oil molar ratio, 1 wt% of catalyst loading and reaction temperature of 333 K whereas the undoped Mg-Al hydrotalcites produced ca. 20% of triacetin conversion when the experiment was conducted under the same conditions.

The main advantage of hydrotalcites catalysts is their availability to withstand feedstock with high FFA and water content. The main drawback of this catalyst comes from the poor physical properties of the catalyst, since they have a low

porosity and low surface area. The performance of hydrotalcites catalysts in biodiesel reactions can be improved by modifying the physical characteristics of the catalyst.

Ion Exchange Resins

Transesterification of biodiesel can be either conducted using an anion or cation exchange resin. Transesterification of Brazillian vegetable oils using cation exchange resin as the catalyst has been conducted by don Reis *et al.* (2005). Palm kernel and Babassu oil were found to produce higher biodiesel yields than soybean oil, probably due to the higher content of shorter fatty acid chains. Amberlyst 15 was reported to produce the highest biodiesel conversion. However, the molar ratio requirement was very high, i.e. up to 800:1 methanol to oil.

Shibasaki-Kitakawa *et al.* (2007) investigated the potential of anion exchange resin as the heterogeneous catalyst. Several types of anion catalyst have been tested for the transesterification of triolein, namely the Diaion PA308, Diaion PA306, Diaion PA306s and HPA 25. Anion exchange resin with a lower cross-linking density and a smaller particle size, Diaion PA306s, was proved to give the highest catalytic activity and resulted in approximately 98.8% purity of biodiesel fuel. In their latest research, Shibasaki-Kitakawa *et al.* (2011) also reported that Diaion PA306s catalyst could act as both catalyst and adsorbent in the transesterification reaction. Impurities such as FFA, methanol, dark brown pigment and by-product glycerine were successfully removed from the product by the adsorption onto the resin. Falco *et al.* (2010) conducted a study of the transesterification of soybean oil using basic and acidic ion exchange resin as the catalyst. In this study, a strongly basic anion exchange resin, BR 1 was reported to give the highest conversion and the selectivity of FAME could potentially reach 100%.

A comparison study between anion and cation exchange resin has been carried out by Li *et al.* (2012). Four types of ion exchange resins, namely Amberlyst 15 (cation), Amberlite IRC-72 (cation), Amberlite IRA-900 (anion) and Amberlite IRC-93 (anion) have been tested in the transesterification of yellow horn

(Xanthoceras sorbifolia Bunge.) seed oil. Amberlite IRA-900 was reported to have the highest conversion yield of 96.3%. Amberlyst 15 was also found to give good conversion yield (83.5%), however, it is still considered a weak catalyst compared to Amberlite IRA-900. Anion exchange resins can also be repeatedly used without any loss in the catalytic activity (Shibasaki-Kitakawa *et al.*, 2010; Li *et al.*, 2012). However, thermal stability became the major problem for ion exchange catalysts. The situation was more severe for the anion resin catalysts because their resistance to high temperature was much lower compared to cation exchange resins.

Enzyme Catalyst

The enzyme catalyst has been discovered to be a potential catalyst for biodiesel production. The enzyme catalyst shows good thermal stability, good separation of products, is capable of being regenerated and reused and has good tolerance towards the high level of FFA in the feedstock. However, the main drawback was the cost of these biocatalysts, since they were found to be more expensive than most of the heterogeneous catalysts. Most of the enzyme catalysts were prepared via immobilisation techniques, where the cell biocatalyst was immobilised within biomass support particles. This is the main advantage of this catalyst since the immobilisation can be achieved spontaneously during batch cultivation and no purification is needed (Fukuda *et al.*, 2001).

Few studies have been carried out using biocatalysts in biodiesel production. Nelson *et al.* (1996) found that M. Miehi, a lipase catalyst resulted in good yield of biodiesel in the transesterification process. An immobilised lipase has also been utilised in the methanolysis of corn oil under supercritical conditions, and this resulted in more than 98% of FAME conversion (Jackson and King, 1996). The utilisation of a lipase catalyst in continuous biodiesel production has also been investigated by Nie *et al.* (2006), where a three-step transesterification with methanol was conducted using a series of columns, packed with immobilised Candida sp. 99-125 lipase. Under the optimal condition, the final conversion ratio of FAME obtained was approximately 90-92%. Another research on continuous systems using immobilised lipase from the *Burkholderias cepacia* (IM BS-30) catalyst was carried out by

Hsu *et al.* (2004). Under the optimal conditions, approximately 96% FAEE yield was achieved.

2.5.2 Free Fatty Acids (FFA)

The FFA content is one of the variables that dictates the feasibility of the biodiesel transesterification process. The acid value is an indicator of FFA content in the triglycerides, where a higher acid value shows that the feedstock contains a higher percentage of FFA. Several studies have been conducted to investigate the effect of FFA in the esterification and transesterification reaction. A study by Naik *et al*. (2008) showed a significant drop in the conversion of FAME when the FFA content was beyond 2%. Therefore, they proposed that a direct base transesterification can only be carried out when the FFA content is lower than 2%. On the other hand, Canakci and Van Gerpen (2001) suggested that the recommended acidity should be below 1 mgKOH g^{-1} triglyceride (ca. 0.5% FFA content) for a direct transesterification reaction. According to Freedman *et al*. (1984), the FFA content in the triglycerides should not be more than 1% in order to hinder the saponification reaction. Theoretically, FFA can react with the base catalyst by neutralisation and saponification reactions and this situation resulted in low yield and conversion to biodiesel. Therefore, a pre-treatment step is needed to esterify the FFA before triglycerides can be converted into FAAE.

2.5.3 Water Content

Water content is also one of the variables that significantly affect the performance of biodiesel production. All materials involved in the transesterification process should be waterless because the presence of water leads to the hydrolysis of FAAE and triglycerides and simultaneously contributes to the formation of soap. The produced soap increases the viscosity of the reaction mixture leading to the formation of a stable emulsion, and this leads to difficulty in the separation process. Canacki and Van Garpen (2001) identified that even a small amount of water (0.1%) in the transesterification process could reduce the conversion of triglycerides in the feedstock. The same situation happened to the esterification process where Ellis *et al.* (2008) found that even a small amount of water, either readily available

inside the feedstock or produced as a by-product in the esterification reaction, can reduce the conversion of FAME due to the saponification reaction. These problems may contribute to the limitation of sources for biodiesel feedstock, especially in the utilisation of waste vegetable oils and crude oils, since they generally contain water and FFA (Tomasevic and Silver-Marinkovic, 2003). A study by Kusdiana and Saka (2001) also showed that water could have higher negative impact on the transesterification process than the presence of FFA in the triglycerides. Meher *et al.* (2006a) have taken several steps to ensure that transesterification is a water-free process, by preparing fresh solutions for potassium hydroxide and methanol.

2.5.4 Molar Ratio of Alcohol to Oil and Type of Alcohol

The molar ratio between oil and alcohol is one of the main factors that influences the conversion of FAAE. Theoretically, the reaction stoichiometry requires three moles of alcohol per mole of triglycerides to yield three moles of FAME and one mole of glycerine. However, in practice, a higher feed mole ratio is employed in order to shift the esterification reaction to the desired product.

Normally, in industrial processes or laboratory work, a molar ratio of 6:1 is chosen because it gives higher conversion, which is more than 98% by weight (Freedman *et al.*, 1984). Short chain alcohol such as methanol, ethanol and butanol are frequently employed in the production of biodiesel. Differences in the kinetic reaction using different types of alcohol insignificantly affect the final properties of biodiesel. Thus, the selection of alcohol usually depends on the cost and the reaction performance. Methanol is commonly used as a solvent because it has a good reactivity with triglycerides, good physico-chemical properties, low cost and is easily available. However, there is a large explosion risk associated with methanol as a solvent and both methanol and methoxide (liquid and vapours) are categorised as toxic and need to be handled carefully (Leung *et al.*, 2010). On the other hand, ethanol also has several good points as a solvent. It comes from renewable sources and is found to produce FAEE with lower cloud point and pour point values as compared to methanol.

Both of these solvents are immiscible with triglycerides at ambient temperatures, and thus mechanical stirring or ultrasonic agitation usually help to improve the mass transfer and simultaneously contribute to the formation of emulsion. The tendency of ethanolysis to produce a stable emulsion is higher compared to methanolysis, and therefore leads to difficulty in the biodiesel purification process. Hanh *et al.* (2009) investigated the influence of short chain alcohols (1-propanol, 2-propanol, 1-butanol, 2-butanol) on the esterification of FFA under ultrasonic agitation. He found that normal chain alcohol makes the reaction rate higher than the secondary alcohol. This is probably due to the sterical hindrance owned by secondary chain alcohols, limiting their access to the reaction centre, which in turn slows down the reaction rate.

An adequate amount of alcohol is very important to optimise biodiesel production. An insufficient amount of alcohol will lead to a reverse reaction, thus lowering the conversion of FAAE. On the other hand, an excessive amount of alcohol neither increases the conversion of FAAE nor the amount of product obtained. It makes the recovery process more difficult and leads to a stable emulsion between FAME and glycerine. This stable emulsion contributes to difficulties in the separation process and eventually raises the production cost. Research by Miao and Wu (2006) also proved that an excessive amount of alcohol was one of the factors that contributes to complexity of the separation process. They identified that a large amount of alcohol, i.e. 70:1 and 84:1 molar ratio decelerated the separation process between FAME and glycerine in biodiesel production. Higher consumption of alcohol also increases the solubility of glycerine, and as a result it decreases the yield of biodiesel as some glycerine will remain in the FAME phase.

2.5.5 Reaction Time and Temperature

The rate of reaction is significantly influenced by the reaction temperature and time (Freedman *et al.*, 1984). According to Formo (1954), if the transesterification reaction is given enough time, the reaction will proceed to near completion even at room temperature. For the reactions operated in ambient pressure, the selection of temperature is usually dependent on the boiling point of the solvent used. If the

chosen temperature is higher that the boiling point of the solvent, it will evaporate the alcohol and it results in lower ester conversion.

The range of temperature that is commonly used by researchers for biodiesel production is 318-353 K for ambient reaction processes and could go up to 473-573 K under pressurised systems. A higher temperature was also used when supercritical methanol (reaction temperature between 623 to 673 K, pressure between 45-65 MPa) was employed for the biodiesel reaction (Kusdiana and Saka, 2001). Leung and Guo (2006) investigated the effect of temperature on the transesterification process, and the findings showed that any temperatures higher than 323 K had a negative impact on the virgin oils but gained a positive feedback for waste oils with higher viscosities. However, this condition is applicable only when FFA removal pre-treatment step is introduced during the early stage of the process. Higher temperature also favours the saponification process and must be avoided (Ramadhas *et al.*, 2005). The conversion rate of FAAE was usually high in the early stage of the transesterification reaction but slowly declined due to the lesser driving force (Freedman *et al.*, 1984).

2.5.6 Mixing Intensity and Mode of Stirring

Mixing is one of the key factors in optimising the production of biodiesel, as oils and fats are partially miscible in a methanol solution. Once the reactants are totally mixed with each other, an increase in stirring speed is unnecessary. Meher *et al.* (2006b) studied the effect of different speeds in the transesterification of Pongamia pinnata with methanol. The reaction was conducted at three stirring speeds, which was at 180, 360 and 600 revolution per minute (rpm). They identified that 180 rpm did not cause any significant impact on the yield of FAME and led to an incomplete reaction. On the other hand, 360 and 600 rpm stirring speeds show the same yield, i.e. 97% FAME after 3 h of reaction. The mode of stirring also plays an important role in the conversion of FAAE. Sharma and Singh (2008) identified that when a magnetic stirrer was replaced with a mechanical stirrer at the same stirring speed, the yield of biodiesel increased from 85% to 89.5%. This was probably due to the formation of a more complete solution using the rigorous mixing introduced by mechanical stirring.

The same finding was also reported by Sharma and Singh (2008) and Leung and Gou (2006). A low frequency of ultrasonic irradiation can also be used for transesterification (Stavarache *et al.*, 2005). Hanh *et al.* (2009) investigated the transesterification of triolein using different types of stirring conditions i.e. mechanical stirring and ultrasonic agitation. Ultrasonic agitation was found to produce a higher conversion yield than the conventional mechanical stirring. In addition, Colucci *et al.* (2005) found that by using ultrasonic mixing, the reaction rate constants were three to five time higher than those reported in the literature for mechanical agitation. Mootabadi *et al.* (2010) found that ultrasonic-assisted transesterification only required an hour to achieved 95% yield compared to 2-4 h with conventional stirring. Generally, by using ultrasonic agitation, a higher FAAE conversion was achieved in a shorter reaction time. However, research by Georgogianni *et al.* (2009) claimed that ultrasonic agitation is only workable when the reaction occurs under the most favourable conditions (2% w/w NaOH, 7:1 molar ratio of methanol to oil and 333 K). Apart from that, the main obstacle is the price of the ultrasonic equipment, which is far more expensive compared to the conventional agitation method.

2.6 SEPARATION AND PURIFICATION OF BIODIESEL PRODUCT

The separation process is one of the most crucial parts of biodiesel production. The product from the transesterification process is normally composed of FAAE, glycerine, alcohol, catalyst and unreacted glycerides. The properties of the fuel are strongly influence by the purity of the biodiesel product. Normally, the by-product glycerine is separated from FAAE using a simple gravitational settling method and left for a certain period of time. The separation process using the settling or centrifugal tank was considered to be cost effective (Gomes *et al.* 2010). Biodiesel can also be separated by centrifugation and membrane purification. Centrifugation techniques offer a faster separation process compared to traditional settling techniques, however the high operating cost becomes a major concern. Membrane purification is the latest technology in biodiesel separation. It was found to produce a high quality of biodiesel (Dube *et al.*, 2007), besides being energy efficient (Lin *et al.*, 1997).

However, problems such as the saponification reaction and an excess of alcohol could lead to difficulty during the separation process. The saponification reaction creates a stable emulsion between glycerine and biodiesel and this emulsion reduces the product yield. On the other hand, excess alcohol tends to act as a solubiliser and sometimes decelerates the separation process. Usually, alcohol is removed after the separation of glycerine and FAAE. Then, the FAAE is subjected to the purification process to remove impurities such as traces of glycerine, methanol, unreacted triglycerides and other by-products. Biodiesel purification methods can be classified into two categories: wet washing technologies and dry washing technologies.

2.6.1 Wet Washing Technologies

Wet washing technologies have been widely used in biodiesel purification (Van Gerpen, 2005). Water becomes the most popular reagent in wet washing technologies since the by-products i.e. glycerine and methanol are highly soluble in water (Berrios and Skelton, 2008). Wet washing can be conducted in three different ways: (i) washing with deionised water, (ii) washing with acid (i.e. phosphoric acid, sulphuric acid) and water and (iii) washing with an organic solvent and water.

Water washing using deionised water is a conventional method used in biodiesel purification. The process starts by adding a small portion of deionised water to the crude biodiesel, and the solution is stirred gently to avoid the formation of emulsion. This washing cycle is repeated until colourless wash water is obtained, and this indicates that all the impurities have been removed. This method is claimed to be the most effective method and has been used intensively in the biodiesel purification field. On the other hand, Glisic and Skala (2009) used a slightly different approach in the purification stage, whereby hot distilled water was utilised instead of ambient temperature deionised water. By improving this step, they successfully produced biodiesel with 99% purity. The main drawback of having water as the washing agent is the substantial generation of waste liquid effluent, and this factor contributes to a higher cost for treatment and waste disposal. Apart from that, water washing also contributes to a significant loss in product yield, due to the retention of product in the water phase (Canakci and Van Gerpen, 2001).

Water washing techniques have been improved by the addition of acid in water solution. Phosphoric acid, sulphuric acid and hydrochloric acid are the most common acids used in the purification of crude biodiesel. The presence of acid in aqueous solution could reduce the purification steps as it simultaneously neutralises the basic constituent in the product, thus producing a better quality of biodiesel. Faccini *et al.* (2011) and Çayli and Küsefoğlu (2008) used acid water with 10% and 5% (v/v) of phosphoric acid to purify the crude biodiesel, followed by hot water washing. On the other hand, Srivastava and Verma (2008) employed 10% of phosphoric acid aqueous solution in their unique bubble washed techniques to purify crude biodiesel. The product was finally washed with distilled water to remove traces of impurities. Alternatively, Karaosmanoğlu *et al.* (1996) and Atapour and Kariminia (2011) used sulphuric acid (1:1) and hydrochloric acid (0.5%) as a neutralisation agent in their biodiesel purification, followed by hot water washing.

An organic solvent that is commonly used in biodiesel purification is petroleum ether (Ma *et al.*, 1998; Wang *et al.*, 2007 and Soriano *et al.*, 2009). This process is usually followed with hot water washing to remove residual soap and catalyst.

2.6.2 Dry Washing Technologies

Nowadays, the conventional wet separation technologies are being progressively replaced by more promising dry washing techniques. The process has the advantages of being waterless, having strong affinity to polar compounds, being easy to integrate into the existing plant, having a significantly lower purification time, producing no wastewater and improving the biodiesel quality (Atadashi *et al.*, 2011; Atadashi *et al.*, 2011c). Adsorbents that are usually used as the drying agent are ion exchange resins (Rohm and Haas BD10 dry and Purolite PD206), silicates (Magnesol and Trisyl), activated carbon, activated clay and activated fibre.

The dry washing process is usually carried out between room temperature and 338 K (Berrios and Skelton, 2008; Faccini *et al.*, 2011), and the process takes 20-30 min to complete. These adsorbents were selected as drying materials because they have the potential to adsorb the hydrophilic components such as glycerine and water and

simultaneously remove metal and soap (Wall *et al.*, 2011). Purification using a dry washing technique is usually followed by an appropriate separation method to remove used adsorbent from the final product.

Intensive studies have been conducted by several research groups to determine the feasibility of dry washing techniques in the biodiesel separation process. Cooke *et al.* (2003) and Faccini *et al.* (2011) studied the performance of magnesol and ion exchange resins to neutralise the impurities in crude biodiesel. They found that magnesol gives better adsorption properties compared to ion exchange resins. This was because this material has a strong affinity for polar compounds, therefore all the impurities (e.g. metal contaminant, glycerine, excess methanol and soap) were easily removed from the product. On the other hand, ion exchange resins have the capability of reducing the glycerine content to a value of 0.01% and effectively remove water, salts and soap from the product. However, the removal of methanol from the product was insignificant (Berrios and Skelton, 2008). Predojević (2008) studied the comparison between dry and wet separation methods in the biodiesel purification process: (i) washing with silica gel, (ii) with 5% phosphoric acid and (iii) with hot distilled water. The results showed that silica gel and phosphoric acid treatments gave the highest yield, at approximately 92%.

2.7 CONCLUSIONS

The production of biodiesel using renewable sources has become the most promising alternative nowadays with the depletion in petroleum resources. It is expected that the demand for biodiesel as fuel will significantly increase in the future. At present, the dominant feedstock for biodiesel production is edible vegetable oil, with different countries using different types of vegetable oils. However, the increasing world population increases the demand for both food and fuels and significantly contributes to the food versus fuel issues. Therefore, the non-edible feedstocks such as a non-edible vegetable oil, animal fats and waste oils are found to be effective feedstocks replacements for reducing the cost of biodiesel. These oils (non-edible feedstocks) contain significant amount of FFA and cannot be directly used in a base catalysed transesterification reaction because FFA could react with the

base catalyst to form soap. The saponification process forms a stable emulsion and leads to difficulties in the process of separation and reutilisation of the catalyst. Several studies on the utilisation of waste oils as raw material have been conducted and it has been found that high yield is achieved using a two-step synthesis of biodiesel. The first stage, the pre-treatment step (esterification process) is needed to reduce the amount of FFA in the feedstock before being subjected to a base catalysed transesterification reaction.

Many biodiesel studies have been conducted using the conventional homogeneous process. However, homogeneous catalysts create lots of challenges during the reaction process (e.g. formation of soap, high level of acidity/basicity in the product, generation of a substantial amount of wastewater, unable to reutilise the catalyst). Therefore, interest has been diverted to the utilisation of heterogeneous catalysts as a promising alternative in developing better biodiesel fuel. The use of heterogeneous catalysts has been proven to simplify the production and purification processes because they can be easily separated from the reaction mixture. This type of catalyst allows multiple usage of the catalyst through regeneration, resulting in a reduction in waste and a reduction in the environmental impact.

However, heterogeneous catalysis reaction still gives a number of drawbacks. Heterogeneous catalysts were found to have slower reaction rates, leaching and poisoning of catalysts and the reaction requires extreme operating conditions such as higher reaction temperature and longer reaction time. The issue of stability for longer catalyst life was also found to be the main problem in most of the heterogeneous catalysts. Therefore, there are still plenty of scopes for improvement, especially on the selection of suitable and sustainable catalyst for low quality biodiesel feedstocks.

This chapter has summarised all the aspects involved in biodiesel production, from the historical background, different types of raw materials, the reaction mechanisms, and parameters that affect the process performance and the separation and purification processes. For this research work, UCO was selected as the feedstock for the biodiesel production and concentrated effort has been put into the development of

a two-stage esterification-transesterification process for biodiesel production. Several types of heterogeneous catalyst were investigated in this two-stage reaction. Within the next chapter (Chapter 3), material and methods involved in this research work were presented and elaborated in detail.

3 MATERIALS AND METHODS

3.1 INTRODUCTION

This chapter represents the materials and experimental methods used in this research work. This chapter is divided into six main sections: materials, catalyst preparation and characterisation, development of analytical technique, physical and chemical analysis of used cooking oil (UCO), esterification reaction, transesterification reaction and separation and purification of biodiesel.

3.2 MATERIALS

Ion exchange resin catalysts (Purolite CT-122, Purolite CT-169, Purolite CT-175, Purolite CT-275, Purolite D5081 and Purolite D5082) were supplied by Purolite International Limited, UK, Amberlyst 15 was purchased from Sigma Aldrich, UK, and Diaion PA306s was supplied by Mitsubishi Chemicals, Japan. All resins were supplied in wet form. The UCO was supplied by Greenfuel Oil Company Limited, UK.

Methanol (>99.5% purity), sodium hydroxide (98+%) pellets, 0.1 M standardised solution acid hydrochloric, 0.1 M standardised solution sodium hydroxide, 0.1 M standardised solution sodium hydroxide in 2-propanol, toulene (99.5%), 2-propanol (99+%), glacial acetic acid (99.85%), chloroform (>99%), methyl linoleate (>99%), sodium chloride, sulphuric acid (95-98%), phenolphthalein, iso-octane (>99.5) and acetonitrile (>99.8%) were purchased from Fisher Scientific, UK and caesium carbonate, potassium bromide (KBr), 12-phosphotungstic acid hydrate ($H_3PW_{12}O_{40}.xH_2O$), *p*-naphtholbenzein, *n*-hexane, methyl heptadecanoate (>99%), methyl linolenate (>99%), methyl oleate (>99%), methyl palmitate (>99%) and methyl stearate (>99%) were purchased from Sigma Aldrich, UK. Other chemicals used were analytical reagent grade.

3.3 CATALYST PREPARATION AND CHARACTERISATION

3.3.1 Catalyst Preparation

3.3.1.1 Cation Exchange Resin

Amberlyst 15, Purolite CT-122, Purolite CT-169, Purolite CT-175, Purolite CT-275, Purolite D5081 and Purolite D5082 are classified as strong acidic cation exchange resins that are made from styrene-divinylbenzene copolymer backbone with sulfonic acid as a functional group. All of these resins were supplied in wet form. These resins were pre-treated before being used as the reaction catalysts. According to Bianchi *et al.* (2009), dry catalysts do not require any pre-treatment as the active sites are already free and available on the surface of the resin and inside the pores, whereas the wet catalysts are pre-conditioned with solvent, rinsed and dried in a vacuum oven (373 K). The ion exchange resin pre-treatment method used in this research work is a common method used by most of the researchers for the preparation of ion exchange resins (Klepáčová *et al.*, 2005; Bianchi *et al.*, 2009; Park *et al.*, 2010; Tesser *et al.*, 2010; Kouzu *et al.*, 2011). All wet resins were immersed in methanol overnight and pre-treated with the methanol in ultrasonic bath. The process takes about 8-10 cycles of rinsing to ensure that all contaminants were removed (i.e. the colour of solvent changed from light brown to colourless). During this washing process, the conductivity of the residual solution was recorded and the process continued until the conductivity of the residual solution was approximately the same with the solvent (i.e. conductivity of methanol: 2.3 $\mu S\ m^{-1}$). Finally, the resins were dried in a vacuum oven at 373 K for 6 h to remove any water and methanol. The dried catalyst was kept in a sealed bottle prior to use.

3.3.1.2 Anion Exchange Resin

Anion exchange resin, Diaion PA306s is a strong basic anion exchange resin made from a styrene-divinylbenzene copolymer backbone with quaternary amine as functional group. This resin was supplied in the chloride form. The anion exchange resin was mixed with 1 M of sodium hydroxide (NaOH) to displace the chloride ions to hydroxyl ions. Mixing was done for 72 h with the replacement of NaOH solution every 24 h. After that, the resin was washed with reverse osmosis (RO) water. During this washing process, the conductivity of the residual solution was recorded

and the process continued until the conductivity of the residual solution was approximately the same as the RO water (i.e. 2.2 μS m^{-1}). The catalyst was then rinsed with methanol, filtered and decanted and left overnight in a closed environment. It was not possible to store the catalyst any longer or the catalyst would lose activity.

3.3.1.3 Heteropolyacids Catalyst

Commercially available 12-tungstophosphoric acid ($H_3PW_{12}O_{40}.xH_2O$) and caesium carbonate (Cs_2CO_3) were used to prepare the Cs-supported heteropolyacids catalyst ($Cs_{2.5}H_{0.5}PW_{12}O_{40}$). The thermogravimetrical analysis (DSC-TGA) was performed to measure the water content in the commercial phosphotungstic acid (HPW). The experiments were conducted using 15–20 mg samples with a heating rate of 10 K/min. The studied temperatures was in the range of 313–1073 K. From the analysis, the content of water in commercial HPW corresponding to $H_3PW_{12}O_{40}.26H_2O$ was determined. The preparation of catalyst is listed step-by-step below:

- 0.1 M of Cs_2CO_3 aqueous solution and 0.08 M of 12-tungstophosphoric acid hydrate aqueous solution were prepared.
- 20 cm^3 of 0.1 M aqueous solution of Cs_2CO_3 was added dropwise to 20 cm^3 of 0.08 M aqueous solution of 12-tungstophosphoric acid hydrate at room temperature, with vigorous stirring.
- The resultant milky suspensions were aged at room temperature overnight, leading to a formation of very fine particles.
- The suspension was dried by slow evaporation at 323 K. The resulting solid was ground into powder.
- The dried catalyst was kept in a sealed bottle. Prior to use, the sample was dried in an oven at 383 K to remove moisture.

Calcination was also carried out on a portion of prepared Cs-supported heteropolyacids catalyst to investigate the effect of calcination on triglycerides conversion. The calcination process was conducted in a furnace at 1073 K for 8 h.

Both catalysts are abbreviated with the reference to their processes; [i.e. $Cs_{2.5}H_{0.5}PW_{12}O_{40}$ is for non-calcined Cs-supported heteropolyacids catalyst and $Cs_{2.5}H_{0.5}PW_{12}O_{40}$ (calcined) is for calcined Cs-supported heteropolyacids catalyst].

3.3.2 Catalyst Characterisation

3.3.2.1 Field Emission Gun-Scanning Electron Microscopy

A Carl Zeiss (Leo) 1530 VP) field emission gun-scanning electron microscope (FEG-SEM) was used to study the morphology of the catalysts. The FEG-SEM analysis was carried out at room temperature and used accelerating voltages between 1 kV to 30 kV. The samples were mounted on a metal stub with carbon conductive pad and the silver metal was placed at both sides of the samples, to act as a conductor. The samples were coated under vacuum with gold in an argon atmosphere prior to observation. For each catalyst, the results of two different magnifications are presented.

3.3.2.2 Elemental Analysis

Elemental analysis for carbon (C), hydrogen (H), nitrogen (N) and sulphur (S) was performed using Thermoquest EA1110 Elemental Analyser. It works by combusting the sample in pure oxygen with tin as a catalyst. Any sulphur, phosphorous or halogens were removed and excess oxygen was reduced, leaving CO_2, H_2O and N_2 as the combustion products. The resultant gases were dried using a magnesium perchlorate trap before being separated on a packed GC column and detected using a thermal conductivity detector. The sulphur determination was carried out separately using an oxygen flask combustion analysis, followed by a titration. The samples were combusted into oxygen flasks containing water and a few drops of hydrogen peroxide. They were left to stand for 40 min before two indicators were added to the solution. The solution was titrated with barium perchlorate until a permanent hint of red was reached. All the results are reported in weight percentage of carbon, hydrogen, nitrogen and sulphur. Analyses were done in duplicate and the average values were reported.

3.3.2.3 Fourier Transform-Infra Red Measurement

The Fourier Transform-Infra Red (FT-IR) spectroscopy analysis was carried out to determine the functional groups in the catalysts. The spectra were recorded on a FT-IR 8400S SHIMADZU analyser. A potassium bromide (KBr) pellet was used to determine the background signal. All the catalysts were grounded into powder and mixed with KBr powder to form a pellet before being inserted in the sample compartment to undergo 64 scans. The spectral range (wavenumbers) for the spectrophotometer was set at 4000 to 600 cm^{-1} and the final output was in % transmittance.

3.3.2.4 True Density Measurement

The true density (ρ_t) was measured using a Micromeritics Helium Pycnometer 1305. Samples with a known mass (m_c) were placed into the pycnometer cell. A constant flow of helium gas was introduced into the cell several times to ensure that void spaces between the particles were filled by helium gas. The actual volume of sample (v) was calculated based on the known parameters, cell volume, expansion medium volume and the charge pressure before and after expansion. Finally, the true density of particles was determined using the standard formula: true density, $\rho_t = \frac{m_c}{V}$. The measurements were made in triplicate and the average values were reported. The reproducibility error was found to be less than 1%.

3.3.2.5 Particle Size Distribution Measurement

The particle size distribution (PSD) measurment was performed using two different techniques depending on the physical appearance of the catalyst. For powder-type/small beads catalysts such as Cs-supported heteropolyacids and Diaion PA306s catalysts, the Malvern Instrument Mastersizer was used to measure the PSD. For larger particle beads such as Purolite ion exchange resins catalysts, the PSD were determined using a standard sieve measurement. The Malvern Mastersizer takes measurement based on laser diffraction described by the Fraunhofer approximation and Mie theory. In this method, the wet dispersion analysis was selected to measure the distribution pattern of the particles. The equipment operating parameters were set to record the background measurement for 60 s followed by the sample

measurement for 60 s. The samples were then introduced into the dispersion module with water as the solvent and a total of two measurement cycles were carried out for each sample and the average was taken to give the final result. For the determination of PSD using sieve measurement, a set of standard sized sieves was selected, cleaned, weighed and arranged in decreasing sieve sizes. A known weight of sample was poured into the top sieve and the sieve tower was placed in a mechanical shaker. The sample was sieved through the sieves and upon completion, each sieve was weighed. From this information, the PSD of each catalyst was determined. The measurements were made in duplicate to ensure the reproducibility of the results.

3.3.2.6 Surface Area, Total Pore Volume and Average Pore Diameter Measurement

Surface area, pore volume and average pore diameter were determined from adsorption isotherms using a Micromeritics ASAP 2020 surface analyser. The samples were degassed using two-stage temperature ramping under a vacuum of <10 mm Hg, followed by sample analysis at 77 K using nitrogen gas. The Brunauer-Emmett-Teller (BET) method was used to calculate the surface area, average pore diameter and total pore volume.

3.3.2.7 Sodium Capacity Determination

Sodium capacity determination experiments were performed to determine the exchange capacity of ion exchange resin catalysts. This experiment was conducted using a conventional titration method. The analysis took place in a 50 mL Erlenmeyer flask with the pre-determined mass of catalyst (ca. 0.5 g) in contact with 50 mL of 0.1 M of volumetric standard aqueous NaOH. The flasks were sealed with parafilm and shaken for 72 h in an orbital shaker. After that, the solution was filtered and 5 mL aliquots were back titrated with 0.1 M volumetric standard hydrochloric acid (HCl) using methyl red as an indicator. The concentration of NaOH, C_{NaOH} in the conical flasks after the solution reached equilibrium was determined by using the following Equation (3.1):

$$C_{NaOH\ final} = \frac{C_{HCl} \times V_{HCl}}{V_{NaOH}} \tag{3.1}$$

where C_{HCl} is concentration of HCl (0.1 M), V_{HCl} and V_{NaOH} are the volume of HCl and NaOH used during the titration process. The concentration of NaOH adsorbed was calculated using the following Equation (3.2):

$$C_{NaOH\ adsorbed} = C_{NaOH\ initial} - C_{NaOH\ final} \quad (3.2)$$

where $C_{NaOH\ initial}$ is the initial concentration of sodium hydroxide (0.1 M) and $C_{NaOH\ final}$ is the final concentration of NaOH, as calculated in Equation 3.1. The sodium capacity (q_{NaOH}) was calculated using the following Equation (3.3):

$$q_{NaOH} = \frac{V_{initial} \times C_{NaOH\ adsorbed}}{m_C} \quad (3.3)$$

where $V_{initial}$ and m_C are the initial volume on NaOH (50 mL) and mass of catalyst (ca. 0.5g) introduced into the conical flask, respectively.

3.4 DEVELOPMENT OF ANALYTICAL METHOD

3.4.1 Preparation of Standard Solutions

The preparation of standard solutions was carried out to establish calibration curves for each fatty acid presence in the UCO mixture. Each of the fatty acid methyl ester (FAME) standards were dissolved in *n*-hexane and stored separately in 15 mL amber bottles. For each standard, five different concentrations were prepared and the concentrations were approximately between 1 and 10 g L^{-1}.

3.4.2 Calibration Curve for Individual Standards

The internal standard method was chosen as the quantification method to determine the response factor and concentration of each component present in the sample. Methyl heptadecanoate was chosen as an internal standard. 9 sets of standard FAME mixtures at different concentrations were prepared. In each sample mixture, 5000 ppm of methyl heptadecanoate was added and this amount was kept constant for all sample mixtures. The mixtures were deposited into 2 mL amber vial and injected into gas chromatography-mass spectrometry (GC-MS). Each sample

preparation and subsequent injection and calculation for each concentration was performed in triplicate to verify the consistency, reliability and reproducibility of the response factor. The peak areas of the analyte and internal standard were measured and calculated as the area ratio between the analyte and the internal standard (see Equation 3.4). The area ratio was plotted against the concentration ratio (see Equation 3.5). The resulted response factors were obtained from the slope of the graph and verified using Equation 3.6.

$$\text{Area ratio of } i^{th} \text{ component, } AR_i = \frac{\text{Area of the } i^{th} \text{ component, } A_i}{\text{Area of the internal standard, } A_{is}} \quad (3.4)$$

$$Concentration \text{ ratio of the } i^{th} \text{ component, } CR_i = \frac{\text{Concentration of the } i^{th} \text{ component, } C_i}{\text{Concentration of the internal standard, } C_{is}} \quad (3.5)$$

$$Response \text{ factor of the } i^{th} \text{ component, } RF_i = \frac{\text{Area ratio of the } i^{th} \text{ component, } AR_i}{\text{Concentration ratio of the } i^{th} \text{ component, } CR_i} \quad (3.6)$$

The resulting response factors were used to determine the composition of fatty acids in the sample. Equation 3.6 was re-arranged to calculate the unknown sample concentration as shown in Equation 3.7:

$$\text{Concentration of the } i^{th} \text{ component of } j^{th} \text{ sample, } C_{ij} = \frac{\text{Area ratio of the } i^{th} \text{ component of } j^{th} \text{ sample, } AR_{ij} \times C_{is}}{\text{Response factor(RF) of the } i^{th} \text{ component, } RF_i} \quad (3.7)$$

3.4.3 Instrumentation and Data Acquisition

The FAME content was assayed using a Hewlett Packard GC-MS model HP-6890 and HP5973 (mass selective detector). The GC-MS was also equipped with a flame ionisation detector (FID). A DB-WAX (J & W Scientific) capillary column of length 30 m and internal diameter of 0.25 x 10^{-3} m packed with polyethylene glycol

(0.25 μm film thickness) was used. Helium was used as a carrier gas at a constant flow rate of 1.1 mL min^{-1}. The temperature of both the injector and the detector was set at 523 K. The injection volume of 1 μL and a split ratio of 10:1 were used as part of the GC-MS analysis method. A ramp method was used to separate all the components in the sample mixture. In the ramp method, the initial oven temperature was held at 343 K and the sample was injected by an auto-injector. The oven temperature was held at 343 K for 2 min after the sample injection. The oven temperature was then ramped from 343 – 483 K at a rate of 40 K min^{-1} and from 483 – 503 K at a rate of 7 K min^{-1}. The oven temperature was held at 503 K for 11 min to remove any remaining traces of the sample. The total run time for each sample was approximately 19.5 min. After the sample run was over, the oven temperature was cooled back to 343 K so that the subsequent run could be started.

3.4.4 Preparation of Derivatised Sample of the UCO

This experimental work was developed in order to determine and quantify the composition of fatty acid and FAME in the UCO. The sample was prepared using British Standard Institution (BSI) standard method, EN ISO 12966-2:2011. The derivatisation process begins by weighing 50 mg of the UCO in a 10 mL ground-glass necked one-mark volumetric flask, followed by the addition of 0.2 mol L^{-1} sodium methoxide in methanol. The solution was boiled until the solution became clear. Two drops of phenolphthalein were added to the solution, followed by the addition of sufficient amount of 1 mol L^{-1} sulphuric acid in methanol solution until the solution becomes colourless and 0.2 mL sulphuric acid was added. The prepared solution was boiled for further five min followed by the addition of 4 mL sodium chloride solution and 1 mL of *iso*-octane. The solution was mixed vigorously and allowed to settle until the two phases were separated. The upper layer, the clear supernatant was analysed by GC-MS.

3.5 PHYSICAL AND CHEMICAL CHARACTERISATION OF USED COOKING OIL (UCO)

3.5.1 Determination of Acid Value and Free Fatty Acids (FFA) Content

The amount of acid in the UCO was determined using ASTM D974 (ASTM Standard D974-08), which was specifically used to determine the acidic or basic constituents in highly coloured fats and oils. The determination of acid or base number was carried out by dissolving approximately 2 g of sample in a mixture of 100:99:1 ratio of toluene, 2-propanol and water to form a single phase solution. The resulting solution was titrated at room temperature with 0.1 M standardised solution of potassium hydroxide in 2-propanol and the end point was detected by a change in the colour of *p*-naphtholbenzein indicator from orange to green.

The acid and the free fatty acids (FFA) values were calculated using Equations 3.8 and 3.9. The value of 27.81 in Equation 3.9 was obtained from the average molecular mass of fatty acids divided by ten. For this research work, the average molecular mass of fatty acids is 278.11 g mol^{-1}. If the molecular mass of fatty acids remains unknown, this value is referred to as one-tenth of the molecular mass of oleic acid (Özbay *et al.*, 2008; Bianchi *et al.*, 2009). If the molecular mass of oleic acid had been used, and it would have resulted in small errors. However, these errors were found to be within the acceptable level. The percentage of FFA was found to be approximately one-half of the acid value as a mere coincidence because the molecular weight of KOH (56.1) is approximately one-fifth of the molecular weight of oleic acid.

$$\text{Acid value, mg KOH/g sample} = \frac{[(A-B) \times M \times 56.1]}{W} \quad (3.8)$$

$$\text{FFA content, \%} = \frac{[(A-B) \times M \times 27.81]}{W} \quad (3.9)$$

where, A and B are KOH solution required for the titration of the sample and blank, mL; M is the molarity of KOH solution, M and W is the sample used, g

3.5.2 Determination of Water Content

Water content was determined by Karl Fischer titration method using a Mitsubishi Moisture Meter (CA-20) as the analytical instrument. This titration was carried out using HYDRANAL – Coulomat A as the anode solution and HYDRANAL – Coulomat CG as the cathode solution. The equipment was calibrated to determine the reliability and reproducibility of the results. Water was selected as the standard and sampling was carried out at room temperature. 100 mg of standard water was introduced into the titration cell by means of a metal syringe needle and the results were generated automatically by the moisture meter. After a good calibration had been obtained, the same procedure was carried out for the samples of interest. The results are reported as a percentage of water in the test samples.

3.5.3 Determination of Triglycerides, Diglycerides and Mononglycerides Composition in the UCO

The determination of monoglycerides, diglycerides and triglycerides in the UCO were carried out using the method established by Haigh *et al.* (2012). The liquid chromatography-mass spectrometry (LC-MS) was carried out using a Waters Acquity ultra performance liquid chromatography (UPLC) system interfaced to a Waters Synapt HDMS quadrupole time-of-flight (TOF) mass spectrometer, using positive ion. A Phenomenex Kinetix C18 UPLC column (150 mm x 2.1 mm x 2.1 μm) was used for the separation. The chromatography used a binary method with acetonitrile as solvent A and 2-propanol as solvent B. The separation was carried out using a binary gradient with a flow rate of 0.15 ml min^{-1} starting with 90% acetonitrile and 10% 2-propanol changing to 30% acetonitrile in 20 min. Quantification was based on the external calibration standard solutions of triolein, diolein and monoolein.

3.5.4 Determination of Bulk Density

Density of UCO was determined using pycnometer. It is one of the precise methods to measure the density of working liquids. A pycnometer is a glass bottle with a close-fitting glass stopper with a capillary hole through it. The purpose of having

capillary hole inside the stopper is to remove the spare liquid after closing the pycnometer, giving a high accuracy of the liquid's volume measurement. Water has been used as the reference material to determine the density of the UCO. The pycnometer was filled with distilled water. The volume of water that filled the pycnometer was calculated using Equation 3.10:

$$\text{Volume of water}, V = \frac{m_{H_2O}}{\rho_{H_2O}} \quad (3.10)$$

where m_{H_2O} is the experimentally determined mass of water. The procedure was repeated for the UCO and the mass of sample was experimental determined. Volume of sample in the pycnometer was assumed to be the same as the volume of the water in the pycnometer. The density of sample was calculated using the following Equation (3.11):

$$\text{Density of liquid}, \rho_L = \frac{m_L}{(m_{H_2O} \times \rho_{H_2O})} \quad (3.11)$$

where,

ρ_L = density of liquid sample (UCO), kg m^{-3}

ρ_{H_2O} = density of water, kg m^{-3}

m_{H_2O} = mass of water, kg

m_L = mass of liquid sample (UCO), kg

3.6 ESTERIFICATION REACTION AND CATALYST REUSABILITY STUDY

3.6.1 Esterification Reaction

The esterification process was carried out in a four-neck 1000 mL cylindrical jacketed-glass reactor. The reactor was equipped with a mechanical stirrer, sampling port and a reflux condenser to prevent loss of methanol due to vaporisation. Heating of the reactor contents was achieved by circulating the water from a water bath and through the reactor jacket. A thermocouple was used to monitor the temperature of the reaction mixtures. Figure 3.1 shows the experimental set-up for the esterification

of FFA while Figure 3.2 shows the reaction scheme for esterification process, respectively. A specified amount of UCO and methanol was added to the reactor and the stirring and heating of the reaction mixtures were started. When the reaction mixtures reached the desired temperature, a known amount of catalyst was added and this time was taken as the zero time for the reaction. The samples were taken periodically from the reactor for FFA analysis. The conversion of FFA was calculated using the following Equation (3.12):

$$\text{Conversion of FFA, } X_F = \frac{C_{F0} - C_F}{C_{F0}} \quad (3.12)$$

where C_{F0} is the initial concentration of FFA of the mixture (i.e. at time, t = 0) and C_F is the concentration of FFA at any time 't'.

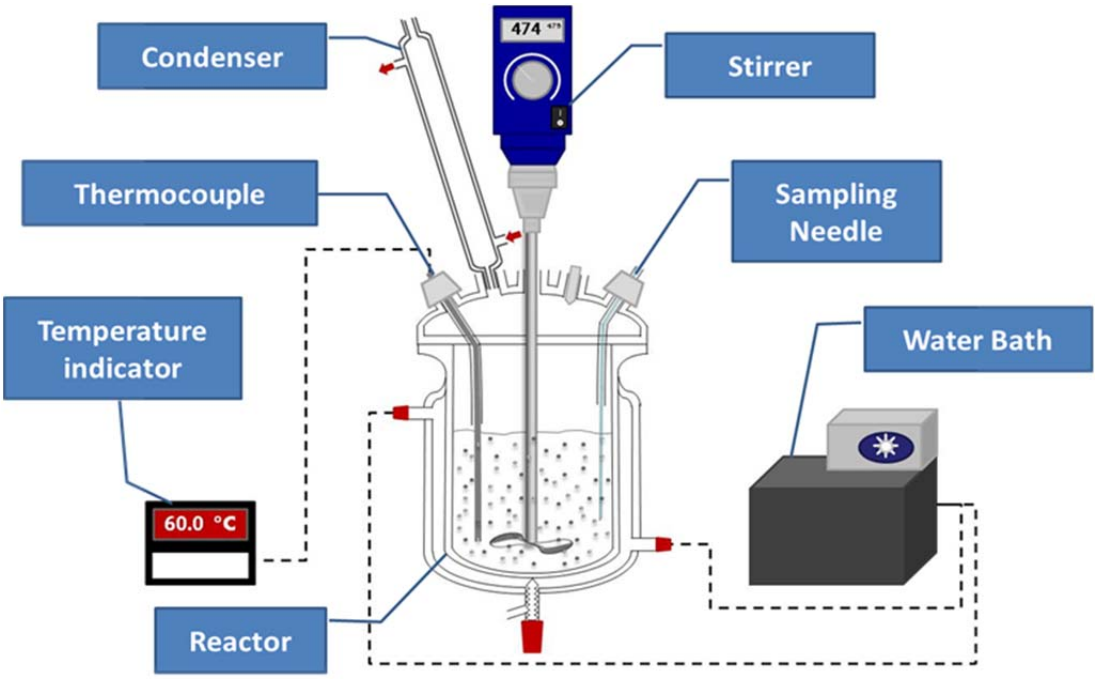

Figure 3.1. Experimental set-up for the esterification of FFA in the UCO using ion exchange resins.

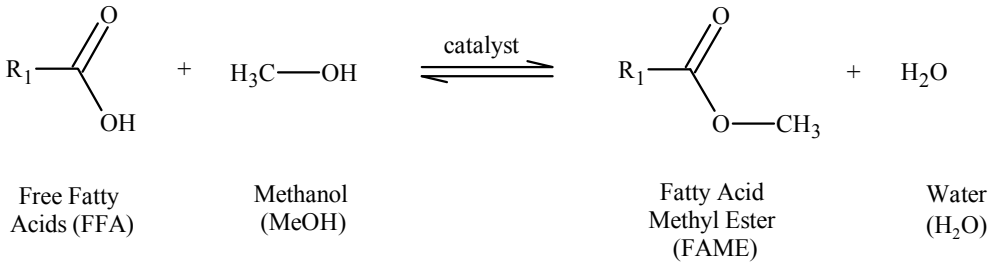

Figure 3.2. Reaction scheme for the esterification process: Conversion of FFA to FAME. R_1 represent the fatty acids group.

Once the experiment was over, the reaction mixture was allowed to cool to room temperature. The reaction mixture was then transferred to a separating funnel and allowed to settle overnight to form two layers; the top layer consisted of excess methanol, water (by-product), traces of FAME and unreacted UCO whereas the bottom layer consisted of unreacted UCO together with traces of methanol, glycerine, FAME and the catalyst. The bottom layer was withdrawn from the separating funnel together with the catalyst and the retained catalyst was washed, dried and stored for further experimental work.

For the esterification reaction, batch kinetic studies on the elimination of mass transfer resistances and the effect of catalyst loading, reaction temperature and feed mole ratio of methanol to UCO on the conversion of FFA were investigated. Pre-treated oil with the optimum FFA conversion was selected for transesterification and prior to transesterification, methanol was removed from the esterified UCO using a rotary evaporator. In terms of the reproducibility of experimental data, selected experiments were repeated 3 times and it was found that the differences were 1-2%. Therefore, it was assumed that a similar error applies to all results. In addition, a blank run without any catalyst was performed and there was no conversion of FFA after 8 h of reaction time. Therefore, it was concluded that the esterification of FFA was only possible in the presence of a catalyst.

3.6.2 Reusability Study of Esterification Catalyst

A detailed reusability study of the esterification catalyst was conducted to determine the catalyst life time. The catalyst that performed best during batch kinetic studies as

compared to other catalysts was chosen for the reusability study. The first phase of this work was to investigate the effect of reusing the same batch of a catalyst for a number of cycles on the conversion of FFA. For this purpose, used catalyst was washed with methanol with the aid of an ultrasonic bath until there were no traces of UCO and a colourless solution was obtained. During this washing process, the conductivity of the residual solution was recorded and the process continues until the conductivity of the residual solution was approximately the same (conductivity of methanol: 2.3 $\mu S\ m^{-1}$). The washed catalyst was filtered and dried in a vacuum oven at 373 K for 6 h. The reusability study was carried out under the optimum process conditions obtained from the batch kinetic studies.

In the second phase of this work, an investigation into the homogeneous contribution was carried out to establish if sulphonic acid groups were leached during the reaction process. A process flow diagram for the reusability study is shown in Figure 3.3. It was performed by reacting pure methanol with unused pre-treated catalyst for 8 h at the optimum reaction temperature and stirring speed. After the experiment was completed, the catalyst was filtered and the solution was used in the subsequent reaction with UCO, in the absence of catalyst. This is referred to as the first cycle of homogeneous contribution study. The filtered catalyst was dried in the vacuum oven at 373 K for 6 h and this catalyst was then used for an experiment with pure methanol and UCO to monitor the conversion trend as a result of the catalyst being treated with methanol. The reaction was carried out under the optimum process conditions and the result was plotted as the first cycle of methanol treated catalyst study.

The spent catalyst from the previous methanol treated catalyst experiment was washed thoroughly with methanol until no evidence of UCO contamination (with the aid of ultrasonic irradiation) was found. The catalyst was then filtered and dried in a vacuum oven at 373 K for 6 h. The experimental work proceeded to the second homogeneous cycle, where the reaction took place between pure methanol and the used catalyst. The catalyst was the same catalyst used in the first cycle of homogeneous contribution study and the first cycle of methanol treated catalyst

study. After the experiment was completed, the catalyst was filtered and the solution was used in the subsequent reaction with UCO, in the absence of catalyst. The reaction was carried out using the optimum reaction conditions. The FFA conversion was monitored and the result was plotted as the second cycle of homogeneous contribution study. The used catalyst obtained from the second cycle of homogeneous contribution study was dried in a vacuum oven at 373 K for 6 h, introduced to UCO and pure methanol and reacted at optimum process conditions to produce the second cycle of methanol treated catalyst study.

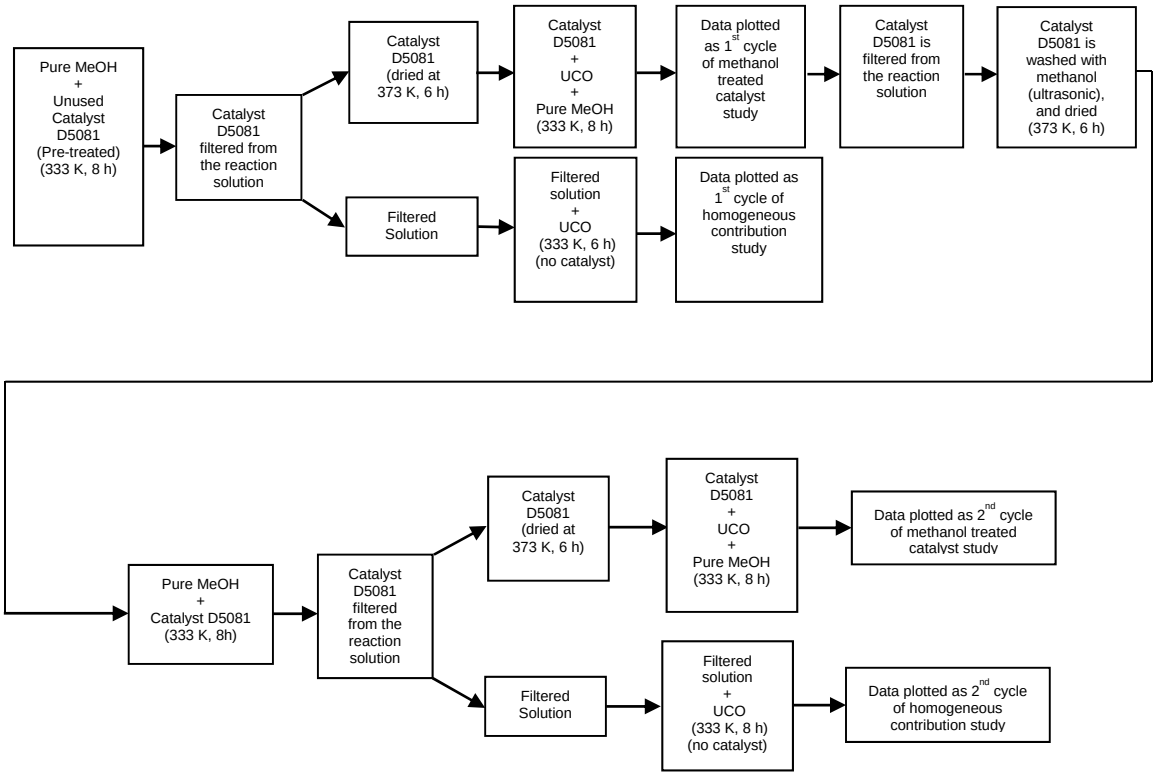

Figure 3.3. Process flow diagram for catalyst reusability study.

3.7 TRANSESTERIFICATION REACTION AND REUSABILITY STUDY

3.7.1 Transesterification Reaction

The feedstock used for the transesterification process was the pre-treated used cooking oil (P-UCO) from the esterification reaction. The experimental set-up and procedure for transesterification was similar to the esterification, except that the size for transesterification reactor was smaller i.e. 250 mL. Figure 3.4 shows the reaction scheme of the transesterification process.

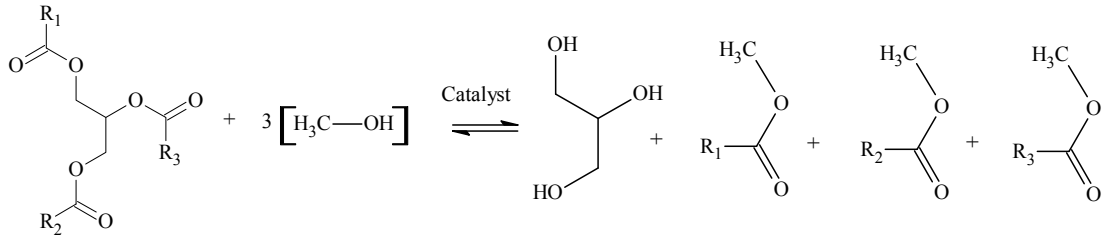

Figure 3.4. A reaction scheme of the transesterification process. R_1, R_2 and R_3 represent the fatty acids group attached to the backbone of triglycerides.

Samples were taken periodically from the reactor for FAME analysis using GC-MS. The results were used to determine triglycerides conversion. The percent conversion of triglycerides was calculated using the following Equation (3.13):

$$\% \text{ Conversion of triglycerides, } X_T = \frac{C_{T0} - C_T}{C_{T0}} \times 100 \quad (3.13)$$

where C_{T0} is the initial concentration of triglycerides in the reaction mixture and C_T is the concentration of triglycerides at any time '*t*'.

Once the experiment was completed, the reaction mixture was allowed to cool to room temperature. The reaction mixture was separated from the spent catalyst, transferred to a separating funnel and allowed to settle overnight. The used catalyst was stored for further experimental work. Batch kinetic studies on the elimination of mass transfer resistances and the effect of catalyst loading, reaction temperature and feed mole ratio of methanol to P-UCO on the conversion of triglycerides were studied. In terms of the reproducibility of experimental data, selected experiments were repeated 3 times and it was found that there was ±2% difference in the results. Therefore, it was assumed that a similar error applies to all results.

3.7.2 Reusability Study of Transesterification Catalyst

A reusability study of the transesterification catalyst was conducted to determine the catalyst life time. The catalyst that performed the best during batch kinetic studies was chosen for the reusability study. This investigation was carried out by studying

the effect of reusing the same batch of catalyst on the conversion of triglycerides. The used catalyst was prepared by three regeneration steps as follows:

1) The used catalyst was washed with glacial acetic acid in methanol to displace the fatty acid ions with acetate ions. Two levels of acid concentrations (17.5 M and 1 M) were selected to investigate the effect of acid concentration on the properties of the washed catalyst. This displacement step was conducted with the aid of an ultrasonic bath until there were no traces of P-UCO and a colourless solution was obtained. The catalyst was then washed using RO water to remove excess of acetic acid solution. During this washing process, the conductivity of the residual solution was recorded and the process continued until the conductivity of the residual solution was approximately the same as the conductivity of the RO water, 2.2 $\mu S\ m^{-1}$.
2) The catalyst was mixed with 1 M NaOH to displace the acetate ions with hydroxyl ions. The mixing was carried out for 72 h using a mechanical stirrer, with replacement of NaOH solution every 24 h. The catalyst was washed with RO water to remove excess NaOH solution. The same conductivity test routine was carried out until the conductivity of the residual solution was approximately the same as the conductivity of the RO water, 2.2 $\mu S\ m^{-1}$.
3) The catalyst was rinsed with methanol and prior to use, then filtered and decanted overnight in a closed environment.

3.8 SEPARATION AND PURIFICATION OF BIODIESEL

Two methods have been selected to purify biodiesel. The first method is wet purification and the second method is dry purification. The first method uses water as the washing agent. For the second method, ion exchange resin Purolite PD206 has been selected as the adsorbent. Purolite PD206 was chosen because this type of adsorbent has a high adsorbent capacity, is easily regenerated and is cost effective for biodiesel purification. The detailed procedure for each method is summarised in the following section.

3.8.1 Wet Purification Process

- The reaction mixture was separated from the spent catalyst, transferred to a separating funnel and allowed to settle overnight (gravitational settling).
- The FAME-rich phase was withdrawn from the separating funnel and introduced to a rotary evaporator to remove traces of methanol. The resulting solution was referred to as unpurified biodiesel.
- The unpurified biodiesel was heated and stirred at 150 rpm until the temperature reached 328 K.
- The unpurified biodiesel was washed thoroughly with 20% of acid water (one-fifth of the total volume of unpurified biodiesel produced from the reaction). The acid water was prepared by adding 2% (v/v) phosphoric acid (H_3PO_4) in distilled water. A constant stirring speed (150 rpm) was used and the mixture was maintained at 328 K for 5 min.
- The mixture was transferred to a separating funnel and two layers were formed: the upper layer consists of FAME and the bottom layer consists of waste water.
- The bottom layer was removed and the washing steps were repeated using 10% (v/v) of hot RO water. The solution was maintained at 328 K for 5 min, transferred to a separatory funnel and two layers were formed, FAME (top) and waste water (bottom). The bottom layer was removed and this step was repeated 3 to 5 times until the resulting waste water was clear.
- The purified biodiesel was separated from the waste water and stored for further analysis.

3.8.2 Dry Purification Process

- The reaction mixture was separated from the spent catalyst, transferred to a separating funnel and allowed to settle overnight (gravitational settling).
- The FAME-rich phase was withdrawn from the separating funnel and introduced to a rotary evaporator to remove traces of methanol. The resulting solution was referred to as unpurified biodiesel.
- The unpurified biodiesel was heated and stirred at 150 rpm until the temperature reached to 338 K.

- 5% (w/w) relative to the mass of the unpurified biodiesel of adsorbent (Purolite PD 206) was added to the unpurified biodiesel.
- The temperature was maintained at 338 K and the solution was stirred at 150 rpm for 30 min.
- The purified biodiesel was separated from the adsorbent and stored for further analysis.

4 CATALYSTS CHARACTERISATION

4.1 INTRODUCTION

This chapter presents the characterisation techniques for biodiesel catalysts. There were three types of catalysts involved in biodiesel production, i.e. the cation exchange resins (Amberlyst 15, Purolite CT-122, Purolite CT-169, Purolite CT-175, Purolite CT-275, Purolite D5081 and Purolite D5082), anion exchange resin (Diaion PA306s) and heteropolyacids supported on a salt catalyst (12-phosphotungtic acid (HPW) supported by caesium salt ($Cs_{2.5}H_{0.5}PW_{12}O_{40}$)). For biodiesel synthesis, two different types of reactions are involved, i.e. esterification followed by transesterification. Purolite D5081, Purolite D5082 and Amberlyst 15 were employed for the esterification and Diaion PA306s, Cs-supported heteropolyacids ($Cs_{2.5}H_{0.5}PW_{12}O_{40}$), Purolite CT-122, Purolite CT-169, Purolite CT-175, Purolite CT-275 and Purolite D5081 were investigated for transesterification. The characterisation of the catalysts was performed using field emission gun-scanning electron microscopy (FEG-SEM) analysis, elemental analysis, Fourier transform-infra red (FT-IR) spectroscopy analysis, surface area measurement, true density measurement and particle size distribution (PSD) measurement. At the end of this chapter, the physical and chemical characterisation of the catalysts will be summarised according to the reaction process.

4.2 FIELD EMISSION GUN-SCANNING ELECTRON MICROSCOPY (FEG-SEM) ANALYSIS

All the cation exchange resins are made from the crosslinking between polystyrene and divinylbenzene (DVB) copolymers, functionalised with sulfonic acid groups. Purolite CT-122 is a gelular strongly acidic catalyst, whilst the rest of cation resins (Purolite CT-122, Purolite CT-169, Purolite CT-175, Purolite CT-275, Purolite D5081 and Purolite D5082) are macroporous strongly acidic catalysts. Gelular resins normally have lower degree of cross-linking while the conventional macroporous resins usually have higher degree of cross-linking. According to the manufacturer (Purolite International Limited), Purolite CT-175, Purolite CT-275, Purolite D5081 and Purolite D5082 are categorised as highly cross-linked resins.

They have an exceptionally high degree of DVB cross-linking as compared to other conventional macroporous resins. Due to the high degree of cross-linking, these catalysts exhibit very little volume change (swelling), have a dense matrix and improved oxidation resistance.

The FEG-SEM images for Purolite and Amberlyst cation exchange resins are presented in Figures 4.1 to 4.7. Figure 4.1 shows the surface morphology of Purolite CT-122, taken at magnification of 1 kX and 20 kX. The FEG-SEM image for this gelular polymer matrix shows a collapsed surface covered with hair line cracks at the lower magnification. These hair line cracks show a smooth-like surface at the higher magnification. In contrast, a more porous structure can be seen for the macroporous resins (Figures 4.2 - 4.7). For cation macroporous resins, the surface morphology was taken at the magnification of 20 kX and 100 kX. From figures 4.2 - 4.7, it can be seen that these resins have a tiny-hole-like surfaces that are specially designed to create a large number of pores that serve as the flow channels within the structure. Another ion exchange resin used in biodiesel synthesis is Diaion PA306s. This resin serves as a strongly basic anion exchange resin with a 4% cross-linking density. Figure 4.8 represent the surface morphology of Diaion PA306s, captured at the lower (20 kX) and higher (100 kX) magnifications. In contrast with gelular cation exchange resins, Diaion PA306s resin, a special gel matrix with an integrated high porosity shows a tiny-hole-like surface with large numbers of pores.

The third classification of catalyst is the heteropolyacids supported salt catalyst. Among the heteropolyacids catalysts, tungstophosphoric acid, also known as phosphotungstic acid has been chosen due to its high acid strength and high thermal stability. Figures 4.9 and 4.10 represent the surface morphology of $Cs_{2.5}H_{0.5}PW_{12}O_{40}$ and $Cs_{2.5}H_{0.5}PW_{12}O_{40}$ (calcined). The images were taken at the magnification of 1 kX and 5 kX. All images show a significant number of very fine particles of heteropolyacids (0.01 - 2 μm). They have an irregular shape and size, and are randomly distributed over the support surface, Cs salts.

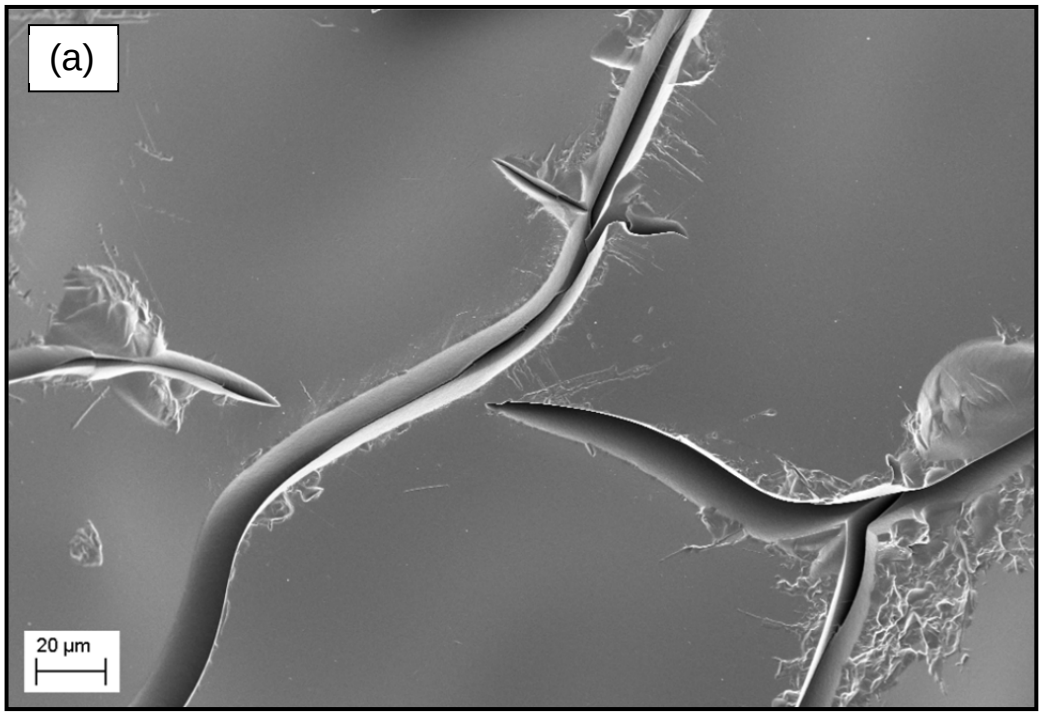

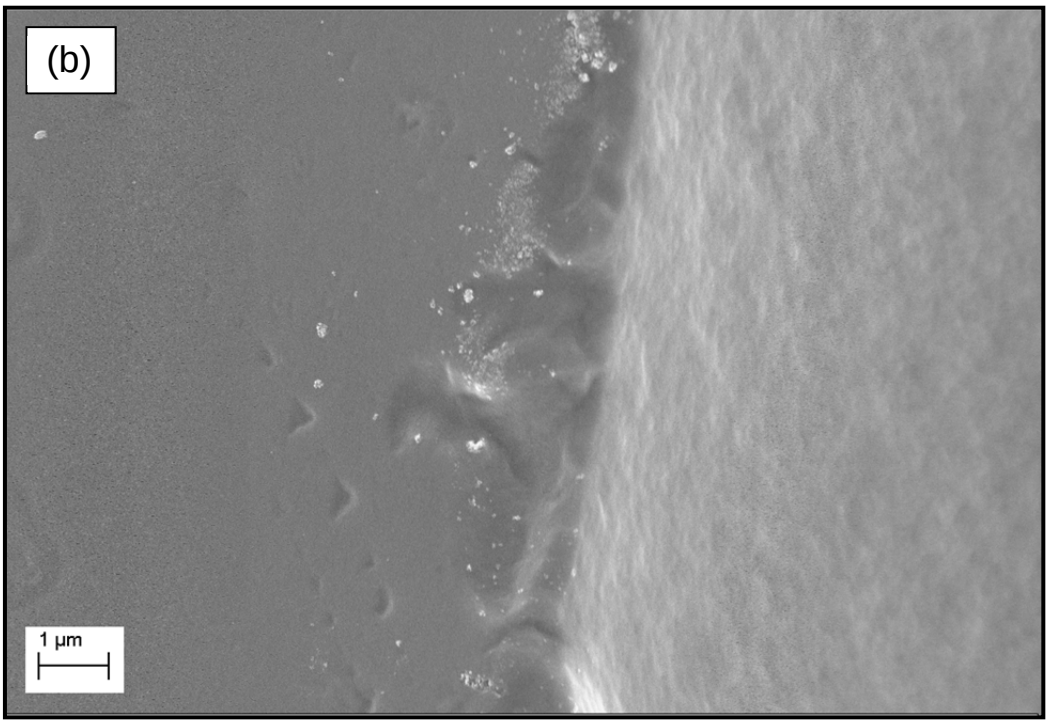

Figure 4.1. The FEG-SEM images of Purolite CT-122. Image (a): magnification 1 kX; image (b): magnification 20 kX.

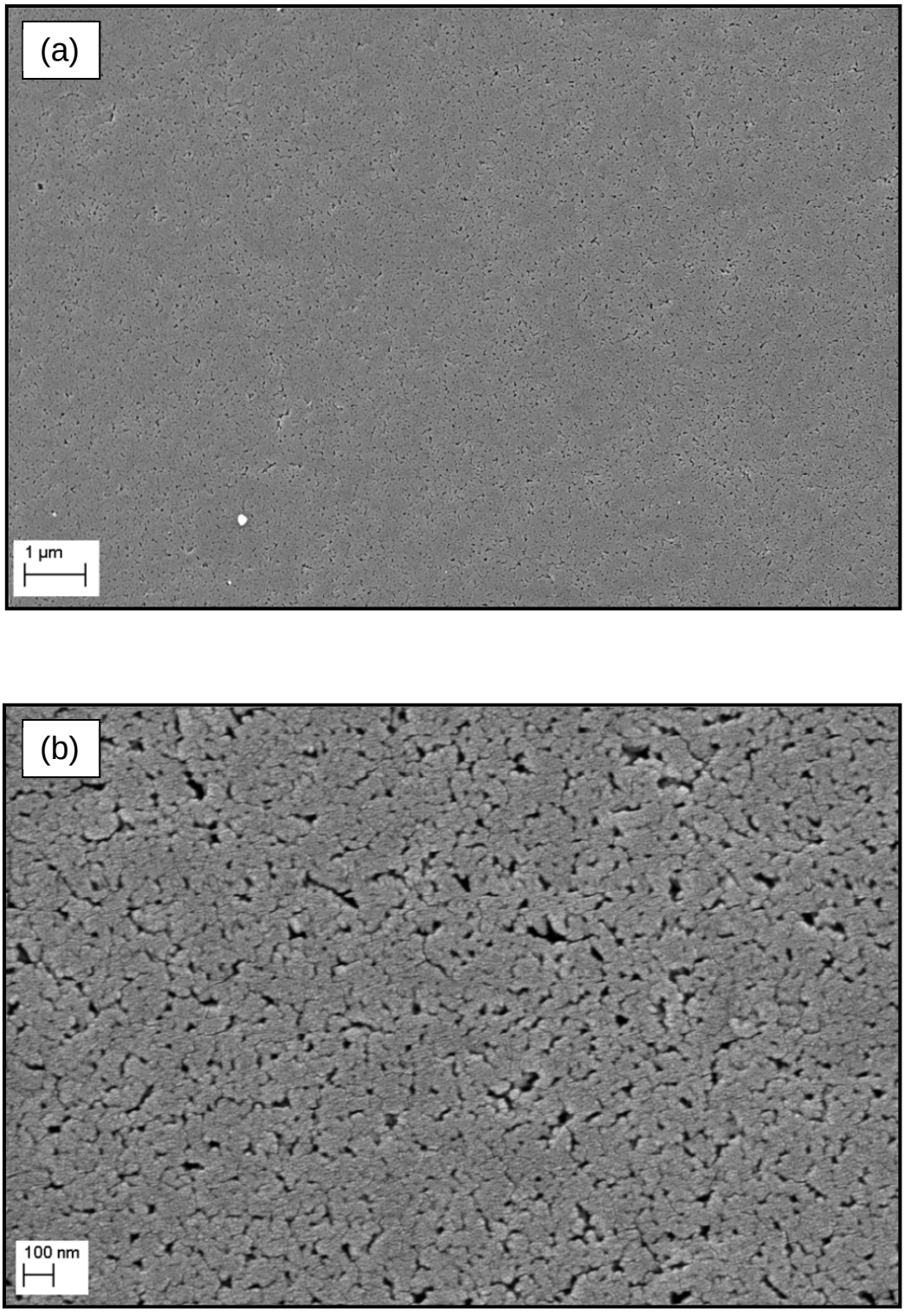

Figure 4.2. The FEG-SEM images of Amberlyst 15. Image (a): magnification 20 kX; image (b): magnification 100 kX.

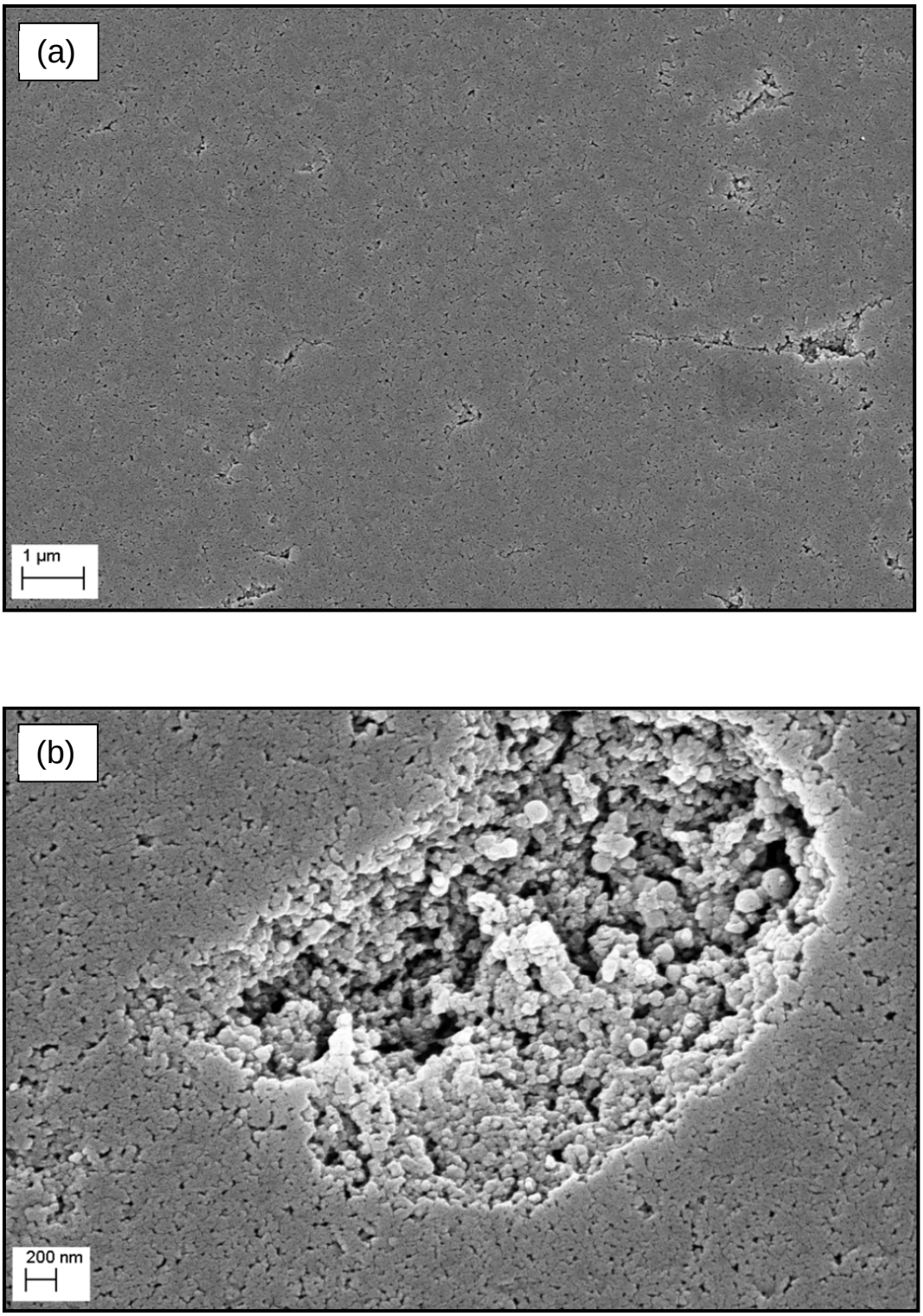

Figure 4.3. The FEG-SEM images of Purolite CT-169. Image (a): magnification 20 kX; image (b): magnification 100 kX.

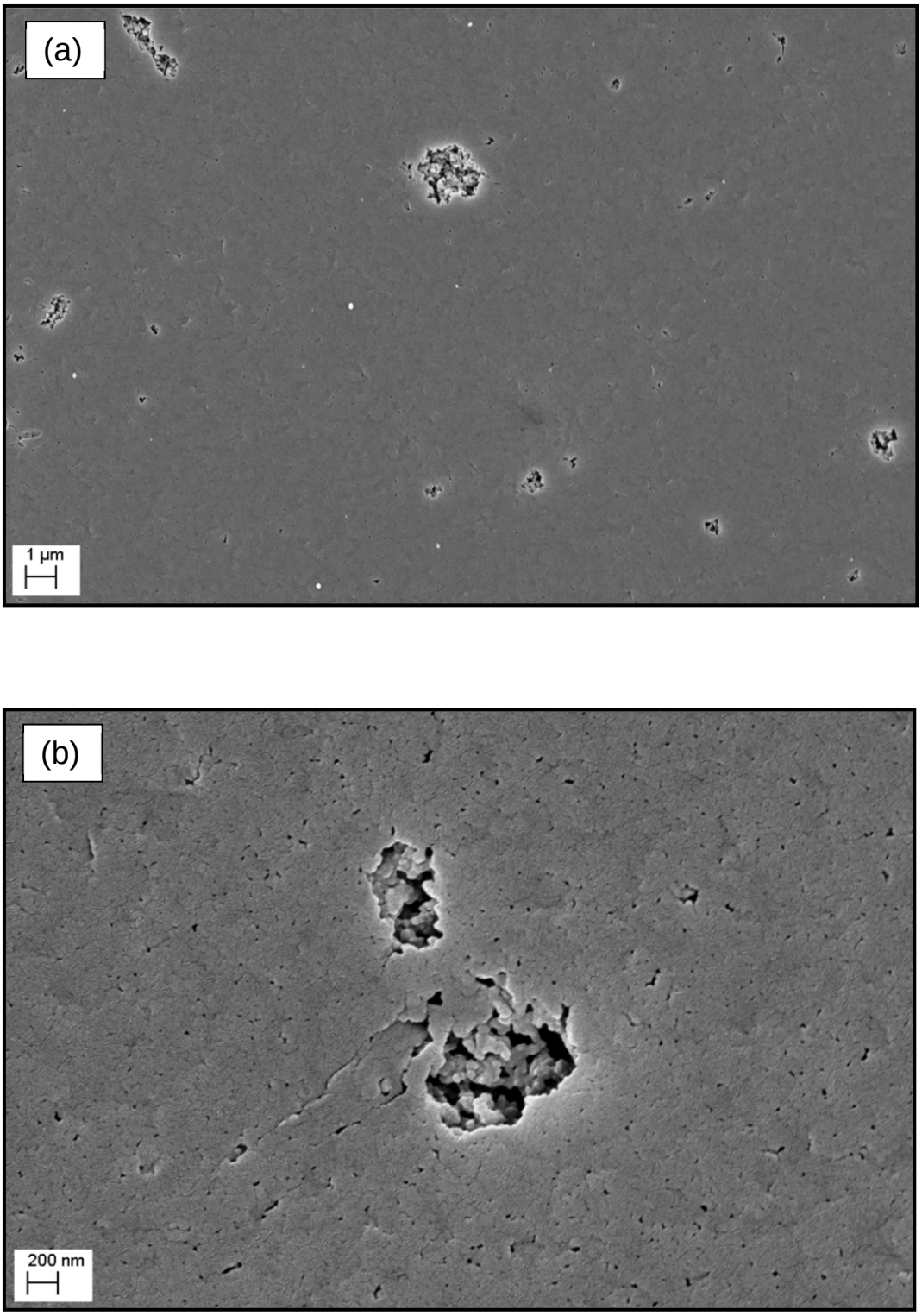

Figure 4.4. The FEG-SEM images of Purolite CT-175. Image (a): magnification 20 kX; image (b): magnification 100 kX.

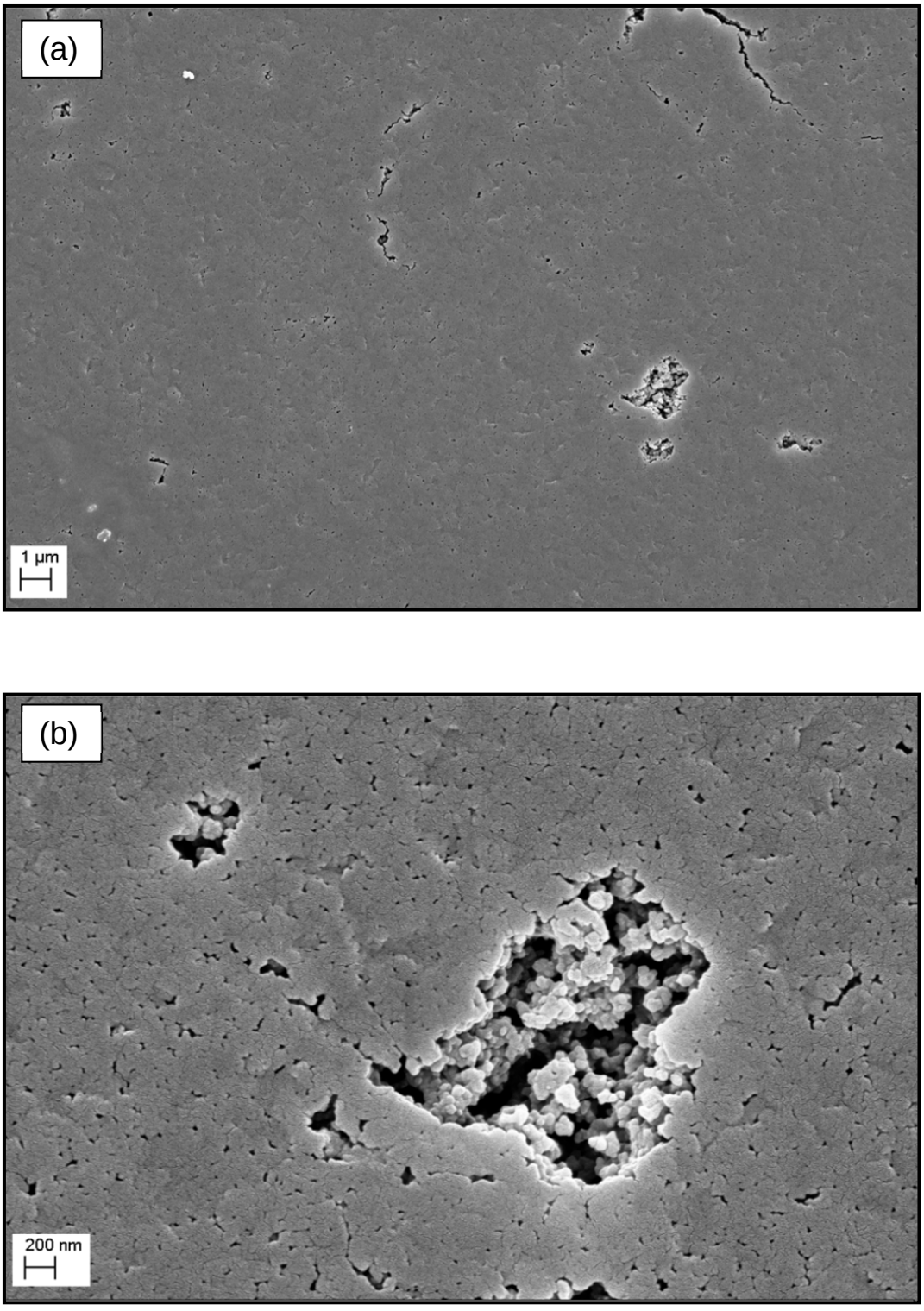

Figure 4.5. The FEG-SEM images of Purolite CT-275. Image (a): magnification 20 kX; image (b): magnification 100 kX.

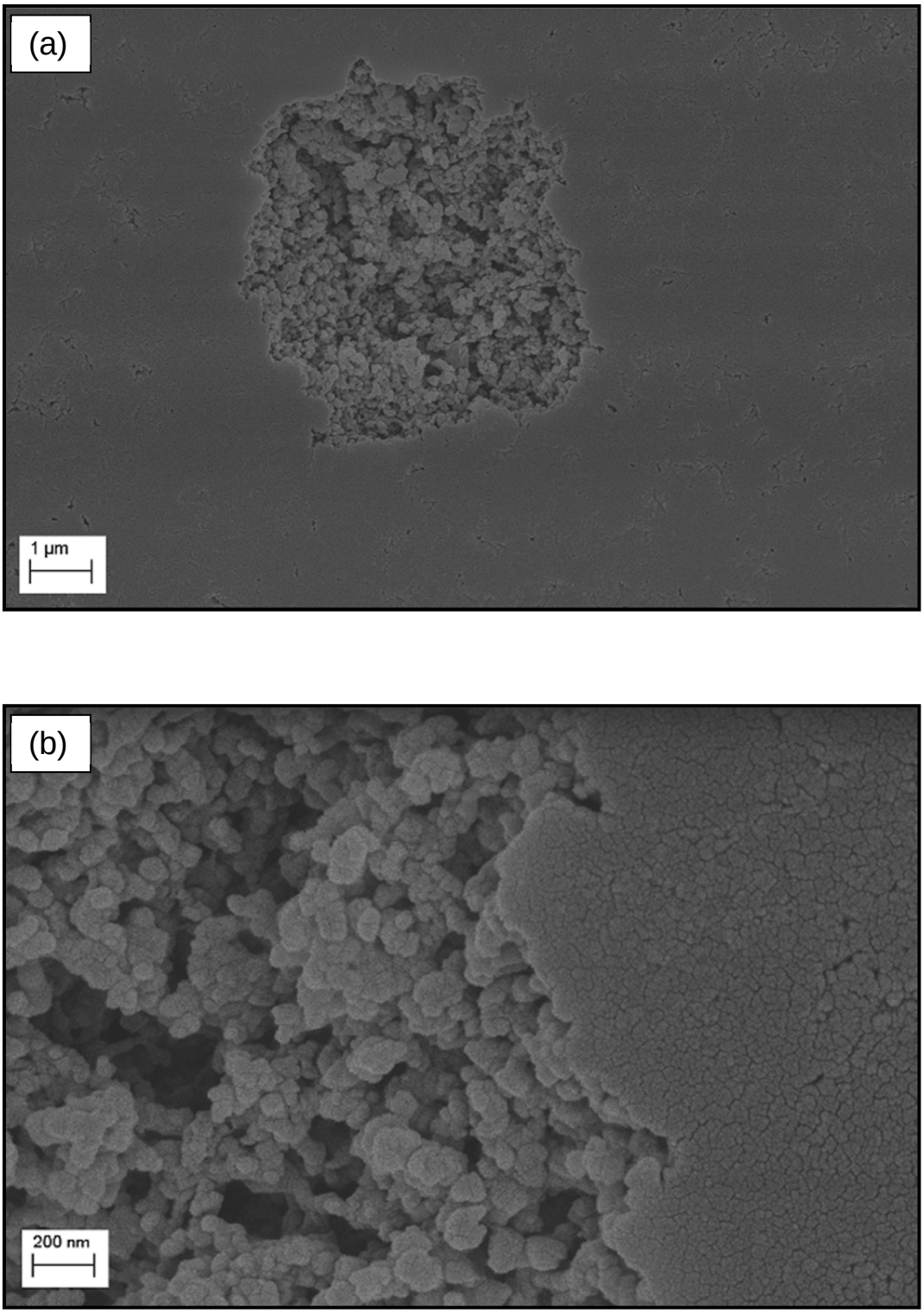

Figure 4.6. The FEG-SEM images of Purolite D5081. Image (a): magnification 20 kX; image (b): magnification 100 kX.

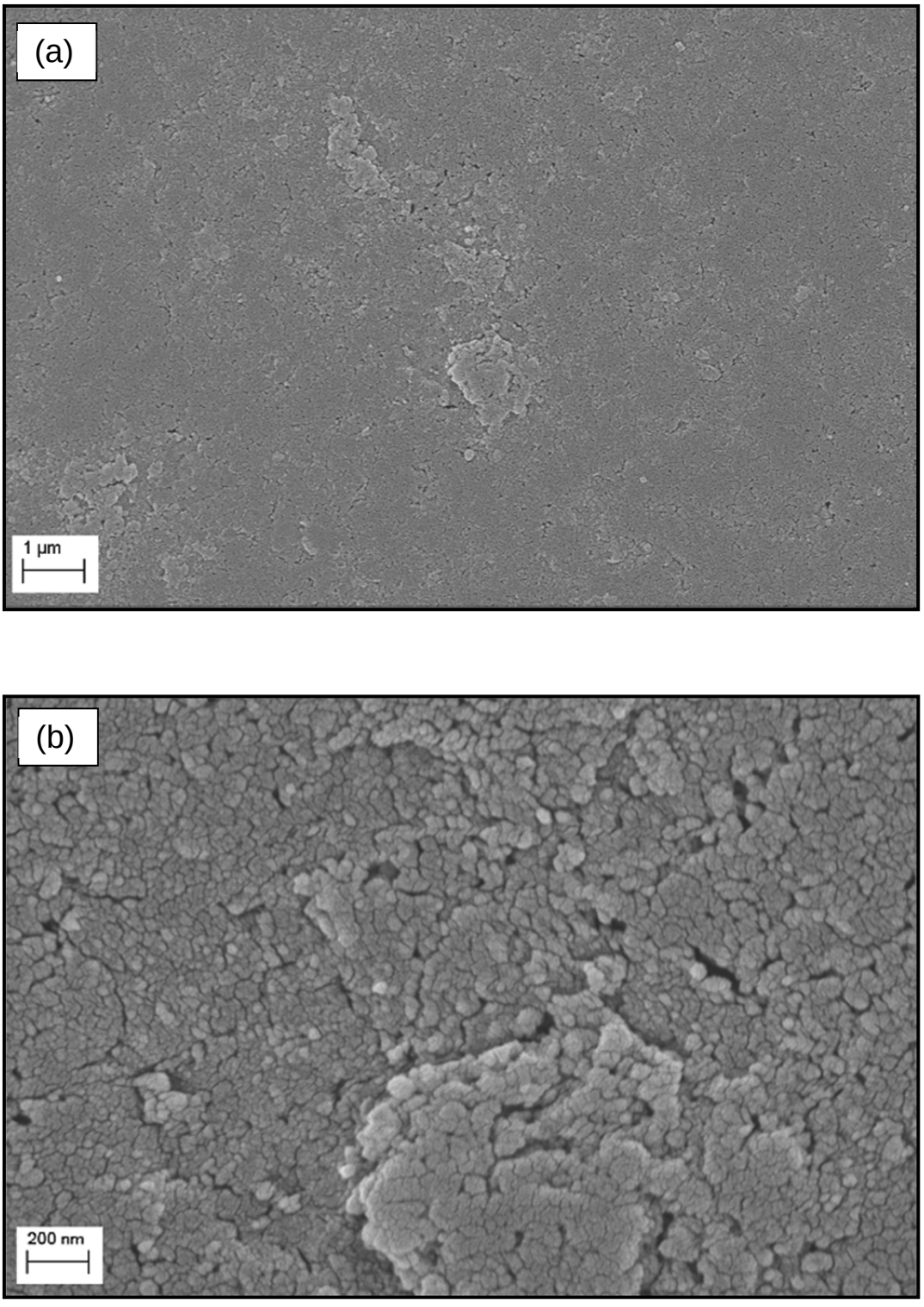

Figure 4.7. The FEG-SEM images of Purolite D5082. Image (a): magnification 20 kX; image (b): magnification 100 kX.

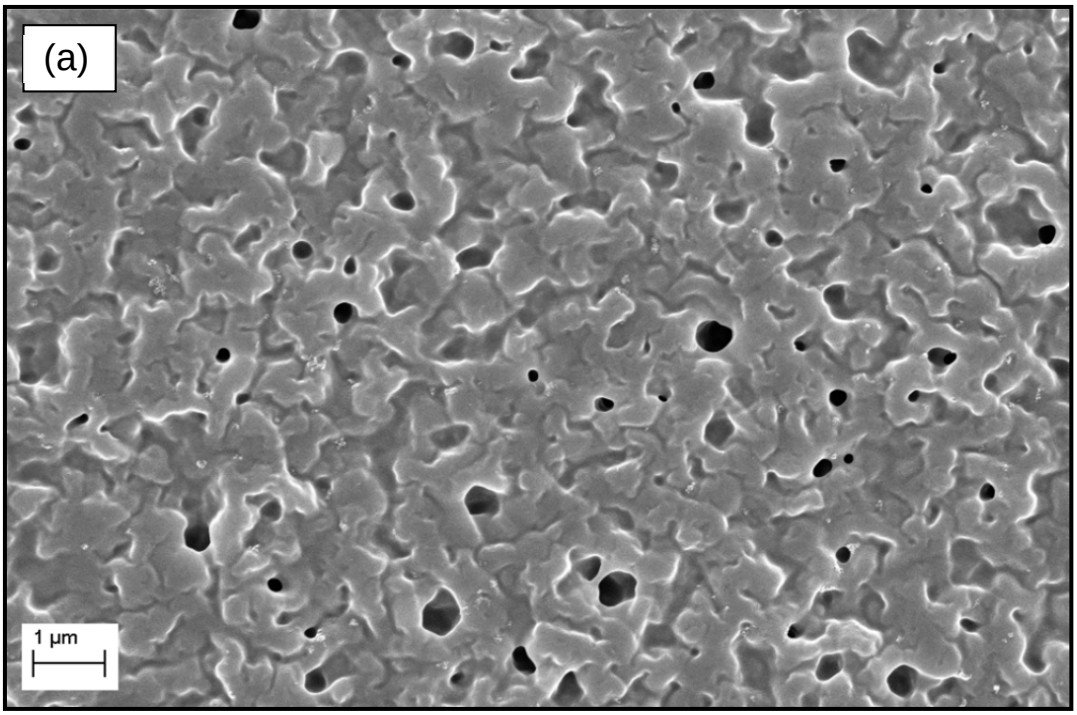

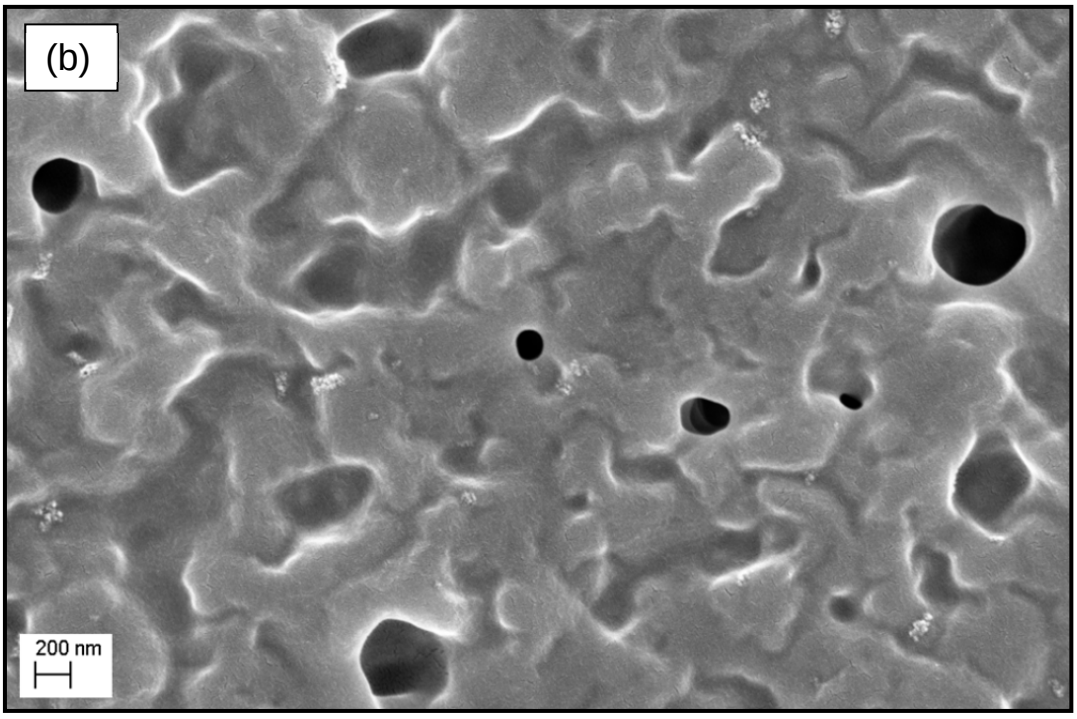

Figure 4.8. The FEG-SEM images of Diaion PA306s. Image (a): magnification 20 kX; image (b): magnification 100 kX.

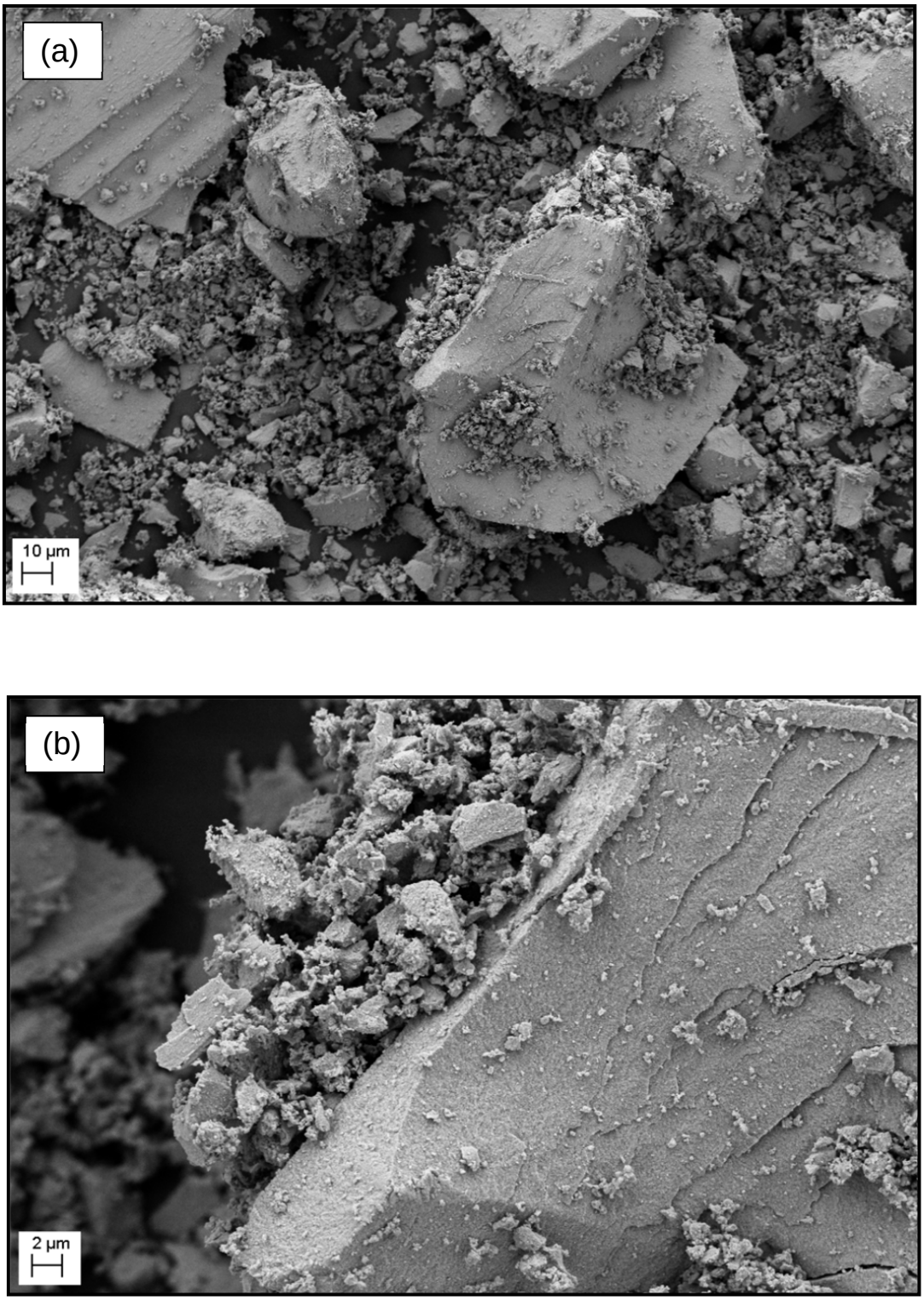

Figure 4.9. The FEG-SEM images of $Cs_{2.5}H_{0.5}PW_{12}O_{40}$ catalyst. Image (a): magnification 1 kX; image (b): magnification 5 kX.

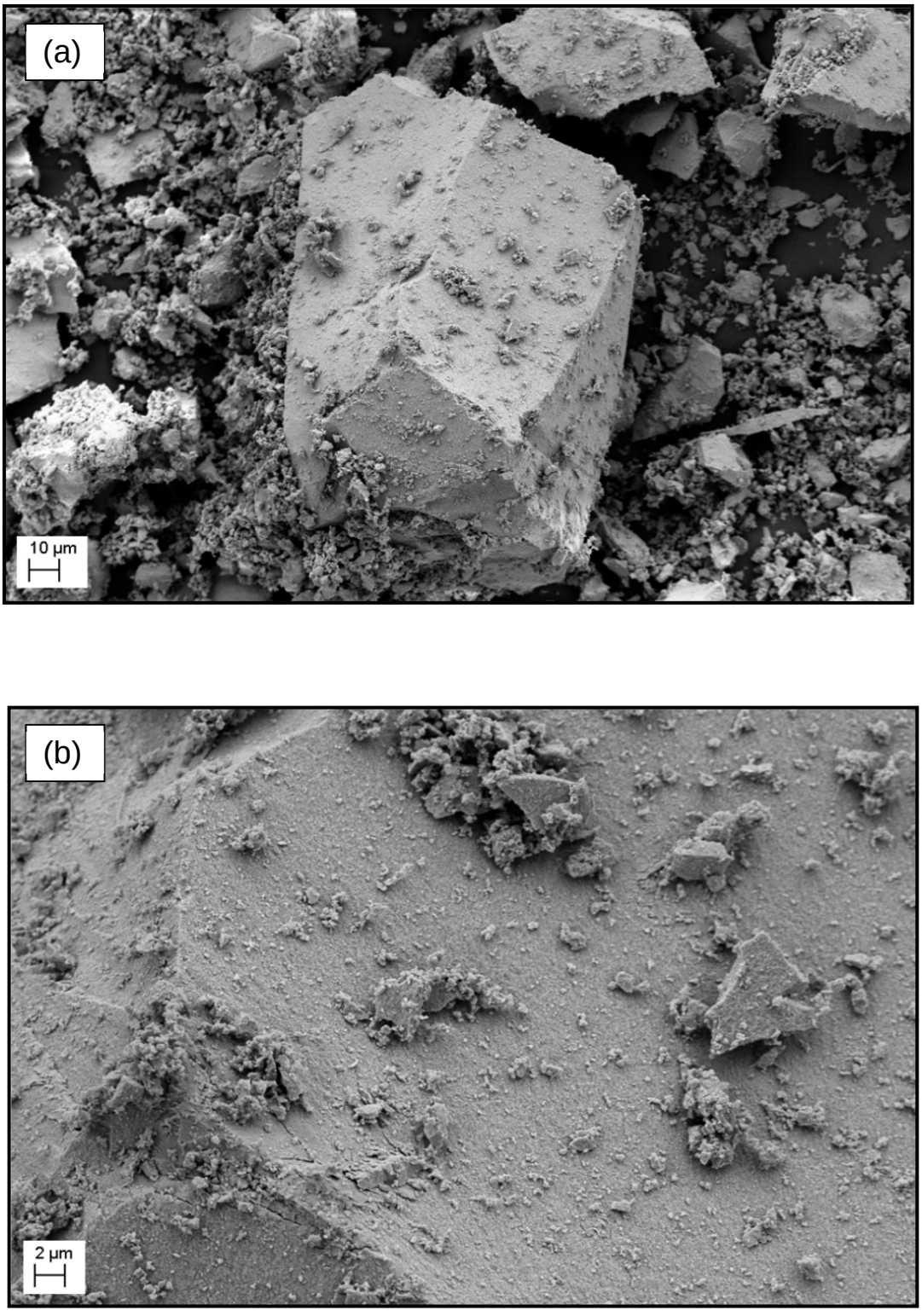

Figure 4.10. The FEG-SEM images of $Cs_{2.5}H_{0.5}PW_{12}O_{40}$ (calcined) catalyst. Image (a): magnification 1 kX; image (b): magnification 5 kX.

4.3 ELEMENTAL ANALYSIS

The results for elemental analysis are presented in Table 4.1. For cation exchange resins, the polymer structure consists of carbon, hydrogen, sulphur and oxygen elements. There was unexpected presence of nitrogen in some of the cation exchange resins, and the value was less than 1%. In this case, nitrogen was assumed to be a contaminant in the sample. For all ion exchange resins, it was assumed that the only other species present was oxygen. Oxygen cannot be measured by elemental analysis and therefore, the percentage of oxygen content was determined by the difference from the total weight percentage of other elements (i.e. carbon, hydrogen, nitrogen and sulphur).

Results from Table 4.1 show that Purolite CT-275 has the highest percentage of sulphur (16.61%) and oxygen (34.20%) whereas Purolite D5081 has the highest amount of carbon (77.04%). In addition, Diaion PA306s was found to have the highest amount of hydrogen (9.42%) and with the presence of quaternary amine group, 4.34% of nitrogen was detected from Diaion PA306s catalyst. For Cs-supported heteropolyacids catalyst, the composition of caesium, hydrogen, phosphorus, tungsten and oxygen are calculated directly from the molecular mass of the compound (3209.8 g mol^{-1}). The result is presented in Table 4.2.

Table 4.1. The elemental analysis results for ion exchange resin catalysts.

Catalyst	% C	% H	% N	% S	% O*
Amberlyst 15	53.14	6.12	0.05	16.17	24.52
Diaion PA306s	55.59	9.42	4.34	0.00	30.65
Purolite CT-122	51.06	5.68	0.06	15.99	27.22
Purolite CT-169	48.88	5.07	0.06	16.58	29.42
Purolite CT-175	47.35	4.74	0.00	15.75	32.17
Purolite CT-275	44.59	4.61	0.00	16.61	34.20
Purolite D5081	77.04	5.32	0.95	4.09	12.61
Purolite D5082	68.87	4.44	0.13	5.92	20.65

*Oxygen by difference

Table 4.2. The elemental analysis results for Cs-supported heteropolyacids catalysts.

Elements	Composition, %
Caesium (Cs)	10.35
Hydrogen (H)	0.02
Phosphorus (P)	0.97
Tungsten (W)	68.72
Oxygen (O)	19.94

*percent composition was calculated from the molecular mass of the compound (3209.8 g mol^{-1})

4.4 FOURIER TRANSFORM-INFRA RED MEASUREMENT

Figures 4.11 to 4.17 show the FT-IR spectra for the strongly acidic cation exchange resins (Amberlyst 15, Purolite CT-122, Purolite CT-169, Purolite CT-175, Purolite CT-275, Purolite D5081 and Purolite D5082). The FT-IR spectra for all cation exchange resins were quite similar with the presence of the expected functional groups. The main functional group found in the spectra is sulfonic group (SO_3^-) stretching in the range from 1226 cm^{-1} - 1217 cm^{-1} (asymmetric) and 1186 cm^{-1} - 1006 cm^{-1} (symmetric). Table 4.3 shows the overall infrared assignment of bands for all cation exchange resins.

Table 4.3. The infrared assignment of bands for cation exchange resins.

Wavenumber (cm^{-1})	Assignment
3700 - 3100	O-H stretching vibration of hygroscopic water
2940 - 2920	C-H_2 stretching vibration (asymmetric)
2860 - 2840	C-H_2 stretching vibration (symmetric)
1740 - 1625	Overtone pattern of benzene ring (weak intensity)
1600 - 1500	C-H deformation and skeletal vibrations in polystyrene/DVB (Singare *et al.*, 2011)
1470 - 1440	C-H deformation vibrations (asymmetric)
1226 - 1217	SO_3^- stretching vibrations (asymmetric)
1186 - 1006	SO_3^- stretching vibrations (symmetric)
902 - 671	C-H out-of-plane deformation vibrations of monosubstituted and disubstitued benzene rings

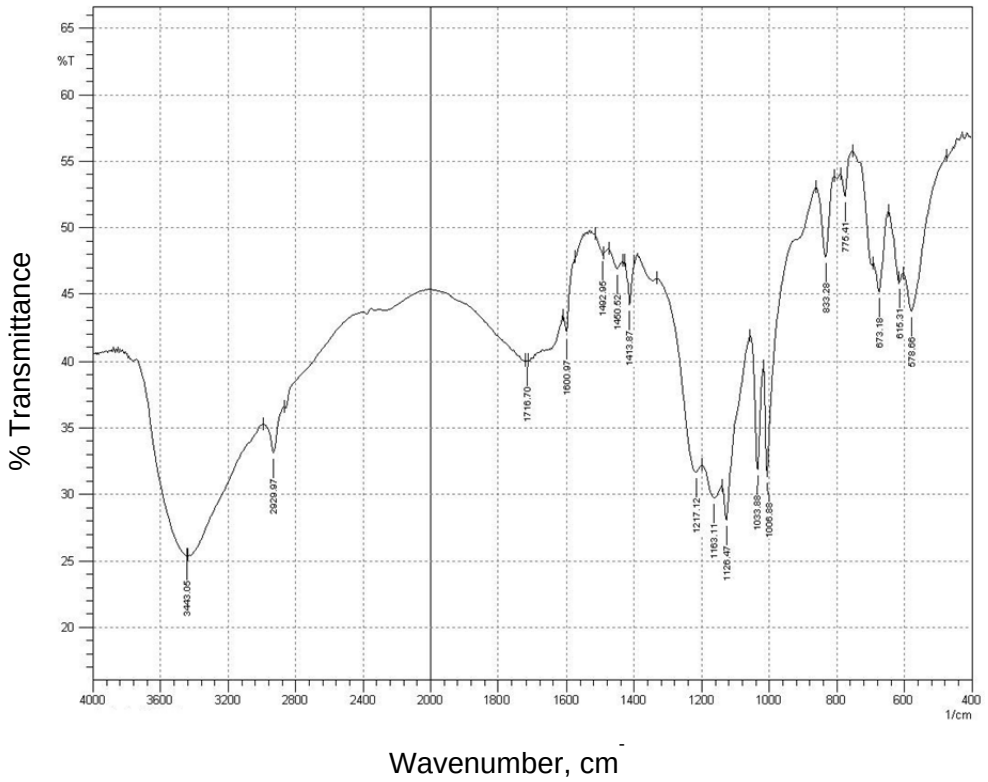

Figure 4.11. The FT-IR spectra of Amberlyst 15 catalyst.

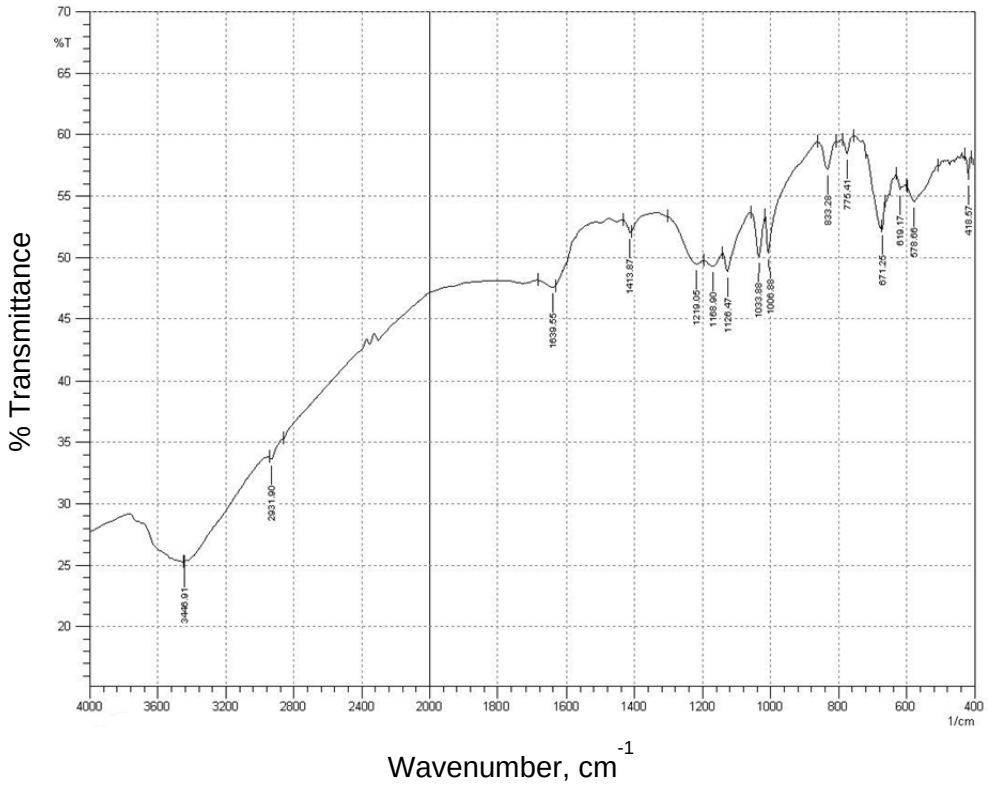

Figure 4.12. The FT-IR spectra of Purolite CT-122 catalyst.

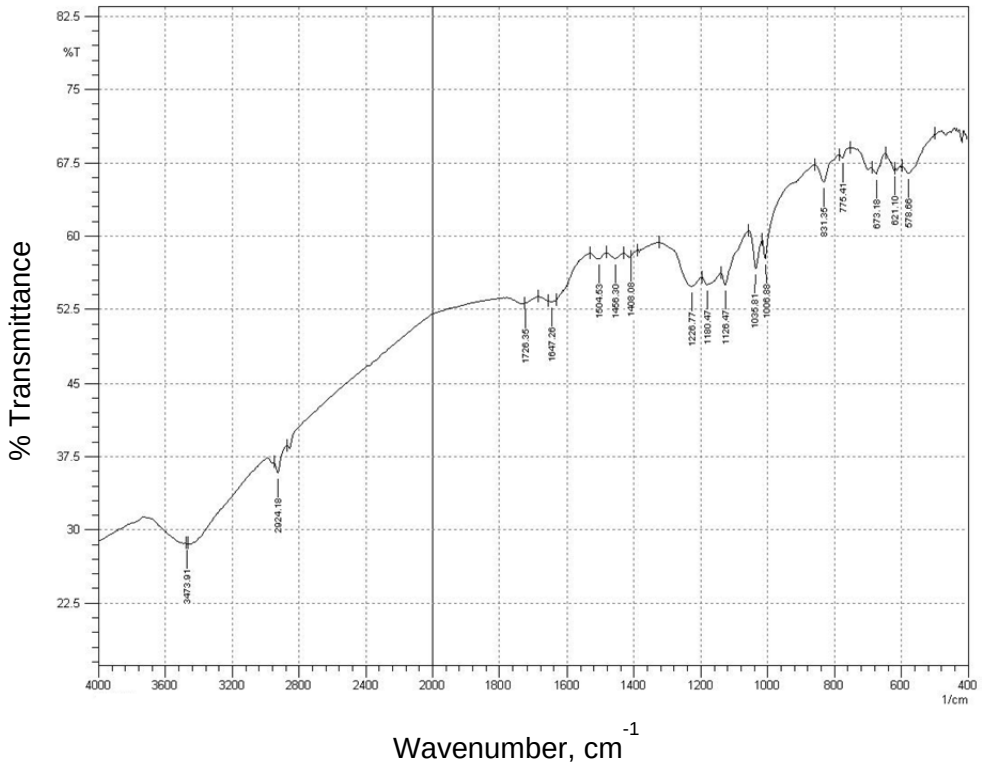

Figure 4.13. The FT-IR spectra of Purolite CT-169 catalyst.

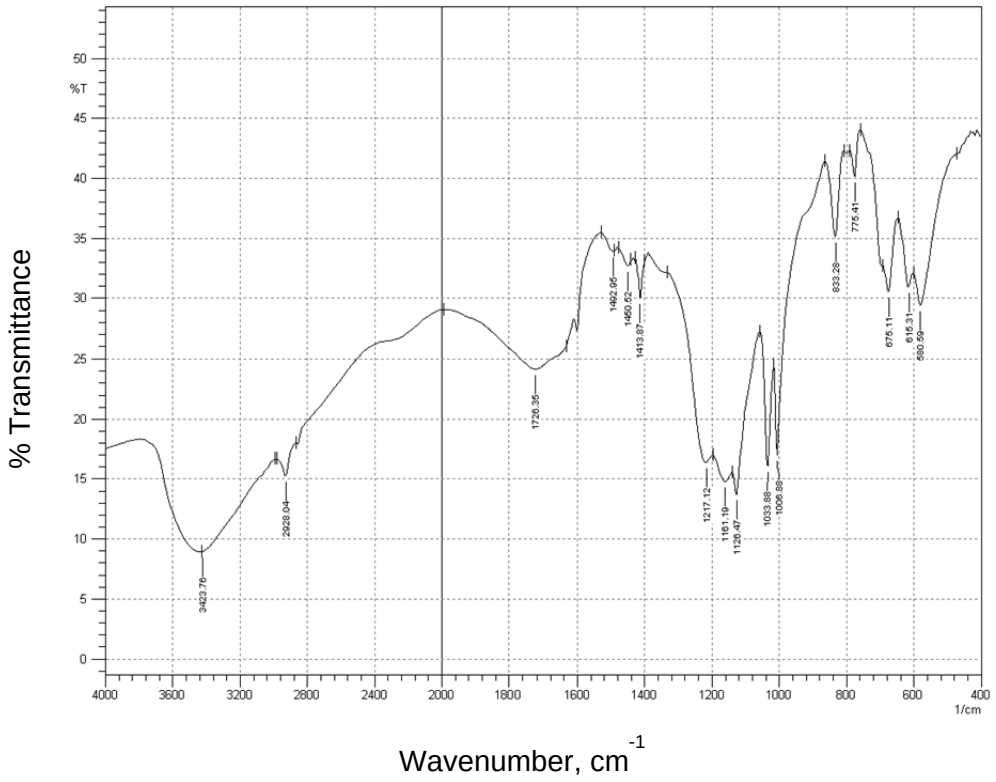

Figure 4.14. The FT-IR spectra of Purolite CT-175 catalyst.

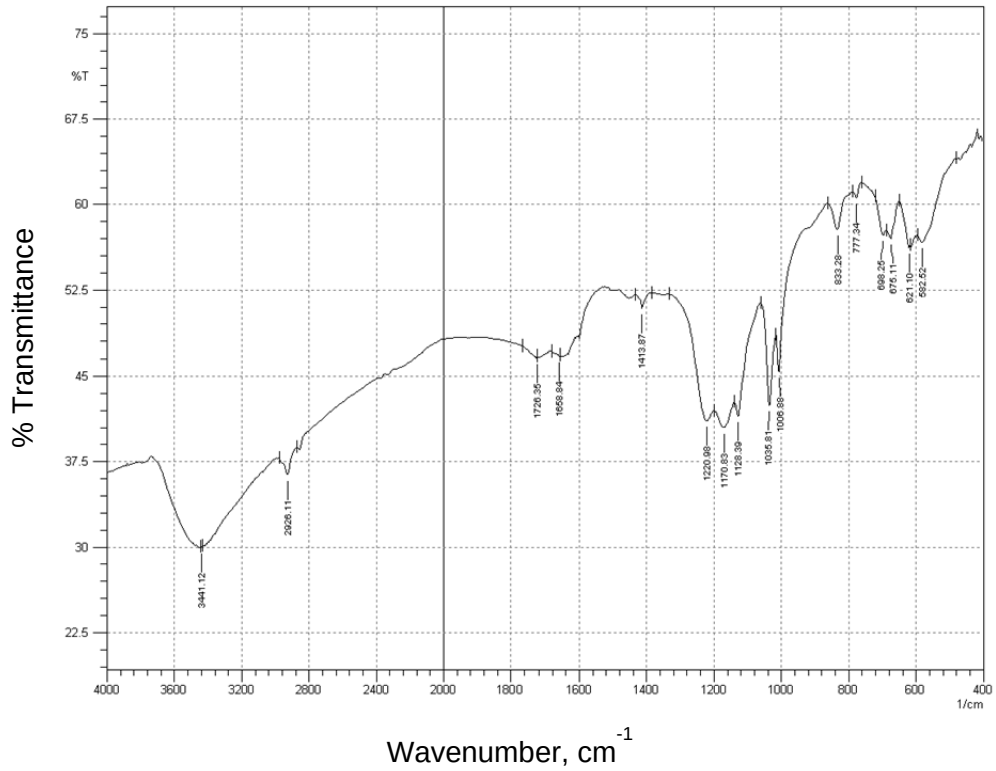

Figure 4.15. The FT-IR spectra of Purolite CT-275 catalyst.

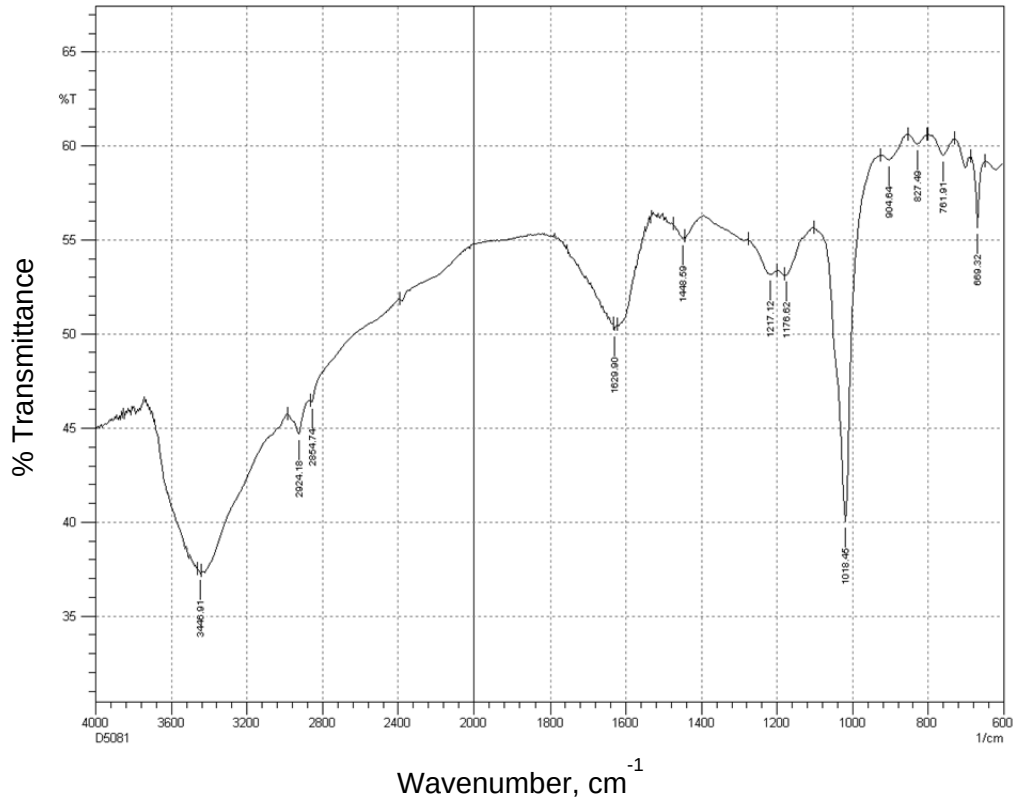

Figure 4.16. The FT-IR spectra of Purolite D5081 catalyst.

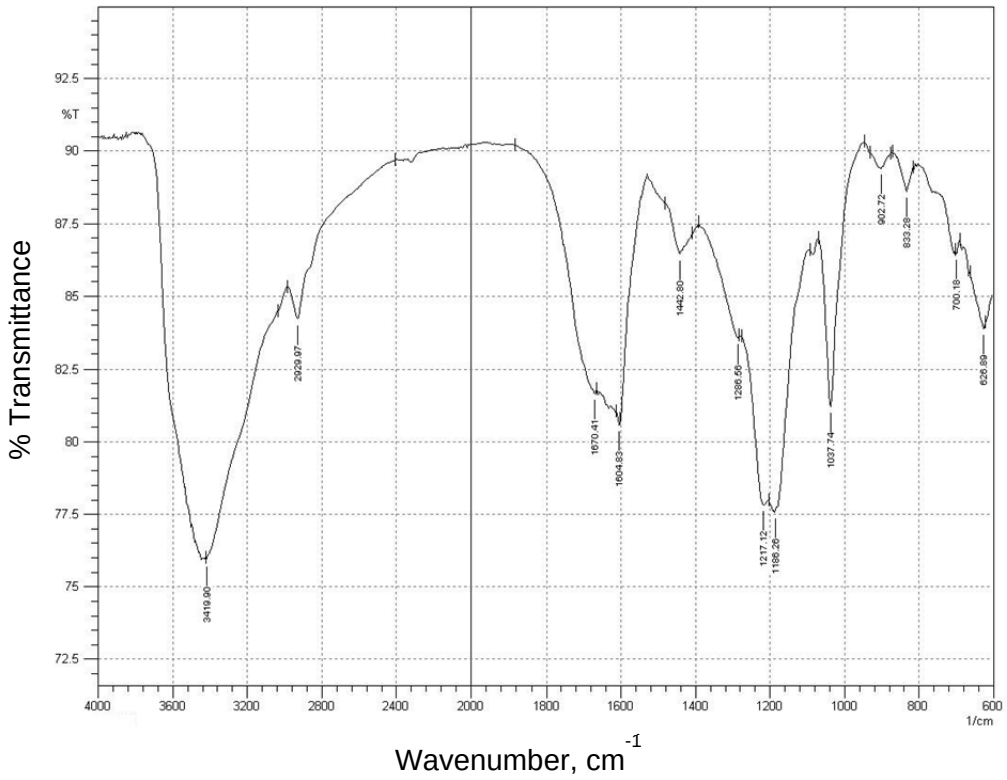

Figure 4.17. The FT-IR spectra of Purolite D5082 catalyst.

The FT-IR spectra for Diaion PA306s was slightly different than the cation exchange resins, as presented in Figure 4.18. This is due to the presence of quaternary ammonium functional group in the structure of anion exchange resin. The characteristic band for this resin is mainly focused on the vibration of -CH, -CH_2, -CH_3, -NH, -NH_2, NH_3, benzene ring and oxygen functionality of the polymers. Table 4.4 shows the infrared assignment of bands for anion exchange resin, Diaion PA306s.

Table 4.4. The infrared assignment of bands for anion exchange resin, Diaion PA306s.

Wavenumber, cm^{-1}	**Assignment**
3419	O-H stretching vibration of hygroscopic water
3018	C-H stretching vibration of benzene ring (Traboulsi *et al.*, 2012)
2928	C-H stretching vibration of CH_2 and CH_3 in CH_3-N (Traboulsi *et al.*, 2012)
1693 - 1631	C-N-H deformation vibrations of secondary amine
1487	N-H vibration (weak intensity)
1475	C-H asymmetric deformation vibrations
1410	O-H deformation vibrations (possibly resulting from the presence of alcohol residual within the resin)
1371	C-H deformation vibrations of the C-H aliphatic group
1220 - 1008	C-H deformation vibrations (in-plane rocking band)
976 - 831	C-H out-of-plane deformation vibrations of monosubstituted and disubstitued benzene rings
923 - 831	C-N stretching vibrations in N-CH_3

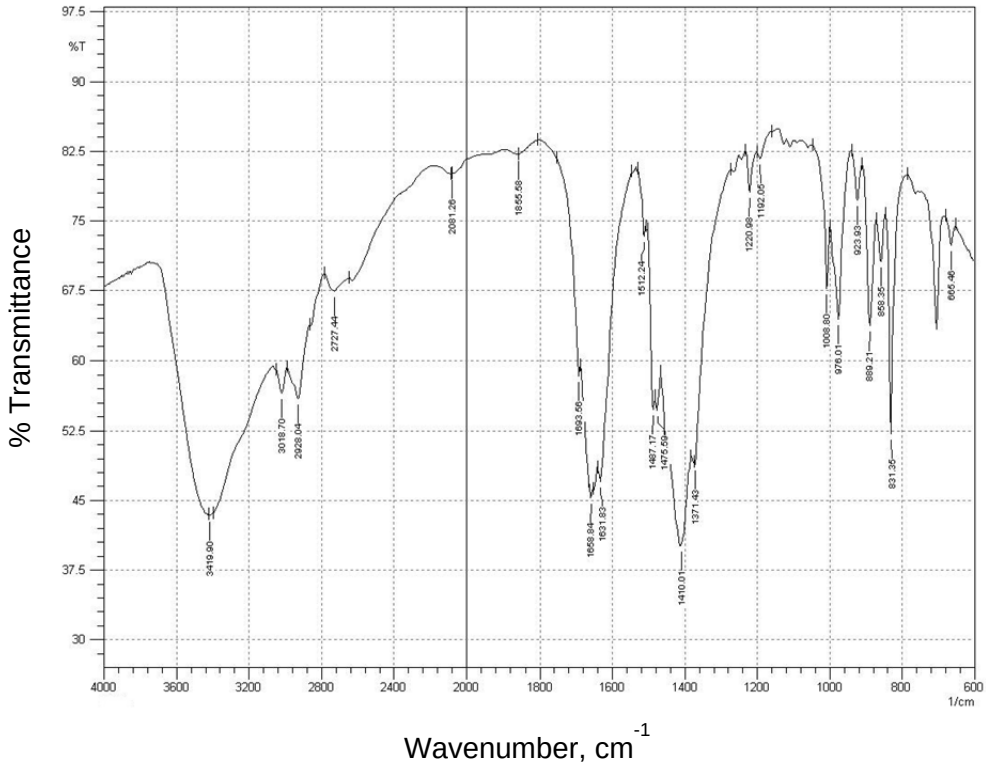

Figure 4.18. The FT-IR spectra of Diaion PA306s catalyst.

The structural form of 12-tungstophosphoric acid is known as a Keggin structure. This structure consists of a central phosphorus atom tetrahedrally coordinated by four oxygen atoms and surrounded by twelve octahedral WO_6 units that share edges and

corners in the structure (Keggin, 1934, Kozhevnikov, 1998). From the structure, it was possible to deduce four types of oxygen, which provide four significant bands in the spectra in the range of 1200-700 cm^{-1}. This is called the fingerprint region for heteropolyacids catalyst (Pope, 1983). The exact position of these bands depends upon the hydration degree (Pazé *et al.*, 2000; Essayem *et al.*, 2001) and the type of counter cation present (Rocchiccioli-Deltcheff *et al.*, 1983). The FT-IR spectra for $Cs_{2.5}H_{0.5}PW_{12}O_{40}$ and $Cs_{2.5}H_{0.5}PW_{12}O_{40}$ (calcined) catalysts are shown in Figures 4.19 and 4.20. From the figures, it can be seen that both catalysts resulted in the same pattern of signal adsorption. Table 4.5 show the infrared assignment of bands for Cs-supported heteropolyacids catalysts.

Table 4.5. The infrared assignment of bands for Cs-supported heteropolyacids catalysts.

Wavenumber (cm^{-1})	Assignment
3419	O-H stretching vibration of hygroscopic water
1629	O-H vibration - correspond to the presence of the protonated water clusters, probably the di-aqua proton $H_5O_2^+$ generated by 12-tungstophosphoric acids or/and water physisorbed onto the caesium salts. (Essayem *et al.*, 2001; Yang *et al.*, 2002)
1080	asymmetric stretching vibration of the P-O bond in the central PO_4 tetrahedral
983	stretching vibration of $W=O_t$ (terminal oxygen in the Keggin structure)
889	W-O-W (corner) vibration (Shiju *et al.*, 2009)
802	W-O-W (edge) vibration (Shiju et al., 2009)

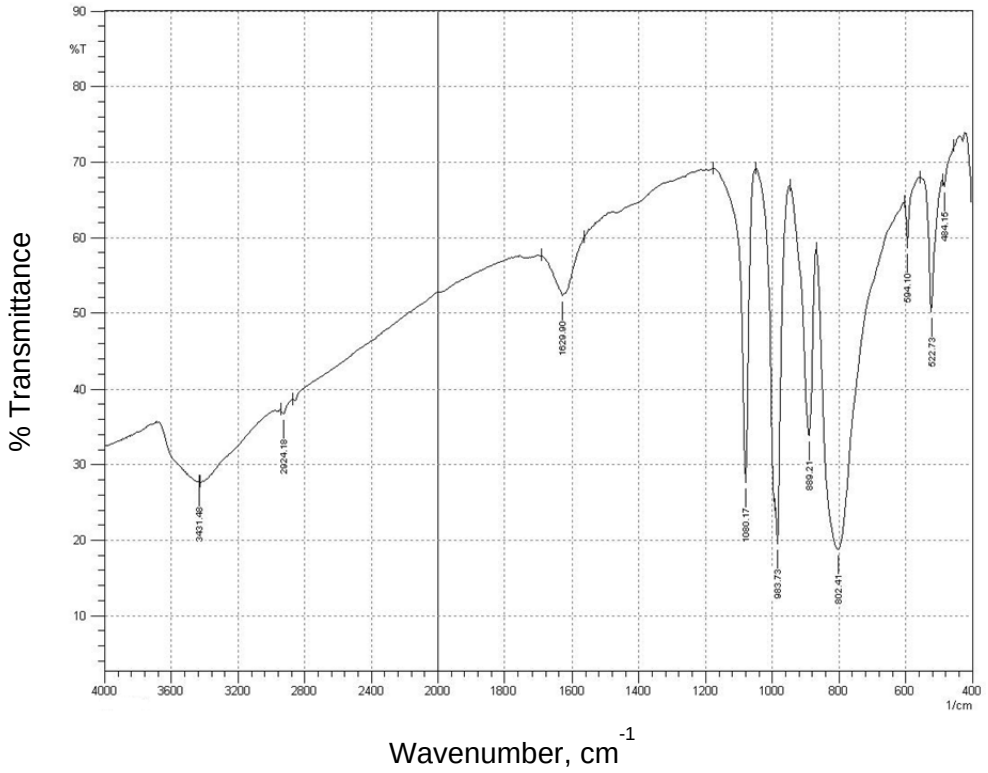

Figure 4.19. The FT-IR spectra of $Cs_{2.5}H_{0.5}PW_{12}O_{40}$ catalyst.

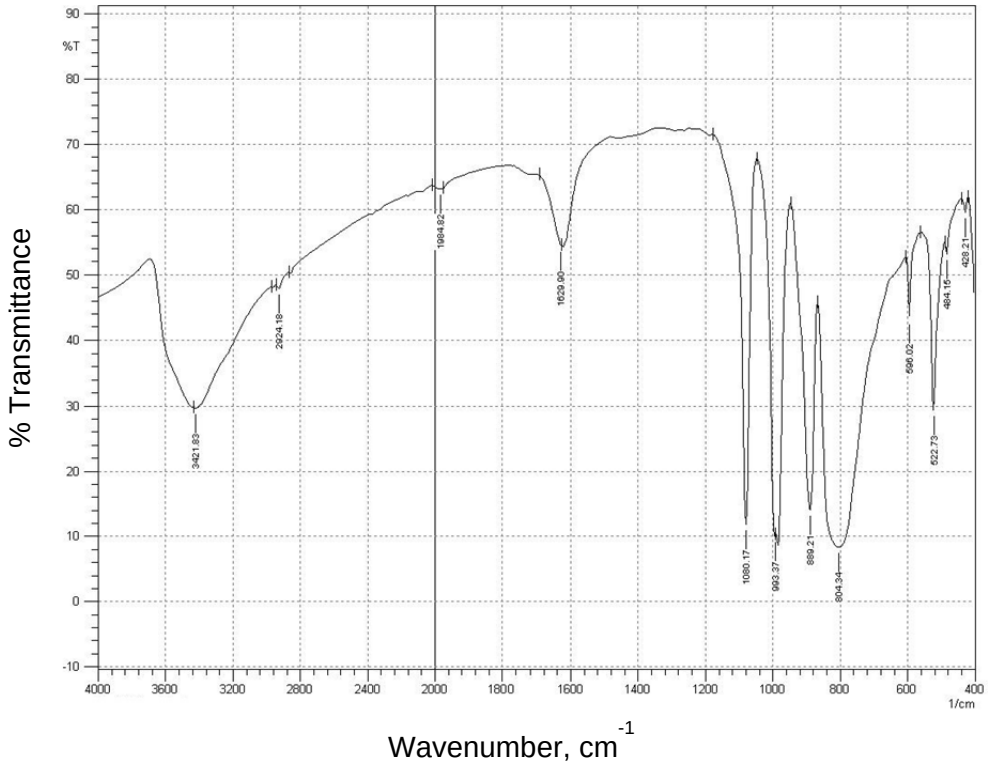

Figure 4.20. The FT-IR spectra of $Cs_{2.5}H_{0.5}PW_{12}O_{40}$ (calcined) catalyst.

4.5 TRUE DENSITY MEASUREMENT

Table 4.6 gives the measured true densities for all catalysts. From the table, it can be seen that Cs-supported heteropolyacids catalysts [$Cs_{2.5}H_{0.5}PW_{12}O_{40}$ and $Cs_{2.5}H_{0.5}PW_{12}O_{40}$ (calcined)] have the highest densities (6.3 g cm^{-1} and 6.4 g cm^{-1}) and the Amberlyst 15 has the lowest density (1.027 g cm^{-1}).

Table 4.6. True density for studied catalysts.

Catalyst	True density (g cm^{-3})
Amberlyst 15	1.027
$Cs_{2.5}H_{0.5}PW_{12}O_{40}$	6.296
$Cs_{2.5}H_{0.5}PW_{12}O_{40}$ (calcined)	6.421
Diaion PA306s	1.236
Purolite CT-122	1.297
Purolite CT-169	1.297
Purolite CT-175	1.296
Purolite CT-275	1.296
Purolite D5081	1.309
Purolite D5082	1.373

4.6 PARTICLE SIZE DISTRIBUTION (PSD) MEASUREMENT

The PSD results for all catalysts are presented in Figures 4.21 - 4.30. Figures 4.21 - 4.23 represent the results for Diaion PA306s, $Cs_{2.5}H_{0.5}PW_{12}O_{40}$ and $Cs_{2.5}H_{0.5}PW_{12}O_{40}$ (calcined) catalysts. The result for Diaion PA306s (Figure 4.21) shows a unimodel PSD, ranging from the smallest particle size of 103 μm to the largest particle size of 647 μm. For Cs-supported heteropolyacids catalysts, the non-calcined catalyst has a unimodal distribution whereas the result for the calcined catalyst results in two significant PSD peaks. For both Cs-supported heteropolyacids catalysts, the PSD range for the first peak was similar with particle distribution ranges from 0.06 - 0.7 μm. The PSD for the second peak of $Cs_{2.5}H_{0.5}PW_{12}O_{40}$ (calcined) lies between 1.7 - 48.2 μm. This results shows that calcination treatment increases the average particle size and distribution, which changes from unimodal to bimodal distribution (Juang and Hon, 1996).

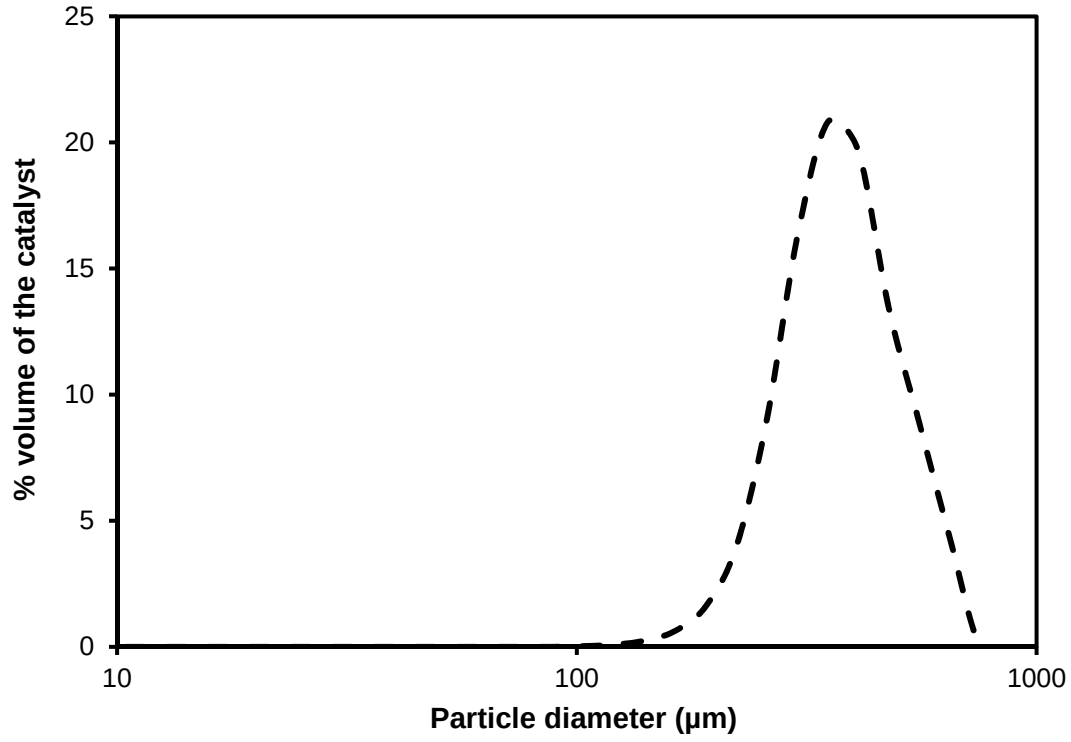

Figure 4.21. The particle size distribution (PSD) of Diaion PA306s catalyst.

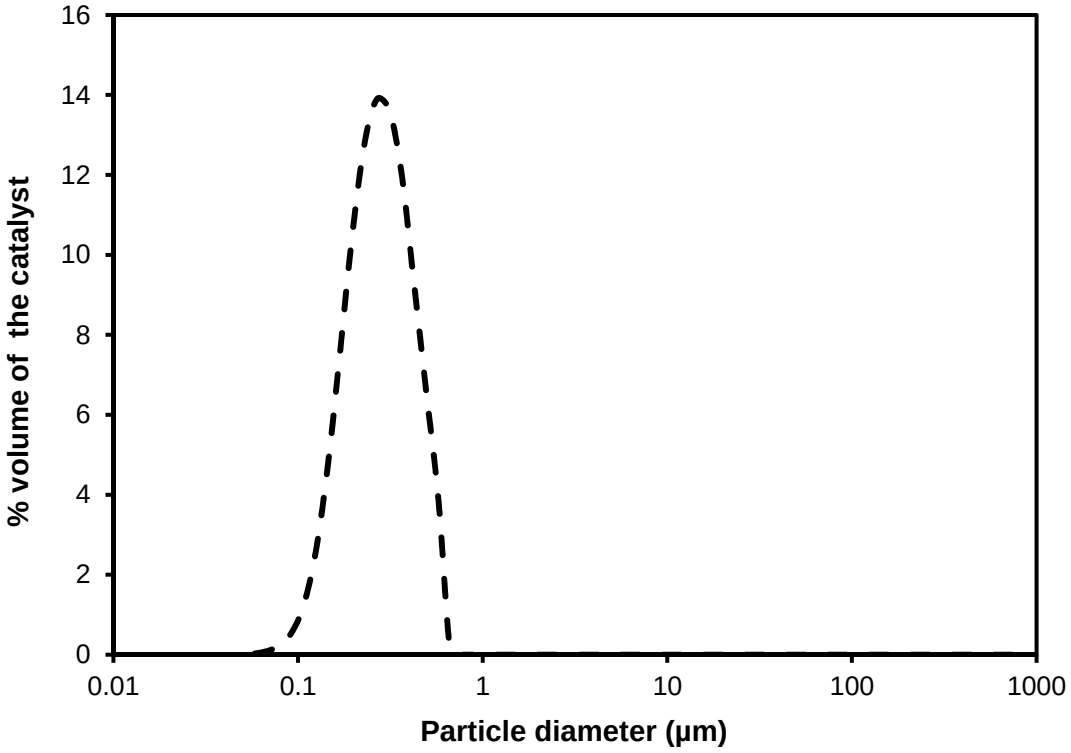

Figure 4.22. The particle size distribution (PSD) of $Cs_{2.5}H_{0.5}PW_{12}O_{40}$ catalyst.

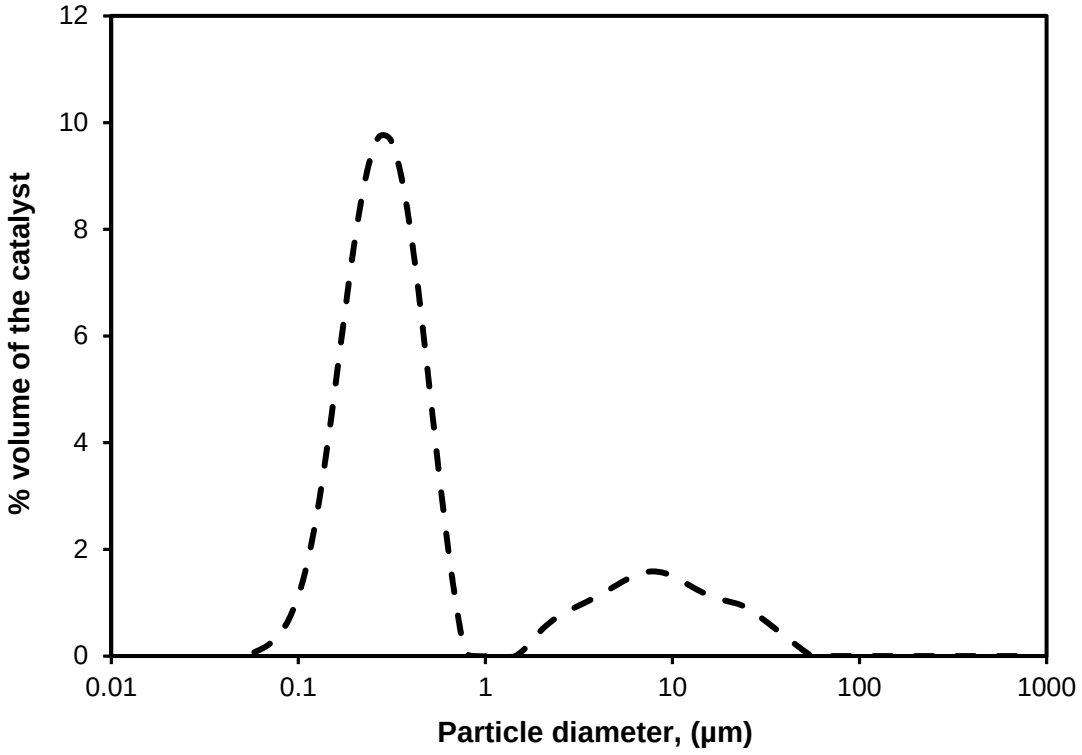

Figure 4.23. The particle size distribution (PSD) of $Cs_{2.5}H_{0.5}PW_{12}O_{40}$ (calcined) catalyst.

Figures 4.24 - 4.30 show the results for Amberlyst 15, Purolite CT-122, Purolite CT-169, Purolite CT-175, Purolite CT-275, Purolite D5081 and Purolite D5082. Amberlyst 15 shows a wide distribution of particles (Figure 4.24), ranging from 210 - 1200 µm. From the distribution, approximately 1% (w/w) of the catalyst was measured to be more than 1000 µm in diameter and 0.4% (w/w) had less than 300 µm in diameter. A majority of the particles (~93% (w/w)) falls within the range of 500 - 1200 µm. In comparison with the other catalysts analysed using sieve analysis, Purolite CT-122 (Figure 4.25) was found to have the narrowest PSD, where the range of particle size lies between 500 - 1000 µm. Nearly 89% (w/w) of the total particles comes between the range of 600 - 1000 µm. Approximately 11% (w/w) of the Purolite CT-122 catalyst was measured to be less than 600 µm in diameter. For Purolite CT-169 (Figure 4.26), the particles are well distributed within the range of 300 - 1000 µm. A majority of particles (88% (w/w)) lie within 500 - 1000 µm. Purolite CT-175 (Figure 4.27) catalyst show very similar distributions to Amberlyst 15, although the distribution is slightly narrower (300 - 1200 µm) than Amberlyst 15.

From the distribution, approximately 2% (w/w) of the catalyst was measured to be more than 1000 µm in diameter and 3% (w/w) having less than 500 µm in diameter. 700 µm sieve was found to retain the largest amount of particles (42% (w/w)). A good distribution of particles was also observed for Purolite CT-275 in Figure 4.28. 500 µm sieve size was found to retain the largest amount of particles (35% (w/w)) whereas the percent retention for the other three sieves are similar (420 µm - 17% (w/w); 600 µm - 19% (w/w) and 710 µm - 23% (w/w)). For Purolite D5081 (Figure 4.29), the highest percentage of particles was observed between the range of 355 - 710 µm (85% (w/w)). 1.7% (w/w) catalyst lies within the range of 210 - 355 µm and the rest (13.3% (w/w)) was higher than 710 µm. The distribution pattern for Purolite D5082 (Figure 4.30) catalyst was similar to Purolite CT-169 with both catalysts having the same range of distribution from 300 - 1000 µm. Particles retained in 500 and 600 µm sieve are 33% (w/w) and 30% (w/w), respectively. The other 30% (w/w) of catalyst falls below 500 µm and another 7% (w/w) particles are higher than 710 µm in diameter.

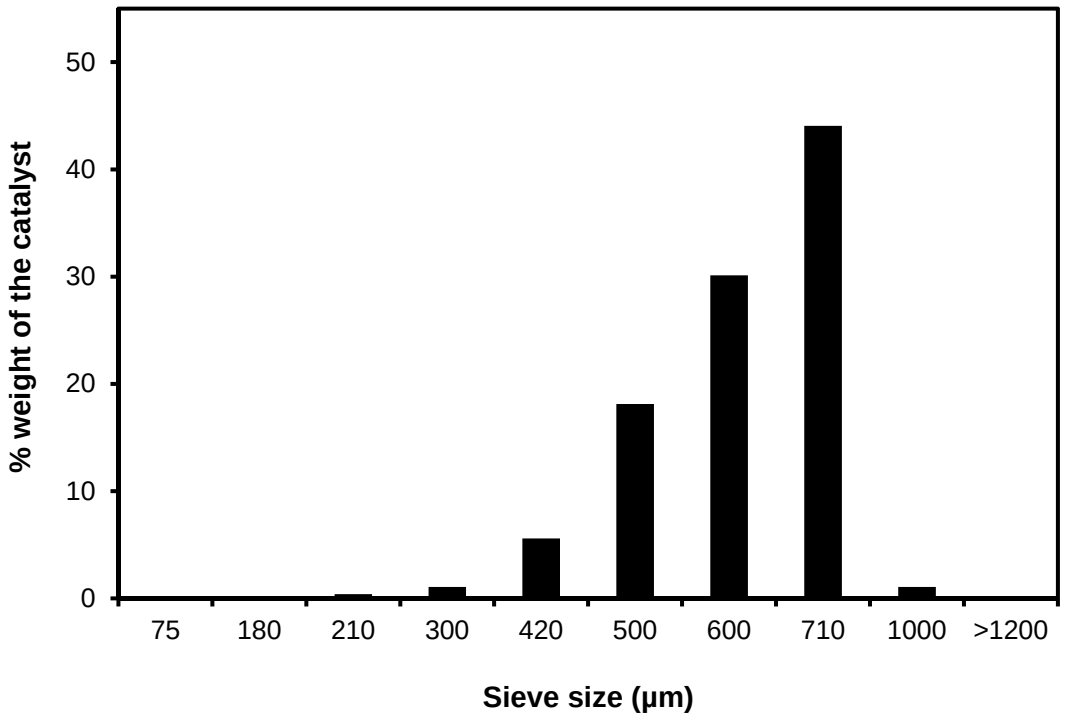

Figure 4.24. The particle size distribution (PSD) of Amberlyst 15 catalyst.

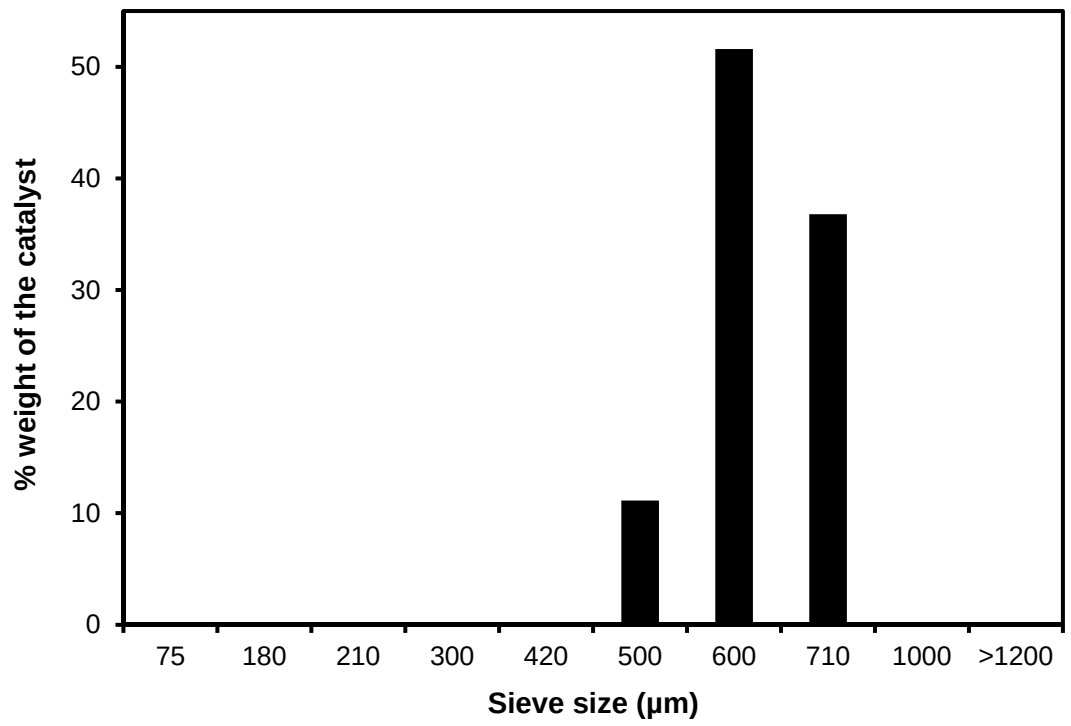

Figure 4.25. The particle size distribution (PSD) of Purolite CT-122 catalyst.

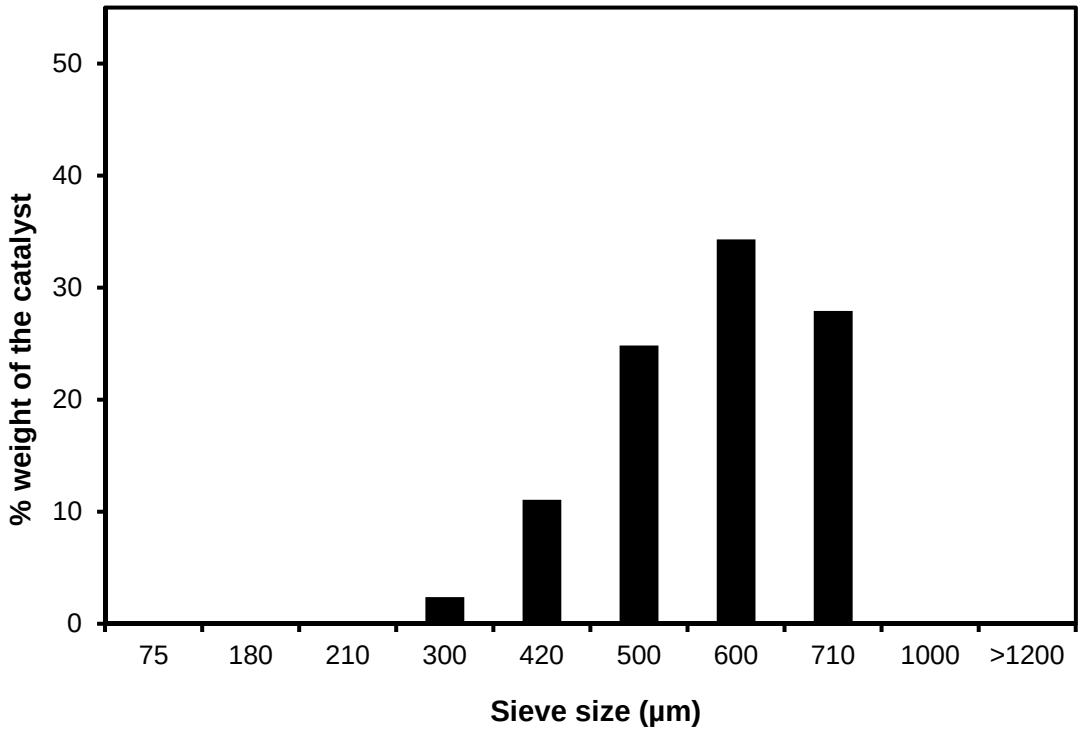

Figure 4.26. The particle size distribution (PSD) of Purolite CT-169 catalyst.

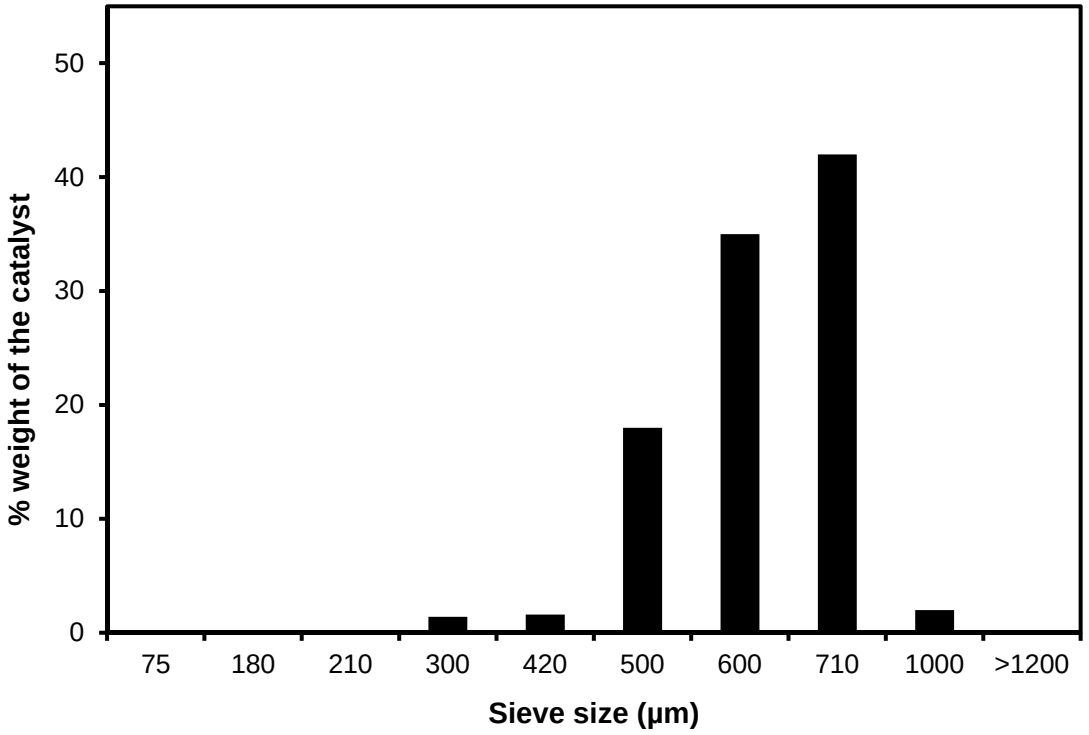

Figure 4.27. The particle size distribution (PSD) of Purolite CT-175 catalyst.

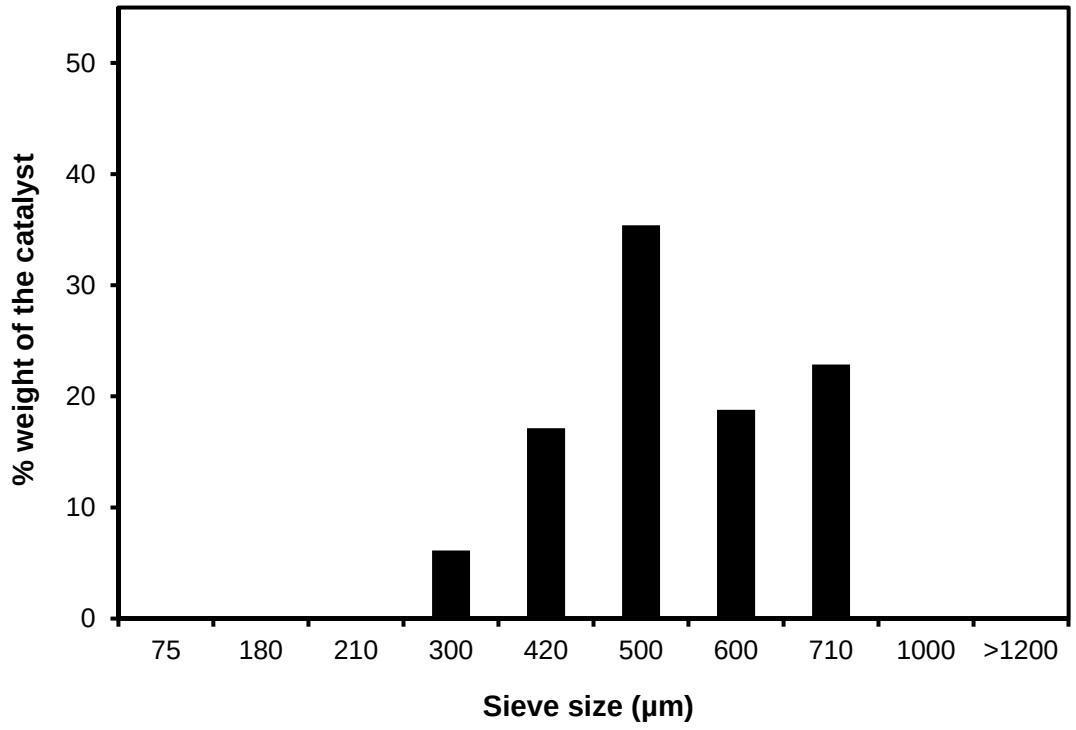

Figure 4.28. The particle size distribution (PSD) of Purolite CT-275 catalyst.

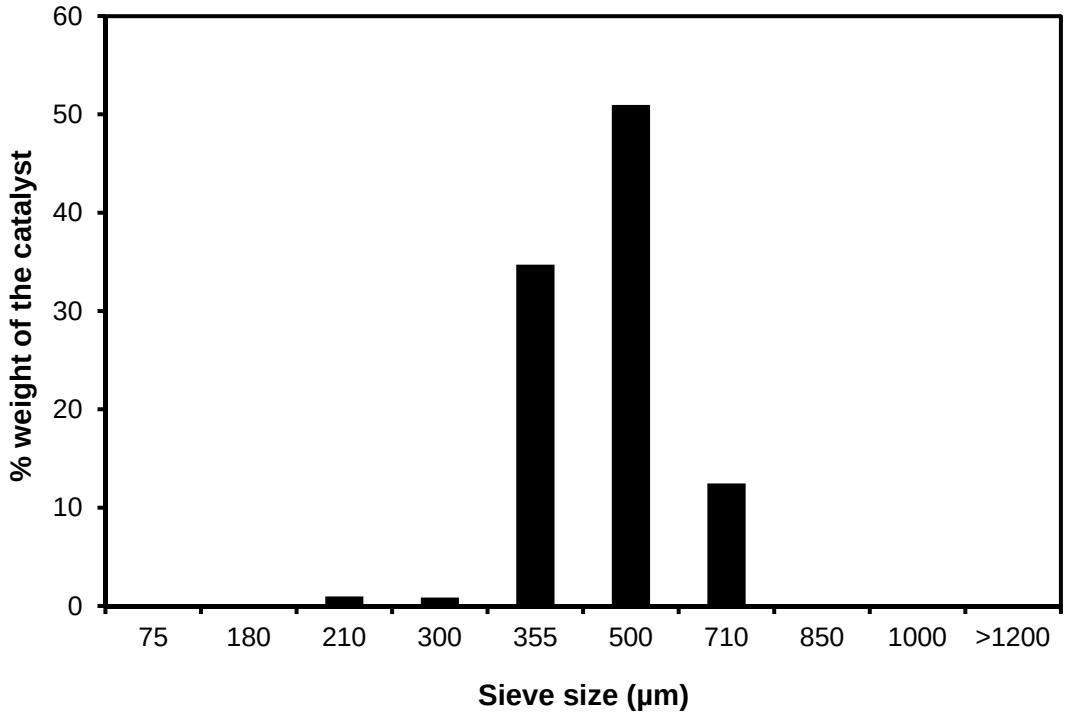

Figure 4.29. The particle size distribution (PSD) of Purolite D5081 catalyst.

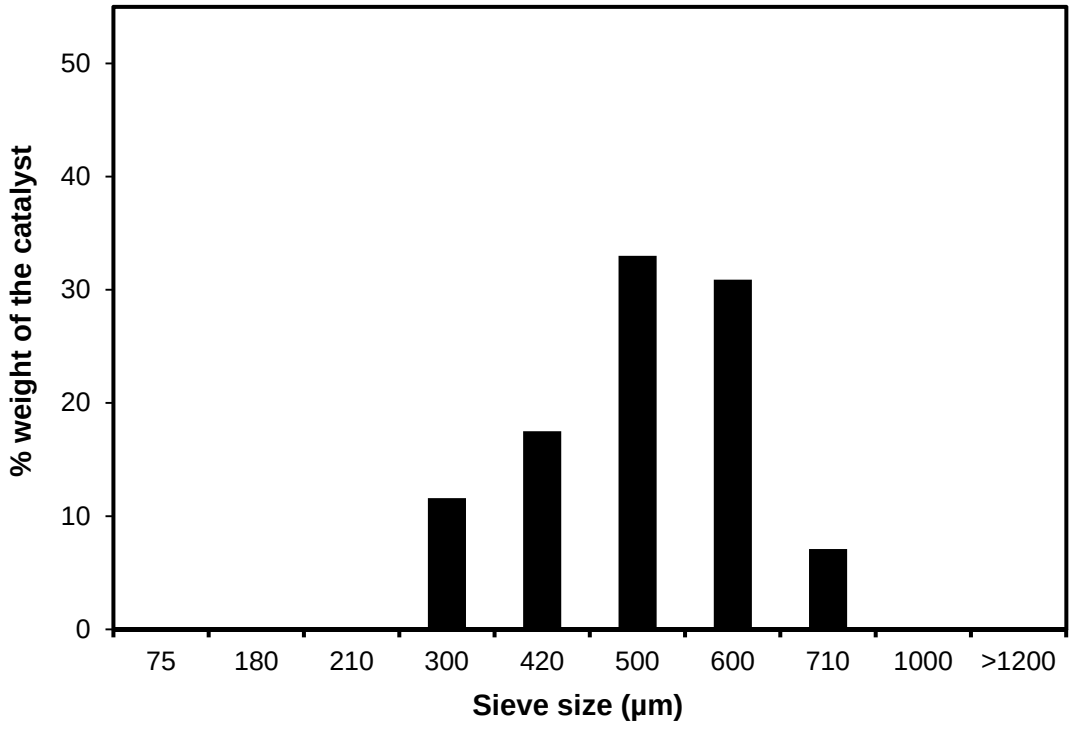

Figure 4.30. The particle size distribution (PSD) of Purolite D5082 catalyst.

4.7 DETERMINATION OF SURFACE AREA, TOTAL PORE VOLUME AND AVERAGE PORE DIAMETER

The results for surface area, average pore diameter and total volume are presented in Table 4.7. It was not possible to obtain the surface area for Purolite CT-122 and Diaion PA306s as the gelular matrix structure of the polymeric resin collapsed during the analysis. Purolite D5081 and Purolite D5082 catalysts have the highest surface areas of 514.2 m^2 g^{-1} and 459.6 m^2 g^{-1} respectively. This was followed by Cs-supported heteropolyacids catalysts [135.1 m^2 g^{-1} for $Cs_{2.5}H_{0.5}PW_{12}O_{40}$ and 119.26 m^2 g^{-1} for $Cs_{2.5}H_{0.5}PW_{12}O_{40}$ (calcined)]. The rest of the catalysts have a similar specific surface area ranging from 20 - 60 m^2 g^{-1}. Purolite D5081 was also found to have the highest total pore volume (0.47 cm^3 g^{-1}), whereas the Cs-supported heteropolyacids catalysts (both calcined and non calcined catalyst) were found to have the lowest total pore volume [0.09 cm^3 g^{-1} for $Cs_{2.5}H_{0.5}PW_{12}O_{40}$ and 0.08 cm^3 g^{-1} for $Cs_{2.5}H_{0.5}PW_{12}O_{40}$(C)]. For average pore diameter analysis, the Cs-supported heteropolyacids catalyst was found to have the lowest average pore diameter [2.57 nm for $Cs_{2.5}H_{0.5}PW_{12}O_{40}$ and 2.64 nm for $Cs_{2.5}H_{0.5}PW_{12}O_{40}$ (calcined)], whilst the highest average pore diameter belongs to CT-169 (27.42 nm).

Table 4.7. Surface area, average pore diameter and total pore volume of studied catalysts.

Catalyst	BET Surface Area(m^2 g^{-1})	Average pore diameter (nm)	Total Pore Volume (cm^3 g^{-1})
Amberlyst 15	45.65	25.39	0.31
$Cs_{2.5}H_{0.5}PW_{12}O_{40}$	135.10	2.57	0.09
$Cs_{2.5}H_{0.5}PW_{12}O_{40}$ (calcined)	119.26	2.64	0.08
Diaion PA306s	#	#	#
Purolite CT-122	#	#	#
Purolite CT-169	37.97	27.42	0.27
Purolite CT-175	23.77	17.37	0.108
Purolite CT-275	20.9	19.60	0.108
Purolite D5081	514.18	3.69	0.47
Purolite D5082	459.62	3.14	0.36

#Data could not be measured

4.8 SUMMARY OF CHEMICAL AND PHYSICAL PROPERTIES OF BIODIESEL CATALYSTS

Physical and chemical properties of esterification and transesterification catalysts are summarised in Tables 4.8 and 4.9, respectively.

Table 4.8. Physical and chemical properties of catalyst used for the esterification process.

Catalyst Properties	Purolite D5081	Purolite D5082	Amberlyst 15
Physical Appearance	Opaque spherical beads	Opaque spherical beads	Opaque spherical beads
Functional Group	Sulfonic acid	Sulfonic acid	Sulfonic acid
Moisture Capacity (%H^+)*	56.9	56.2	52-57
Polymer structure	Macroporous Polystyrene cross-linked DVB	Macroporous Polystyrene cross-linked DVB	Macroporous Polystyrene cross-linked DVB
Cross-linking level	Highly cross-linked	Highly cross-linked	Medium cross-linked
Temperature limit (K)*	393	393	393
BET Surface Area (m^2 g^{-1})	514.18	459.62	53
Total Pore Volume (cm^3 g^{-1})	0.47	0.36	0.4
Average pore diameter (nm)	3.69	3.14	30
True Density (g cm^{-3})	1.309	1.373	1.027

* Manufacturer data

Table 4.9. Physical and chemical properties of catalysts used for transesterification process.

Catalyst Properties	**Purolite CT-122**	**Purolite CT-169**	**Purolite CT-175**	**Purolite CT-275**
Physical Appearance	Golden spherical beads	Opaque spherical beads	Opaque spherical beads	Opaque spherical beads
Functional Group	Sulfonic acid	Sulfonic acid	Sulfonic acid	Sulfonic acid
Moisture Capacity (%H^+)*	78 - 82	51 - 57	50 - 57	51 - 59
Polymer structure	Gelular Polystyrene cross-linked DVB	Macroporous Polystyrene cross-linked DVB	Macroporous Polystyrene cross-linked DVB	Macroporous Polystyrene cross-linked DVB
Cross-linking level	Low cross-linked	Medium cross-linked	Highly cross-linked	Highly cross-linked
Temperature limit, (K)*	403	393	418	418
BET Surface Area, (m^2 g^{-1})	#	37.97	23.77	20.9
Total Pore Volume (cm^3 g^{-1})	#	0.27	0.108	0.108
Average pore diameter (nm)	#	27.42	17.37	19.6
True Density (g cm^{-3})	1.297	1.297	1.296	1.296

* Manufacturer data, #Data could not be measured

Table 4.9. (continued) Physical and chemical properties of catalysts used for transesterification process.

Catalyst Properties	Purolite D5081	Diaion PA306s	$Cs_{2.5}H_{0.5}PW_{12}O_{40}$	$Cs_{2.5}H_{0.5}PW_{12}O_{40}$ (calcined)
Physical Appearance	Opaque spherical beads	White beads	Opaque spherical beads	Opaque spherical beads
Functional Group	Sulfonic acid	Quaternary ammonium	b	b
Moisture Capacity (%H^+)*	56.9	66 - 76	a	a
Polymer structure	Macroporous Polystyrene cross-linked DVB	Gelular Polystyrene cross-linked DVB	b b	b b
Cross-linking level	Highly cross-linked	Low cross-linked	b	b
Temperature limit, (K)*	393	333	a	a
BET Surface Area (m^2 g^{-1})	514.18	#	135.10	119.26
Total Pore Volume (cm^3 g^{-1})	0.47	#	0.09	0.08
Average pore diameter (nm)	3.69	#	2.57	2.64
True Density (g cm^{-3})	1.309	1.297	6.296	6.281

*Manufacturer data, [a]Data not available, [b]Data not applicable, [#]Data could not be measured

4.9 CONCLUSIONS

In this chapter, the physical and chemical characterisation of biodiesel catalysts have been carried out and discussed in detail. The FEG-SEM analysis shows the morphology of esterification and transesterification catalysts. For cation exchange resin catalysts, the gelular polymer matrix shows a collapsed surface surrounded with hair line cracks whereas for macroporous resin, a more open structure can be seen with a smooth and highly porous surface. In contrast with gelular cation exchange resins, the gelular anion resin Diaion PA306s was found to have a special gel matrix with extended porous structure, having a tiny-hole-like surface with large numbers of pores. For Cs-supported heteropolyacids catalysts, an irregular shape and size of heteropolyacids particles was observed to randomly distribute over the support surfaces, Cs salts.

From the elemental analysis results, analysis between the esterification catalysts shows that Purolite D5081 has the highest amount of carbon (77.04%) whereas Amberlyst 15 has the highest proportion of hydrogen (6.12%), sulphur (16.17%) and oxygen (24.52%) as compared to other esterification catalysts. For the transesterification catalysts, Diaion PA306s was found to have the highest amount of carbon (55.59%) and hydrogen (9.42%) whereas Purolite CT-275 was found to have the highest amount of sulphur (16.62%) and oxygen (34.20%) as compared to other transesterification catalysts. In addition, with the presence of quaternary amine group in Diaion PA306s catalyst, 4.34% of nitrogen was detected from Diaion PA306s catalyst.

From the FT-IR spectroscopy analysis, all catalysts came out with expected functional groups in their individual spectra such as sulfonic acid and quaternary amine group for cation and anion exchange resin, respectively. The results from PSD measurements show that both Cs-supported heteropolyacids and anion exchange resin catalysts give smaller distribution of particle size as compared to cation exchange resin catalysts. True density measurement for esterification catalysts shows that Purolite catalysts i.e. Purolite D5081 and Purolite D5082 have comparably the same values of densities which were approximately 1.3 g cm^{-3} and Amberlyst 15 has a slightly lower density, i.e. 1.027 g cm^{-3}. For transesterification catalysts, Cs-supported heteropolyacids catalysts [$Cs_{2.5}H_{0.5}PW_{12}O_{40}$ and $Cs_{2.5}H_{0.5}PW_{12}O_{40}$ (calcined)] were found to have the highest densities (6.3 g cm^{-3} and 6.4 g cm^{-3}) while the rest of transesterification catalysts have similar densities, ca. 1.2 g cm^{-3}.

Results from the surface area measurement show that Purolite D5081 has the highest BET surface area (514.2 m^2 g^{-1}) and total pore volume (0.47 cm^3 g^{-1}) whereas Amberlyst 15 shows the highest average pore diameter (25.39 nm) among all the esterification catalysts investigated. For the transesterification catalyst, the highest average pore diameter (27.42 nm) and total pore volume (0.27 cm^3 g^{-1}) belongs to Purolite CT-169 whereas the highest BET surface area (135.10 m^2 g^{-1}) belongs to Cs-supported heteropolyacids catalyst, $Cs_{2.5}H_{0.5}PW_{12}O_{40}$. It was not possible to

obtain the surface area for Purolite CT-122 and Diaion PA306s as the gelular matrix structure of the polymeric resin collapsed during the analysis.

The information on catalyst characterisation is very important since they serve as a fundamental knowledge on the chemical and physical properties of the catalysts. This information is used later to elucidate the relationship between the catalytic performance and the physical and chemical properties of the catalyst. In the next chapter (Chapter 5), the development of analytical techniques is carried out to determine the component and composition of used cooking oil (UCO), followed by the characterisation of UCO via chemical and physical characterisation methods.

5 DEVELOPMENT OF ANALYTICAL TECHNIQUES AND PHYSICAL AND CHEMICAL CHARACTERISATION OF USED COOKING OIL (UCO)

5.1 INTRODUCTION

This chapter is divided into two sections. The first section focuses on the development of analytical techniques to determine the component and composition of used cooking oil (UCO) and the second section presents the characterisation of UCO using chemical and physical characterisation method. In the first section, determination of components in the feedstock, development of a calibration curve for all standards, quantification of fatty acids in the UCO and a study on the ageing of the standards were carried out. In the second section, results on the characterisation of the UCO was presented including the determination of the acid value and free fatty acids (FFA) content, moisture content analysis, triglycerides, diglycerides and monoglycerides analysis and bulk density measurement.

5.2 QUANTITATIVE ANALYSIS OF FATTY ACIDS COMPOSITION USING GAS CHROMATOGRAPHY-MASS SPECTROMETRY (GC-MS)

5.2.1 Introduction

There are several analytical methods that can be used for the identification and quantification of components in fats and oil. These techniques include the application of high performance liquid chromatography-mass spectrometry (HPLC-MS), size exclusion chromatography-mass spectrometry (SEC-MS), ^{1}H-nuclear magnetic resonance (^{1}H-NMR) and gas chromatography-mass spectrometry (GC-MS). GC-MS is one of the popular techniques to allow the identification and quantification of individual component in fats and oils. It is a very reliable method, fast, easy to conduct and widely used to analyse the content of fats and oils (Li *et al.*, 2008). Several works have been carried out to develop a faster and more reliable method (Bading and De Jong, 1983; Cruz-Hernandez and Destaillats, 2009). Cruz-Hernandez and Destaillats (2009) developed a gas chromatography (GC) method by modifying the length of the GC column and the film thickness of the GC

column. They claimed that this new method offers many key advantages including increased sample throughput, reduced analytical expenses and increased laboratory productivity. A comprehensive method for both short and long chain fatty acid characterisation in lipids has also been studied by Bading and De Jong (1983). In most cases, a capillary column was chosen instead of a packed column, as this type of column would give more reliable and accurate results (Slover and Lanza, 1979).

The UCO and biodiesel are categorised as one of the lipid derivatives. Therefore, their compositions are very complex. A very precise and appropriate method is required to analyse their content. There are two main steps involved in fatty acid analysis. First step is the preparation of fatty acids to fatty acid methyl ester (FAME) and the second step is the quantification of FAME by GC-MS. The preparation of FAME is very important to determine the composition of fatty acids in the given sample. The derivatisation method can be performed either by hydrolysis or methylation. The most popular method is by the derivatisation of fatty acids to FAME by methylation (David *et al.*, 2005). This method is well accepted due to the robustness and reproducibility of the chromatographic data. In addition, this method requires less reagents and no expensive equipment. FFA can also be detected directly by using polar stationary phase (such as a HP-FFAP column). However, this method is least favoured as compared to the derivatisation method because it is only specific to the FFA content (David *et al*., 2005).

In GC-MS analysis, the compound is determined by injection of pure standard in a reproducible condition. Each component will have their own retention time and usually came out as an absolute peak, unless there are peaks that have a very close retention times or the columns are not capable to separate the components, it will come out as a shoulder or a very broad peak. Quantification of chromatographic data is conducted to measure the amount/concentration of each component inside the sample. There are several methods for analysing GC-MS results such as normalisation, normalisation with response factor, external standard and internal standard. The external and the internal standardisation techniques are the most popular (Grob and Barry, 2004). In the external standard method, the

chromatographic analysis of the standard and the sample are carried out separately under exactly the same conditions. The area of the component in the standard is compared with the area of component in the sample to determine the concentration of the component. On the other hand, in the internal standard method, a chosen reference standard, also known as internal standard is added directly to the sample being analysed and the area of the component peak is compared to the area of the internal standard to determine its composition. The internal standard method was found to give more accurate results as compared to the external standard method. However, selection of a suitable compound as an internal standard is a challenge (Grob and Barry, 2004). There are several requisition of selecting internal standard including that it must be miscible with the samples being analysed, must elute from the column, must be within the analysed samples peak, preferably similar with the functional group type of the sample of interest and that it must be adequately separated from all the samples components. Furthermore, the standard also needs to be non-reactive towards any component in the samples and able to withstand the same analytical condition as the sample of interest. As a result, methyl heptadecanoate was chosen as an internal standard and was used throughout the analysis.

In this work, a new, fast and simple GC-MS method was developed to characterise the properties of the UCO and biodiesel. The objectives of this section are four-fold: (i) to identify the biodiesel components, (ii) to obtain the response factor for each component, (iii) to quantify the UCO composition and (iv) to study the influence of standard ageing to the FAME composition.

5.2.2 Chromatogram Analysis of Derivatised UCO

Figure 5.1 shows the chromatogram of the derivatised UCO sample. From the chromatogram, all the main components in the samples were identified and they were completely separated and eluted from each other. For the purpose of clarity, the solvent peaks (*n*-hexane and methanol) are not shown in Figure 5.1. Methyl palmitate appears at a retention time of 8.324 min followed by methyl heptadecanoate (C17:0 – internal standard) which appeared at a retention time of

8.950 min. Methyl stearate (C18:0), methyl oleate (C18:1) and methyl linoleate (C18:2) peaks appears at a retention time of 9.712, 9.914 and 10.349 min respectively. Finally, methyl linolenate (C18:3) appears at a retention time of 11.005 min. As the methylation process converts fatty acids to FAME by derivatisation, it could be concluded that there are five main components present in the UCO, namely palmitic acid, stearic acid, oleic acid, linoleic acid and linolenic acid. All the five FAME components along with methyl heptadecanoate (internal standard) were verified using MS which are presented in Figures 5.2 – 5.7.

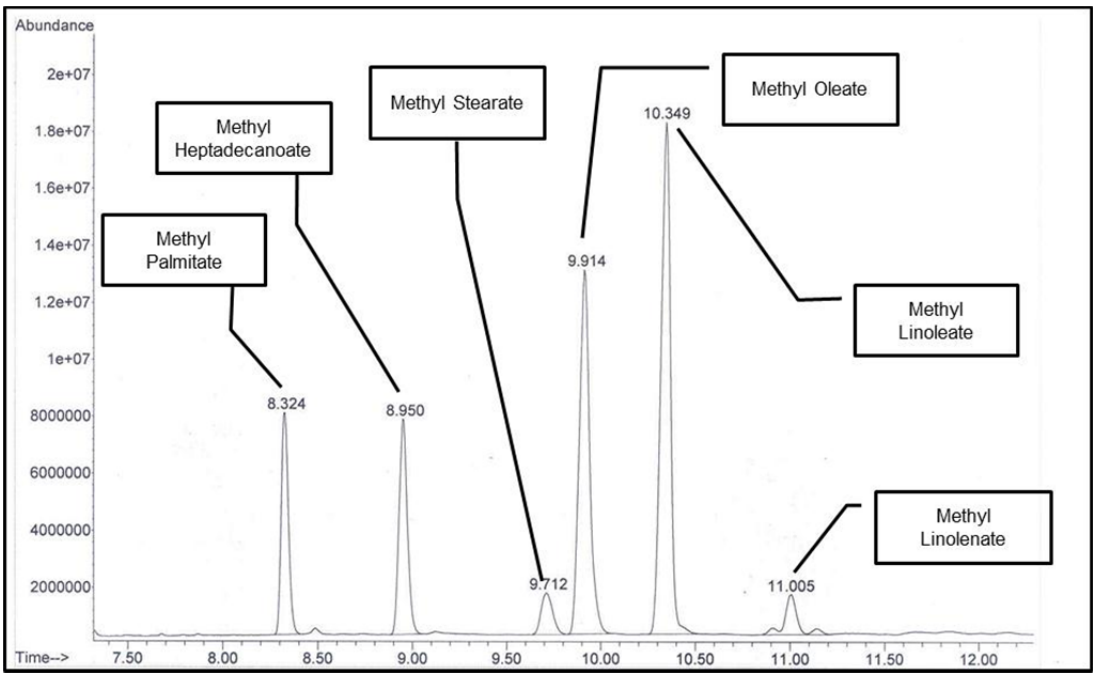

Figure 5.1. A typical chromatogram of the derivatised UCO.

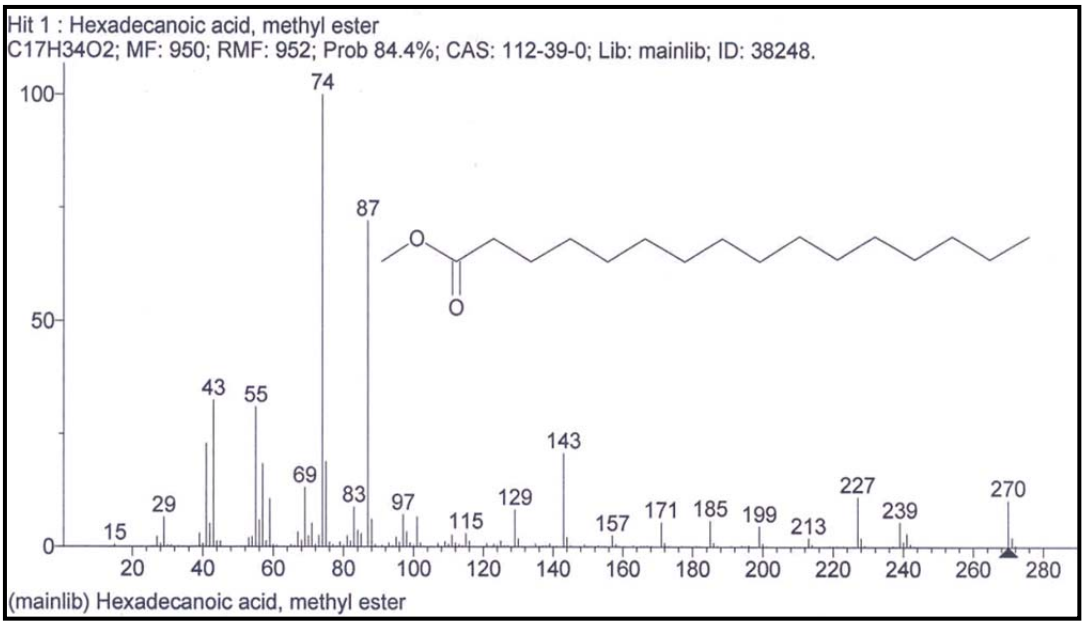

Figure 5.2. An image of MS result obtained from MS library (Component: Methyl Palmitate).

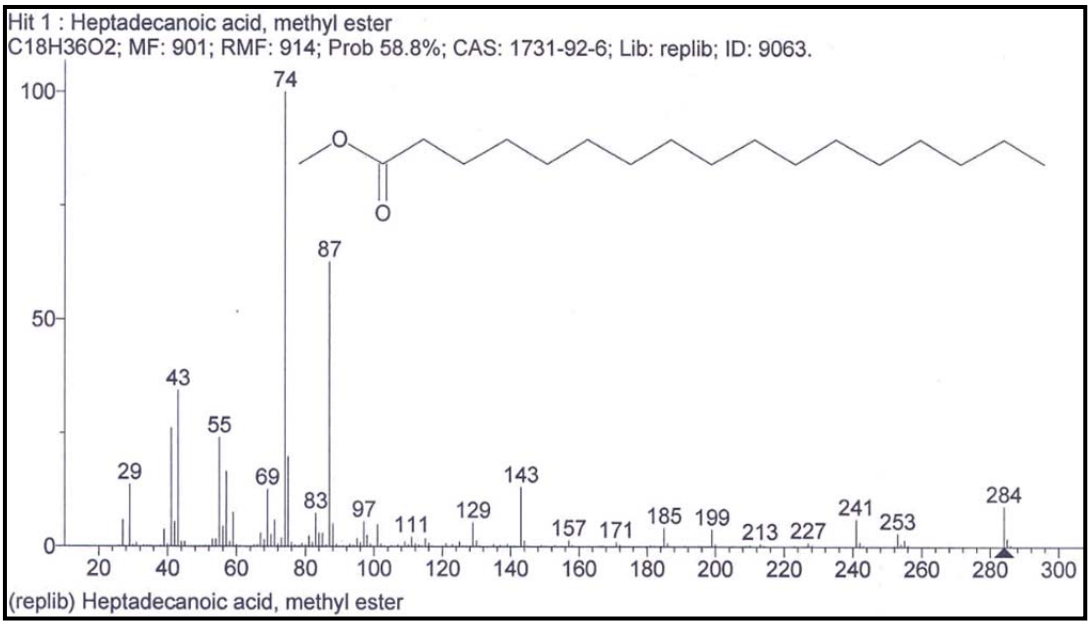

Figure 5.3. An image of MS result obtained from MS library (Component: Methyl Heptadecanoate –Internal Standard).

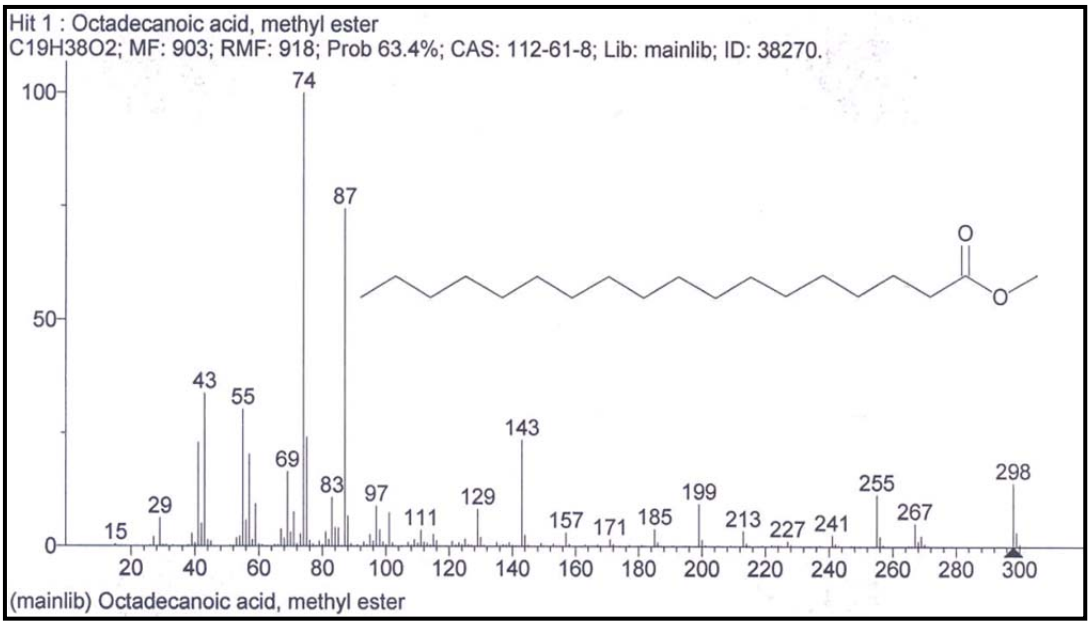

Figure 5.4. An image of MS result obtained from MS library (Component: Methyl Stearate).

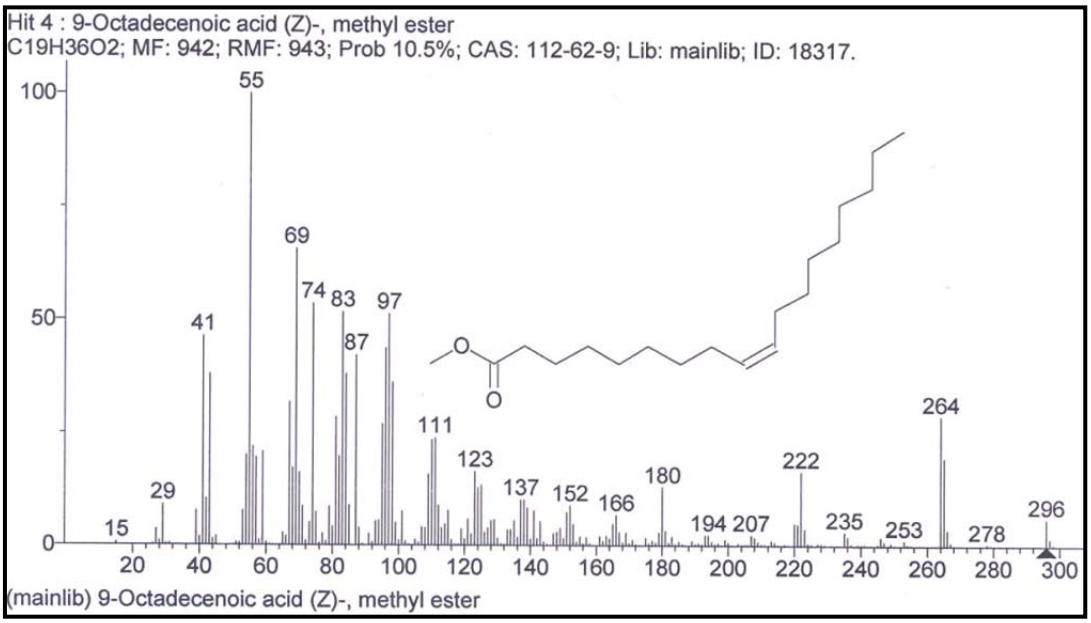

Figure 5.5. An image of MS result obtained from MS library (Component: Methyl Oleate).

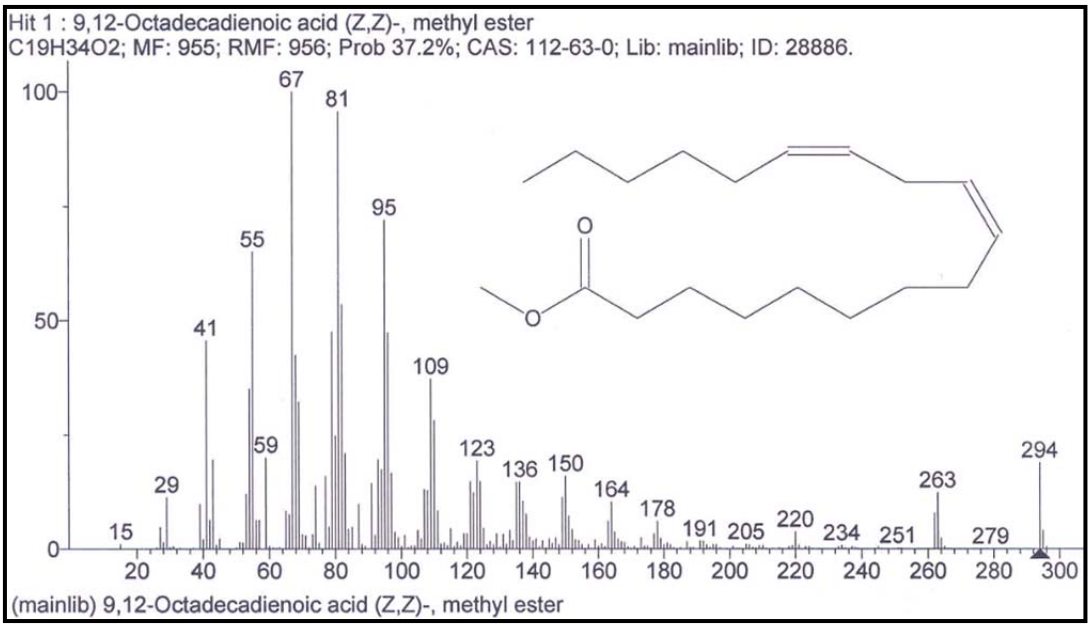

Figure 5.6. An image of MS result obtained from MS library (Component: Methyl Linoleate).

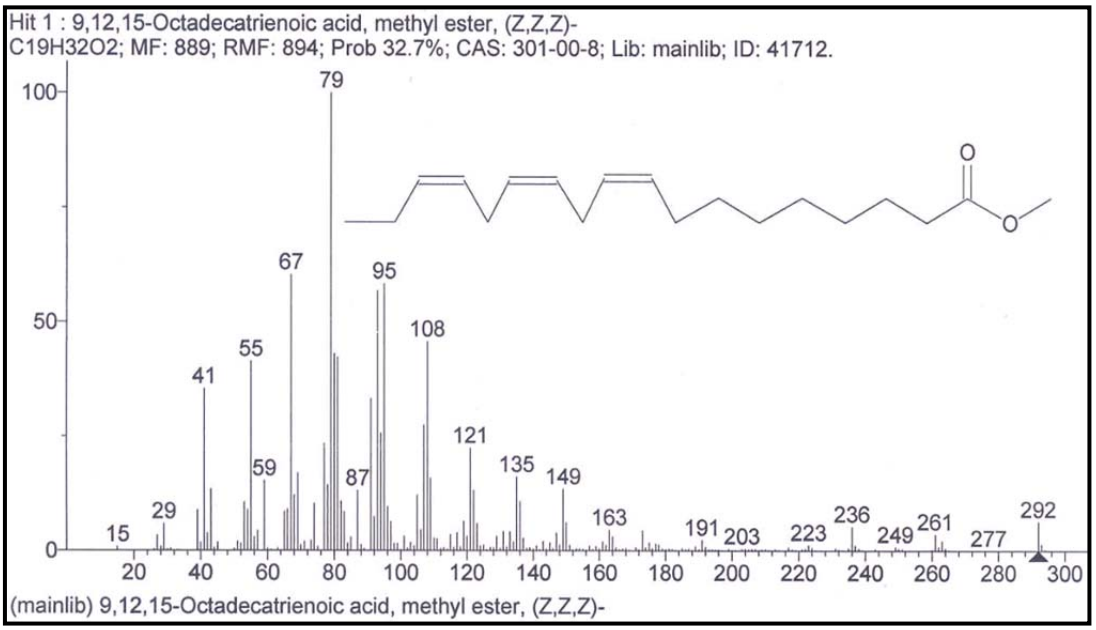

Figure 5.7. An image of MS result obtained from MS library (Component: Methyl Linolenate).

5.2.3 Calibration Curve for Individual Standards

Figures 5.8 – 5.12 show the calibration curves for all the FAME standards, whilst Table 5.1 summarises the linear equation, r-squared values and response factor for all

the five components. The results show a very consistent response factor and r-squared values (> 0.99) for all the species. The resulting response factors were used to determine the composition of fatty acids in the sample. The methylation process does not alter the fatty acids composition of the feedstock, thus the composition of FAME was assumed to be the same as the composition of fatty acids in the feedstock. Table 5.2 summarises the fatty acids composition in the UCO. Table 5.2 clearly shows that oleic and linoleic acid comprise more than 77% of the total fatty acids in the sample; palmitic acid content is 13.62% and the remaining fraction is comprised of linolenic acid (4.64%) and stearic acid (4.14%).

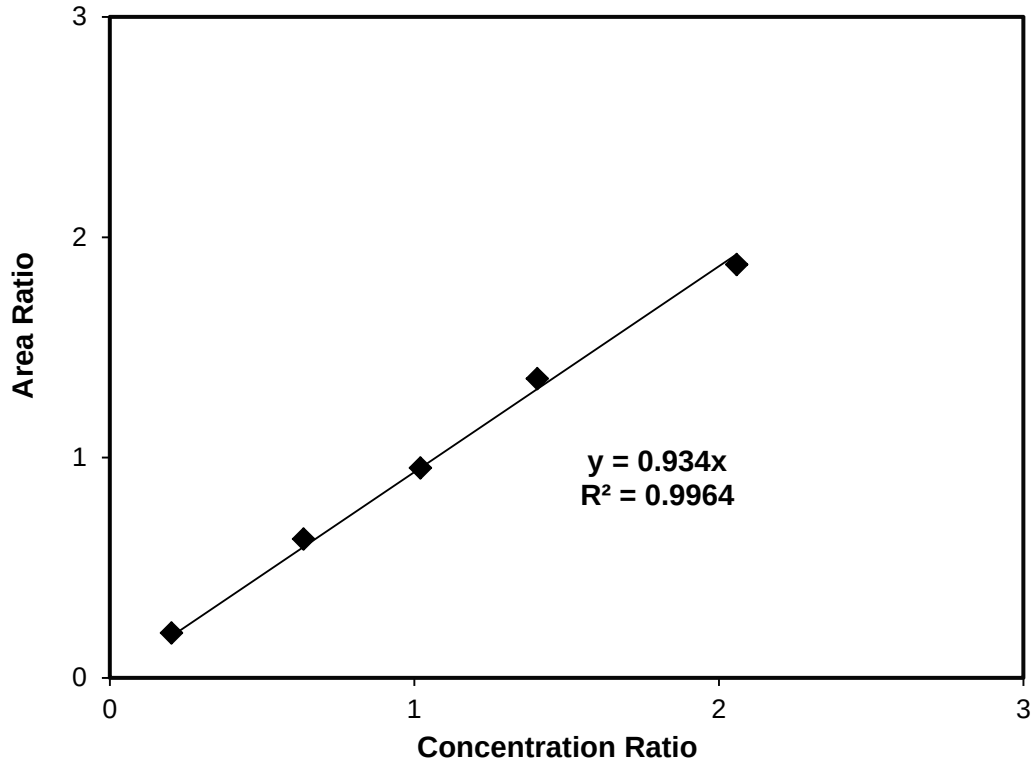

Figure 5.8. Calibration curve for methyl palmitate.

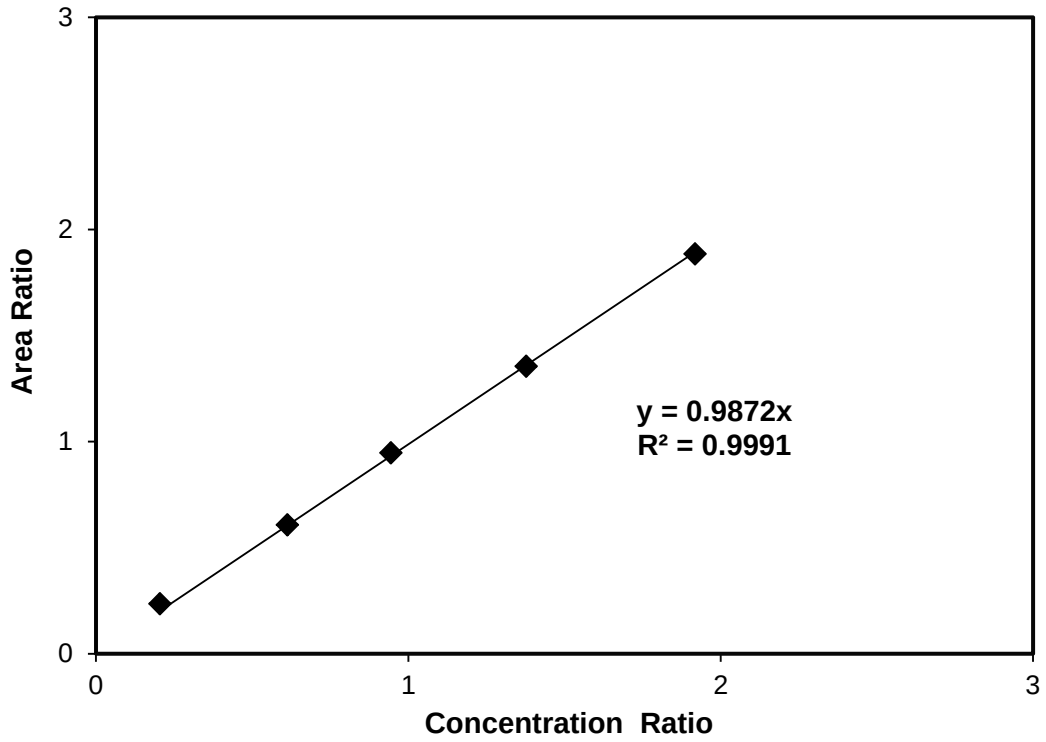

Figure 5.9. Calibration curve for methyl stearate.

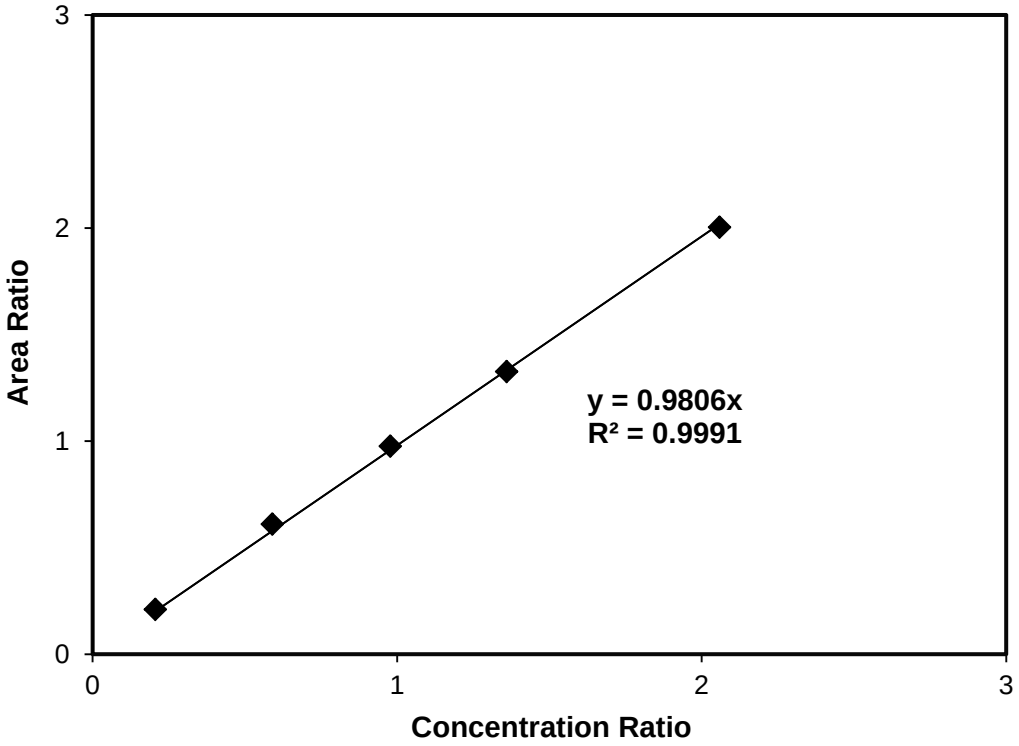

Figure 5.10. Calibration curve for methyl oleate.

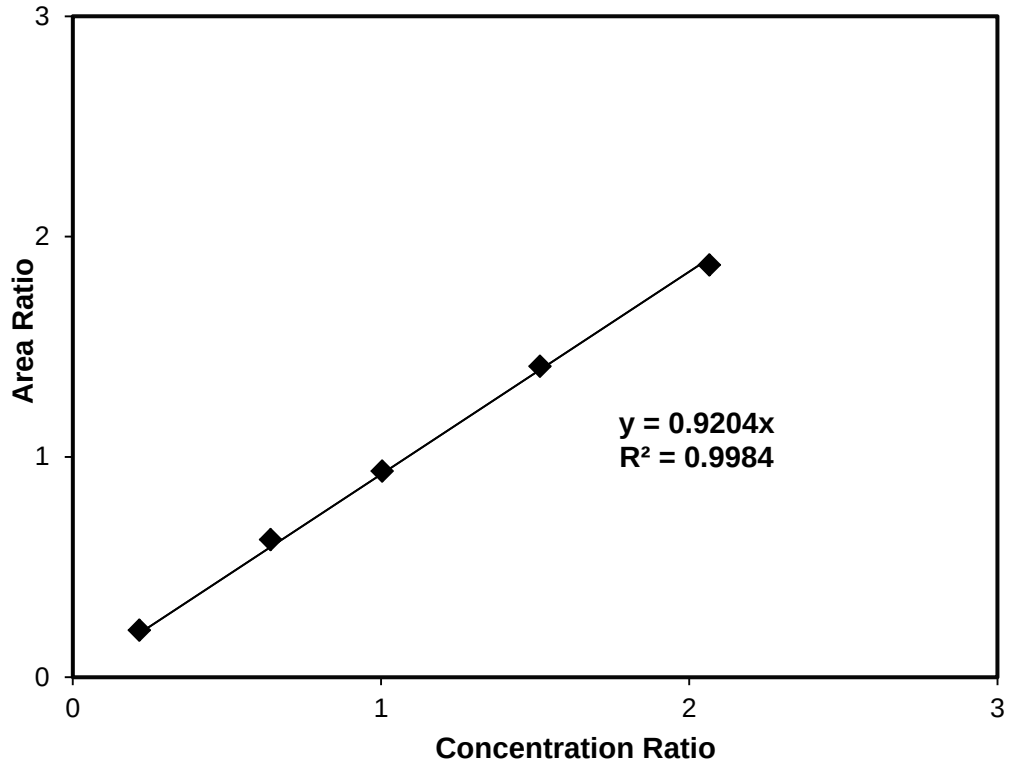

Figure 5.11. Calibration curve for methyl linoleate.

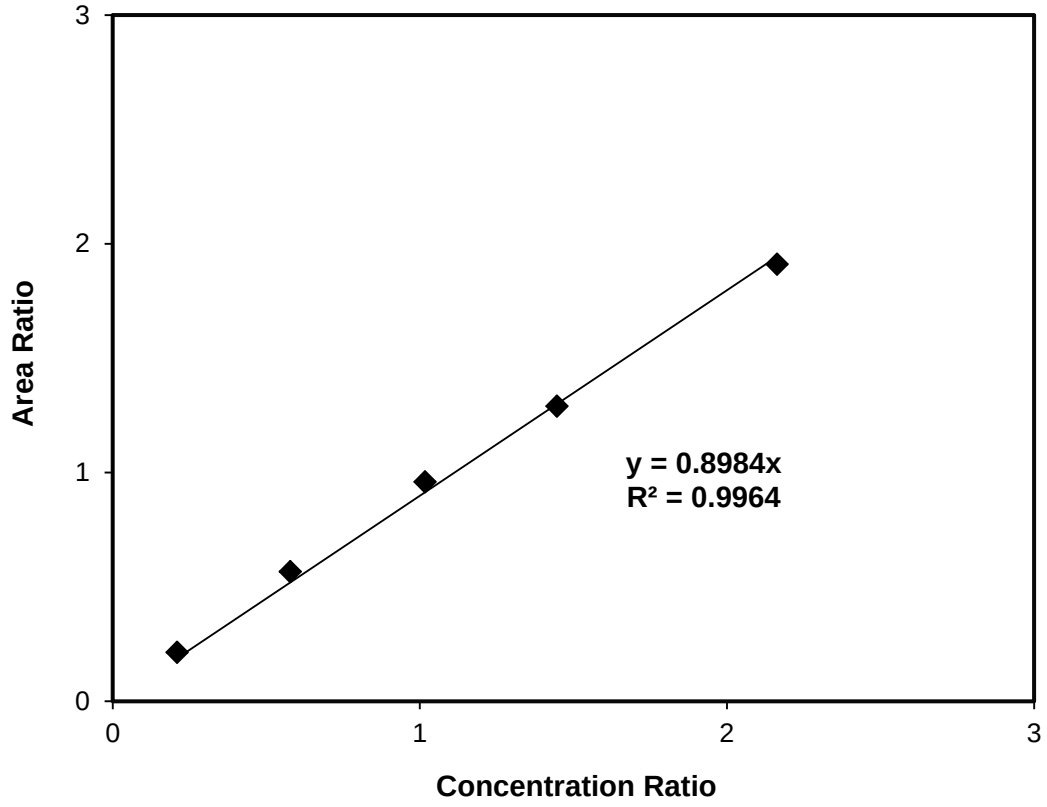

Figure 5.12. Calibration curve for methyl linolenate.

Table 5.1. Linear equation, R-squared values and response factor values for each component.

Component	Linear Equation	R-squared values	Response factor
Methyl Palmitate	$Y = 0.9340\,X$	0.9964	0.9340
Methyl Stearate	$Y = 0.9872\,X$	0.9991	0.9872
Methyl Oleate	$Y = 0.9806\,X$	0.9991	0.9806
Methyl Linoleate	$Y = 0.9204\,X$	0.9984	0.9204
Methyl Linolenate	$Y = 0.8984\,X$	0.9964	0.8984

Table 5.2. Composition of fatty acids in UCO.

Component	% Composition
Palmitic acid	13.62
Stearic acid	4.14
Oleic acid	33.75
Linoleic acid	43.85
Linolenic acid	4.64

5.2.4 Ageing of the Fatty Acid Methyl Ester (FAME) Standards

The ageing of the FAME standards over a time period was studied to check the reliability and reproducibility of the response factor. Fresh stock solutions of FAME standards were prepared and stored at -20°C. At regular time intervals covering over two weeks, mixtures of standards from stored FAME standards were prepared and injected in GC-MS. Response factors were monitored and the results are presented in Figure 5.13. It can be seen from Figure 5.13 that during the first few days of the ageing studies, the value of the response factor for all FAME standards were quite consistent and the error of each FAME standards were negligible. However, as the ageing studies continued over the second week, the difference was more significant especially in case of methyl palmitate, where the error in the response factor was found to be more than 20%. Results from the mass spectrometry indicate that the standards did not experience any decomposition, deterioration or formation of other compounds. Therefore, it was assumed that the situation might be due to the evaporation of the solvent over a number of days during the storage of individual FAME solutions. These errors in the response factor of FAME significantly affect the reliability of the calculated FAME content. Therefore, it was recommended to use standard solutions that were stored less than a week to obtain more accurate and reproducible results for all the experiments.

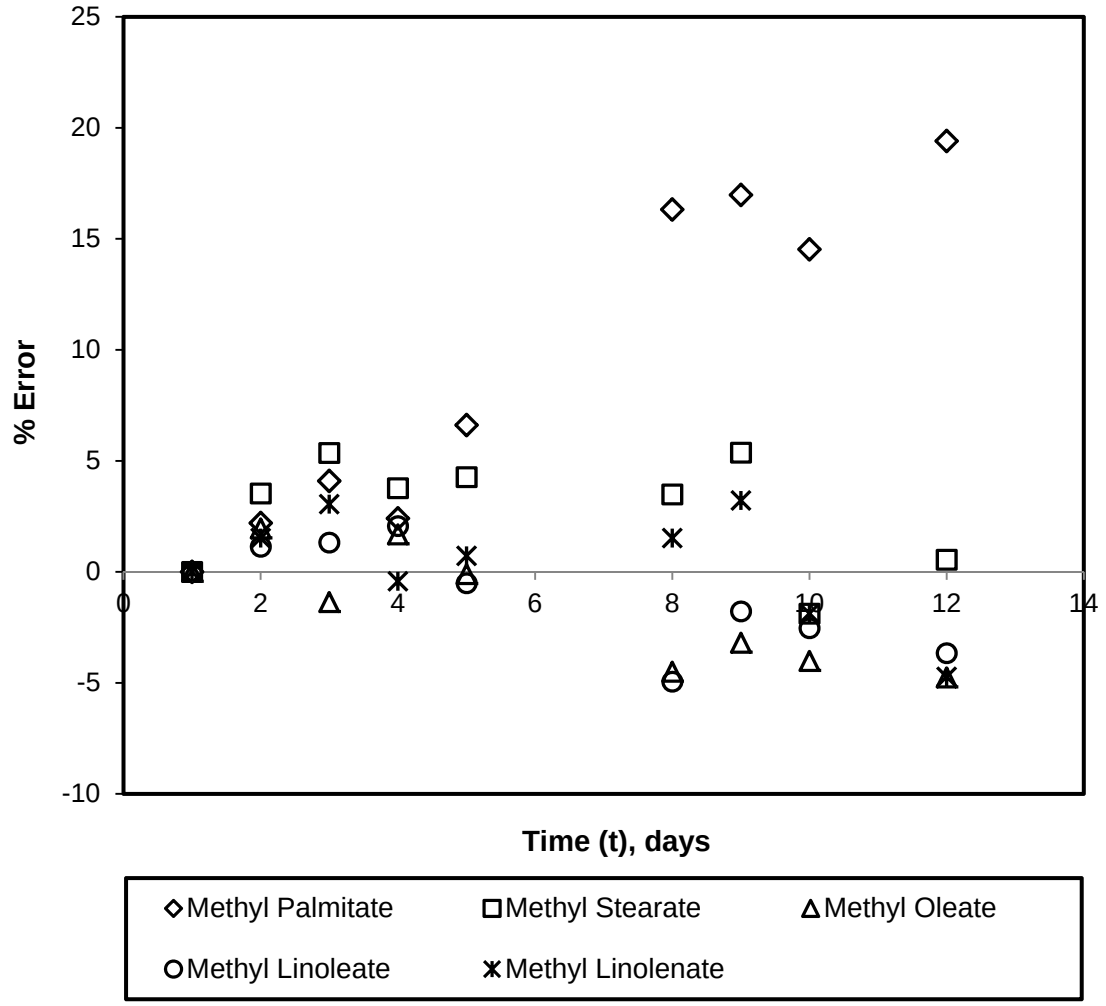

Figure 5.13. Ageing studies for the FAME standards.

5.3 PHYSICAL AND CHEMICAL CHARACTERISATION OF USED COOKING OIL (UCO)

The physical and chemical analyses of the UCO were conducted and the results are presented in Table 5.3. It was found that the percentage of FFA was 6.1%, which was far beyond the allowable limit (<1%) for a direct transesterification process. Therefore, a pre-treatment process should be conducted via the esterification reaction to convert FFA to valuable FAME, or commercially known as biodiesel.

Table 5.3. Chemical and physical characteristics of the UCO.

Analysis	**Values**
Acid value	12.2 mg KOH g^{-1}
Free fatty acids (FFA)	6.1 %
Glycerides Composition	
Monoglycerides	1%
Diglycerides	15%
Triglycerides	84%
Moisture content	0.4%
Density	923.15 kg m^{-3}

5.4 CONCLUSIONS

This study has successfully developed a simple, fast and reliable method for the determination of fatty acids composition in the UCO. The developed method can further be used for biodiesel analysis. There were five components present in the derivatised sample including methyl palmitate, methyl stearate, methyl oleate, methyl linoleate and methyl linolenate with response factors of 0.9340, 0.9872, 0.9806, 0.9204 and 0.8984 respectively. The calibration curve for all the standards showed excellent linearity correlation coefficient (R-squared > 0.99). The composition of fatty acids in the UCO are 13.62%, 4.14%, 33.75%, 43.85% and 4.64% for palmitic acid, stearic acid, oleic acid, linoleic acid and linolenic acid, respectively. An ageing study concluded that the recommended storage period for the FAME standards should not be more than a week for more reliable and accurate results. The physical and chemical analysis of the UCO were conducted and summarised in Table 5.3. As a pre-treatment process is required to convert FFA to valuable FAME, a comprehensive study on the esterification of FFA has been carried out and presented in the Chapter 6.

6 ESTERIFICATION OF FREE FATTY ACIDS (FFA) IN USED COOKING OIL (UCO) USING ION EXCHANGE RESINS AS CATALYSTS

6.1 INTRODUCTION

In recent years, the major obstacle for biodiesel's commercialisation from vegetable oil has been the high cost of the raw feedstock. According to Zhang *et al.* (2003b) approximately 70-95% of biodiesel cost comes from the price of raw feedstock. Therefore, cheap non-edible vegetable oil, animal fats and waste oils have been found to be effective feedstock replacements to reduce the cost of biodiesel (Ramadhas *et al.*, 2005; Supple *et al.*, 2002; Tomasevic and Silver-Marinkovic, 2003; Behzadi and Farid, 2007; Canakci, 2007). According to Balat (2011), the price of used cooking oil (UCO) is 2 -3 times cheaper than virgin vegetable oils, thus it can significantly reduce the production cost of biodiesel.

In this chapter, the utilisation of ion exchange resins in the pre-treatment stage of UCO has been explored. Three types of cation exchange catalysts (Amberlyst 15, Purolite D5081, and Purolite D5082) have been investigated. All the three catalysts were subjected to batch kinetics studies and the catalyst that performed the best in terms of FFA conversion was selected for further optimisation of batch kinetic studies. Elimination of mass transfer resistances and the effect of catalyst loading, reaction temperature and methanol to UCO feed mole ratio on the conversion of FFA were investigated. The experiments were conducted in a jacketed batch reactor to determine the optimum condition for the esterification process prior to the transesterification. Finally, reusability of the catalyst was studied at optimum condition obtained from the batch kinetic studies.

6.2 SCREENING OF ION EXCHANGE RESIN CATALYSTS

In order to identify the best ion exchange resin catalysts for further experimental work, all three resins, Amberlyst 15, Purolite D5081 and Purolite D5082 were subjected to the same reaction conditions: 1% (w/w) of catalyst loading, 333 K reaction temperature, 6:1 methanol to UCO feed mole ratio and 350 rpm impeller

stirring speed. After 8 h, the conversion of FFA was 88% using Purolite D5081 catalyst, whilst the conversion of FFA using Purolite D5082 and Amberlyst 15 was 78% and 28%, respectively. The results are presented in Figure 6.1.

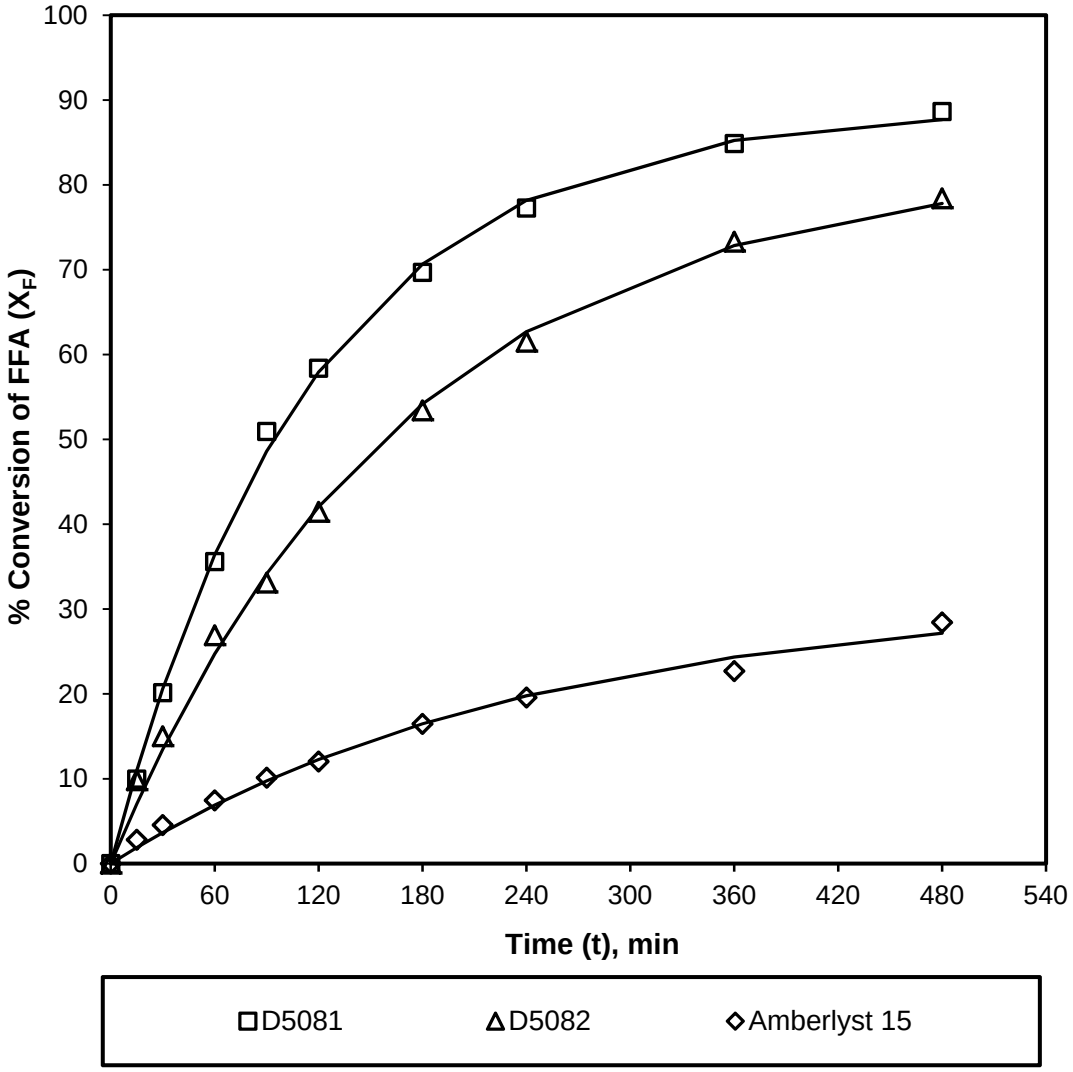

Figure 6.1. Effect of different types of ion exchange resin catalysts on the FFA conversion. Experimental conditions: Stirring speed: 350 rpm; catalyst loading: 1% (w/w); reaction temperature: 333 K; feed molar ratio (methanol:UCO): 6:1.

The differences in the physical and chemical properties of various resins can be used to explain the differences in catalytic activity, such as the surface area measurement and elemental analysis (see Chapter 4, Table 4.8, Table 6.1 and Table 6.2). These analyses show that even though Purolite D5081 has the lowest sulphur content, it exhibits the highest specific surface area and total pore volume. It means that even

though only a little sulfonic acid was present in Purolite D5081 resin, the sulfonic acid group was close to external area and easily accessible. Therefore, there are more accessible active sites for the reaction to occur and hence attains the equilibrium at a faster rate. In addition, results from PSD analysis (see Chapter 4, Figure 4.29) also shows that Purolite D5081 has the smallest average catalyst particles as compared to the other two resins. This means there is a larger surface area for this resin and this finding fits with the analysis from the surface area measurement (Chapter 4, Table 4.8).

Table 6.1. Elemental analysis for fresh and used ion exchange resin catalysts.

Catalyst	% C	% H	% N	% S	% O*
Fresh Amberlyst 15	53.14	6.12	0.05	16.17	24.52
Used Amberlyst 15**	54.53	5.05	0.06	15.94	24.42
Fresh D5081	77.04	5.32	0.95	4.09	12.61
Used D5081 **	77.41	5.69	0.93	3.32	12.66
Fresh D5082	68.87	4.44	0.13	5.92	20.65
Used D5082**	69.07	4.53	0.03	5.41	20.97

*Oxygen by difference
**Washed catalyst after 1st cycle of reusability study

Table 6.2. Sodium capacity for fresh and used ion exchange resin catalysts.

Catalyst	Fresh Resin (mmol g^{-1})	Used Resin (mmol g^{-1})
Amberlyst 15	4.78	4.45
D5081	1.59	1.39
D5082	1.79	1.59

On the other hand, even though Amberlyst 15 has the largest average pore diameter, the result from the esterification reaction (Figure 6.1) shows that Amberlyst 15 has the lowest conversion of FFA compared to Purolite D5081 and D5082 resins. This is because Amberlyst 15 has the lowest specific surface area and lowest pore volume as compared to Purolite resins. Therefore, in the case of Amberlyst 15, there are less active catalytic sites available for the reaction to occur. The specific surface area and

total pore volume were also found to be slightly higher for Purolite D5081 as compared to Purolite D5082. Hence, the reaction using Purolite D5081 as a catalyst gives slightly higher conversion compared to Purolite D5082.

The level of divinylbenzene (DVB) cross-linking also contributes significantly to the level of FFA conversion. From Figure 6.1, it can be seen that resins with high DVB cross-linking (Purolite D5081 and D5082) result in higher FFA conversion compared to lower DVB cross-linked resin (Amberlyst 15). The highly cross-linked resin produces a tougher matrix that is more resistance to chemical (oxidation) and physical (strength) breakdown. The FT-IR spectroscopy analysis was also carried out and there was no noticeable change of functional groups for all the resin samples. Since Purolite D5081 showed the best catalytic performance as compared to other catalysts, it was used for further experimental work.

6.3 OPTIMISATION OF ESTERIFICATION PROCESS IN A JACKETED BATCH REACTOR

6.3.1 Investigation on the Effect of Mass Transfer Resistances

There are two types of mass transfer resistances involved in ion exchange catalysis. The first is the external mass transfer resistance, which takes place across the solid-liquid interface while the second is the internal mass transfer resistance, associated with the differences in particle size of the catalysts. Mixing is one of the key factors to optimise the production of biodiesel as it increases the interaction between the reactants (methanol and UCO) and the catalyst, predominantly at the early stage of the reaction. However, after the reaction mixture reaches the stage where the reactant and the catalyst are well-mixed, there is no additional benefit from increasing the stirring speed. This phenomenon is due to the external mass transfer resistance.

In order to investigate the influence of external mass transfer resistance, three different stirring rates were investigated for the reaction process and the conversion patterns of FFA were observed. Figure 6.2 shows the trend for FFA conversion for three levels of impeller agitation speed, 350, 475 and 600 rpm. The FFA conversion

between the selected stirring rates gave almost an identical trend when the agitation speed increased from 350 rpm to 600 rpm. The conversion of FFA was 90 ± 2% for agitation speed of 350, 475 and 600 rpm, respectively. As the stirring speed only has a negligible impact on FFA conversion, it was confirmed that the external mass transfer resistance has negligible effect on the esterification reaction. As a conclusion, stirring rate of 350 rpm and above was selected for subsequent experiments as there was no evidence of external mass transfer resistance.

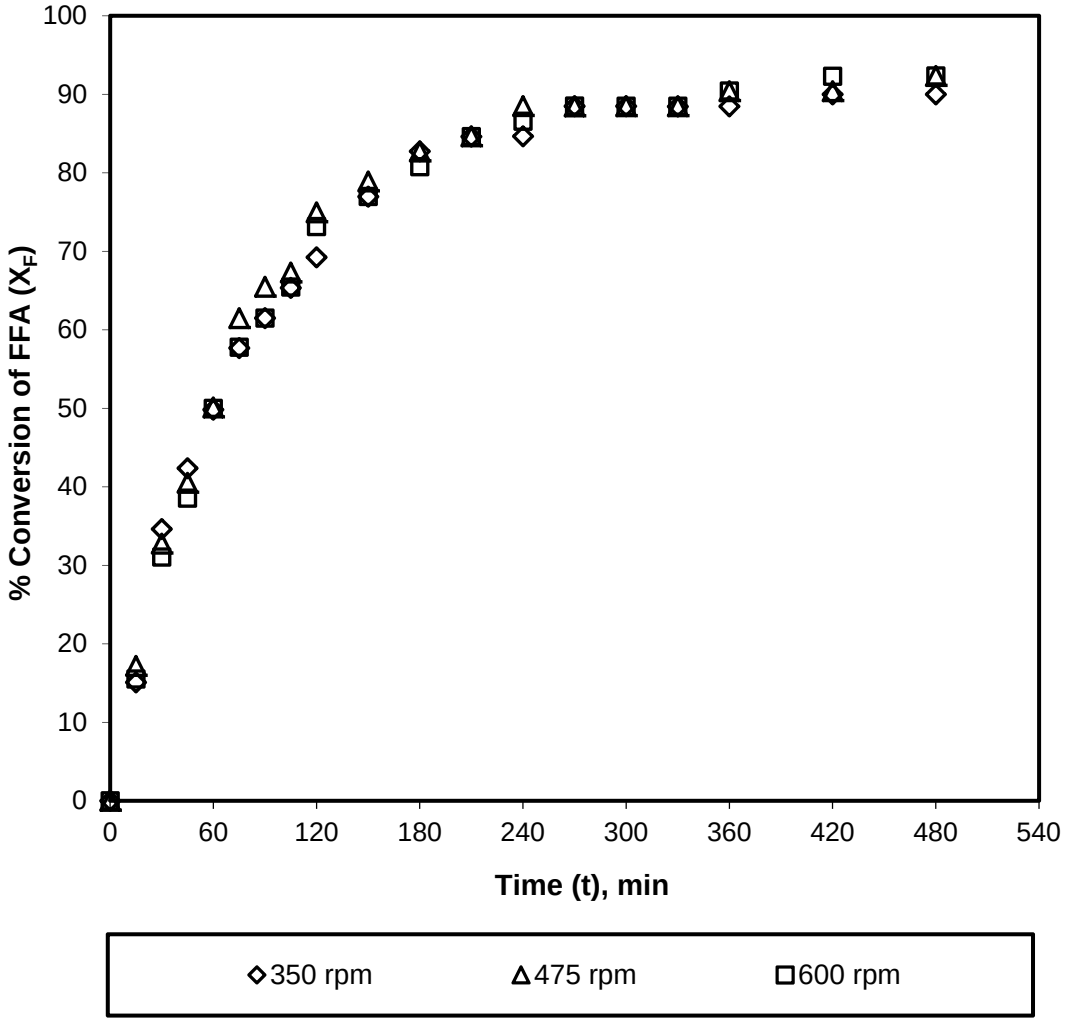

Figure 6.2. Effect of stirring speed on the FFA conversion – External mass transfer resistance. Experimental conditions: Catalyst: Purolite D5081; catalyst loading: 1.25% (w/w); reaction temperature: 333 K; feed molar ratio (methanol:UCO): 6:1.

Internal mass transfer resistance refers to the resistance of movement of reactant molecules inside the pores of the catalyst. In order to investigate the impact of internal mass transfer resistance, a series of experiments were conducted using different ranges of PSD (425-500 μm, 280-800 μm and 600-710 μm). This method has been widely used in catalytic reaction process (Helfferich, 1962; Yadav and Kulkarni, 2000; Silva and Rodrigues, 2006; Russbueldt and Hoelderich, 2009; Tesser *et al.*, 2009; Kouzu *et al.*, 2011). The defined PSD was obtained using a standard sieve measurement. The method was similar to the PSD measurement described in Chapter 3, section 3.3.2.5. Figure 6.3 shows the effect of internal mass transfer resistances on the conversion of FFA.

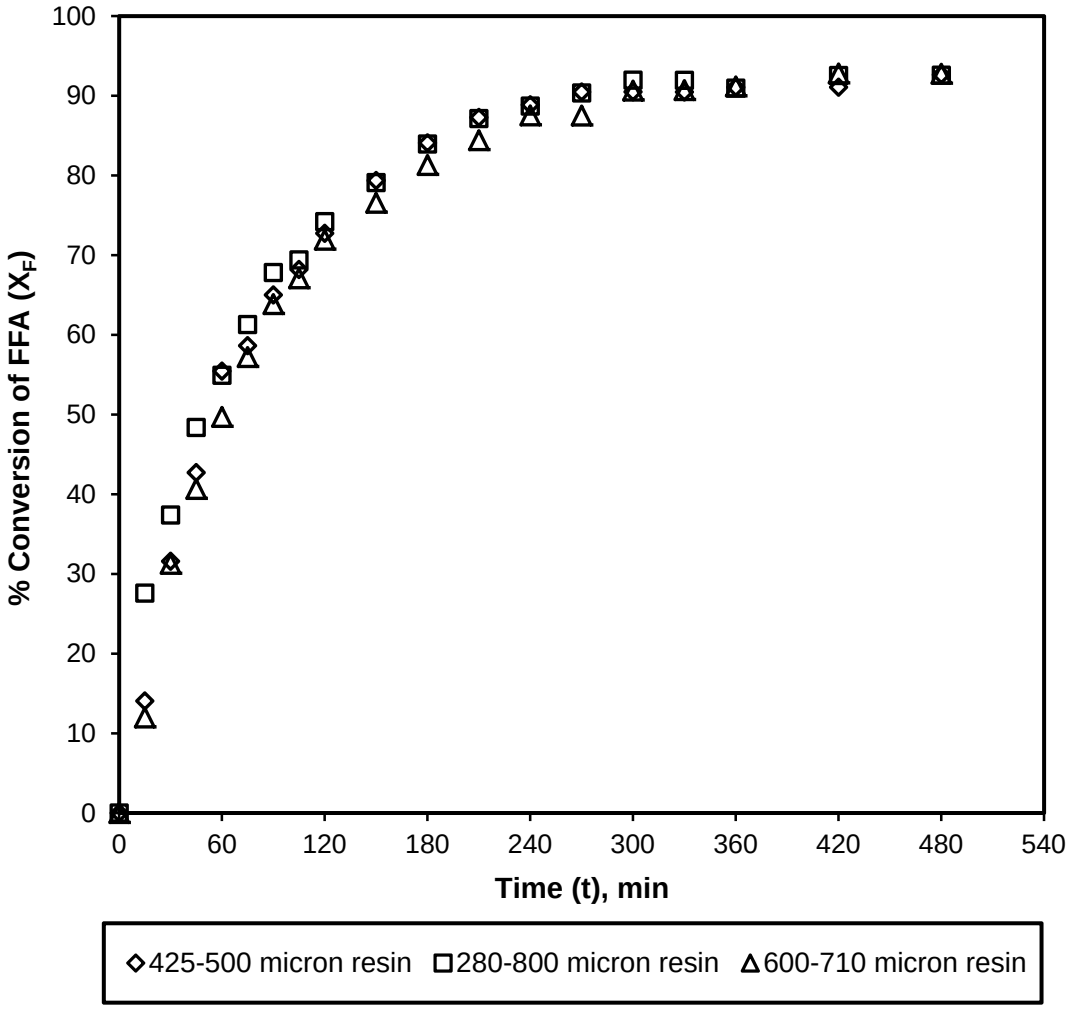

Figure 6.3. Effect of resin size on the FFA conversion – Internal mass transfer resistance. Experimental conditions: Catalyst: Purolite D5081; stirring speed: 475 rpm; catalyst loading: 1.25% (w/w); reaction temperature: 333 K; feed molar ratio (methanol:UCO): 6:1.

From Figure 6.3, it can be seen that 280-800 μm particle range gives a slightly higher conversion compared to the other two particle ranges. This is because this range (280-800 μm) covers a wide range of particle size and therefore the possibility of having smaller particles is higher. This situation contributes to higher conversion of FFA as smaller particle provide larger surface area. To support the argument, comparison was made between 600-710 and 425-500 μm range and it was found that the conversion for 600-710 μm particle size was a bit lower than 425-500 μm particle size in the first 5 h of reaction. Nevertheless, the final conversions of FFA for all three particle ranges were approximately the same at the end of 8 h reaction. This finding proved the previous theory of having smaller particle size contributes to a larger surface area and thus increases the FFA conversion. However, the difference between each range was very small (less than ±2%) and the final conversions were approximately the same. Therefore the effect of internal mass transfer limitation can be eliminated. As a conclusion, all further experiments were carried out with the catalyst as supplied, without sieving.

6.3.2 Effect of Catalyst Loading

A catalyst is needed to improve the rate of the esterification reaction. In this particular work, catalyst loading is defined as the ratio of mass of the catalyst to the mass of the reactants fed. The effect of catalyst loading is shown in Figure 6.4. The reaction temperature was set at 333 K with 6:1 methanol to UCO molar ratio. The reaction took approximately 8 h to reach equilibrium.

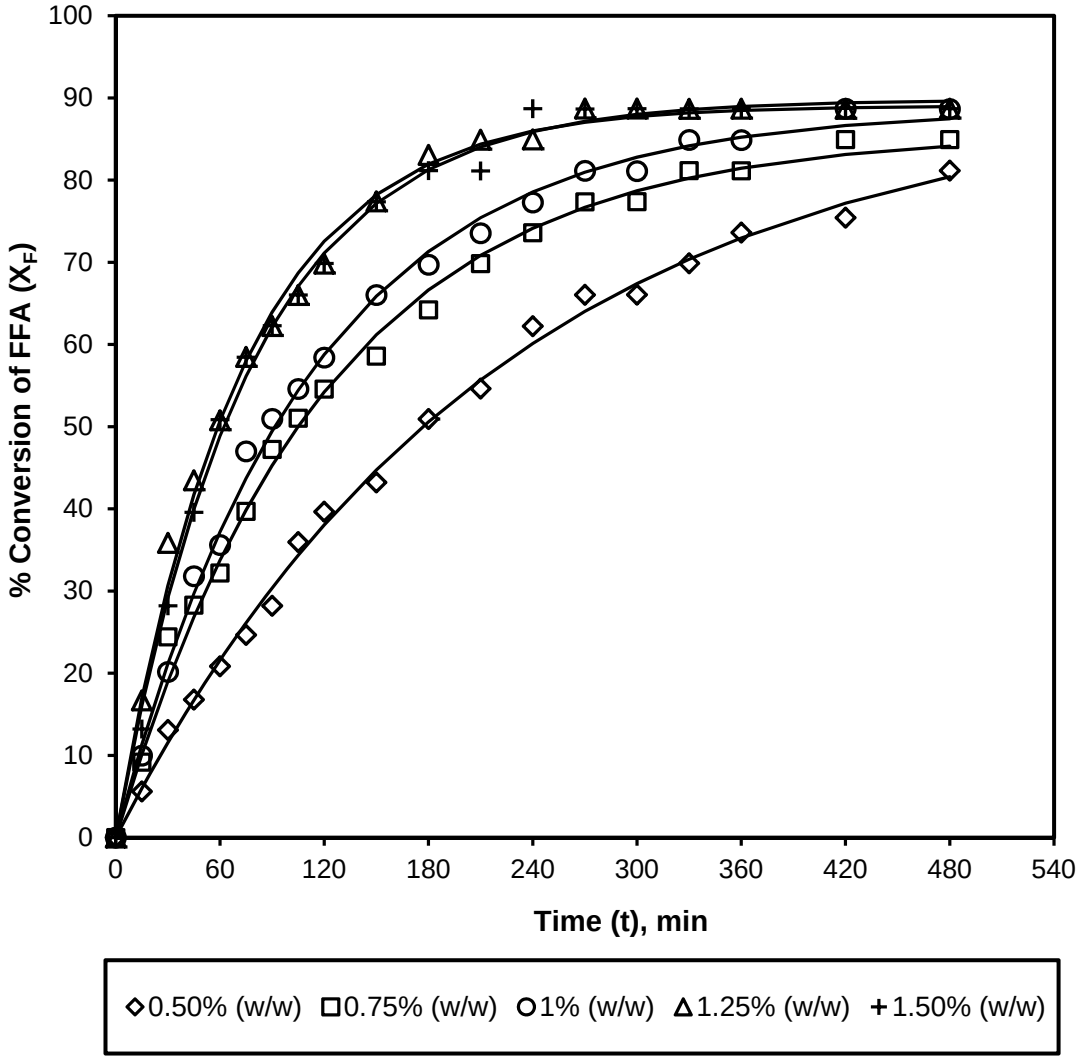

Figure 6.4. Effect of catalyst loading on the FFA conversion. Experimental conditions: Catalyst: Purolite D5081; stirring speed: 350 rpm; reaction temperature: 333 K; feed molar ratio (methanol:UCO): 6:1.

The result shows that the conversion is greatly influenced by the amount of catalyst, especially at the early stage of the esterification reaction. This is attributed to the fact that as the catalyst loading increases, the number of active catalytic sites increases and a shorter time is required for the reaction to reach the equilibrium. Conversion of FFA with less than 0.75% (w/w) catalyst loading gives approximately 81-85% conversion. As catalyst loading increased to 1.5% (w/w)), the change in conversion was less significant with the final conversion for 1.25% (w/w) and 1.5% (w/w) being almost identical (ca. 90%). This phenomenon indicates that as the catalyst loading increases, the conversion and the rate of reaction increases. However as the number

of catalytic sites increases (≥ 1.25% (w/w) catalyst loading), the benefits are reduced as there are sufficient active catalytic sites for the reactant molecules to catalyse the reaction. Furthermore, a higher dosage of catalyst also contributes to more viscous reaction mixture, leading to an increase in mass transfer resistance in the multiphase system (Reddy *et al.*, 2006). In the case of the esterification of FFA, it was found that once the catalyst loading was increased to 1.25% (w/w), there were sufficient catalyst sites for this reaction to occur. The turnover frequency (TOF) for esterification reaction is 1.07 h^{-1}. 1.25% (w/w) catalyst loading was chosen as the optimum catalyst loading and was used for all further esterification reactions.

6.3.3 Effect of Reaction Temperature

According to Freedman *et al.* (1984), the rate of reaction is strongly influenced by the temperature. However, given enough time, the reaction will proceed near to completion even at room temperature (Formo, 1954). The commonly employed reaction temperature ranges from as low as room temperature up to 338 K. For the esterification of FFA, the choice of reaction temperature range was determined by the findings of Leung and Guo (2006). They investigated the effect of reaction temperature on the biodiesel process and suggested that any temperature higher than 323 K has a negative impact on the virgin oils but has a positive impact for waste oils. Esterification of FFA was investigated at different reaction temperatures (323, 328, 333 and 335 K) and the results are shown in Figure 6.5.

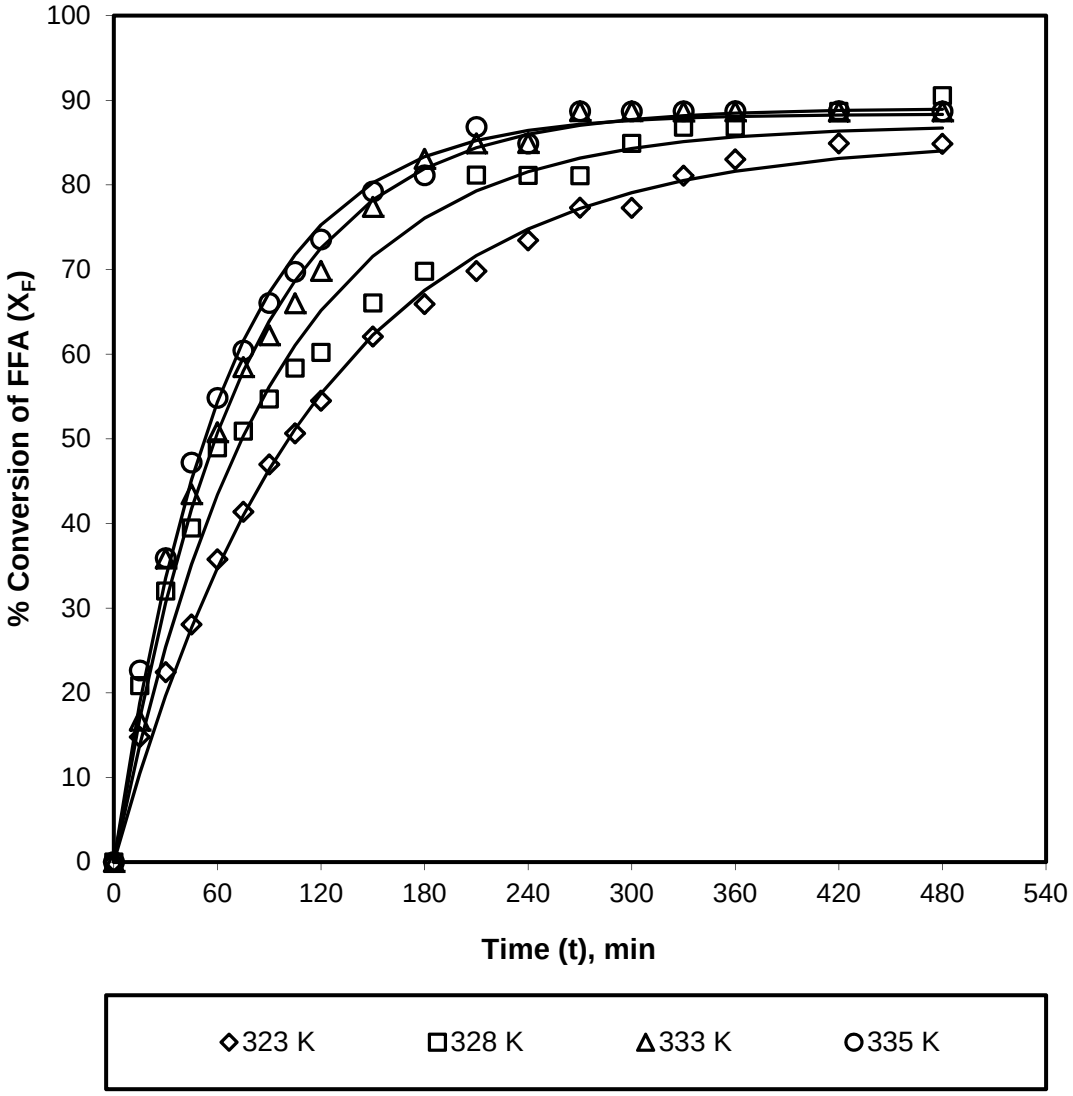

Figure 6.5. Effect of reaction temperature on the FFA conversion. Experimental conditions: Catalyst: Purolite D5081; stirring speed: 350 rpm; catalyst loading: 1.25% (w/w); feed molar ratio (methanol:UCO): 6:1.

As a general rule it is expected that the FFA conversion will increase with an increase in reaction temperature. In addition, it has been observed that an increase in reaction temperature will leads to a reduction in viscosity of UCO, which enhances the contact between methanol and UCO leading to a higher conversion of FFA. After 8 h of reaction, conversion of FFA at 328, 333 and 335 K was approximately 90% whereas for 325 K, the conversion of FFA was about 84%.

A significant decrease in the volume of the reaction mixture was also observed when a trial experiment was conducted at 338 K, just above the boiling point of methanol, 337.7 K. This was expected as there will be some changes to the system when this temperature is reached, with considerable amount of methanol present in the headspace of the reactor as vapour (Gao *et al.*, 2008; Yan *et al.*, 2008). Liu *et al.* (2009) claimed that beyond 338 K, methanol started to vaporise rapidly, forming large number of bubbles to form a foam, that resulted in a decrease in the FFA conversion. Generally, in typical biodiesel reaction process, low reaction temperature will result in low reaction rates whilst higher reaction temperatures lead to excessive methanol loss due to evaporation. After consideration of the safety issues, cost implications and the conversion trends for each temperature, the optimum reaction temperature proposed for further experiments is 333 K.

6.3.4 Effect of Methanol to UCO Molar Ratio

Another important variable that contributes to the performance of esterification reaction is the feed mole ratio of alcohol to UCO. As shown in Figure 3.4 (Chapter 3), the reaction stoichiometry requires three moles of alcohol per mole of triglycerides to yield three moles of FAME and one mole of glycerine. However, in practice, higher feed mole ratio is employed in order to shift the esterification reaction to the desired product. Figure 6.6 shows the effect of methanol to UCO feed mole ratio on the conversion of FFA. The feed mole ratio of methanol to UCO was calculated based on the average molecular mass of fatty acids composition, which is approximately 278.11 g/mol.

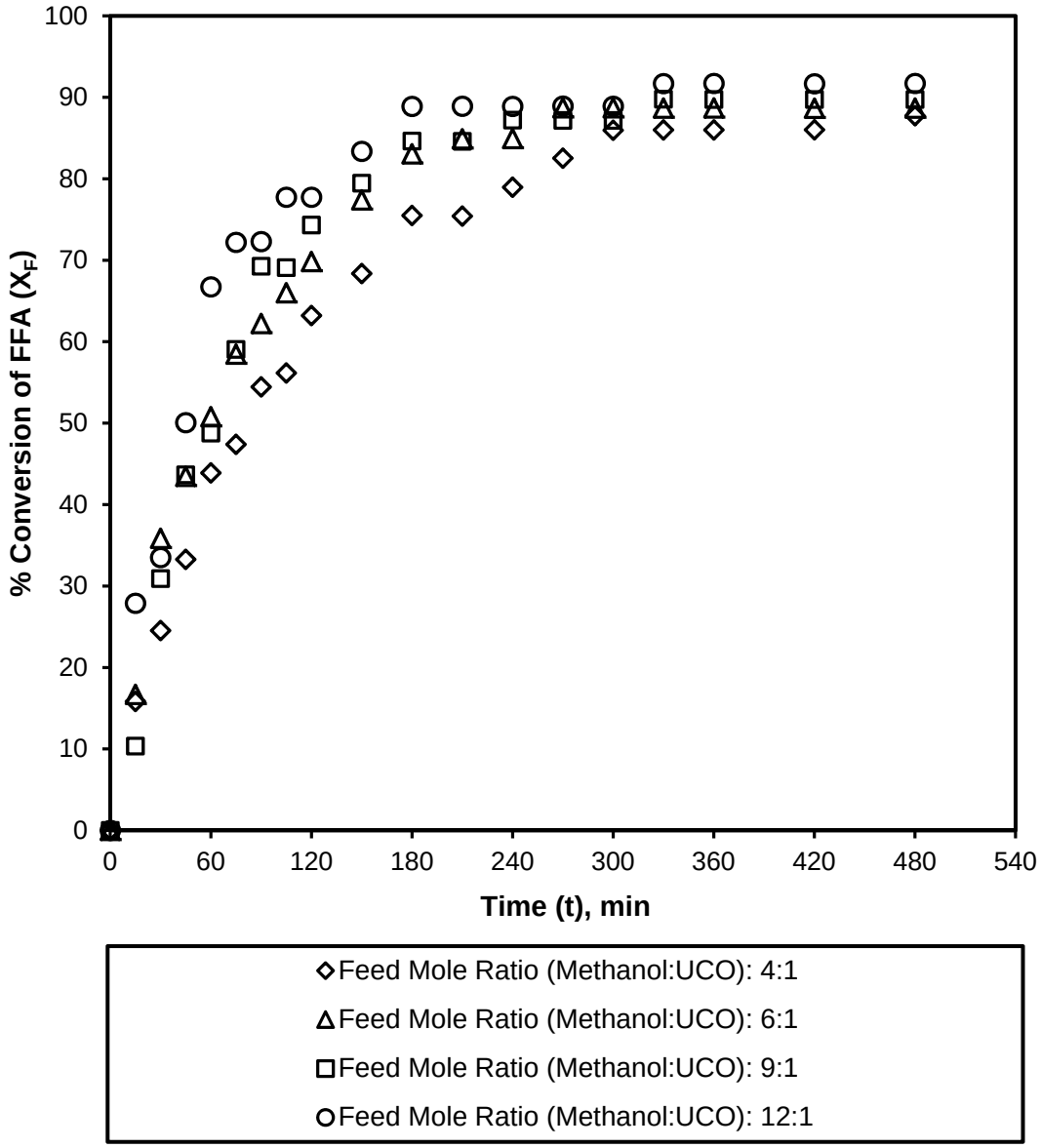

Figure 6.6. Effect of feed mole ratio (methanol:UCO) on the FFA conversion. Experimental conditions: Catalyst: Purolite D5081; stirring speed: 350 rpm; catalyst loading: 1.25% (w/w); reaction temperature: 333 K.

From Figure 6.6 it can be seen that the conversion increased slightly with an increase in methanol to UCO molar ratio. However, differences in the conversion of FFA between different methanol to UCO feed mole ratios were less noticeable, giving 1-2% increments in the FFA conversion as the methanol to UCO molar ratio increases. At 4:1 methanol to UCO feed mole ratio, the FFA conversion was 88% and at 12:1 methanol to UCO feed mole ratio, the FFA conversion was 92%, as

shown in Figure 6.6. In comparison, the methanol to UCO feed mole ratio of 4:1 gives the lowest conversion of FFA than the other three methanol to UCO feed mole ratios. It is because lower concentration gives lower conversion due to standard reaction kinetics and longer reaction time is needed to reach equilibrium. The reaction time can be shortened using a higher feed mole ratio of methanol to UCO. However, the costs will be higher due to higher methanol recovery requirements. Furthermore, a high feed mole ratio of methanol to UCO will also lead to difficulties in the separation process and hinders separation by gravity (Leung and Gou, 2006; Encinar *et al.*, 2007). This will also lead to a decrease in the yield of the product as some glycerine will remain in the pre-treated oil phase. Excess methanol could also drive the combination of methyl ester and glycerine to monoglycerides, which will increase the viscosity of the reaction mixture (Liu *et al.*, 2009). By taking into account the safety issues, and the capital and operating costs of the process, a feed mole ratio of 6:1 (methanol: UCO) was chosen as the optimum molar ratio for the esterification reaction.

6.4 CATALYST REUSABILITY STUDY

A reusability study of Purolite D5081 was conducted to determine the catalyst life time. A series of reactions, using the same batch of catalyst, were carried out at the optimum process conditions: 475 rpm stirring speed, 1.25% (w/w) catalyst loading, 333 K reaction temperature, 6:1 methanol to UCO feed mole ratio, and. The results are shown in Figure 6.7 and from these data it can be seen that the conversion decreased by approximately 8-10% per cycle (i.e. fresh catalyst gives ca. 92% conversion, the first cycle gives ca. 84% conversion, the second cycle gives ca. 73% conversion and the third cycle gives ca. 62% conversion). Potential reasons for the loss of activity include contamination of the external or internal surface of the catalyst and sulphur leaching.

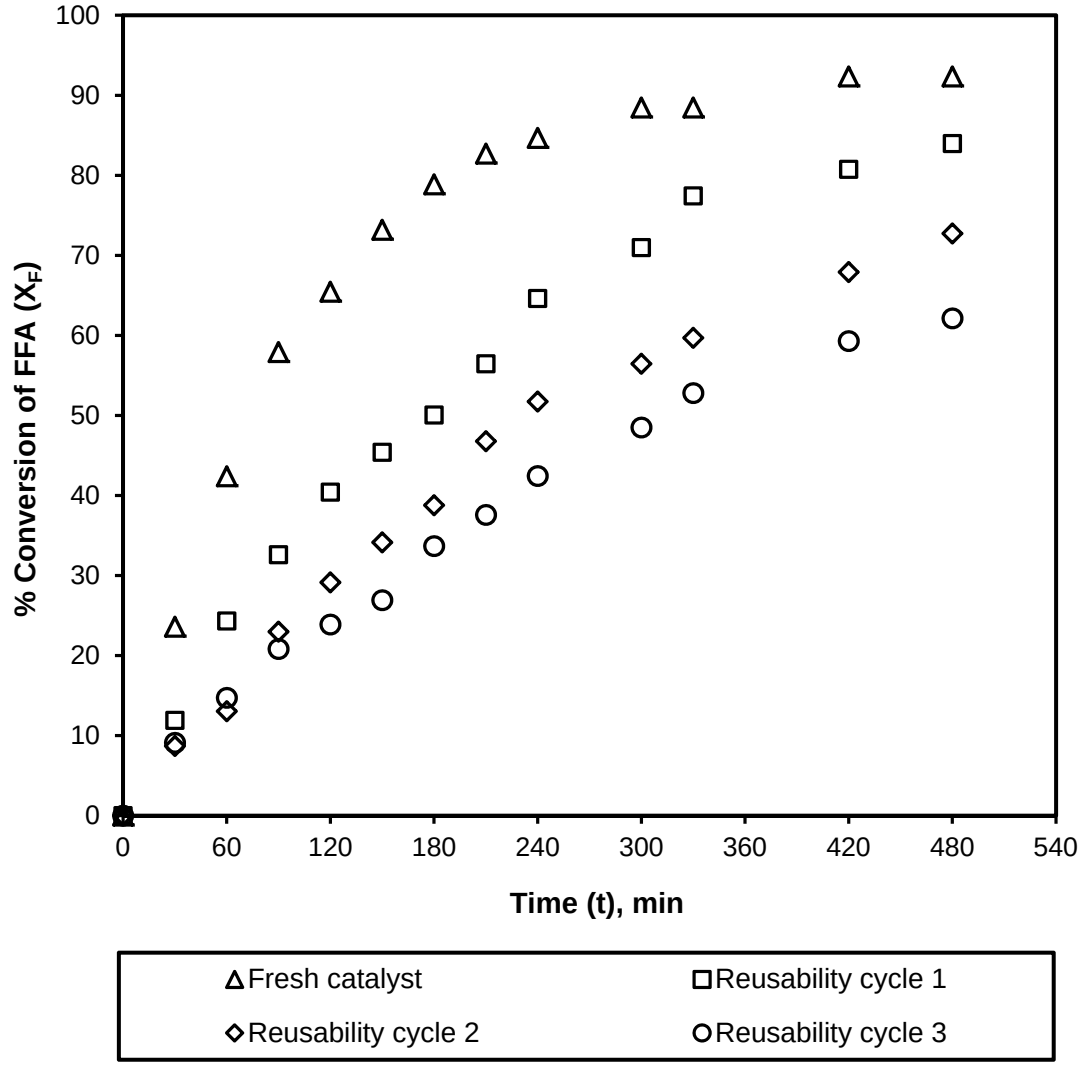

Figure 6.7. Effect of catalyst reusability on the conversion of FFA. Experimental conditions: Catalyst: Purolite D5081; stirring speed: 475 rpm; catalyst loading: 1.25% (w/w); reaction temperature: 333 K; feed molar ratio (methanol:UCO): 6:1.

A scanning electron microscopy (SEM) analysis was carried out to determine if the surface of the catalyst was contaminated by the reaction mixture and the effect of various cleaning regimes. Purolite D5081 was cleaned by placing the catalyst in a flask of methanol which was subsequently placed in an ultrasonic bath, the method is detailed in Chapter 3, section 3.6.2. To determine the effect of ultrasonication, Purolite D5082 was cleaned using methanol but without ultrasonication. A series of SEM micrographs is shown in Figure 6.8 which shows the comparison of fresh and used catalyst (after the first run) as well as comparing the effect of cleaning regimes. Figures 6.8 (a) and (b) show a sample of Purolite D5081 before and after

esterification and it can be seen that there is no trace of UCO on the surface of the used catalyst in Figure 6.8 (b). Figures 6.8 (c) and (d) show a sample of Purolite D5082 and in this case it can be seen that there is UCO present on the surface of the catalyst, indicating incomplete washing of the catalyst. This observation fits with the results of the elemental analysis for used D5082 (Table 6.1) which shows there is a slight increase in residual carbon. On this basis it was decided that ultrasonication was needed as part of the cleaning process in order to ensure UCO was removed from the surface of the catalyst. It is expected that by using ultrasonication to clean the catalyst there is no contamination on the surface of the catalyst and as a result this is not contributing to catalyst deactivation.

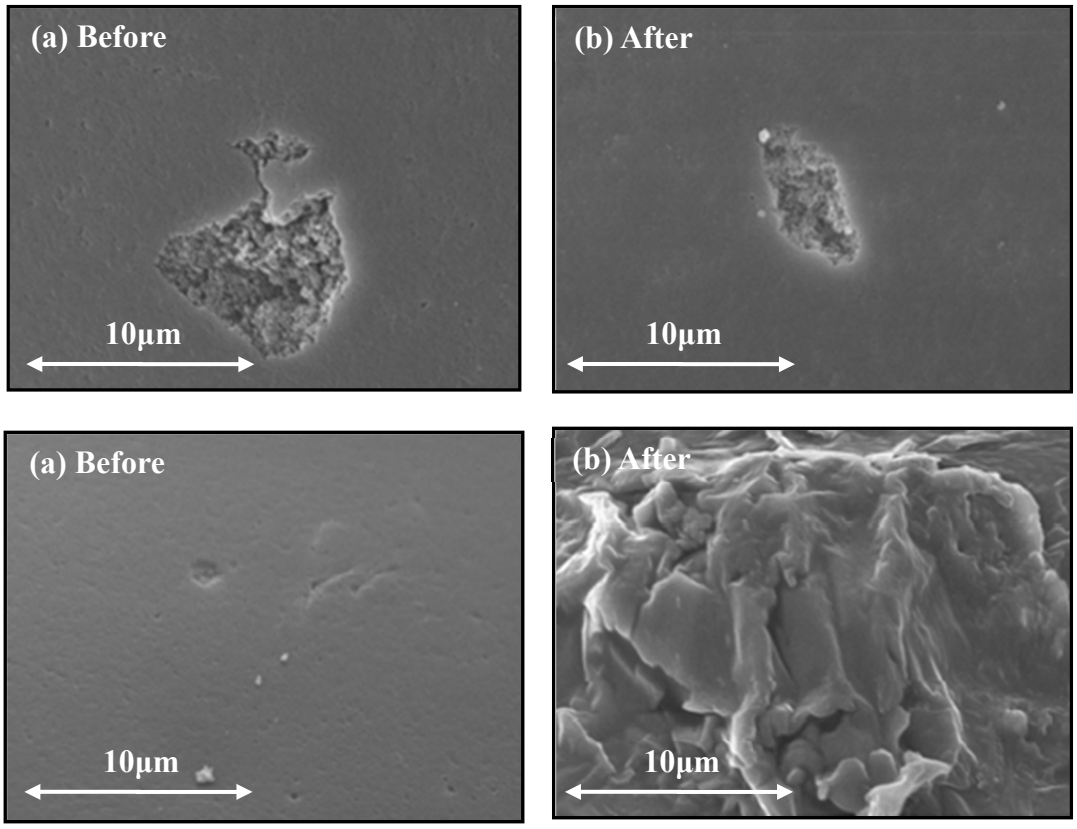

Figure 6.8. SEM analysis of Purolite catalysts taken at 5 kX magnification: Figure 6.8 (a) and Figure 6.8 (b) is Purolite D5081 before and after esterification process and Figure 6.8 (c) and Figure 6.8 (d) is Purolite D5082 before and after esterification process.

It was found that the mass of catalyst increased slightly after each reaction cycle and it has been assumed that this was due to the triglycerides inside the pores of the resin.

The BET analysis showed that Purolite D5081 resin has highest total pore volume of 0.47 cm^3 g^{-1}; which was slightly higher than other conventional ion exchange resins. This means it is possible for the triglycerides molecules to be retained within the resin and contribute to pore blockage. This may also reduce the accessibility of the active catalyst sites and may lead to higher internal mass transfer resistance and finally contribute to decreasing catalytic activity.

Sulphur leaching occurs due to detachment of sulphonic acid from the polymer matrix. Water is one of the products formed during the esterification reaction and in theory it could hydrolyse sulphonic acid groups to form homogenous sulphuric acid (H_2SO_4). An elemental analysis was carried out to determine the level of sulphur within various resin samples and the results are shown in Table 6.1. Fresh D5081 resin had a sulphur content of 4.1%, and after the first reaction cycle this decreased by nearly 20% to 3.3%. Ion exchange capacity results in Table 6.2 show a decrease of acid content for fresh and used catalyst of approximately 13%. This indicates that there is sulphur leaching contributing to the reduction in catalytic activity.

To further investigate the leaching of homogeneous species in the reaction mixture and UCO blockage within the resin pores, a series of experiments were carried out using Purolite D5081 as catalyst. The experimental work and the process flow diagram were highlighted in Chapter 3, section 3.6.2. Figure 6.9 shows the conversion of FFA during the uncatalysed reaction between the treated-methanol solution and UCO and the result clearly shows that there was a significant FFA conversion (ca. 87%) for the first cycle of homogeneous contribution study. This confirms the occurrence of sulphonic acid leaching, believed to be due to the detachment of sulphonic acid groups from the catalyst surface, followed by the hydrolysis of sulphonic acid species with water to form homogeneous species. Data plotted for the second cycle shows that the conversion of FFA is very low after the first homogenous contribution cycle (< 5%) indicating that there is no further leaching of the sulphonic acid group in methanol in the subsequent cycles.

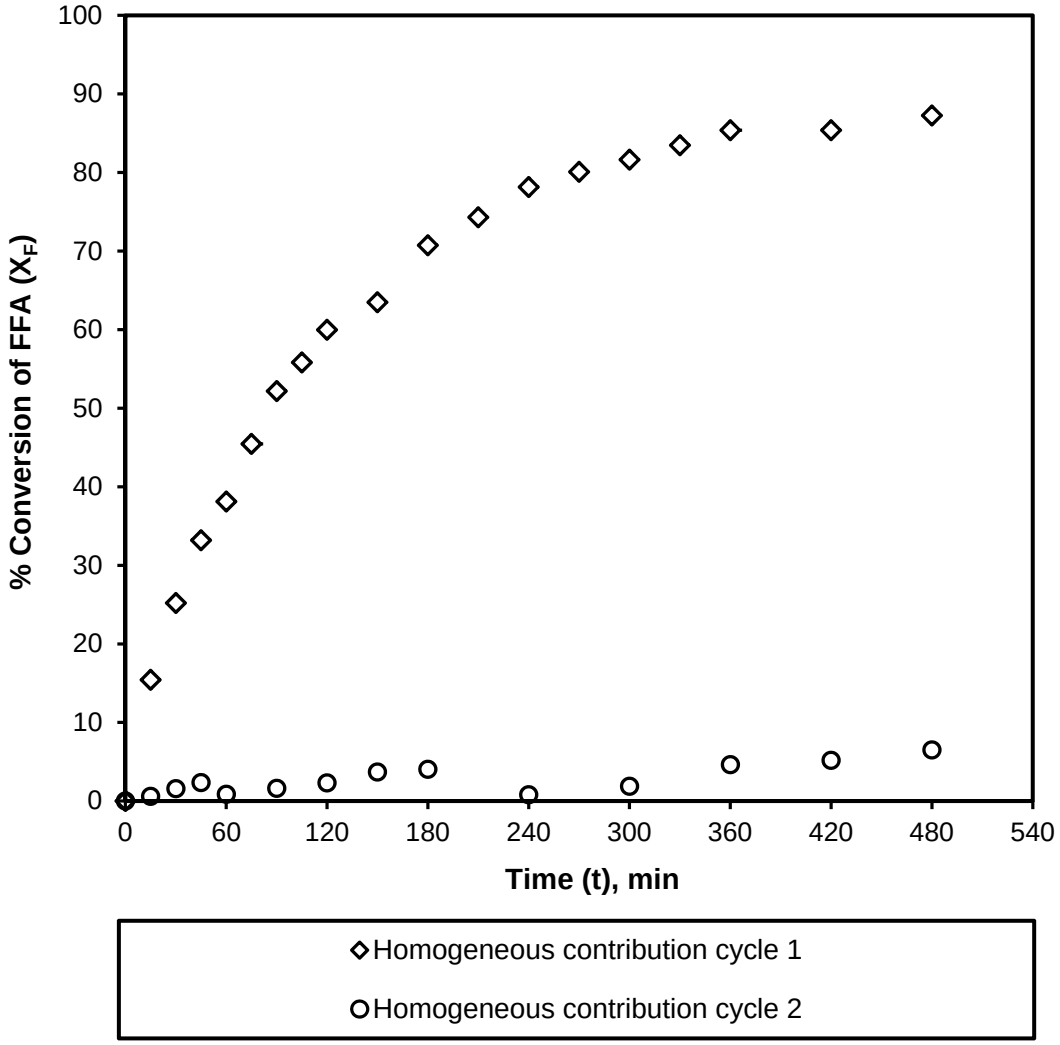

Figure 6.9. Effect of homogeneous contribution on the conversion of FFA. Experimental conditions: catalyst: Purolite D5081; stirring speed: 475 rpm; reaction temperature: 333 K.

In addition, the catalyst deactivation has also been investigated using the Purolite D5081 catalyst that was previously filtered from the methanol solution. The results are shown in Figure 6.10. It can be seen that the conversion of FFA for the second cycle was slightly lower compared to the first cycle, reducing from 90% to 77%. This was solely due to the blockage of large molecules of UCO molecules and based on the evidence that the leaching of sulphonic acid was negligible during the second cycle of the reaction (see Figure 6.9).

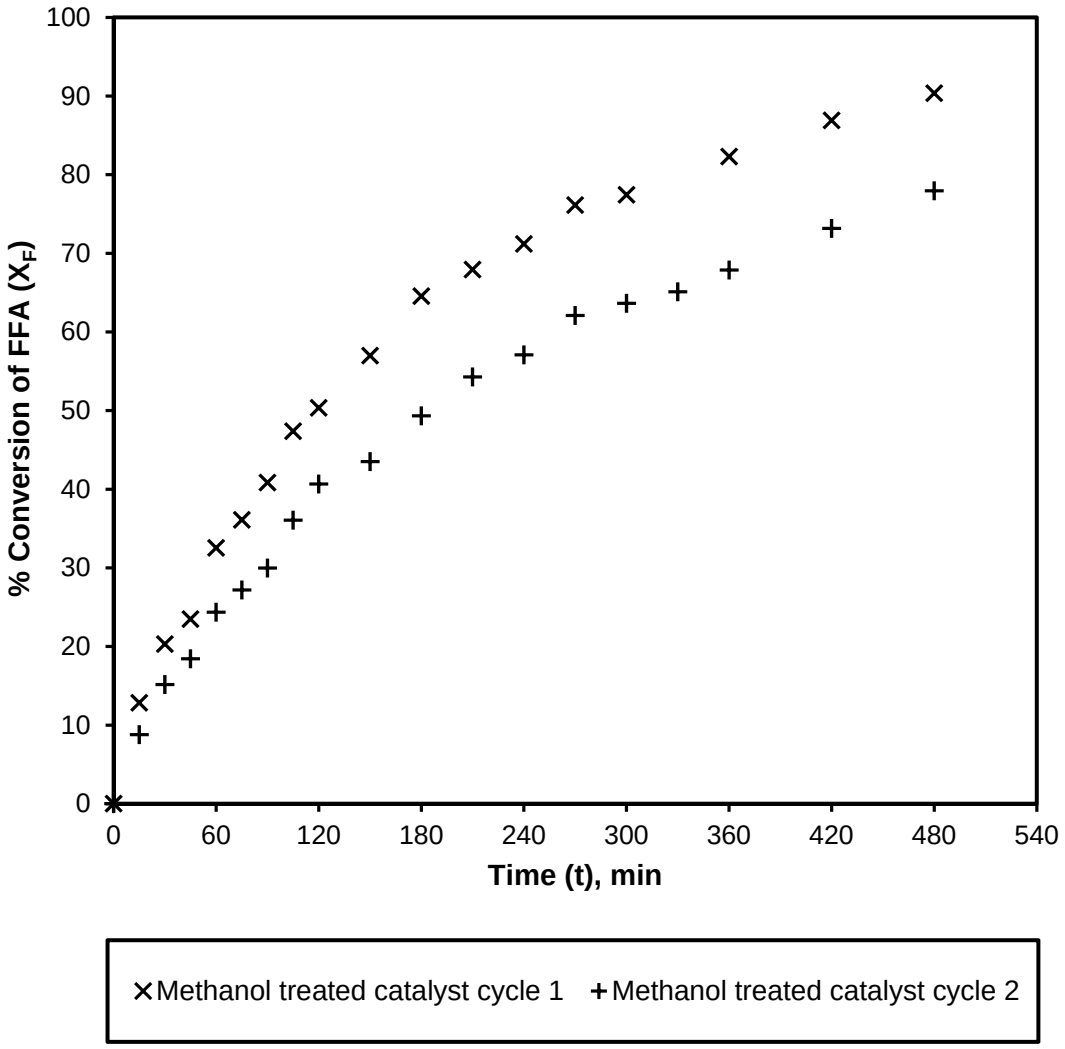

Figure 6.10. Study of FFA conversion using methanol treated catalyst. Experimental conditions: Catalyst: Purolite D5081; stirring speed: 475 rpm; catalyst loading: 1.25% (w/w); reaction temperature: 333 K; feed molar ratio (methanol:UCO): 6:1.

Figure 6.11 shows the comparison between the reusability study and methanol treated catalyst study. The difference in FFA conversion between the fresh catalyst (92%) and first methanol treated catalyst cycle (90%) is believed to be due to the sleaching of sulphonic acid groups, since both the experiments were conducted using the same experimental parameters. The only difference was the condition of the catalyst, where in the former experiment, fresh catalyst was used and for the latter one, methanol-treated-catalyst was used. This finding was verified using the homogeneous contribution study shown in Figure 6.9. Furthermore, it can be seen from Figure 6.11 that the first cycle of methanol treated catalyst study gives FFA

conversion of ca. 90%, that is 6% higher than the conversion of FFA achieved for the first cycle from the reusability study i.e. ca. 84%. For the former experiment, the resin itself was not introduced to any UCO mixture. So, there was no possibility of any triglyceride blockage during the reaction and hence the FFA conversion was slightly higher. Therefore, it could be assumed that the 6% reduction in conversion was solely due to blockage of large UCO molecules in the pores of catalyst particles. The same trend was also observed during the second cycle for both cases where the calculated FFA conversion difference was about the same.

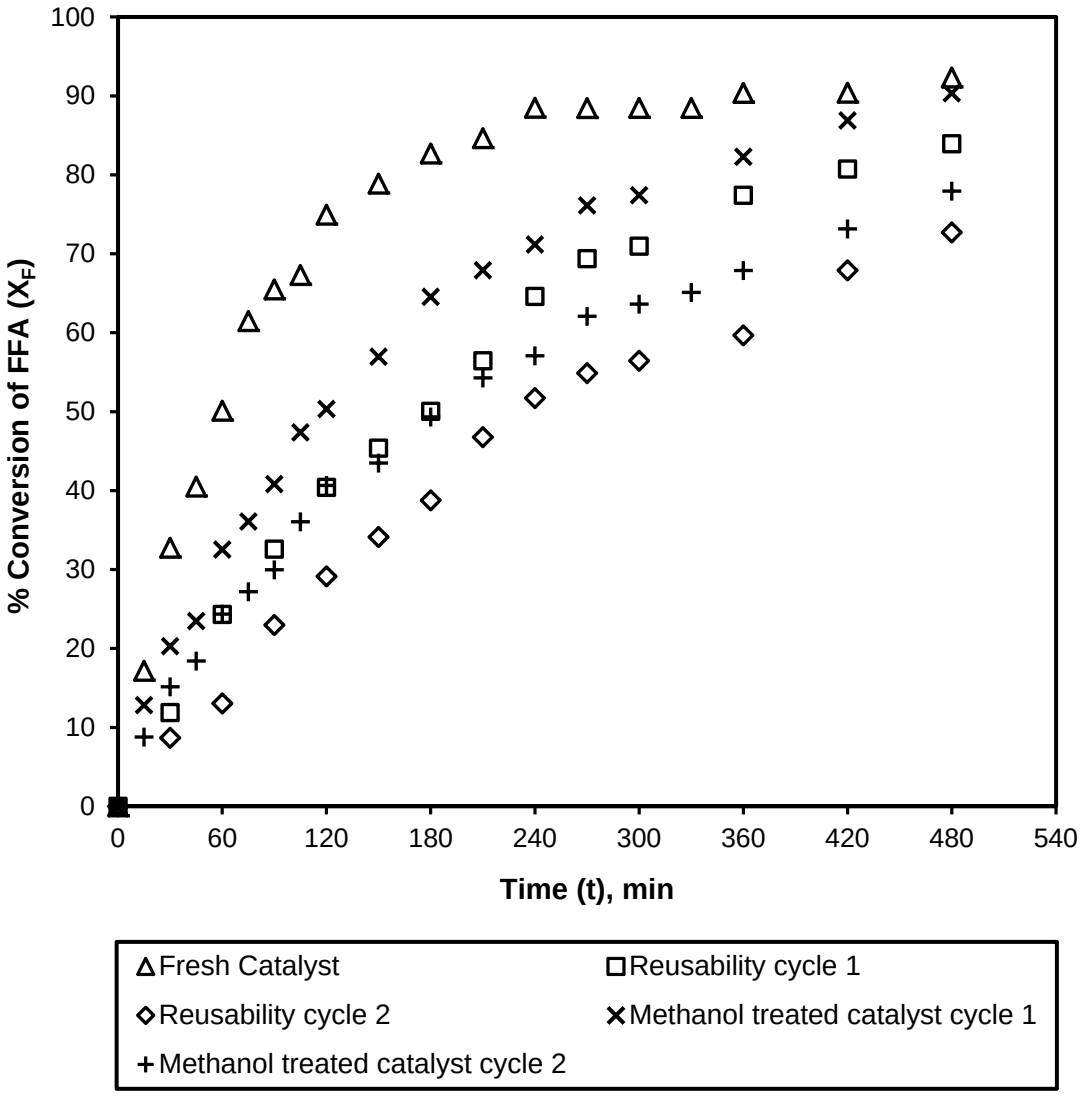

Figure 6.11. Comparison between the reusability study and the methanol treated catalyst study on the conversion of FFA. Experimental conditions: Catalyst: Purolite D5081; stirring speed: 475 rpm; catalyst loading: 1.25% (w/w); reaction temperature: 333 K; feed molar ratio (methanol:UCO): 6:1.

Therefore, it could be concluded that the reduction of FFA conversion in subsequent cycles (either from the reusability study or the methanol treated catalyst study) was largely due to the blockage of the large carboxylic acids in the pores of the resin, since the possibility of sulphonic acid groups leaching throughout the process was small. When both conditions (reusability and methanol treated catalyst study) were evaluated individually, sulphur leaching and pore blockage were observed, which resulted in a reduction in FFA conversion with an increased cycle number.

Overall, it could be concluded that there are two main factors that contribute to the catalyst deactivation during the reusability study. The first factor is the contamination and blockage of the UCO onto and within the surface of the catalyst, and the second factor is the leaching of the sulphonic acid functional groups ($-SO_3H$) attached to the ion exchange polymeric resin matrix.

6.5 CONCLUSIONS

Esterification pre-treatment of the UCO using various types of ion exchange resin catalysts have been investigated. Amongst all the catalysts investigated, Purolite D5081 resin showed the best catalytic performance as compared to the other two resins, Amberlyst 15 and Purolite D5082. This is probably due to the catalytic properties of Purolite D5081 resin, as it has the highest specific surface area and largest total pore volume. At the optimum reaction condition of 1.25% (w/w) catalyst loading, 333 K reaction temperature, 6:1 methanol to UCO molar ratio and 475 rpm stirring speed, Purolite D5081 achieved a FFA conversion of 92%. During the reusability study, the conversion of the catalyst dropped by 10% after each cycle. A series of experiments have been conducted through the homogeneous contribution study and the results confirmed that resin pore blockage and sulphur leaching are the two dominant factors that decreased the catalytic performance of Purolite D5081 catalyst. In the following chapter, batch kinetic modelling of FFA concentration will be presented. MATLAB 7.0 software was used to simulate both homogeneous and heterogeneous kinetic models and the results were correlated with FFA concentration data obtained from batch kinetic experiments.

7 KINETIC MODELLING OF FREE FATTY ACIDS (FFA) ESTERIFICATION

7.1 INTRODUCTION

The study of reaction kinetics is a study of the rate of chemical reactions, which involves investigation of various experimental conditions and understanding how these factors could influence the rate of a chemical reaction. Study of reaction kinetics is usually accompanied by the development of a mathematical model used for the prediction of many practical processes, especially in designing similar industrial processes. Concentration of reactants, physical state of the reactants, reaction temperature, reaction time and physical and chemical properties of the catalyst are the main factors that influence the reaction rate.

The rate of reaction can be defined as the change in the concentration of any of the reactants or products per unit time. The rate of reaction is often linked in the form of a mathematical equation called rate law. The rate law can be determined empirically from the experimental results or through theoretical prediction. From the rate law, the order of reaction can be determined. The order of reaction is the power of the concentration in the rate law expression with respect to the reactant. The order of reaction can be classified into four categories: the zero order reaction, first order reaction, second order reaction and mixed order (higher order) reaction.

Kinetic modelling is a study of molecular interaction based on the elementary reaction. There are several kinetic models that are commonly used in chemical reactions, the pseudo homogeneous (PH) or known as Quasi homogeneous (QH), Eley-Rideal (ER) and Langmuir-Hinshelwood-Hougen-Watson (LHHW) models. Different kinetic models have been used in esterification process and the results are summarised in Table 7.1.

Table 7.1. Review of different types of systems, order of the reaction and kinetic models for esterification.

Process	Catalyst	Reactor Configuration	Order of reaction	Kinetic model	References
Oleic acid esterification in triglycerides	Relite CFS	Batch reactor	Second order	PH	Tesser *et al.* (2005)
FFA esterification in vegetable oil	Purolite CT-275	Batch reactor	Second order	PH	Pasias *et al.* (2006)
FFA esterification in sunflower oil	Sulphuric acid	Batch reactor	First order (forward reaction), second (reverse reaction)	PH	Berrios *et al.* (2007)
Esterification of myristic acid	*p*-Toulene sulfonic acid, Amberlyst 15 and Degussa	Batch reactor	Second order	-	Yalçinyuva *et al.* (2007)
FFA esterification in low grade CPO	Sulphuric acid	Batch reactor	First order	PH	Satriana and Supardan (2008)
Esterification of artificially acidified soybean oil	Amberlyst 15	Stirred tank reactor, bed loop reactor	Second order	PH and ER	Tesser *et al.* (2009)
FFA esterification in waste cooking oil	$Fe_2(SO_4)_3$/C	Batch reactor	Second order	LHHW	Gan *et al.* (2009)
Esterification and transesterificatio n in used frying oil	Sulphuric acid	Batch reactor	First order (forward reaction), second (reverse reaction)	PH	Berrios *et al.* (2010)
Simulated pure oleic acid and palm oil	Tungstated zirconia	Batch reactor	First and second order models	PH	Zubir and Chin (2010)
Myrisctic acid esterification in presence of triglycerides	Sulfated zirconia	Batch reactor	Second order	PH	Rattanaphra *et al.* (2011)

Several studies on kinetic models have been conducted using single fatty acid esterification (e.g. lactic acid, myristic acid and palmitic acid) with different kinds of ion exchange resins. Sanz *et al.* (2002) studied the kinetics of lactic acid esterification reaction with methanol (MeOH), catalysed by different acidic resins, such as Dowex 50W8x, Dowex 50W2x, Amberlyst 36 and Amberlyst 15 dry. They used three types of kinetic models, QH, ER and LHHW, to correlate the

experimental data. The QH model was found to fit the experimental data well since the reaction medium reported was a highly polar mixture. Similar work on lactic acid esterification was carried out by Qu *et al.* (2009) with *iso*-butanol and *n*-butanol as solvent and Weblyst D009 (acidic ion exchange resin) as a catalyst. Experimental data was correlated using the same kinetic models (PH, LHHW and ER). All models showed a reasonably good results but the PH model was preferred due to its simple mathematical model (Qu *et al.*, 2009).

Investigation of the kinetic modelling of free fatty acids (FFA) esterification in waste oils was also carried out by several researchers. For instance, Pasias *et al.* (2006) investigated on the esterification of FFA in used vegetable oils using Purolite CT-275. They correlated their experimental data using PH model and good agreement was obtained between the experimental data and calculated values. Using the same PH model, they successfully predicted the optimum conversion of two other oils with higher FFA content. Berrios *et al.* (2007) investigated the kinetic of FFA esterification in used frying oil using sulphuric acid as a catalyst. The acid value conversion was fitted satisfactory to the PH kinetic model using first order for the forward reaction and second order for reverse reaction. By using the same kinetic model, a kinetic study of FFA esterification in low grade crude palm oil was investigated (Satriana and Supardan, 2008). Results revealed that the reaction was irreversible and followed a first order kinetic law. Gan *et al.* (2009) studied the kinetic of FFA esterification in waste cooking oil with $Fe_2(SO_4)_3$/C as a catalyst and the experimental data were modelled using the LHHW kinetic model. They found that the proposed kinetic model was favourably consistent with the experimental results.

On the other hand, there are several kinetic models conducted on artificially modified feedstock, ideally made to investigate the performance of ion exchange resin catalysts in highly acidified oil. For example, Tesser *et al.* (2005) studied the reaction kinetics of oleic acid esterification in triglycerides using the sulfonic acid resin (Relite CFS) as catalyst. They modelled the reaction kinetics using the PH model (second order reaction) and the experimental data was found to have a satisfactory

agreement with the calculated values. This research work has been extended by Tesser *et al.* (2009) using Amberlyst 15 as a catalyst with two different reaction configurations; the batch stirred tank reactor and bed loop reactor. Two types of kinetic models (PH and ER) were compared and it was found that the ER model was a superior model as compared to the PH model for the esterification of high FFA oil. The kinetic model of myristic acid esterification in the presence of triglycerides using sulfated zirconia as a catalyst was investigated by Rattanaphra *et al.* (2011). A second order reversible PH model was demonstrated to fit the experimental data and this model gave a satisfactory interpretation of the experimental data. A similar finding was reported by Yalçinyuva *et al.* (2007) when they investigated the esterification of myristic acid using homogeneous (*p*-toulene sulfonic acid) and heterogeneous (Amberlyst 15 and Degussa) catalysts. Their experimental data have been interpreted with a second order kinetic model and a good agreement was achieved between the experimental data and the model.

Several authors have also investigated on the effect of phase partitioning of various components between the liquid and the absorbed phase. These phenomena are accountable to resins with remarkable swelling properties as most of the swollen resins shows a high tendency to incorporate both water (H_2O) formed during the reaction and alcohol used as the esterification agent. This phenomenon will lead to a different concentration environment within the pores as compared to the bulk phase concentration. Therefore, for this kind of system, additional information is required to simulate the real reaction mechanism. Ali and Merchant (2006) studied the esterification of myristic acid with isopropyl alcohol using ion exchange resin catalysts (Dowex 50Wx8-400, Amberlite IR-120, and Amberlyst 15) as catalysts. They correlated the experimental data using five kinetic models: PH, ER, LH, modified Langmuir Hinshelwood (ML), and Pöpken (PP). The ML model was found to gives the best prediction of reaction kinetics for the gel-type catalyst while the PP model showed good agreement with the experimental results for the macroreticular catalyst. They also claimed that the partitioning phenomena play a fundamental role in reaction kinetics. Tesser *et al.* (2010b) have developed a detailed kinetic model to demonstrate the effect of partitioning phenomena in the esterification of FFA using

Amberlyst 15 and Relite CFS as catalysts. The developed model successfully interpreted all the experimental data and they claimed that the model was suitable for data prediction in larger production scale, such as an industrial tubular reactor or a continuous plant.

In this research work, a detailed study on the kinetic behaviour of FFA esterification using Purolite D5081 as catalyst was carried out. Several kinetic models have been investigated: the PH, LHHW and ER models. Three kinetic models were commonly used in the esterification of FFA. In the previous chapter, studies on the effect of mass transfer resistances (Chapter 5, section 6.3.1) showed that the reaction was not affected by the mass transfer resistances. Therefore in this kinetic study, external and internal mass transfer limitation is considered to be negligible and hence not considered. For the heterogeneous models, a reaction-on-surface kinetics and rate law were developed based on the following assumptions:

- The surface of the catalyst contains a fixed number of sites.
- All the catalytic sites are identical.
- The reactivity of these sites depends only on the temperature. They do not depend on the nature or amount of other material present on the surface during the reaction.

Kinetic parameters such rate constant and adsorption coefficient were determined using MATLAB using the built-in ODE45 solver, the fourth order Runge-Kutta method to solve the differential equations numerically. The fourth order Runge-Kutta method has been commonly used to numerically integrate the differential moles balance in esterification reaction (Tesser *et al.*, 2009; Kapil *et al.*, 2011). The developed kinetic models were used to correlate experimental data from the esterification reaction. The optimum condition was achieved by minimising the sum of residual square (SRS) between the experimental and calculated mole fraction of all the species involved. The SRS value is a measure of the discrepancy between the experimental data and model estimation. A small SRS value indicates a tight fit of

the model to the data. The best fitted model were further investigated to determine the activation energy of the esterification reaction.

7.2 THE KINETIC MODELS OF FFA ESTERIFICATION

7.2.1 Pseudo Homogeneous (PH) Model

The PH model is widely used in the esterification system and is reported to produce a good correlation between the experimental and simulated data (Tesser *et al.*, 2005; Pasias *et al.*, 2006; Qu *et al.*, 2009).

The general mole balance equation is presented in Equation 7.1.

$$\text{Accumulation} = \text{Input} - \text{Output} - \text{Reacted} \tag{7.1}$$

For this study, a batch reactor has been used to obtain the experimental data. There was no input and output flow during the reaction and hence, Equation 7.1 was simplified to Equation 7.2.

$$\text{Accumulation} = -\text{Reacted} \tag{7.2}$$

The overall esterification process is shown in the following stoichiometric reaction equation which can be expressed mathematically in Equation 7.4.

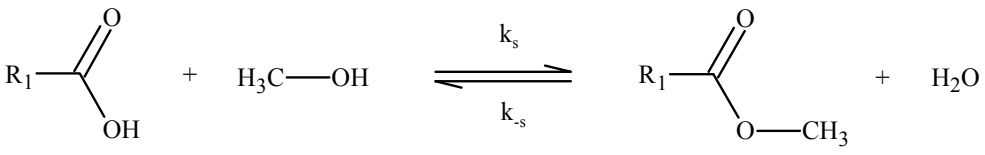

Free Fatty Acids (FFA)	Methanol (MeOH)	Fatty Acid Methyl Ester (FAME)	Water (H_2O)
(A)	(B)	(C)	(D)

(7.3)

$$M_{mix}\ \frac{dC_{FFA}}{dt} = -(-r_{FFA})m_{cat} \tag{7.4}$$

where, C_{FFA} is the concentration of FFA, $-r_{FFA}$ is the reaction rate of FFA, M_{mix} is mass of the reaction mixture and m_{cat} is mass of the Purolite D5081 catalyst.

The PH kinetic model was built based on the following assumptions:

(a) The rate of non-catalysed reaction was negligible relative to the catalysed reaction.
(b) MeOH to FFA molar ratio used was very high, and therefore MeOH concentration was assumed to be constant throughout the reaction process.
(c) The diffusion rate of reactants and products onto the catalyst surface assumed to be negligible.
(d) There was no fatty acid methyl ester (FAME) present in the reaction at time, t = 0.

It was proposed that the reaction was a pseudo *n* order in the forward reaction and second order in the reverse reaction. Therefore, based on these assumptions, the following kinetic rate law was derived.

$$(-r_{FFA}) = -\frac{dC_{FFA}}{dt} = \left(k_f' C_{FFA}\right)^n - \left(-k_r C_{FAME} C_{H_2O}\right) \quad (7.5)$$

where, $k_f' = k_f \times C_{MeOH,0}$, $-r_{FFA}$ is the reaction rate of FFA, k_f' and k_r are the reaction rate constant for forward (esterification) and reverse (hydrolysis) reaction, *n* is the order of forward reaction, $C_{MeOH,0}$ is the initial concentration of MeOH and C_{FFA}, C_{FAME} and C_{H_2O} are the concentration of FFA, FAME and H_2O in the reaction mixture, respectively. For simplification, FFA, MeOH, FAME and H_2O were denoted as A, B, C and D.

Therefore, Equation 7.5 becomes:

$$(-r_A) = -\frac{dC_A}{dt} = \left(k_f' C_A\right)^n - (-k_r C_C C_D) \quad (7.6)$$

Equation 7.4 is directly combined with Equation 7.6 to obtain a new mass balance correlation and shown in Equation 7.7.

$$M_{mix}\ \frac{dC_A}{dt} = -\left((k_f' C_A)^n - (-k_r C_C C_D)\right) m_{cat} \tag{7.7}$$

where, M_{mix} is mass of the reaction mixture and m_{cat} is mass of the Purolite D5081 catalyst. The relationship between the reactants and the products were re-arranged and transformed into the moles of FFA (N_A) term using the following four equations:

$$C_A = \frac{N_A}{M_{mix}} \tag{7.8}$$

$$C_B = \frac{N_{B0} - N_B}{M_{mix}} = \frac{N_{B0} - (N_{A0} - N_A)}{M_{mix}} \tag{7.9}$$

$$C_C = \frac{N_C}{M_{mix}} = \frac{N_{A0} - N_A}{M_{mix}} \tag{7.10}$$

$$C_D = \frac{N_D}{M_{mix}} = \frac{N_{D0} + N_D}{M_{mix}} = \frac{N_{D,0} + (N_{A0} - N_A)}{M_{mix}} \tag{7.11}$$

where, N_{A0}, N_{B0}, N_{C0} and N_{D0} are the number of moles of component A, B, C and D at time = 0 and N_A, N_B, N_C and N_D are the number of moles of component A, B, C and D at time = *t*. Equation 7.7 has been re-arranged with C_A, C_C and C_D terms from Equations 7.8 - 7.11 to derive a new non-linear differential equation (Equation 7.11). Equation 7.9 is not applicable for the PH model will be used later in the heterogeneous model derivation. Time, *t* and moles of FFA, N_A acted as the independent and dependent variables and by solving Equation 7.12, the model prediction of moles of FFA, N_A against time could be developed.

$$\frac{dN_A}{dt} = -\left[\left(k_f^{'} \frac{N_A}{M_{mix}}\right)^n - \left(-k_r \left(\frac{N_{A0} - N_A}{M_{mix}}\right)\left(\frac{N_{D0} + (N_{A0} - N_A)}{M_{mix}}\right)\right)\right] m_{cat} \tag{7.12}$$

7.2.2 Langmuir-Hinshelwood-Hougen-Watson (LHHW) Model

The LHHW model is widely used for the simulation and optimisation of industrial reactors. The LHHW model was also found to successfully describe the esterification reaction (Gan *et al.*, 2009; Srilatha *et al.*, 2011). This model is applicable when the study focuses on the kinetics of surface-catalysed reactions, where the rate determining step is the surface reaction between the adsorbed molecules. The derivatisation of LHHW model was developed by Carberry (1976). The LHHW kinetic model for the esterification of FFA was developed based on the following assumptions:

(a) The rate of non-catalysed reaction was negligible relative to the catalysed reaction.
(b) The adsorption of MeOH, H_2O, FFA and FAME occurs on the surface of the resins. Triglycerides are considered to be non-adsorbing compounds.
(c) The rate determining step is controlled by the surface reaction. A dual site adsorption mechanism is used for the reaction between FFA and MeOH adsorbed on the surface of the catalyst.
(d) The adsorption equilibrium constants are assumed to be independent of the reaction temperature in the investigated temperature range.
(e) The adsorption sites are uniformly energetic and a monolayer catalytic coverage is assumed.
(f) The adsorption and desorption of reactants and products were fast and therefore at equilibrium.
(g) There was no fatty acid methyl ester (FAME) present in the reaction at time, $t = 0$.

It was proposed that the reaction is second order for forward and reverse reactions. For an esterification reaction sequence based on the LHHW model, the mechanism involves the chemisorption of FFA and MeOH as molecules, followed by a reaction between chemisorbed FFA and MeOH molecules to form FAME and H_2O molecules, and finally the desorption of FAME and H_2O. The scheme is summarised by the following mechanism, where S represents the vacant surface site.

Step 1: Chemsorption of FFA $FFA + S \leftrightarrow FFA.S$

Step 2: Chemisorption of MeOH $MeOH + S \leftrightarrow MeOH.S$

Step 3: Surface reaction $FFA.S + MeOH.S \leftrightarrow FAME.S + H_2O.S$

Step 4: Desorption of FAME $FAME.S \leftrightarrow FAME + S$

Step 5: Desorption of H_2O $H_2O.S \leftrightarrow H_2O + S$

The mechanism can also be written as:

Step 1: $A + S \leftrightarrow A.S$

Step 2: $B + S \leftrightarrow B.S$

Step 3: $A.S + B.S \leftrightarrow C.S + D.S$

Step 4: $C.S \leftrightarrow C + S$

Step 5: $D.S \leftrightarrow D + S$

where, A, B, C and D are FFA, MeOH, FAME and H_2O, respectively.

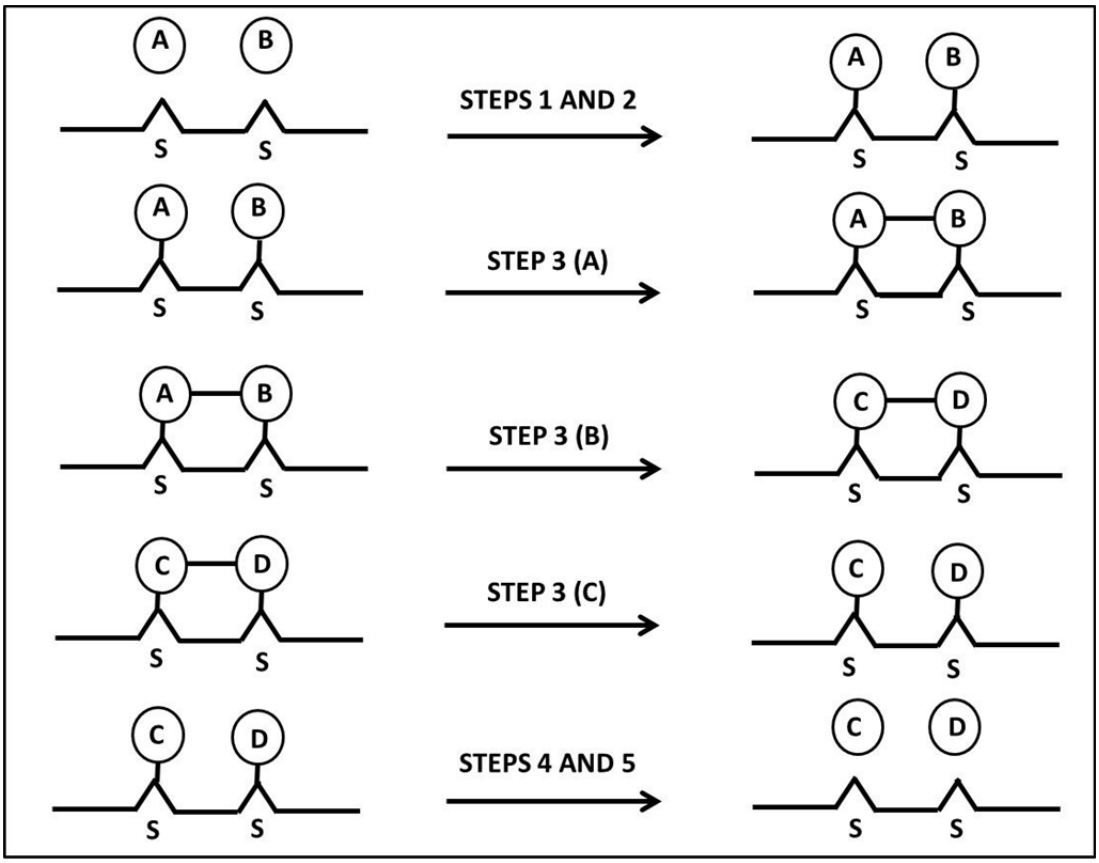

Figure 7.1. Sequence of elementary steps for LHHW model. Reactants A and B adsorb as molecules (Steps 1 and 2), molecules A and B reacted to form adsorbed molecules C and D [Steps 3 (A), (B) and (C)] which subsequently desorb (Steps 4 and 5).

Assuming that bimolecular surface reaction (Step 3) is the rate determining step, the overall rate of reaction between adsorbed A and adsorbed B is given by Equation 7.13:

$$(-r_A) = r_s = k_f \theta_A \theta_B - k_r \theta_C \theta_D \tag{7.13}$$

where, r_s is the rate of surface reaction, k_f and k_r are the rate constants for the forward and reverse reactions and $\theta_{A,}\, \theta_{B,}\, \theta_C$ and θ_D is the fraction of sites occupied by species A, B, C and D respectively. The adsorption and desorption steps, 1, 2, 4 and 5 are assumed to be in equilibrium.

The net rate of adsorption for each species are written as an elementary chemical reaction and presented in Equations 7.14 - 7.17:

$$r_{ads(A)} = k_{a(A)} C_A \theta_V - k_{d(A)} \theta_A \quad (7.14)$$

$$r_{ads(B)} = k_{a(B)} C_B \theta_V - k_{d(B)} \theta_B \quad (7.15)$$

$$r_{ads(C)} = k_{a(A)} C_C \theta_V - k_{d(C)} \theta_C \quad (7.16)$$

$$r_{ads(D)} = k_{a(D)} C_D \theta_V - k_{d(D)} \theta_D \quad (7.17)$$

where, k_a and k_d are the rate constants for adsorption and desorption, C is the concentration of species in the bulk fluid and θ_V is the fraction of vacant sites. The active catalyst sites can either be vacant or occupied by the adsorbed molecules A, B, C and D. The summation between the vacant and occupied sites is equal to one and the site balances are, therefore, written as Equation 7.18. This equation has been re-arranged to Equation 7.19 to have the term for the fraction of vacant sites, θ_V as the subject of the formula.

$$\theta_A + \theta_B + \theta_C + \theta_D + \theta_V = 1 \quad (7.18)$$

$$\theta_V = 1 - \theta_A - \theta_B - \theta_C - \theta_D \quad (7.19)$$

At equilibrium, the net rate of adsorption for all species is equal to zero. Therefore, Equations 7.14 - 7.17 can be written to give the equilibrium surface coverage of each molecules and given by Equations 7.20 - 7.23:

$$\theta_A = K_A C_A \theta_V \quad (7.20)$$

$$\theta_B = K_B C_B \theta_V \quad (7.21)$$

$$\theta_C = K_C C_C \theta_V \quad (7.22)$$

$$\theta_D = K_D C_D \theta_V \quad (7.23)$$

where K_A, K_B, K_C and K_D are the adsorption equilibrium constants for species A, B, C and D respctively and formulated from the ratio of the adsorption and desorption rate constant, $K_i = k_a/k_d$. The equilibrium surface coverage of each species is

substituted into Equation 7.13 to generate the rate expression in terms of concentration, C and fraction of vacant sites, θ_V (Equation 7.24).

$$(-r_A) = k_f K_A C_A K_B C_B \theta_V^2 - k_r K_C C_C K_D C_D \theta_V^2 \quad (7.24)$$

Substitution of the fractional coverage terms (Equations 7.20 - 7.23) into Equation 7.19 gives:

$$\theta_V = 1 - K_A C_A \theta_V - K_B C_B \theta_V - K_C C_C \theta_V - K_D C_D \theta_V \quad (7.25)$$

This equation can be re-arranged to give explicit expression for θ_V and is shown in Equation 7.26.

$$\theta_V = \frac{1}{(1+K_A C_A+K_B C_B+K_C C_C+K_D C_D)} \quad (7.26)$$

Substitution of Equation 7.26 into Equation 7.24 gives:

$$(-r_A) = \frac{k_f K_A C_A K_B C_B - k_r K_C C_C K_D C_D}{(1+K_A C_A+K_B C_B+K_C C_C+K_D C_D)^2} \quad (7.27)$$

Equation 7.27 can be written differently by incorporating the reaction equilibrium constant. Assuming that the surface reaction reached its equilibrium, the net reaction will be equal to zero and therefore Equation 7.13 can be re-arranged to the following form:

$$k_f \theta_A \theta_B = k_r \theta_C \theta_D \quad (7.28)$$

The equilibrium constant can be expressed as a ratio of the forward and reverse rate constants, being defined as:

$$K_{eq} = \frac{k_f}{k_r} \quad (7.29)$$

Substitution of Equation 7.29 into Equation 7.28 gives:

$$K_{eq} = \left(\frac{\theta_C \theta_D}{\theta_A \theta_B}\right)_{eq} \tag{7.30}$$

Substitution of the value of θ_A, θ_B, θ_C and θ_D from Equation 7.20 - 7.23 into Equation 7.30 gives:

$$K_{eq} = \left(\frac{K_C C_C \theta_V K_D C_D \theta_V}{K_A C_A \theta_V K_B C_B \theta_V}\right) = \left(\frac{K_C C_C K_D C_D}{K_A C_A K_B C_B}\right) = \left(\frac{K_C K_D}{K_A K_B}\right)\left(\frac{C_C C_D}{C_A C_B}\right) \tag{7.31}$$

The concentration terms for all species involved could be expressed in terms of equilibrium constant, K for the overall reaction, as presented in Equation 7.32.

$$K = \frac{C_C C_D}{C_A C_B} \tag{7.32}$$

Substituting the value of K from Equation 7.32 in Equation 7.31 to get

$$K_{eq} = \frac{K_C K_D}{K_A K_B} \; K \tag{7.33}$$

The final rate equation is obtained by the substitution of Equation 7.33 into Equation 7.27, re-arranged and expressed as:

$$(-r_A) = \frac{k_f K_A K_B \left(C_A C_B - \frac{1}{K} C_C C_D\right)}{(1 + K_A C_A + K_B C_B + K_C C_C + K_D C_D)^2} \tag{7.34}$$

where $K = K_{eq}(K_A K_B / K_C K_D)$. Equation 7.34 is substituted into Equation 7.4 to obtain a new mass balance correlation and shown in Equation 7.35.

$$M_{mix} \frac{dC_A}{dt} = -\left(\frac{k_f K_A K_B \left(C_A C_B - \frac{1}{K} C_C C_D\right)}{(1 + K_A C_A + K_B C_B + K_C C_C + K_D C_D)^2}\right) m_{cat} \tag{7.35}$$

Substitution of C_A, C_B, C_C and C_D terms from Equations 7.8 - 7.11 into Equation 7.35 gives a new non-linear differential equation (Equation 7.36).

$$\frac{dN_A}{dt} = -\left(\frac{k_f K_A K_B \left(\left(\frac{N_A}{M_{mix}}\right)\left(\frac{N_{B0}-(N_{A0}-N_A)}{M_{mix}}\right) - \frac{1}{K}\left(\frac{N_{A0}-N_A}{M_{mix}}\right)\left(\frac{N_{A0}-N_A}{M_{mix}}\right)\right)}{\left(1+K_A\left(\frac{N_A}{M_{mix}}\right)+K_B\left(\frac{N_{B0}-(N_{A0}-N_A)}{M_{mix}}\right)+K_C\left(\frac{N_{A0}-N_A}{M_{mix}}\right)+K_D\left(\frac{N_{A0}-N_A}{M_{mix}}\right)\right)^2} \right) m_{cat} \quad (7.36)$$

7.2.3 Eley-Rideal (ER) Model

The ER model is a special case of the LHHW model when the surface reaction involves the reaction between the adsorbed molecule and a molecule in the bulk fluid. Based on several previous works on the esterification of FFA, the ER model was also found to successfully describe the esterification reaction (Steinigeweg and Gmehling, 2003, Tesser *et al*., 2005; Lerkkasemsan *et al.*, 2011). The ER kinetic model was developed based on the following assumptions:

(a) The rate of non-catalysed reaction was negligible relative to the catalysed reaction.

(b) The adsorption of MeOH, H_2O, FFA and FAME occurs on the surface of the resins. Triglycerides are considered to be non-adsorbing compounds.

(c) The rate determining step is controlled by the surface reaction. A single site adsorption mechanism is used for the reaction between one reactant adsorbed on the surface of the catalyst with another reactant coming from the bulk fluid.

(d) The adsorption equilibrium constants are assumed to be independent of the reaction temperature in the investigated temperature range.

(e) The adsorption sites are uniformly energetic and a monolayer catalytic coverage is assumed.

(f) The adsorption and desorption of reactants and products were fast and therefore at equilibrium.

(g) There was no fatty acid methyl ester (FAME) present in the reaction at time, t = 0.

It was proposed that the reaction is second order for forward and reverse reactions. For an esterification reaction sequence based on the ER model, the reaction mechanism differs in terms of the components which are adsorbed onto the catalyst. There are two possible cases for ER model; ER model (Case I) where the adsorbed MeOH is reacting with FFA in the fluid or ER model (Case II) where the adsorbed FFA reacts with MeOH in the fluid.

The mechanism for Case I involves the chemisorption of MeOH onto the catalyst surface, followed by a reaction between chemisorbed MeOH and FFA molecules from the bulk fluid to form FAME and H_2O molecules and finally the desorption of H_2O molecules from the catalyst surface. FFA and FAME are assumed to be in the bulk fluid. The scheme is summarised by the following mechanism, where S represents the vacant surface site.

ER Mechanism: Case I

Step 1: Chemsorption of FFA $MeOH + S \leftrightarrow MeOH.S$

Step 2: Surface reaction $FFA + MeOH.S \leftrightarrow FAME + H_2O.S$

Step 3: Desorption of FAME $H_2O.S \leftrightarrow H_2O + S$

The mechanism for Case II involves the chemisorption of FFA onto the catalyst surface, followed by a reaction between chemisorbed FFA and MeOH molecules from the bulk fluid to form FAME and H_2O molecules and finally the desorption of FAME from the catalyst surface. H_2O and MeOH are assumed to be in the bulk fluid. The scheme is summarised by the following mechanism, where S represents the vacant surface site.

ER Mechanism: Case II

Step 1: Chemsorption of FFA $FFA + S \leftrightarrow FFA.S$

Step 2: Surface reaction $FFA.S + MeOH \leftrightarrow FAME.S + H_2O$

Step 3: Desorption of FAME $FAME.S \leftrightarrow FAME + S$

The illustrations of the ER mechanism (Case I and Case II) are presented in Figures 7.2 and 7.3, respectively.

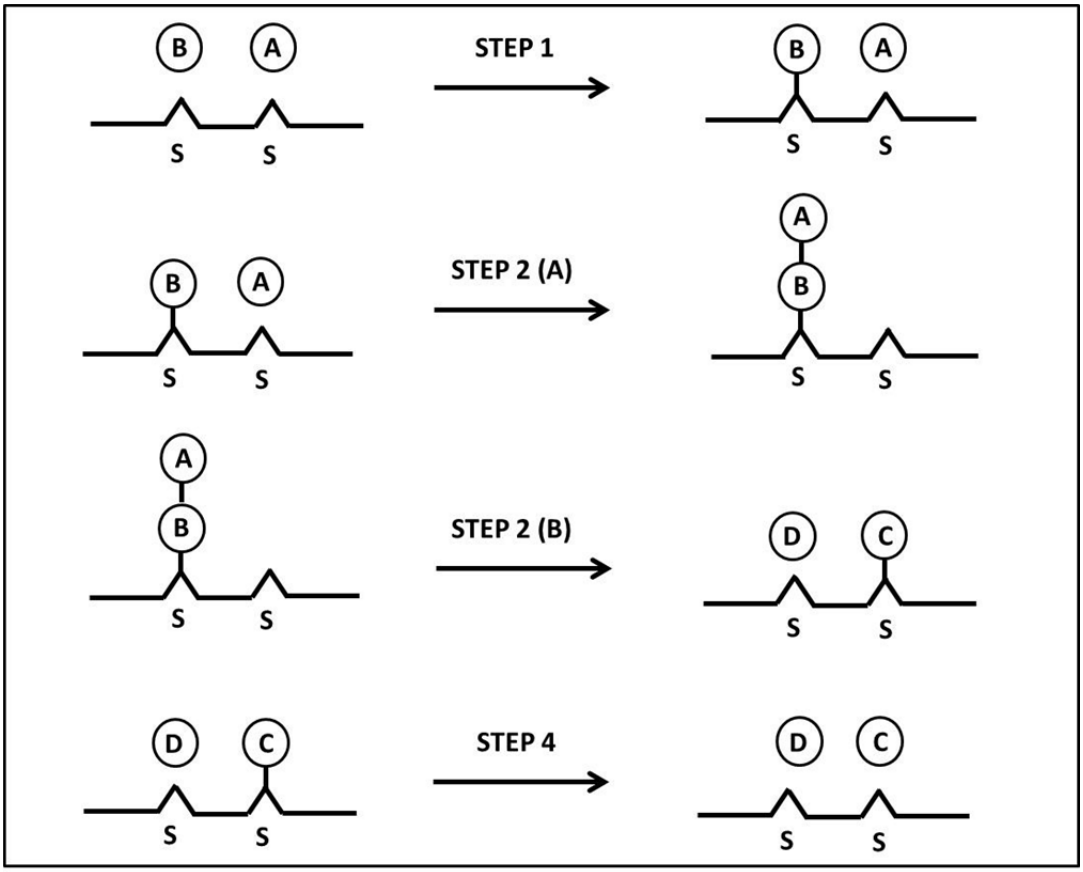

Figure 7.2. Sequence of elementary steps for ER model (Case I). Molecule B adsorbed on the catalyst surface (Step 1), which then reacted with molecules A in the bulk fluid to form molecules C and D [Steps 2 (A) and (B)] and subsequently molecules D desorbed from the catalyst surface (Step 3).

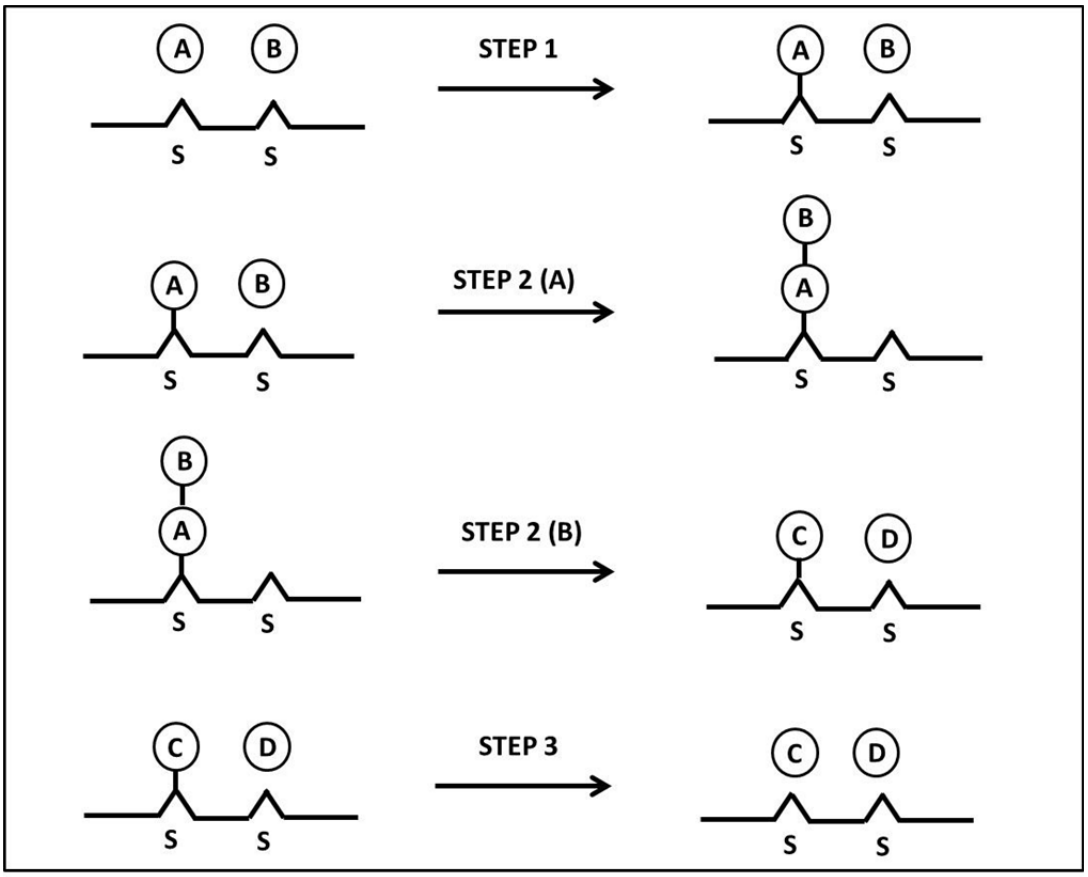

Figure 7.3. Sequence of elementary steps for ER model (Case II). Molecule A adsorbed on the catalyst surface (Step 1), which then reacted with molecules B in the bulk fluid to form molecules C and D [Steps 2 (A) and (B)] and subsequently molecules C desorbed from the catalyst surface (Step 3).

The previous scheme for Case I and Case II mechanisms of ER model can be also written as follows:

ER Mechanism: Case I

Step 1: $B + S \leftrightarrow B.S$

Step 2: $A + B.S \leftrightarrow C + D.S$

Step 3: $D.S \leftrightarrow D + S$

ER Mechanism: Case II

Step 1: $A + S \leftrightarrow A.S$

Step 2: $A.S + B \leftrightarrow C.S + D$

Step 3: $C.S \leftrightarrow C + S$

where, A, B, C and D are FFA, MeOH, FAME and H_2O, respectively.

Assuming that bimolecular surface reaction (Step 2) is the rate determining step, the overall rate of reaction between species A and adsorbed B (Case I) and species B and adsorbed A (Case II) are presented in Equations 7.37 and 7.38:

$$(-r_A) = r_s = k_f C_A \theta_B - k_r C_C \theta_D \quad (7.37)$$

$$(-r_A) = r_s = k_f C_B \theta_A - k_r C_D \theta_C \quad (7.38)$$

where r_s is the rate of surface reaction, k_f and k_r are the rate constants for the forward and reverse reactions, θ_A, θ_B, θ_C and θ_D are the fraction of sites occupied by species A, B, C and D and C_A, C_B, C_C and C_D are concentration of species A, B, C and D in the bulk fluid, respectively. The adsorption and desorption steps, step 1 and 3 are assumed to be in equilibrium. For the further derivation of ER model, only Case I will be presented as both cases are similar. For Case II, the final equation will be presented at the end of the derivation process.

The net rate of adsorption for species B and D are written as an elementary chemical reaction and presented in Equations 7.39 and 7.40:

$$r_{ads(B)} = k_{a(B)} C_B \theta_V - k_{d(B)} \theta_B \quad (7.39)$$

$$r_{ads(D)} = k_{a(D)} C_D \theta_V - k_{d(D)} \theta_D \quad (7.40)$$

where k_a and k_d are the rate constants for adsorption and desorption, C is the concentration of species in the bulk fluid and θ_V is the fraction of vacant sites. The active catalyst sites can either be vacant or occupied by the adsorbed molecules B

and D. The summation between the vacant and occupied sites is equal to one and the site balances are therefore written as Equation 7.41. This equation has been re-arranged to give Equation 7.42 to have fraction of vacant sites, θ_V as the subject of formula.

$$\theta_B + \theta_D + \theta_V = 1 \quad (7.41)$$

$$\theta_V = 1 - \theta_B - \theta_D \quad (7.42)$$

At equilibrium, the net rate of adsorption for all species is equal to zero. Therefore, Equations 7.39 and 7.40 can be written to give the equilibrium surface coverage of each molecule, given by Equations 7.43 and 7.44:

$$\theta_B = K_B C_B \theta_V \quad (7.43)$$

$$\theta_D = K_D C_D \theta_V \quad (7.44)$$

where K_B and K_D are the adsorption equilibrium constants for species B and D respectively and formulated from the ratio of the adsorption and desorption rate constant, $K_i = k_a/k_d$. The equilibrium adsorbed surface coverage term for each species is substituted into Equation 7.37 to generate the rate expression in terms of the bulk fluid concentration and θ_v (Equation 7.45).

$$(-r_A) = k_f K_B C_A C_B \theta_V - k_r K_D C_C C_D \theta_V \quad (7.45)$$

Substitution of the fractional coverage terms (Equations 7.43 and 7.44) into Equation 7.42 gives:

$$\theta_V = 1 - K_B C_B \theta_V - K_D C_D \theta_V \quad (7.46)$$

This equation can be re-arranged to give an explicit expression for θ_v and shown in Equation 7.47.

$$\theta_V = \frac{1}{(1+K_B C_B+K_D C_D)} \tag{7.47}$$

Substitution of Equation 7.47 into Equation 7.45 gives:

$$(-r_A) = \frac{k_f K_B C_A C_B - k_r K_D C_C C_D}{(1+K_B C_B+K_D C_D)} \tag{7.48}$$

Equation 7.48 can be written differently by incorporating the reaction equilibrium constant. Assuming that the surface reaction reached its equilibrium, the net reaction will be equal to zero and therefore Equation 7.37 can be re-arranged to the following form:

$$k_f C_A \theta_B = k_r C_C \theta_D \tag{7.49}$$

The equilibrium constant for the surface reaction can be expressed as a ratio of the forward and reverse reaction, being defined as:

$$K_{eq} = \frac{k_f}{k_r} \tag{7.50}$$

Substitution of Equation 7.50 into Equation 7.49 gives:

$$K_{eq} = \left(\frac{\theta_D C_C}{\theta_B C_A}\right)_{eq} \tag{7.51}$$

Substitution of Equations 7.43 and 7.44 into Equation 7.51 gives:

$$K_{eq} = \left(\frac{K_D C_D \theta_V C_C}{K_B C_B \theta_V C_A}\right) = \left(\frac{K_D C_C C_D}{K_B C_A C_B}\right) = \left(\frac{K_D}{K_B}\right)\left(\frac{C_C C_D}{C_A C_B}\right) \tag{7.52}$$

The concentration terms for all the species involved can be expressed in terms of the equilibrium constant for the overall reaction, as shown in Equation 7.53.

$$K = \frac{C_C C_D}{C_A C_B} \tag{7.53}$$

The relationship among the equilibrium constants could also be generated by substituting Equation 7.53 into Equation 7.52 and the equation expressed as:

$$K_{eq} = \frac{K_D}{K_B} K \tag{7.54}$$

The final rate equation is obtained by the substitution of Equation 7.54 into Equation 7.48, re-arranged and expressed as:

$$\text{Case I:} \qquad (-r_A) = \frac{k_f K_B \left(C_A C_B - \frac{1}{K} C_C C_D \right)}{(1 + K_B C_B + K_D C_D)} \tag{7.55}$$

where $K = (K_B/K_D)K_{eq}$. The similar derivation method is used for Case II and the final rate equation can be expressed as:

$$\text{Case II:} \qquad (-r_A) = \frac{k_f K_A \left(C_A C_B - \frac{1}{K} C_C C_D \right)}{(1 + K_A C_A + K_C C_C)} \tag{7.56}$$

where $K = (K_A/K_C)K_{eq}$. Equations 7.55 and 7.56 are then substituted into Equation 7.4 to obtain a new mass balance correlation and shown in Equations 7.57 and 7.58.

$$\text{Case I:} \qquad M_{mix} \frac{dC_A}{dt} = -\left(\frac{k_f K_B \left(C_A C_B - \frac{1}{K} C_C C_D \right)}{(1 + K_B C_B + K_D C_D)} \right) m_{cat} \tag{7.57}$$

$$\text{Case II:} \qquad M_{mix} \frac{dC_A}{dt} = -\left(\frac{k_f K_A \left(C_A C_B - \frac{1}{K} C_C C_D \right)}{(1 + K_A C_A + K_C C_C)} \right) m_{cat} \tag{7.58}$$

Substitution of C_A, C_B, C_C and C_D terms from Equations 7.8 - 7.11 into Equations 7.57 and 7.58 gives a new non-linear differential equations (Equations 7.59 and 7.60).

$$\text{Case I: } \frac{dN_A}{dt} = -\left(\frac{k_f K_B\left(\left(\frac{N_A}{M_{mix}}\right)\left(\frac{N_{B0}-(N_{A0}-N_A)}{M_{mix}}\right)-\frac{1}{K}\left(\frac{N_{A0}-N_A}{M_{mix}}\right)\left(\frac{N_{A0}-N_A}{M_{mix}}\right)\right)}{\left(1+K_B\left(\frac{N_{B0}-(N_{A0}-N_A)}{M_{mix}}\right)+K_D\left(\frac{N_{A0}-N_A}{M_{mix}}\right)\right)}\right) m_{cat} \tag{7.59}$$

$$\text{Case II: } \frac{dN_A}{dt} = -\left(\frac{k_f K_A\left(\left(\frac{N_A}{M_{mix}}\right)\left(\frac{N_{B0}-(N_{A0}-N_A)}{M_{mix}}\right)-\frac{1}{K}\left(\frac{N_{A0}-N_A}{M_{mix}}\right)\left(\frac{N_{A0}-N_A}{M_{mix}}\right)\right)}{\left(1+K_A\left(\frac{N_A}{M_{mix}}\right)+K_C\left(\frac{N_{A0}-N_A}{M_{mix}}\right)\right)}\right) m_{cat} \tag{7.60}$$

7.2.4 Criteria for Acceptance of Kinetic Models

The estimated rate constant and adsorption coefficient values from each individual kinetic model should be positive. For the heterogeneous kinetic model, it was assumed that the reaction rate was controlled by the adsorption of the reactant molecules onto the catalyst surface. Therefore, if negative values of the adsorption coefficient are obtained, the results would be meaningless. Gangadwala *et al.* (2003) studied kinetic of acetic acid esterification with *n*-butanol as a solvent and they found that the LHHW model gave negative values for adsorption coefficients and hence they concluded that LHHW model was not suitable for the analysed system. Similar findings were reported by Patel and Saha (2007) when they investigated esterification of acetic acid with *n*-hexanol using ion exchange resins as catalysts. They reported that the heterogeneous models were unable to predict the experimental data since the modelling results gave negative values for adsorption coefficients.

7.3 RESULTS AND DISCUSSIONS

The kinetic data for the esterification reaction was correlated with three kinetic models, the PH, LHHW and ER models. Based on the assumptions, the rate of reactions were derived for PH, LHHW and ER (Case I and Case II) models and

presented in Equations 7.6, 7.34, 7.55 and 7.56. From the non-linear differential equations (Equations 7.12, 7.36, 7.59 and 7.60), depending on the kinetic model, two reaction rate constants, k_f and k_r and up to four adsorption coefficient (K_A, K_B, K_C and K_D) are unknown. These unknowns must be determined to describe the reaction system. A built-in ODE45 solver in MATLAB 7.0 was used to numerically integrate the differential molar balances describing the concentration of FFA in the system. Optimum kinetic parameters were determined by minimising the sum of residual squares (SRS) between experimental and calculated moles of FFA. The equation is shown as below:

$$\text{SRS} = \sum_{i=1}^{N_{exp}} \left(N_A^{exp} - N_A^{calc}\right)^2 \tag{7.61}$$

where N_{exp} is the number of experimental data and N_A^{exp} and N_A^{calc} are the experimental and calculated moles of FFA.

Experimental data were successfully fitted by the PH model whereas results obtained from both heterogeneous kinetic models gave negative values for adsorption coefficients. The fitted values for heterogeneous models are given in Table 7.2.

Table 7.2. Fitted values for LHHW and ER (Case I and II) models.

Models/ Temperature (K)	Forward Rate Constant, k_f	Reverse Rate Constant, k_r	Adsorption Coefficient K_A	K_B	K_C	K_D
Langmuir-Hinshelwood-Hougen-Watson						
323	5.44E-01	1.24E-03	6.06E+02	-7.83E+01	8.39E+01	-1.32E+02
328	7.11E-01	1.30E-03	6.56E+02	-8.33E+01	1.06E+02	-1.33E+02
333	8.15E-01	9.10E-04	4.52E+02	-5.09E+01	1.19E+02	-8.29E+01
335	7.62E-01	8.55E-04	4.78E+02	-4.62E+01	8.52E+01	-6.09E+01
Eley Rideal (Case I)						
323	8.44E-03	6.00E-05	n/a	-8.14E-02	n/a	-0.221E+01
328	1.81E-01	4.17E-05	n/a	-4.15E-02	n/a	-0.121E+01
333	1.49E-03	5.00E-05	n/a	-7.16E-02	n/a	-0.229E+01
335	7.70E-04	1.20E-04	n/a	-8.36E-02	n/a	-0.101E+01
Eley Rideal (Case II)						
323	0.439 E+01	6.68E-02	-2.00E-04	n/a	-2.30E-01	n/a
328	0.240 E+01	1.01E-01	-5.00E-04	n/a	-1.77E-01	n/a
333	0.351 E+01	5.47E-02	-4.00E-04	n/a	-3.39E-01	n/a
335	0.225 E+01	1.00E-01	-8.00E-04	n/a	-2.22E-01	n/a

*Units for forward and reverse rate contants are $kg^2\ kg_{cat}^{-1}\ mol^{-1}\ s^{-1}$.

As some of the adsorption coefficients give negative values, the results would be meaningless and hence they were not considered. Furthermore, from the ER model (Case I) route, the mechanism shows that this model cannot lead to reaction and the inhibition was due to the competition of active sites between the reactants. Schmitt and Haase (2006) revealed similar findings when they developed several kinetic models for the synthesis of *n*-hexyl acetate. It was concluded that the heterogeneous kinetic models failed to correctly describe the reaction kinetics. For this analysis, PH model was chosen for further analysis since both LHHW and ER models were unable to predict the experimental data.

Figure 7.4 shows the moles of FFA versus reaction time profile for the esterification performed at different reaction temperatures. From Figure 7.4, a good agreement between the experimental and the calculated moles of FFA were observed for all the experimental data points. The pseudo order for forward reaction was found to give the optimum value of n = 1.6. The calculated results for the PH model kinetic parameters are summarised in Table 7.3. The forward and reverse rate constants, k_f and k_r increased with an increase in reaction temperature (see Table 7.3). However, the increase of reverse rate constant, k_r values with the increase of reaction temperature are considered to be very small and this indicates that the reverse reaction, the hydrolysis process was hardly took place in the reaction.

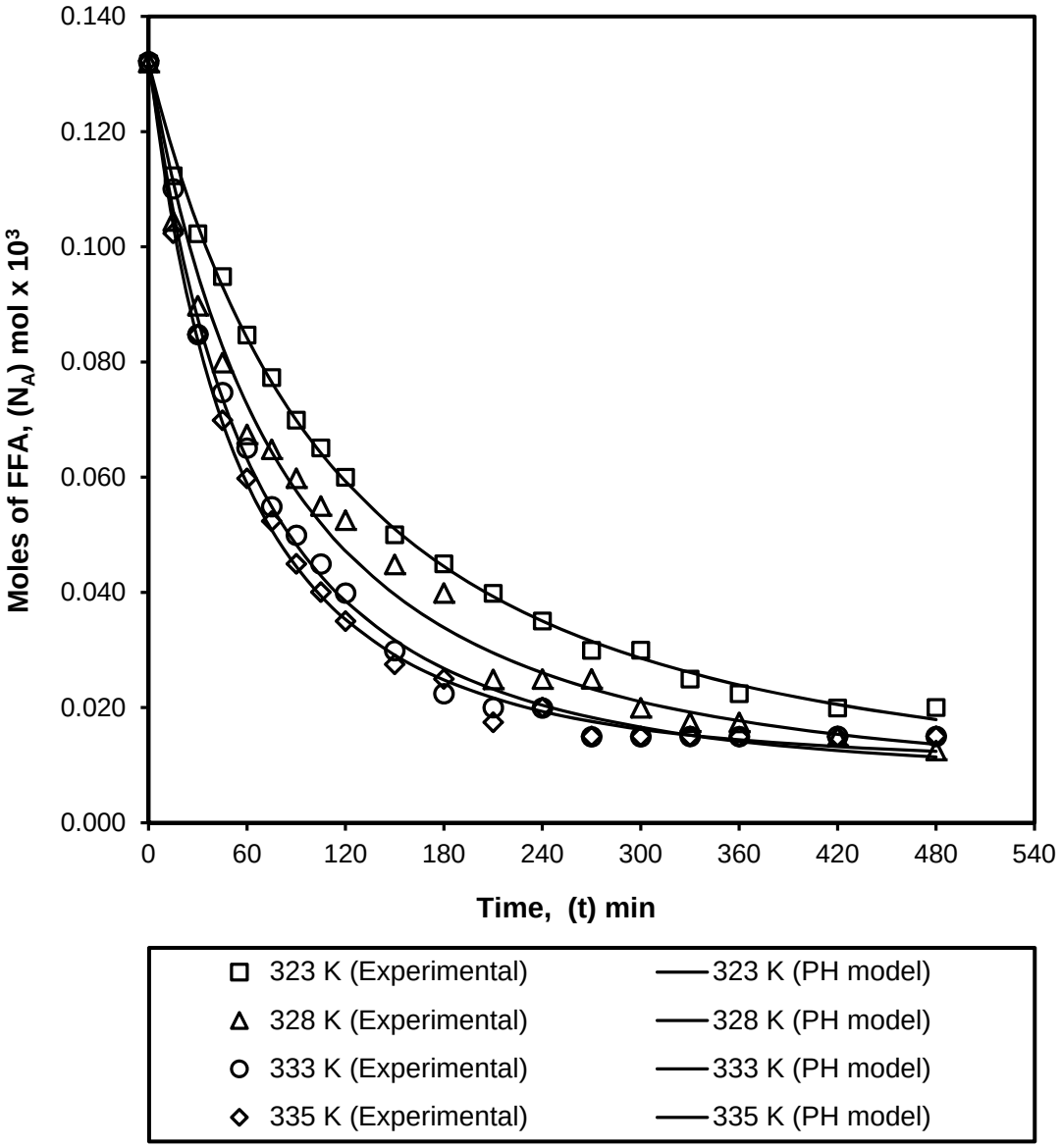

Figure 7.4. The effect of reaction temperatures on the moles of FFA. Experimental conditions: Catalyst: Purolite D5081; catalyst loading: 1.25% (w/w); feed molar ratio (MeOH:UCO): 6:1; stirring speed: 350 rpm.

Table 7.3. Estimated values of the rate constants (forward and reverse reaction) and the corresponding values of SRS for PH model.

Temperature, T (K)	Forward Rate Constant, k_f ($kg^{2.6}$ kg_{cat}^{-1} $mol^{-1.6}$ s^{-1})	Reverse Rate Constant, k_r (kg^2 kg_{cat}^{-1} mol^{-1} s^{-1})	Sum of Residual Square (SRS)	Equilibrium Constant, K_{eq}
323	1.9302	9.10E-04	3.79E-05	2121.13
328	2.7003	1.79E-03	2.47E-04	1510.01
333	3.5000	2.51E-03	1.04E-04	1394.46
335	3.9500	4.31E-03	4.59E-05	917.18

The influence of reaction temperature on the reaction rate was determined by fitting the rate constant, k_f and k_r to the Arrhenius-Van't Hoff equation, as shown in the following equation:

$$k_f = \mathrm{A_f} \exp\left(-\frac{E_o}{RT}\right) \tag{7.62}$$

$$k_r = \mathrm{A_r} \exp\left(-\frac{E_o}{RT}\right) \tag{7.63}$$

where $\mathrm{A_f}$ and $\mathrm{A_r}$ are the Arrhenius pre-exponential factors for the forward and reverse reactions, E_o is the activation energy of the reaction, R is the gas constant and T is the reaction temperature. The Arrhenius plot for the esterification of FFA with MeOH is shown in Figure 7.5. The activation energy for the esterification and hydrolysis reactions calculated from Figure 7.5 are reported in Table 7.4. The reported activation energy values in Table 7.4 are in good agreement with those values reported in the literature for similar systems, with the consideration that different reaction system, temperature range, type of catalyst and catalyst loading were involved. The value for the hydrolysis activation energy also agrees with the values of reverse rate constants, indicating that higher amount of energy is required for hydrolysis reverse reaction to occur. Table 7.5 shows the comparison of activation energy calculated from the current work with the previous FFA kinetics modelling studies reported in the literature.

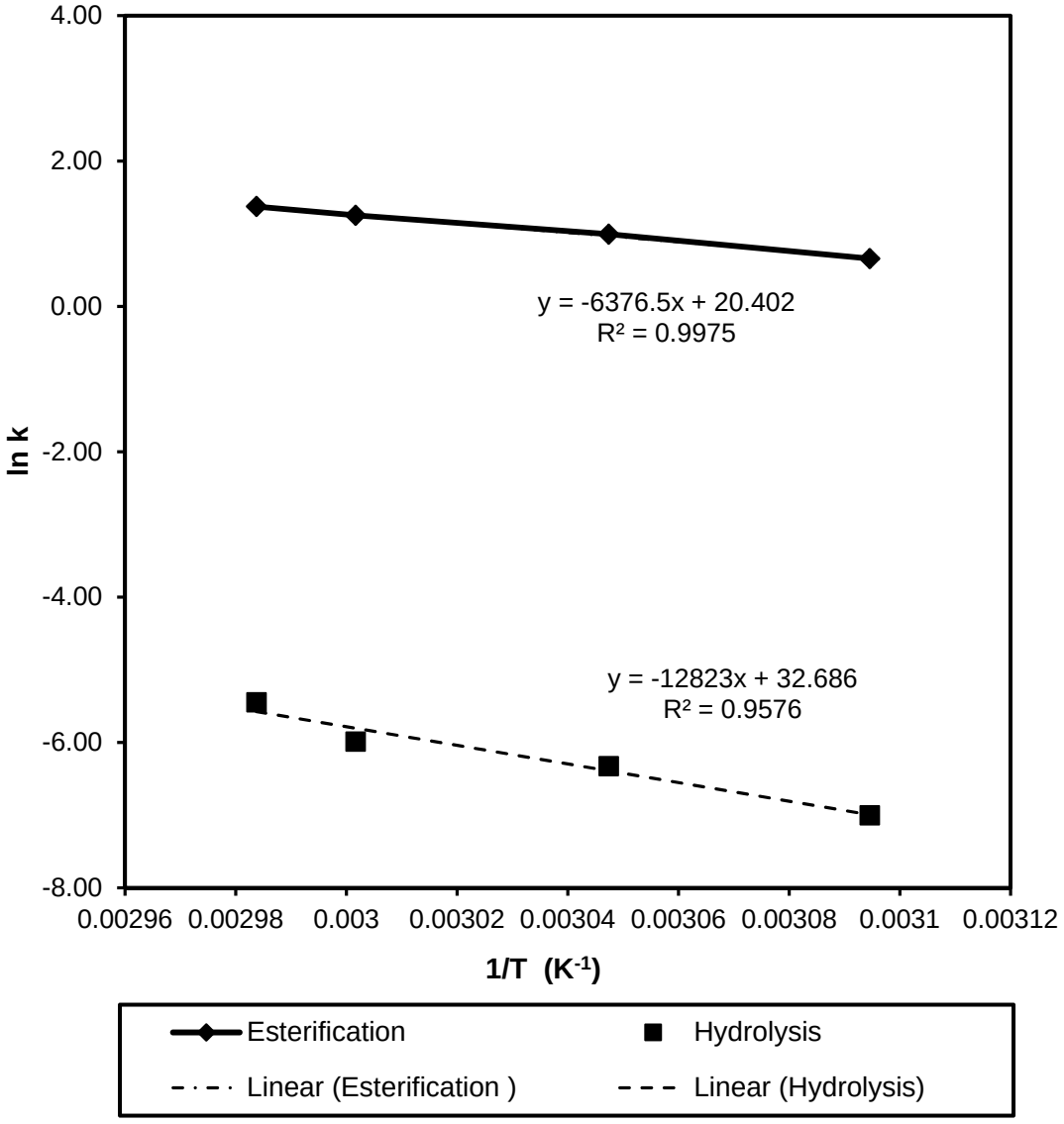

Figure 7.5. The Arrhenius plot for the esterification of FFA using Purolite D5081 as a catalyst.

Table 7.4. Activation energy and the pre-exponential factor for esterification and hydrolysis reactions.

Reaction	Activation Energy (kJ mol^{-1})	Pre-Exponential Factor	R^2
Esterification	53	7.25E+08	0.9975
Hydrolysis	107	1.57E+14	0.9576

Table 7.5. Comparison of activation energies for the esterification reaction using homogeneous and heterogeneous acid catalysts.

Reaction	Catalyst	Reaction Temperature (K)	Kinetic Model (order of reaction)	Activation Energy (kJ mol^{-1})	References
Used cooking oil (UCO) + MeOH	Purolite D5081	323 - 335	PH (first order - forward reaction, second order - reverse reaction)	53	This work
Oleic acid + MeOH	Relite CFS	323 - 358	PH (second order)	58.62	Tesser *et al.* (2005)
High acidity vegetable oil + MeOH	CT-275	363 - 393	PH (second order)	70.34	Pasias *et al.* (2006)
Sunflower oil + MeOH	Sulphuric acid	30 - 333	PH (first order - forward reaction, second order - reverse reaction)	50.75 (5 wt % acid) 44.56 (10 wt% acid)	Berrios *et al.* (2007)
Low grade crude palm oil (CPO) + MeOH	Sulphuric acid	313 - 333	PH (first order)	30.4	Satriana and Supardan, (2008)
Waste cooking oil + MeOH	$Fe_2(SO_4)_3/C$	338 - 368	LHHW (second order)	18.59	Gan *et al.* (2009)
Palmitic acid + MeOH	TPA/ZrO_2	318 - 338	LHHW (second order)	34.2	Srilatha *et al.* (2011)

7.4 CONCLUSIONS

The kinetic modelling of FFA esterification was successfully carried out using Purolite D5081 as a catalyst. Esterification reaction was carried out using 1.25% (w/w) catalyst loading, 6:1 MeOH:UCO feed mole ratio, 350 rpm stirring speed and reaction temperatures ranging from 323 - 335 K. The experimental data from the esterification reaction were fitted to three kinetic models: PH, LHHW and ER. Experimental data was successfully represented by the PH model and good agreement between the experimental and the calculated values was obtained. Both heterogeneous kinetic models gave negative values for the adsorption coefficients and hence were not considered further. The forward rate constant, k_f increased with an increase in reaction temperature. However, the increase of reverse rate constant, k_r values with the increase in reaction temperature are considered to be very small

and this indicates that the reverse reaction (hydrolysis process) hardly took place in the reaction. The activation energies for the esterification and hydrolysis reactions were found to be 53 and 107 kJ mol^{-1}, respectively. These results proved that the hydrolysis reverse reaction requires more energy to occur as compared to esterification reaction, hence validated the proposed model. The SRS values for PH kinetic model vary between 1.04 x 10^{-4} and 4.59 x 10^{-5}.

8 TRANSESTERIFICATION OF PRE-TREATED USED COOKING OIL (P-UCO) TO BIODIESEL USING HETEROGENEOUS CATALYSTS

8.1 INTRODUCTION

In this chapter, the transesterification of used cooking oil (UCO) to biodiesel using heterogeneous catalysts is discussed in detail. Prior to transesterification, methanol was removed from the esterified UCO using a rotary evaporator. The resulting product referred to as the pre-treated UCO (P-UCO) was used as a feedstock for the transesterification reaction. This chapter highlights the use of acid and base heterogeneous catalysts for biodiesel synthesis. Initial batch kinetics studies were carried out for all heterogeneous catalysts and the catalyst that performed the best in terms of triglycerides conversion as compared to other catalysts was selected for further optimisation of batch kinetic studies. Elimination of mass transfer resistances and the effect of catalyst loading, reaction temperature and methanol to P-UCO feed mole ratio on triglycerides conversion were investigated. The experiments were conducted in a jacketed batch reactor to determine the optimum condition for the transesterification process. A reusability study of the best catalyst was performed at the optimum conditions, followed by the separation and purification of biodiesel. Finally, characterisation of the purified biodiesel product was carried out and is summarised at the end of this chapter.

8.2 SCREENING OF ACIDIC AND BASIC HETEROGENEOUS CATALYSTS

The transesterification of biodiesel using different types of heterogeneous catalysts has been investigated to select the best catalyst for further optimisation work. There are three groups of catalysts involved in this work. They are (i) cation exchange resins (Purolite CT-122, Purolite CT-169, Purolite CT-175, Purolite CT-275, Purolite D5081), (ii) anion exchange resin (Diaion PA306s) and (iii) Cs-supported heteropolyacids catalysts [$Cs_{2.5}H_{0.5}PW_{12}O_{40}$ and $Cs_{2.5}H_{0.5}PW_{12}O_{40}$(calcined)], respectively. All catalysts were tested under the same reaction conditions, 1.5% (w/w) of catalyst loading, 333 K reaction temperature, 18:1 methanol to P-UCO feed

mole ratio and 350 rpm impeller stirring speed. The results are collected in Figure 8.1. which shows that after 8 h, the conversion of triglycerides was ca. 50% using Diaion PA306s catalyst, ca. 10% using Purolite CT-275 and ca. 7% using Purolite CT-122 and Purolite CT175. For Cs-supported heteropolyacids catalysts [$Cs_{2.5}H_{0.5}PW_{12}O_{40}$ and $Cs_{2.5}H_{0.5}PW_{12}O_{40}$ (calcined)] and Purolite D5081, there was no measureable formation of FAME. Of all the catalysts investigated, Diaion PA306s gave the highest triglyceride conversion of ca. 50%.

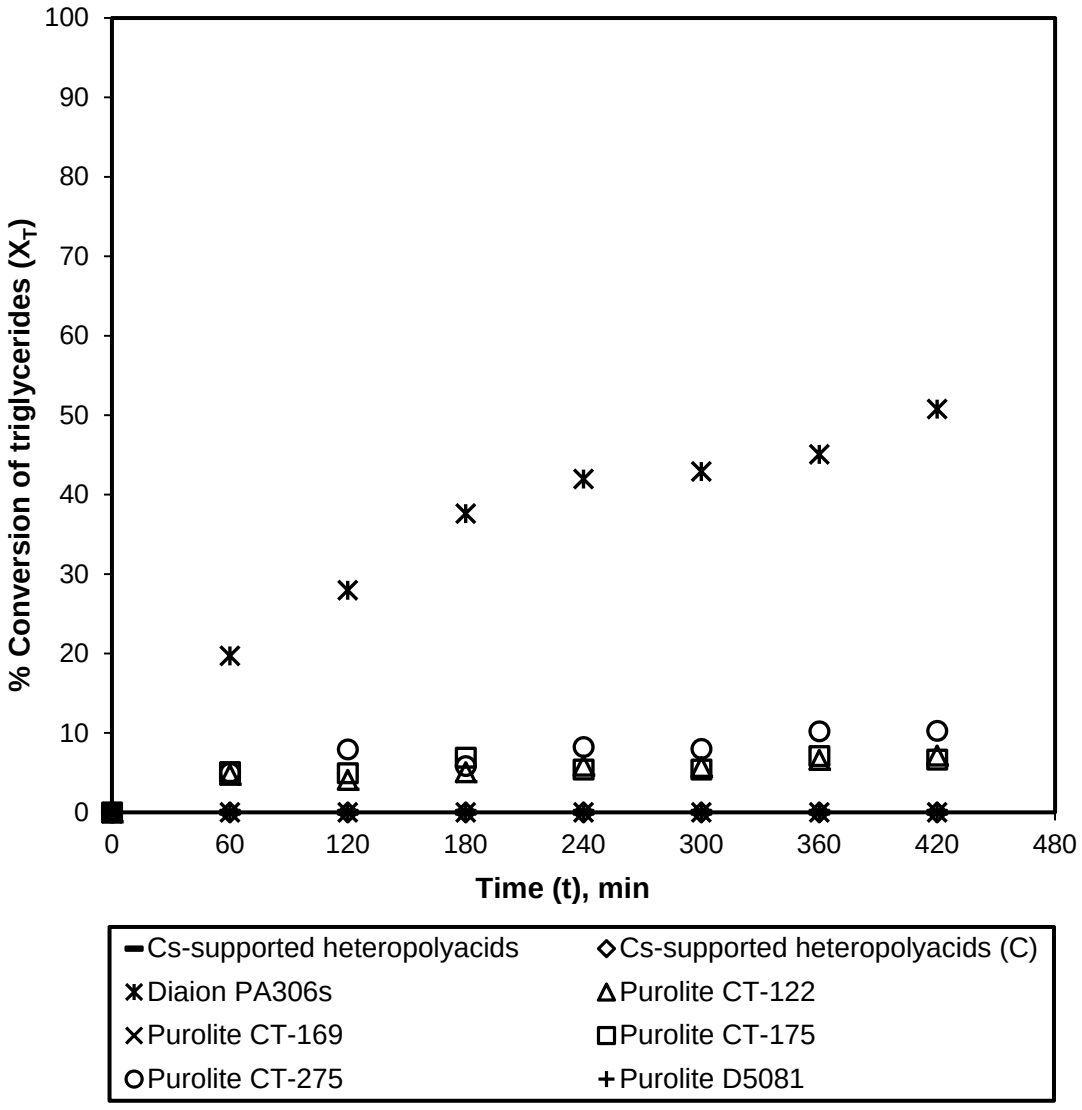

Figure 8.1. Effect of different types of catalysts on triglycerides conversion. Experimental condition: Stirring speed: 350 rpm, catalyst loading: 1.5% (w/w); reaction temperature: 333 K; feed mole ratio (methanol:P-UCO): 18:1.

A huge difference in catalytic performance was observed between Diaion PA306s and the other catalysts and it was expected to be closely related to the acidity and basicity of the catalysts. In this case, Diaion PA306s was classified as a strongly basic anion exchange resin, whilst the rest of the catalysts are categorised as strongly acidic. Base catalysed transesterification has been proven to be a favourable technology and can achieve a high purity and biodiesel yield in a short time (Muniyappa *et al.*, 1996; Antolìn *et al.*, 2002).

In addition, differences in chemical and physical properties may also contribute to the performance of the catalysts. Amongst the catalysts investigated, Diaion PA306s is a low cross-linked resin, with small particles. However, these criteria may not contribute to the catalytic performance since the other low cross-linked catalyst, Purolite CT-122 was only able to give ca. 7% of triglycerides conversion. In addition, there was no conversion of triglycerides when Cs-supported heteropolyacids catalyst, $Cs_{2.5}H_{0.5}PW_{12}O_{40}$ with smallest particle size distribution was used as a catalyst. In contrast, Purolite CT-275, which has a high degree of cross-linking gives a slightly higher triglycerides conversion of ca. 10%. This shows that the basicity of the catalyst is responsible for its transesterification activity and not particle size distribution, specific surface area, average pore diameter or the cross-linked density. Mazzotti *et al.* (1997) and Shibasaki-Kitakawa *et al.* (2007) also reported that the adsorption strength of the alcohol on the anion exchange resin was much higher as compared to cation exchange resins and therefore anion exchange resin resulted in higher activity than cation exchange resin. Since Diaion PA306s showed the best catalytic performance, it was used for the subsequent transesterification reactions.

8.3 OPTIMISATION OF TRANSESTERIFICATION PROCESS IN A JACKETED BATCH REACTOR

8.3.1 Elimination of Mass Transfer Resistances

As mentioned earlier in Chapter 6, there are two types of mass transfer resistances involved in ion exchange catalysis. The first is external mass transfer resistance, which takes place across the solid-liquid interface, whilst the second is the internal

mass transfer resistance associated with the differences in particle size of the catalysts. To evaluate the effect of external mass transfer resistance, the transesterification reactions were performed using different stirring speeds under the same reaction conditions. Three different agitation speeds were used, 300, 350 and 450 rpm and the result is shown in Figure 8.2. Triglyceride conversion between the selected stirring rates gave almost an identical conversion when the agitation speed increased from 300 to 450 rpm. The final conversion of triglycerides at 8 h for all the mentioned stirring speed was ca. 40%. As the stirring speed above 300 rpm only has a negligible impact on triglycerides conversion, it was confirmed that the external mass transfer resistance has negligible effect on the transesterification reaction. Hence, a stirring rate of 350 rpm and above was selected for subsequent experiments.

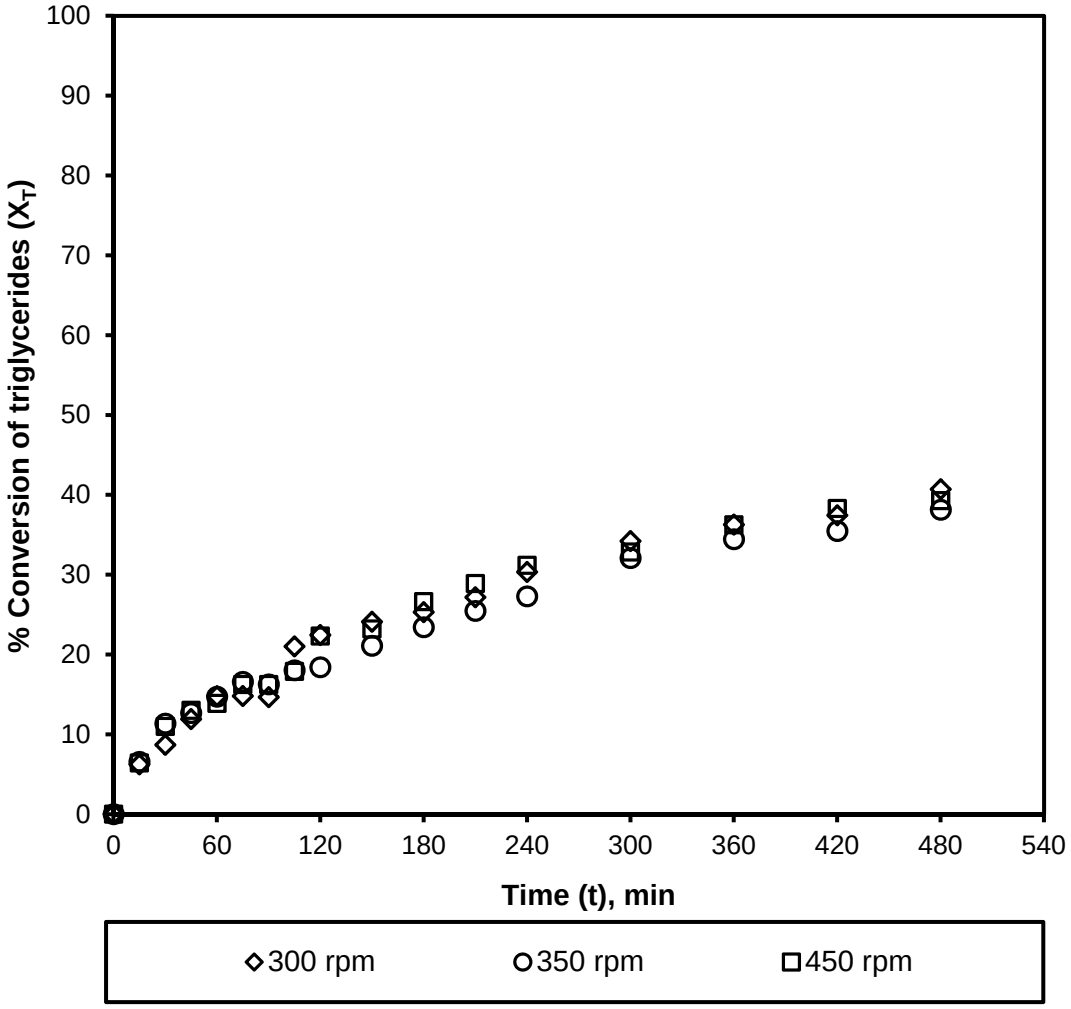

Figure 8.2. Effect of stirring speed on triglycerides conversion - External mass transfer resistance. Experimental conditions: Catalyst: Diaion PA306s; catalyst loading: 1.5% (w/w); reaction temperature: 323 K; feed mole ratio (methanol:P-UCO): 18:1.

The effect of internal mass transfer resistance can be studied by measuring reaction rates for different average catalyst particle sizes. In this case, absence of internal mass transfer resistance could not be verified because the catalyst was supplied in wet form in the swelling condition. This type of catalyst (anion exchange resin) cannot be heated to more than 333 K, otherwise it affects the stability of the catalyst. As the water content cannot be totally removed below 333 K, separation by a sieving will not represent the actual size of catalyst particle. Therefore, PA306s resin was used as received, without sieving for all transesterification reaction.

8.3.2 Effect of Catalyst Loading

The catalyst concentration was found to affect the conversion of triglycerides. To explore this possibility, the effect of catalyst concentration on triglycerides conversion was investigated using different catalyst loadings, 1.5% (w/w), 3% (w/w), 4.5% (w/w), 5.5% (w/w), 9% (w/w) and 10% (w/w). The weight of the catalyst was based on the dry basis calculation. Figure 8.3 shows the effect of catalyst loading on the conversion of triglycerides. The reaction temperature was set at 323 K with 18:1 methanol to P-UCO feed mole ratio and 350 rpm stirring speed.

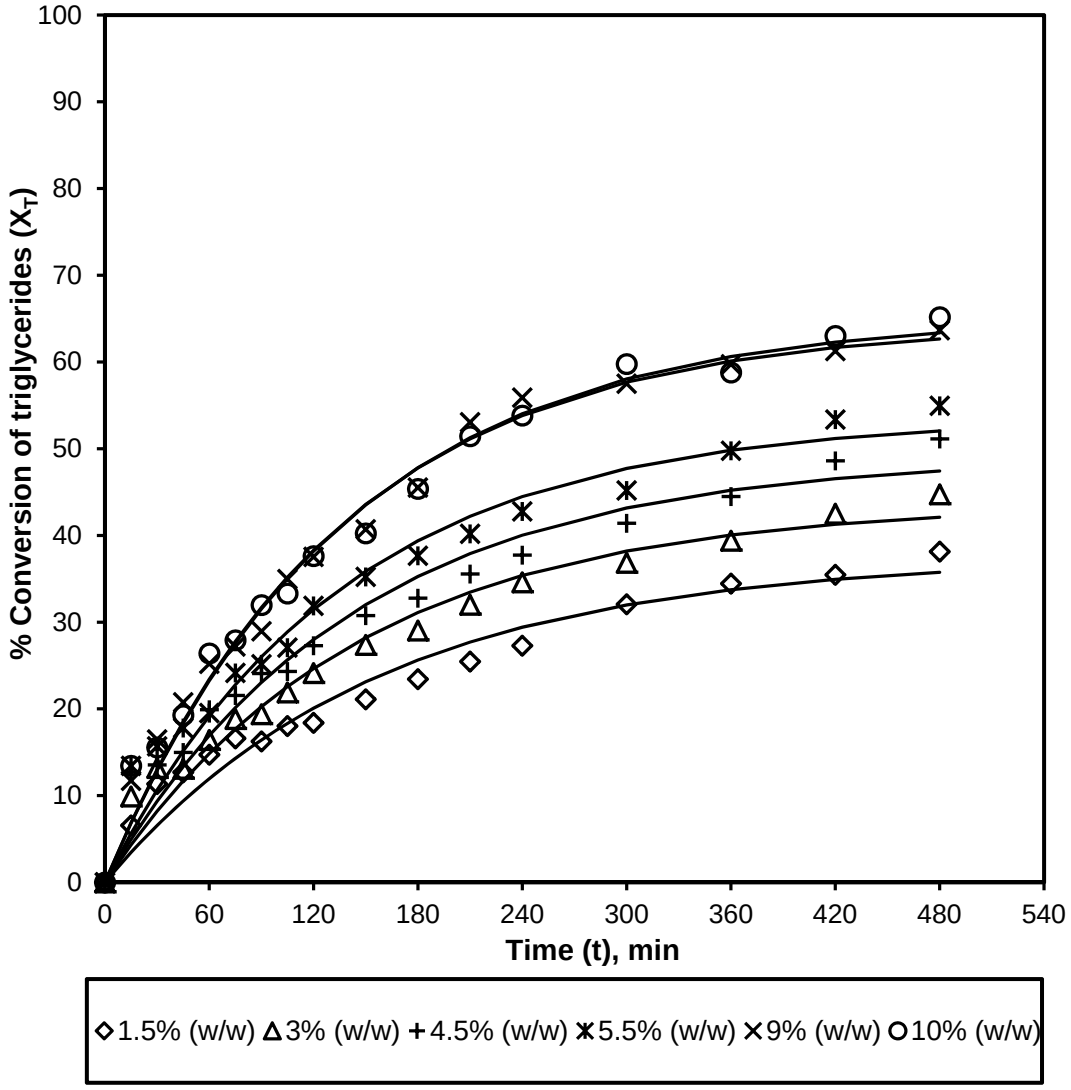

Figure 8.3. Effect of catalyst loading on triglycerides conversion. Experimental conditions: Catalyst: Diaion PA306s; stirring speed: 350 rpm; reaction temperature: 323 K; feed mole ratio (methanol:P-UCO): 18:1.

As observed from Figure 8.3, increasing the catalyst concentration was found to increase triglycerides conversion. This behaviour was expected since with an increase in the number of active catalytic sites, triglycerides conversion increases. An increase in the conversion of triglycerides was more significant when the catalyst loading increased from 1.5% (w/w) to 3% (w/w) (ca. 38% to 45%) and from 4.5% (w/w) to 5.5% (w/w) (i.e. ca. 51% to 55%) than when it increased from 9% (w/w) to 10% (w/w) (ca. 64% to 65%). As the reaction proceeds, the changes in triglycerides conversion become less significant, indicating that the system is approaching equilibrium. Based on the observation for 9% (w/w) and 10% (w/w) catalyst loading, it could be concluded that a further increase in catalyst concentration would cause negligible increase in the conversion of triglycerides (ca. 64% to 65%). Furthermore, higher catalyst dosage leads to a more viscous reaction mixture that will increase the mass transfer resistance in the multiphase system (Reddy *et al.*, 2006). Therefore, using a very high amount of catalyst is unnecessary for this reaction. The turnover frequency (TOF) for transesterification reaction is 2.31 h^{-1}. For all further transesterification study, 9% (w/w) was chosen as the optimum catalyst loading.

8.3.3 Effect of Reaction Temperature

The reaction temperature plays an important role in increasing triglycerides conversion. In order to investigate the effect of reaction temperature, transesterification reaction was carried out in the temperature range of 313 to 333 K. Figure 8.4 shows the plot of triglycerides conversion over time at various reaction temperatures. From Figure 8.4, triglycerides conversion was found to increase with an increase in reaction temperature. A similar trend was observed by other researchers (Liu *et al.*, 2009) when they studied the effect of reaction temperature on biodiesel transesterification using different types of ion exchange catalysts. Figure 8.4 also shows a significant difference in triglycerides conversion when the reaction temperature increases from 313 to 328 K. After 8 h of reaction, the final conversion of triglycerides at 313, 325 and 328 K was approximately 50%, 64% and 75%, respectively.

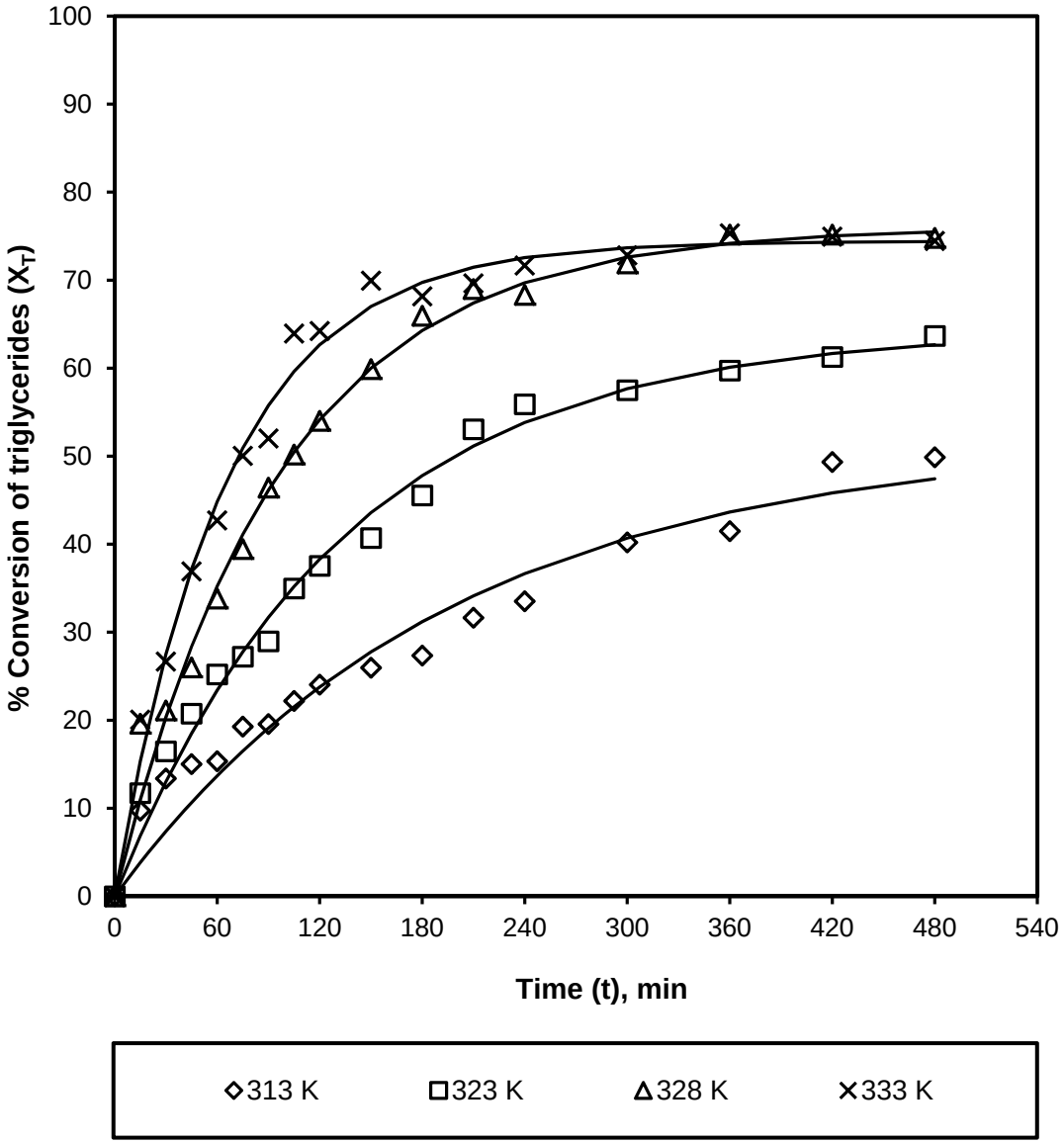

Figure 8.4. Effect of reaction temperature on triglycerides conversion. Experimental conditions: Catalyst: Diaion PA306s; stirring speed: 350 rpm; catalyst loading: 9% (w/w); feed mole ratio (methanol:P-UCO): 18:1.

As mentioned earlier in Chapter 6, an increase in reaction temperature leads to a reduction in the viscosity of triglycerides, which enhances the contact between methanol and triglycerides. From Figure 8.4, it was also observed that triglycerides conversion for the 328 and 333 K reaction temperatures are similar although the time for the conversion to reach steady state was faster for 333 K. As the final conversion for 325 and 328 K was approximately the same with ca. 75% conversion, an increase in temperature will only increase the operating cost. Therefore, 325 K was chosen as

the optimum reaction temperature and proposed for further transesterification reactions.

8.3.4 Effect of Methanol to P-UCO Feed Mole Ratio

The feed mole ratio of methanol to P-UCO is one of the parameters that affect the conversion of triglycerides. Stoichiometrically, the methanolysis of triglycerides requires three moles of methanol per mole of triglyceride to yield three moles of FAME and one mole of glycerine. The reaction mechanism was shown in Figure 8.1. Given that the transesterification is a reversible reaction, excess methanol should help the conversion of triglycerides. The molar mass of UCO was determined to be 871.82 g mol^{-1} and this was used to calculate the feed mole ratio of methanol to P-UCO. Figure 8.5 shows the effect of feed mole ratio of methanol to P-UCO on the conversion of triglycerides.

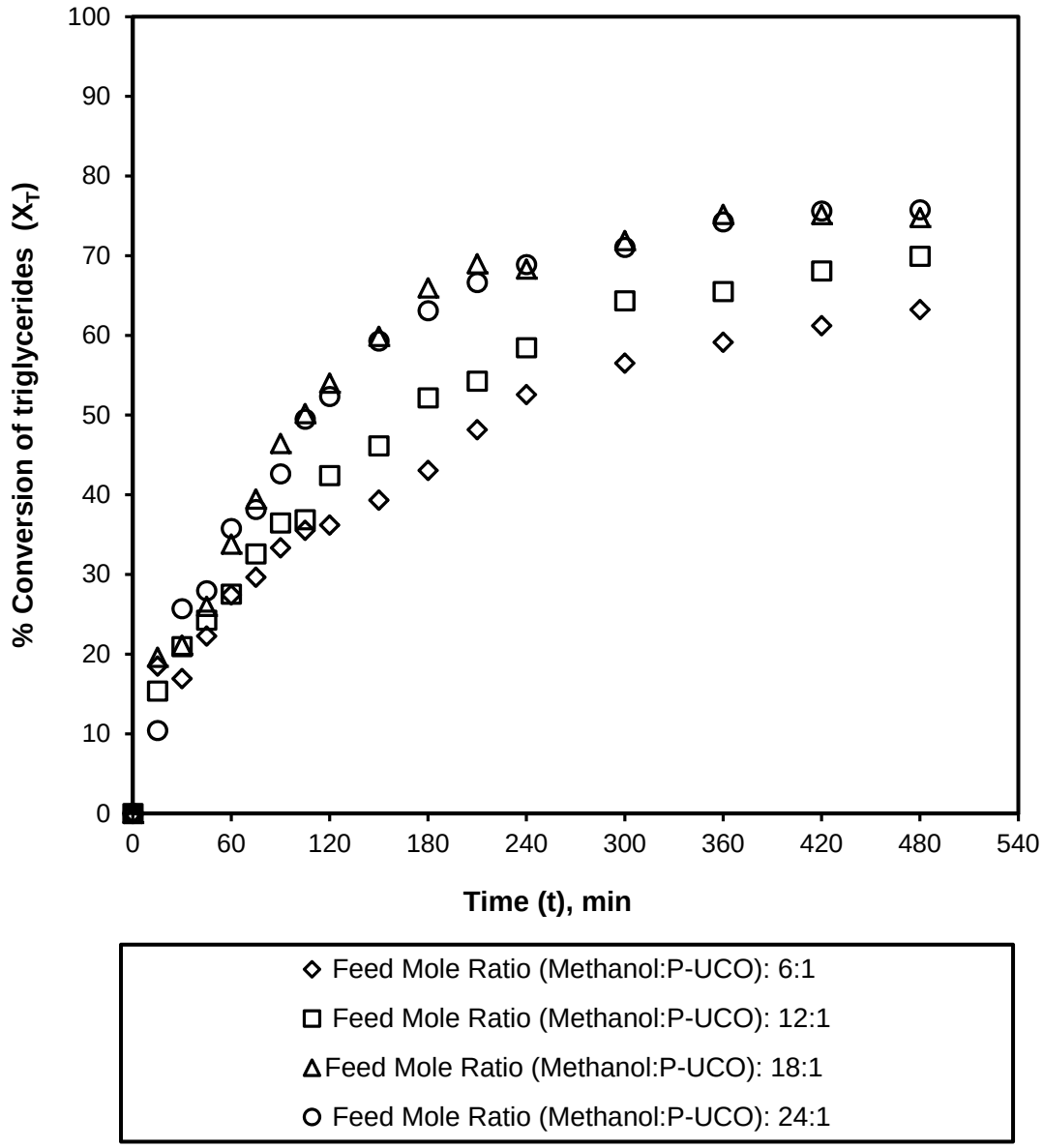

Figure 8.5. Effect of feed mole ratio (methanol:P-UCO) on triglycerides conversion. Experimental conditions: Catalyst: Diaion PA306s; stirring speed: 350 rpm; catalyst loading: 9% (w/w); reaction temperature: 328 K.

As observed from Figure 8.5, the conversion of triglycerides increased with an increase in methanol to P-UCO feed mole ratio from 6:1 to 18:1. The conversion of triglycerides using 6:1, 12:1 and 18:1 methanol to P-UCO feed mole ratio at 8 h are 63%, 69% and 75%, respectively. From Figure 8.5, it can be seen that a further increase in feed mole ratio of methanol to P-UCO from 18:1 to 24:1 did not result in an increase in conversion of triglycerides and the final triglycerides conversion for both feed mole ratios were approximately same, i.e. 75%. A significantly high feed

mole ratio is not preferable in biodiesel production because it makes the separation process difficult (Murugesan *et al.*, 2008). A higher consumption of methanol also requires larger unit operations including reactors, separation column and methanol recovery equipment that will increase the overall cost of the process (Zhang *et al.*, 2003b; Chai *et al.*, 2007; Yan *et al.*, 2010). An optimum operating ratio should be selected on the basis of overall economics and equilibrium conversion and therefore, a feed mole ratio of 18:1 methanol to P-UCO was selected as the optimum ratio and used for further transesterification reaction.

8.4 CATALYST REUSABILITY STUDY

Reusability of the catalyst is an important step as it reduces the cost of biodiesel production. The preparation of spent catalyst for the reusability study was detailed in Chapter 3, section 3.7.2. During the preparation of used catalyst, the displacement of fatty acid ion with acetate ion was investigated using acetic acid concentrations of 17.5 M and 1 M, respectively. Two analyses (FEG-SEM and elemental analysis) were conducted before the displacement process was finalised.

The FEG-SEM analysis was carried out to observe any changes on the surface of the catalysts after being treated with acetic acid. Figure 8.6 compares the FEG-SEM analysis for (a) fresh Diaion PA306s, (b) used Diaion PA306s (1 M acetic acid treatment) and (c) used Diaion PA306s (17.5 M acetic acid treatment) catalysts captured at 500x magnification.

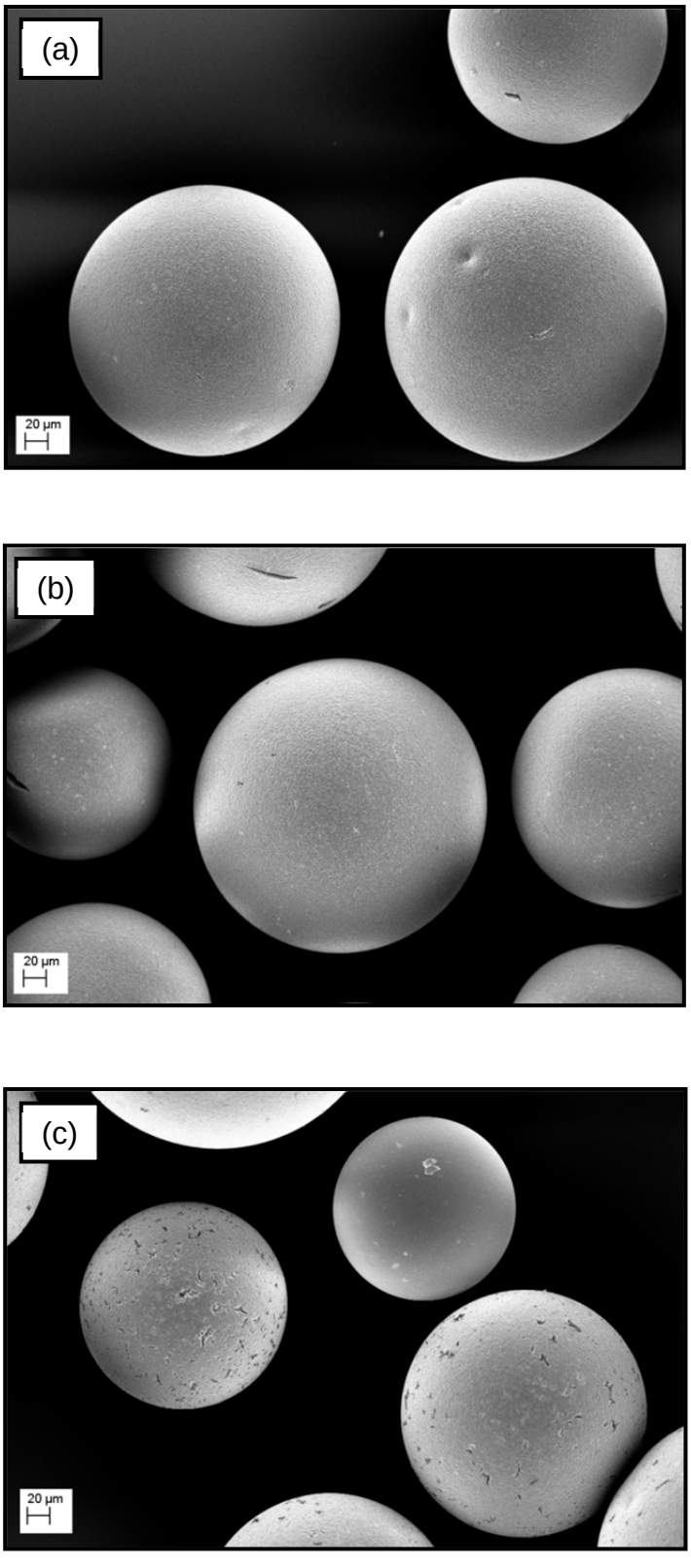

Figure 8.6. The FEG-SEM images of Diaion PA306s catalysts, taken at 500x magnification: (a) Fresh Diaion PA306s, (b) used Diaion PA306s (1 M acetic acid treatment) and (c) used Diaion PA306s (17.5 M acetic acid treatment).

From Figure 8.6, it can be seen that the surface morphology of fresh and used Diaion PA306s (1 M of acetic acid treatment) catalysts appears as a smooth surface whereas a noticeable deterioration of the surface was found when Diaion PA306s catalyst was treated with 17.5 M acetic acid. This suggests that the concentration of acetic acid is too high. Table 8.1 shows the results of the elemental analysis. From Table 8.1, it can be seen that the used Diaion PA306s catalysts treated with 17.5 and 1 M acetic acid resulted in a slightly lower carbon and hydrogen values as compared to the fresh Diaion PA306s. The reduction of carbon and hydrogen values in used Diaion PA306s catalyst treated with 17.5 M of acetic acid was also found to be slightly higher than the used Diaion PA306s catalyst treated with 1 M of acetic acid. This indicates that there are some changes or damage to the structure of Diaion PA306s catalyst when higher acetic acid concentration was used and this could contribute to a loss in catalytic activity. Therefore, acid displacement using 1 M acetic acid solution was selected and further displacement was carried out as described in Chapter 3, section 3.7.2.

Table 8.1. Elemental analysis of fresh and used Diaion PA306s

Catalysts	**Elemental Analysis**			
	%C	**%H**	**%N**	**%O***
Fresh Diaion PA306s	55.59	9.42	4.34	30.65
Used Diaion PA306s (1 M acetic acid)	55.44	9.20	4.31	31.05
Used Diaion PA306s (17.5 M acetic acid)	54.51	8.84	4.35	32.30

*Oxygen by difference

The reusability study was carried out under the optimum reaction conditions, 9% (w/w) catalyst loading, 328 K reaction temperature, 18:1 methanol to P-UCO feed mole ratio and 350 rpm stirring speed. The result of reusability study was compared with the optimum result obtained using fresh Diaion PA306s catalyst and shown in Figure 8.7. It was observed that the Diaion PA306s catalyst gave a similar conversion of triglycerides using fresh and used catalysts. The conversion of triglycerides for both catalysts after 8 h of reaction time was approximately 75%. It

was concluded that the catalyst can be used several times without losing catalytic activity.

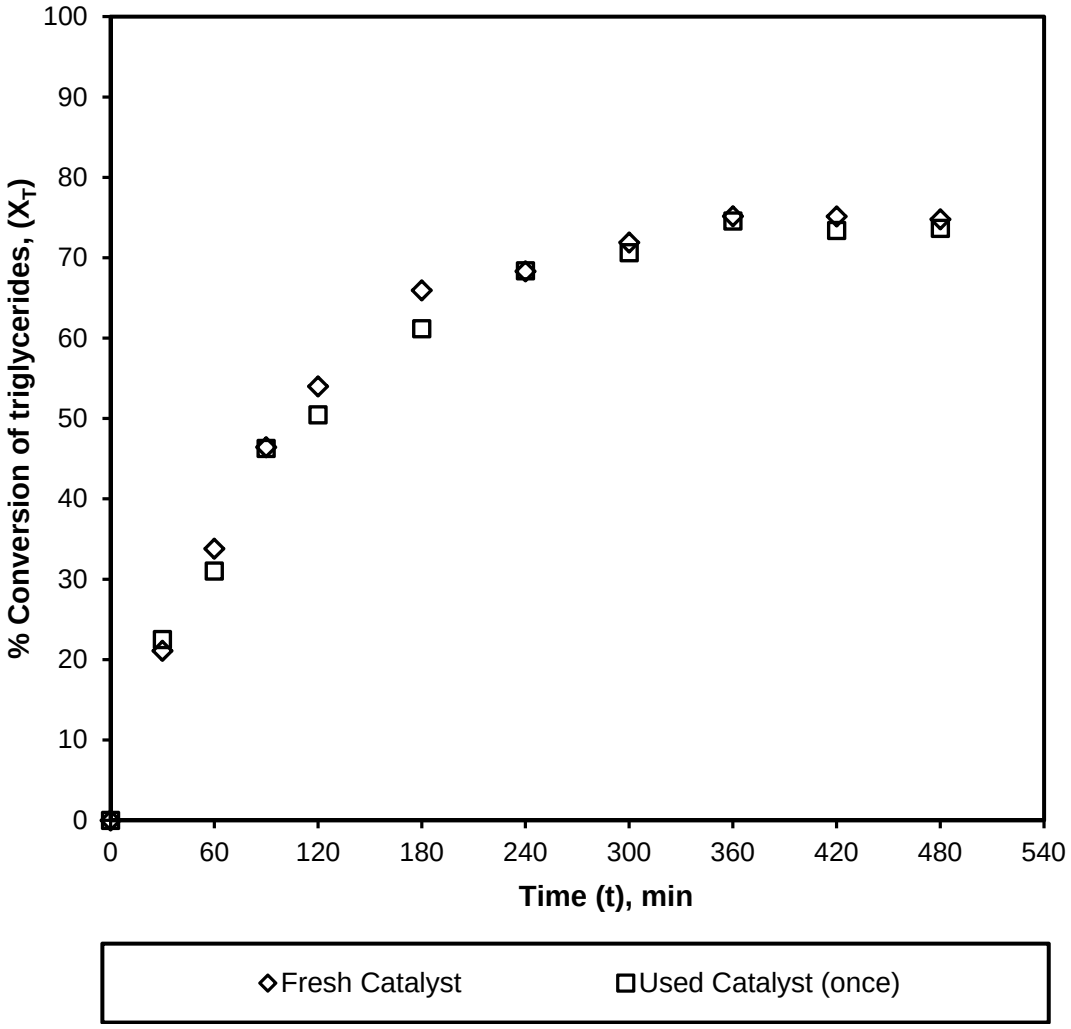

Figure 8.7. Effect of catalyst reusability on the conversion of triglycerides. Experimental conditions: Catalyst: Diaion PA306s; stirring speed: 350 rpm; catalyst loading: 9% (w/w); reaction temperature: 328 K; feed mole ratio (methanol:UCO): 18:1.

8.5 SEPARATION AND PURIFICATION PROCESS

Once the transesterification reaction was completed, the reaction mixture was allowed to cool to room temperature. The reaction mixture was separated from the catalyst and transferred to a separating funnel. Figure 8.8 shows the separation of the products in the separating funnel. Phase separation can be observed within 5-10 min and is completed within 24 h.

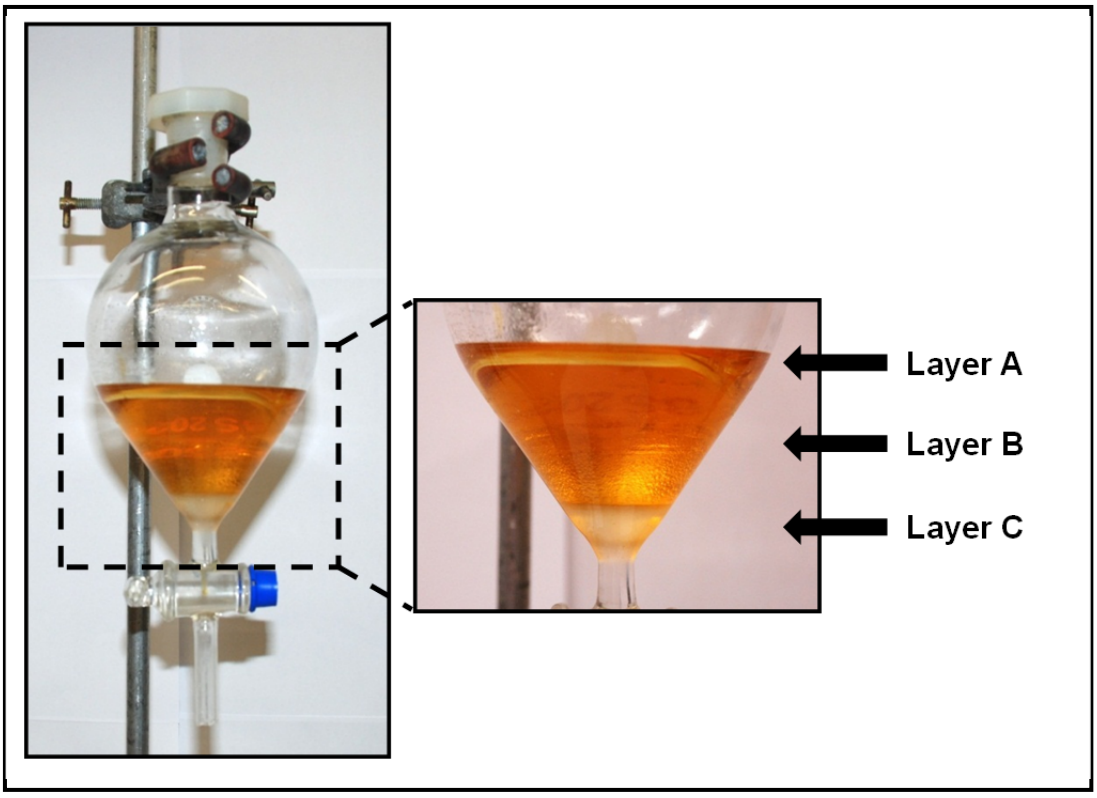

Figure 8.8. Separation of the biodiesel product. The top layer (Layer A) was a thin layer of methanol-rich phase, the middle layer (Layer B) was the bulk layer of FAME-rich phase and the bottom layer (Layer C) was the glycerine-rich phase.

The reaction mixture was allowed to settle overnight to form three layers. The top layer (Layer A) was a thin layer of methanol-rich layer, the middle layer (Layer B) was the biggest and was the layer of FAME-rich phase and the bottom layer (Layer C) was the glycerine-rich phase. The layers were sequentially withdrawn from the separating funnel and the middle layer was put in a rotary evaporator to remove excess methanol. The unpurified biodiesel cannot be used directly in a diesel engine oil because it contains impurities including unreacted P-UCO, free fatty acids (FFA), water, metal ions and glycerine. These impurities may contribute to various problems such as corrosion, low oxidation stability, deposits in the injectors, filter blockage, bacterial growth, and crystallisation (Berrios *et al.*, 2011). According to Shibasaki-Kitakawa *et al.* (2011), the biodiesel impurities such as the residual oil, free fatty acids (FFA), water and dark brown pigment can be removed from the product by adsorption on Diaion PA306s catalyst. Figure 8.9 shows the comparison of used UCO, P-UCO and unpurified biodiesel. It can be clearly seen from Figure 8.9 that

the colours transformed from dark brown to light yellow, and at the same time, colour of the resin beads changed from off-white to dark brown. This indicates that the Diaion PA306s was responsible for removing the dark brown pigments from the feedstock. However, without further analyses, the presence of other impurities cannot be ignored. Therefore, two types of washing techniques, wet and dry washing, were carried out during the purification process and these products were compared with unpurified biodiesel. Both methods have been detailed in Chapter 3, section 3.8.

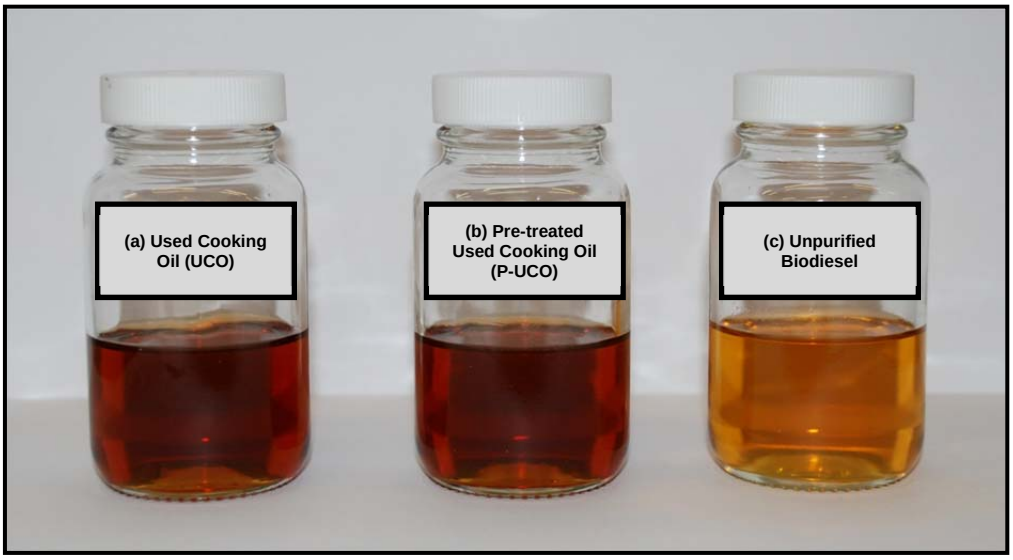

Figure 8.9. Samples of feedstock and products. (a) Used cooking oil (UCO), (b) pre-treated used cooking oil (P-UCO) and (c) unpurified biodiesel.

Table 8.2 shows the purity of FAME using wet and dry washing and the results were compared with the unpurified biodiesel. Images of the biodiesel product after the different washing techniques are presented in Figure 8.10. Results in Table 8.2 show a similar percentage of FAME for all purified and unpurified samples. The dry washing treatment using PD 206 gave the highest percentage of FAME purity of ca. 75%. By having the advantage of being water-free, there is less production of waste water, purified biodiesel from the dry washing treatment was selected for further testing.

Table 8.2. Purity of FAME using different treatment processes. (i) Ion exchange treatment, (ii) water treatment and (iii) unpurified biodiesel.

Treatment Processes	Purity of FAME, %
Ion Exchange resin (PD 206) Treatment	75.4 ± 1
Water Treatment	72.3 ± 2
Unpurified biodiesel	71.6 ± 0.5

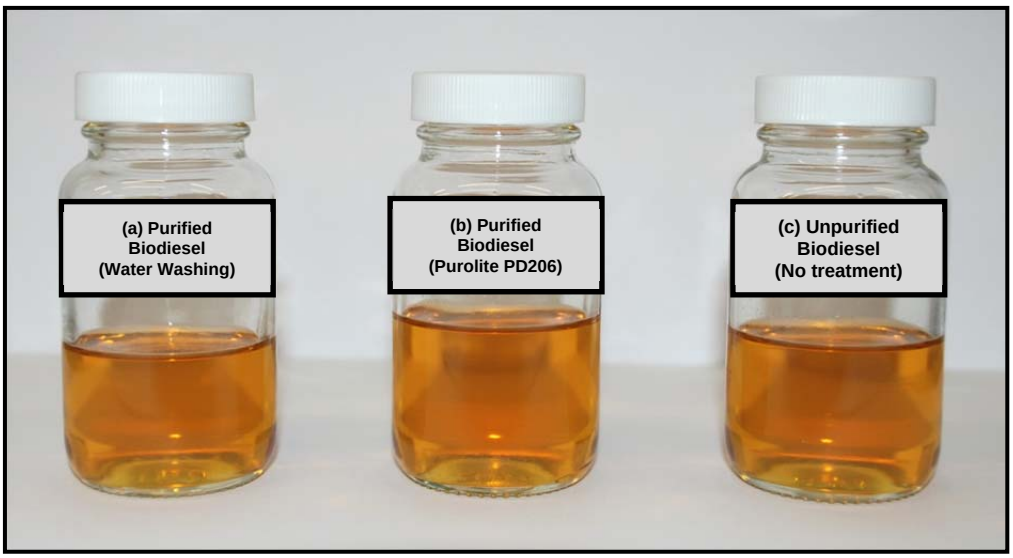

Figure 8.10. Biodiesel (a) Wet washing (water treatment), (b) dry washing [ion exchange (Purolite PD206) treatment] and (c) unpurified biodiesel.

The purified biodiesel from the dry washing process was tested for monoglycerides, diglycerides, triglycerides and glycerine content. The same analyses were conducted on unpurified biodiesel and the results are presented in Table 8.3. It can be seen from Table 8.3 that biodiesel from the dry washing technique shows a lower percentage of glycerides and glycerine content as compared to the unpurified biodiesel. The finding contradicts with the findings by Shibasaki-Kitakawa *et al.* (2011) as they claimed that all the impurities can be removed simultaneously using Diaion PA306s resin. Therefore, the product from the dry washing method was selected for further analysis.

Table 8.3. Analysis of monoglycerides, diglycerides, triglycerides and glycerine content (total and free glycerine).

Component	Ion Exchange Resin (PD 206) Treatment % (m/m)	Unpurified Biodiesel % (m/m)
Monoglycerides	0.85	1.35
Diglycerides	0.1	2.74
Triglycerides	0.47	1.91
Free glycerine	0.03	0.05
Total glycerine	0.33	0.9

8.6 PRODUCT CHARACTERISATION

The chemical and physical properties of the purified biodiesel are summarised in Table 8.4. From the table, it can be seen that the purity of FAME was quite low (ca. 75%) and the remaining 25% was predicted to be the unreacted triglycerides. However, it was not possible to quantify the amount of triglycerides presents in the sample because there were no established methods available to quantify the triglycerides at higher concentration. Apart from that, the loss of FAME could also possibly due to the separation and purification processes as there is a possibility that some of the FAME might retained in the methanol-rich layer. Therefore, further investigation needs to be carried out in future study to investigate the loss of FAME during the reaction and separation processes. From Table 8.4, it can be seen that some of the other parameters (e.g. free and total glycerine, and water content) also did not meet the strict requirements of the biodiesel standard. However, the rest of the results were very close to the values given in the standards and with further improvements on the process, the properties of biodiesel could be improved.

Table 8.4. Chemical and physical properties of purified biodiesel.

Properties	**Unit**	**Standard Method**	**Purified biodiesel (PD 206)**	**Standard**	
				EN 14214	**ASTM D6751**
Acid Value	mg KOH/g	ASTM D974	0.10	< 0.50	< 0.5
Density at 15°C	kg/m^3	EN ISO 12185	0.89 ± 0.005	0.86-0.90	-
Iodine value	g I_2/100 g	EN 1411	54	< 120	-
FAME	% (w/w)		75.40	≥ 96.5	-
Methyl palmitate	%		15.13	-	-
Methyl stearate	%	EN14103	5.57	-	-
Methyl oleate	%		33.61	-	-
Methyl linoleate	%		38.51	-	-
Methyl linolenate	%		7.19	-	-
Group I metal (Na+K)	mg/kg	EN 14109	0 (Na) 9 (K)	< 5.0	< 5.0
Group II metal (Ca+Mg)	mg/kg	EN 14538	0 (Ca) 2 (Mg)	< 5.0	< 5.0
Monoglycerides	% m/m		0.85	< 0.80	-
Diglycerides	% m/m		0.10	< 0.20	-
Triglycerides	% m/m	EN 14105	0.47	< 0.20	-
Free glycerine	% m/m		0.03	< 0.02	< 0.02
Total glycerine	% m/m		0.33	< 0.25	< 0.24
Methanol	% m/m	EN 14110	0.00	< 0.20	< 0.2
Phosphorus content	mg/kg	EN 14107	10	< 4	< 10
Sulfur content	mg/kg	EN ISO 20846	1	< 10	< 15
Viscosity at 40°C	mm^2/s	EN ISO 3104	4.2 ± 0.01	3.5-5.00	1.9-6.00
Water content	mg/kg	EN ISO 12937	548	< 500	< 0.05 vol % (water and sediment)

8.7 CONCLUSIONS

Transesterification of P-UCO using various types of catalysts has been investigated. Amongst the catalysts investigated, Diaion PA306s catalyst showed the best catalytic performance and the reason was due to the acidity and basicity of the catalysts. As a result, Diaion PA306s was selected for the optimisation study. At the optimum reaction conditions of 9% (w/w) catalyst loading, 328 K reaction temperature, 18:1 methanol to P-UCO feed mole ratio and 350 rpm stirring speed, triglycerides conversion was ca. 75%. The remaining 25% was predicted to be the unreacted triglycerides. During the reusability study, the Diaion PA306s catalyst gave similar triglycerides conversion after being reused once (at the same conditions). Therefore,

it was concluded that the catalyst can be used several times without losing catalytic activity. Two types of washing techniques, wet and dry washing, were carried out during the purification process and the results for purified biodiesels were compared with unpurified biodiesel. Biodiesel produced from the dry washing technique shows the lowest percentage of glycerides and glycerine content and therefore was chosen as the best treatment for the purification of biodiesel. The chemical and physical characterisation of purified biodiesel has been carried out. The characterisation results shows that some of the parameters (e.g. FAME purity, triglycerides, monoglycerides, free and total glycerine, and water content) did not meet the strict requirements of the biodiesel standard and therefore, further work needs to be carried out in future studies to improve the quality of biodiesel. The conclusions from this research work and the recommendations for future work will be summarised in Chapter 9.

9 CONCLUSIONS AND RECOMMENDATIONS FOR FUTURE WORK

9.1 CONCLUSIONS

Synthesis of biodiesel from used cooking oil (UCO) using ion exchange resins as catalysts has been successfully investigated. The following conclusions can be drawn from the current research.

Detailed characterisation of various types of heterogeneous catalysts including Amberlyst 15, Purolite CT-122, Purolite CT-169, Purolite CT-175, Purolite CT-275, Purolite D5081, Purolite D5082, Diaion PA306s and Cs-supported heteropolyacids catalysts, $Cs_{2.5}H_{0.5}PW_{12}O_{40}$ and $Cs_{2.5}H_{0.5}PW_{12}O_{40}$ (calcined) have been carried out. Catalyst characterisation provided significant fundamental knowledge of the chemical and physical properties of the catalysts. This information was used to correlate the relationship between the catalytic performance and the physical and chemical properties of the catalysts.

A simple, fast and reliable method for fatty acid methyl ester (FAME) quantification was successfully developed using gas chromatography-mass spectrometry (GC-MS). The calibration curve for all FAME standards showed excellent linearity and the correlation coefficient (r-squared) obtained was > 0.99. An ageing study concluded that the recommended storage period for the FAME standards should not be more than a week for more reliable and accurate results.

Determination and quantification of UCO were carried out using GC-MS. From the UCO chromatogram, five main components were identified, and they are palmitic acid, stearic acid, oleic acid, linoleic acid and linolenic acid with a composition of 13.62%, 4.14%, 33.75%, 43.85% and 4.64%, respectively. The physical and chemical analyses of the UCO were conducted and the results are as follows: acid value: 12.2 mg KOH g^{-1}; free fatty acids (FFA) content: 6.1%; density: 923.15 kg m^{-3}; triglycerides content: 84%; diglycerides content: 15%; monoglycerides content: 1% and moisture content: 0.4%. It was found that the

composition of FFA was 6.1%, which was above the allowable limit (<1%) for a direct transesterification process. Feedstock with a high FFA content cannot be used directly in a base catalysed transesterification reaction because it contributes to neutralisation and saponification and thus decreases the yield of biodiesel. Therefore, a pre-treatment stage (esterification process) is needed to convert FFA to valuable FAME before base catalysed transesterification.

Pre-treatment of UCO by esterification using various types of ion exchange resin catalysts has been investigated. Three types of ion exchange resin catalysts i.e. Amberlyst 15, Purolite D5081, and Purolite D5082 were selected for initial batch kinetics studies. Of all the catalysts investigated, Purolite D5081 resin showed the best catalytic performance as compared to Amberlyst 15 and Purolite D5082. This is probably due to the catalytic properties of Purolite D5081 resin, as it has the highest specific surface area and largest total pore volume. As a result, Purolite D5081 was selected for further optimisation of batch kinetic studies. During the optimisation study, stirring speed and difference in particle size was found to have a negligible impact on FFA conversion. Therefore, it was concluded that the internal and external mass transfer resistances have negligible effect on the esterification reaction. Under optimum reaction conditions of 475 rpm stirring speed, 1.25% (w/w) catalyst loading, 333 K reaction temperature and 6:1 methanol to UCO molar ratio, Purolite D5081 achieved FFA conversion of 92%. During reusability study, the conversion of FFA dropped by 10% after each cycle. A series of experiments were conducted for the homogeneous contribution study and it could be concluded that there are two main factors that contribute to the Purolite D5081 catalyst deactivation during the reusability study. The first factor is the contamination and blockage of the UCO onto and within the surface of the catalyst, and the second factor is the leaching of the sulphonic acid functional groups ($-SO_3H$) attached to the ion exchange polymeric resin matrix.

The kinetic modelling of FFA esterification with methanol was successfully carried out using Purolite D5081 as a catalyst. The esterification reaction was carried out using 1.25% (w/w) catalyst loading, 6:1 methanol:UCO feed mole ratio and the

reaction temperature ranging from 323 - 335 K. The experimental data from esterification reaction were correlated using three kinetic models: pseudo homogeneous (PH), Eley-Rideal (ER) and Langmuir-Hinshelwood-Hougen-Watson (LHHW). Experimental data obtained from batch kinetics studies were successfully fitted to the PH model and a good agreement between experimental and calculated values was obtained. Both heterogeneous kinetic models gave negative values for the adsorption coefficients and hence were not considered for further kinetic modelling. The forward rate constant, k_f increased with an increase in reaction temperature. However, an increase of reverse rate constant, k_r with an increase in reaction temperature is considered to be very small. This indicates that the reverse reaction i.e. hydrolysis hardly took place during batch kinetic studies. The activation energies for the esterification and hydrolysis reactions were found to be 53 and 107 kJ mol^{-1}, respectively. These results proved that the hydrolysis reverse reaction requires more energy to occur as compared to esterification reaction, hence validated the proposed model. The SRS values for PH kinetic model vary between 1.04 x 10^{-4} and 4.59 x 10^{-5}.

Transesterification of pre-treated cooking oil (P-UCO) using various types of heterogeneous catalysts has been investigated. Amongst the catalysts investigated, Diaion PA306s catalyst showed the best catalytic performance and this was believed to be closely related to the acidity and basicity of the catalysts. Diaion PA306s was selected for the optimisation of the transesterification reaction. Under the optimum reaction conditions of 350 rpm stirring speed, 9% (w/w) catalyst loading, 328 K reaction temperature and 18:1 methanol to P-UCO feed mole ratio, triglycerides conversion was ca. 75%. During the reusability study, Diaion PA306s catalyst gave a similar conversion of triglycerides after being reused once. Therefore, it was concluded that the resin can be used several times without losing catalytic activity. Several purification methods have been investigated and dry washing method was chosen as the best alternative for biodiesel purification.

9.2 RECOMMENDATIONS FOR FUTURE WORK

The following recommendations are suggested for future work.

9.2.1 Esterification-Transesterification Reaction

- For commercialisation purposes, it is necessary to compare the performance of Purolite D5081 with commercialised catalysts available in the market for FFA esterification (e.g. Amberlyst BD20). Previously, Amberlyst BD20 resin has been proposed as the comparison catalyst but due to commercial reasons, Rohm and Haas was not able to supply the catalysts.
- Further work is necessary to investigate the blockage and leaching behavior of Purolite D5081. Investigation of several possible solutions such as improvement on the clean-up process and the resin regeneration procedure and investigation of the manufacturing process of Purolite D5081 could be carried out to improve the life time.
- An extended study could be carried out to improve triglyceride conversion in transesterification reaction. Improvement on the conversion of triglycerides could be carried out by implementing the two-stage transesterification reaction. In the two-stage transesterification of the UCO, the first stage of reaction was performed under the optimum conditions, 350 rpm stirring speed, 9% (w/w) catalyst loading, 328 K reaction temperature and 18:1 methanol to UCO molar ratio. After the first reaction finished, the methanol and glycerol-rich phase was separated from the FAME-rich phase and this FAME-rich phase introduced to the second stage of transesterification. The second stage of transesterification will be carried out using fresh methanol and catalyst. For the second stage of transesterification, an optimisation study could be carried out to determine the optimum Diaion PA306s catalyst loading and methanol to P-UCO molar ratio.

9.2.2 Separation and Purification of Biodiesel

- An extended study on the separation and purification of the biodiesel could be carried out by further investigation of different types of adsorbents such as ion exchange resin, silicates, activated clays and activated carbon. The optimisation of purification parameters such as adsorbent loading, purification time and temperature, mixing intensity and reusability of spent adsorbent could be conducted to increase the yield of biodiesel.
- A study of the purification of by-product glycerin could be carried out. The glycerin has been partially purified using the Diaion PA306s catalyst by successfully removing the dark brown pigments. Further purification steps are needed to remove other impurities such as FFA, FAME, water and methanol and thus, higher purity of glycerin could be obtained.

9.2.3 Economic Analysis

- An economic analysis could be carried out to determine the feasibility of biodiesel production using ion exchange resins as catalysts. A comparison between homogeneous and heterogeneous processes could be conducted to determine the best option for biodiesel synthesis.

9.2.4 Kinetic Modelling

- An extensive study on the batch kinetic modelling for the transesterification reaction could be carried out. This investigation could extensively cover all process parameters including the effect of temperature, catalyst loading, feed mole ratio of methanol to P-UCO, partitioning phenomena and non-ideal mixing behavior. In addition, a comparison between different kinetic models (i.e. homogeneous and heterogeneous) could be studied to determine the suitability of the proposed model with the experimental data.

10 REFERENCES

Ahmad, A. L., Yasin, N. H. M., Derek, C. J. C. & Lim, J .K. 2011, "Microalgae as a sustainable energy source for biodiesel production: A review", *Renewable & Sustainable Energy Reviews*, vol. 15, no. 1, pp. 584-593.

Alba-Rubio, A. C., Santamaría-González, J., Mérida-Robles, J. M., Moreno-Tost, R., Martín-Alonso, D., Jiménez-López, A. & Maireles-Torres, P. 2010, "Heterogeneous transesterification processes by using CaO supported on zinc oxide as basic catalysts", *Catalysis Today*, vol. 149, no. 3-4, pp. 281-287.

Albuquerque, M. C. G., Jiménez-Urbistondo, I., Santamaría-González, J., Mérida-Robles, J. M., Moreno-Tost, R., Rodríguez-Castellón, E., Jiménez-López, A., Azevedo, D. C. S., Cavalcante Jr., C. L. & Maireles-Torres, P. 2008, "CaO supported on mesoporous silicas as basic catalysts for transesterification reactions", *Applied Catalysis A: General*, vol. 334, no. 1-2, pp. 35-43.

Al-Widyan, M. I. & Al-Shyoukh, A. O. 2002, "Experimental evaluation of the transesterification of waste palm oil into biodiesel", *Bioresource Technology*, vol. 85, no. 3, pp. 253-256.

Ali, S. H. & Merchant, S. Q. 2006, "Kinetics of the esterification of acetic acid with 2-propanol: Impact of different acidic cation exchange resins on reaction mechanism", *International Journal of Chemical Kinetics*, vol. 38, no. 10, pp. 593-612.

Anderson, M. W., Terasaki, O., Ohsuna, T., Philippou, A., Mackay, S. P., Ferreira, A., Rocha, J. & Lidin, S. 1994, "Structure of the microporous titanisilicate ETS-10", *Nature*, vol. 367, no. 6461, pp. 347-351.

Antolìn, G., Tinaut, F. V., Briceño, Y., Castaño, V., Pérez, C. & Ramìrez, A. I. 2002, "Optimisation of biodiesel production by sunflower oil transesterification", *Bioresource Technology*, vol. 83, no. 2, pp.111-114.

Atabani, A. E., Silitonga, A. S., Badruddin, I. A., Mahlia, T. M. I., Masjuki, H. H. & Mekhilef, S. 2012, "A comprehensive review on biodiesel as an alternative energy resource and its characteristics", *Renewable & Sustainable Energy Reviews*, vol. 16, no. 4, pp. 2070-2093.

Atadashi, I. M., Aroua, M. K. & Abdul Aziz, A. R. 2011a, "Biodiesel separation and purification : A review", *Renewable Energy*, vol. 36, no. 2, pp. 437-443.

Atadashi, I. M., Aroua, M. K., Abdul Aziz, A. R. & Sulaiman, N. M. N. 2011b, "Membrane biodiesel production and refining technology: A critical review", *Renewable & Sustainable Energy Review*s, vol. 15, no. 9, pp. 5051-5062.

Atadashi, I.M., Aroua, M. K., Abdul Aziz, A. R. & Sulaiman, N. M. N. 2011c, "Refining technologies for the purification of crude biodiesel", *Applied Energy*, vol. 88, no. 12, pp. 4239-4251.

Atapour, M. & Kariminia, H-R. 2011, "Characterization and transesterification of Iranian bitter almond oil for biodiesel production", *Applied Energy*, vol. 88, no. 7, pp. 2377-2381.

Bading, H. T. and De Jong, C. 1983, "Glass capillary gas chromatography of fatty acid methyl esters. A study of conditions for the quantitative analysis of short- and long-chain fatty acids in lipids", *Journal of Chromatography*, vol. 279, pp. 493–506.

Bai, H-X., Shen, X-Z., Liu, X-H. & Liu, S-Y. 2009, "Synthesis of porous CaO microsphere and its application in catalyzing transesterification reaction for biodiesel", *Transactions of Nonferrous Metals Society of China*, vol. 19, no. 0805167, pp. S674-S677.

Balat, M. 2011, "Potential alternatives to edible oils for biodiesel production – A review of current work", *Energy Conversion & Management*, vol. 52, no. 2, pp. 1479-1492.

Barakos, N., Pasias, S. & Papayannakos, N. 2008, "Transesterification of triglycerides in high and low quality oil feeds over an HT2 hydrotalcite catalyst", *Bioresource Technology*, vol. 99, no. 11, pp. 5037-5042.

Barrault, J., Bancquart, S. & Pouilloux, Y. 2004, "Selective glycerol transesterification over mesoporous basic catalysts", *Comptes Rendus Chimie*, vol. 7, no. 6-7, pp. 593-599.

Barthomeuf, D. 1996, "Basic zeolites: Characterization and uses in adsorption and catalysis", *Catalysis Reviews-Science & Engineering*, vol. 38, no. 4, pp. 521-612.

Behzadi, S. & Farid, M. M. 2007, "Review: examining the use of different feedstock for the production of biodiesel", *Asia Pacific Journal Chemical Engineering*, vol. 2, no. 5, pp. 480-486.

Berrios, M., Siles, J., Martin, M. A. & Martin, A. 2007, "A kinetic study of the esterification of free fatty acids (FFA) in sunflower oil", *Fuel*, vol. 86, no. 15, pp. 2383-2388.

Berrios, M. & Skelton, R. L. 2008, "Comparison of purification methods for biodiesel", *Chemical Engineering Journal*, vol. 144, no. 3, pp. 459-465.

Berrios, M., Martin, M.A., Chica, A. F. & Martin, A. 2010a, "Study of esterification and transesterification in biodiesel production from used frying oils in a closed system", *Chemical Engineering Journal*, vol. 160, no. 2, pp. 473-479.

Berrios, M., Martín, M. A., Chica, A. F. & Martín, A. 2011, "Purification of biodiesel from used cooking oils", *Applied Energy*, vol. 88, no. 11, pp. 3625-3631.

Beynese, C. R., Hinnekens, H. & Martens, J. 1996, "*Esterification process*", US Patent 5,508, 457.

Bianchi, C. L., Boffito, D. C., Pirola, C. & Ragaini, V. 2009, "Low temperature de-acidification process of animal fat as a pre-step to biodiesel production", *Catalysis Letters*, vol. 134, no. 1-2, pp. 179-183.

Boehman, L. 2005, "Biodiesel Production and Processing", *Fuel Processing Technology*, vol. 86, no. 10, pp. 1057-1058.

Brito, A., Borges, M. E. & Otero, N. 2007a, "Zeolite Y as a heterogeneous catalyst in biodiesel fuel production from used vegetable oil", *Energy & Fuels*, vol. 21, no. 6, pp. 3280-3283.

Brito, A., Garcia, F., Borges, M. E., Diaztt, M. C., Arvelo, R. & Otero, N. 2007b, "Reuse of fried oil to obtain biodiesel: Zeolites Y as a catalyst", *International Journal of Chemical Reactor Engineering*, vol. 5, no. A104.

Canakci, M & Van Gerpen, J. 2001, "Biodiesel production from oils and fats with high free fatty acid", *Transactions of the American Society of Agricultural Engineers*, vol. 44, no. 6, pp.1429-1436.

Canakci, M. 2007, "The potential of restaurant waste lipids as biodiesel feedstocks", *Bioresource Technology*, vol. 98, no. 1, pp. 183-190.

Cantrell, D. G., Gillie, L .J., Lee, A. F. & Wilson, K. 2005, "Structure-reactivity correlations in MgAl hydrotalcite catalysts for biodiesel synthesis", *Applied Catalysis A: General*, vol. 287, no. 2, pp. 183-190.

Cao, F. H., Chen, Y., Zhai, F. Y, Li, J, Wang, J. H., Wang, X. H., Wang, S. T. & Zhu, W. M. 2008, "Biodiesel production from high acid value waste frying oil catalyzed by superacid heteropolyacid", *Biotechnology & Bioengineering*, vol. 101, no. 1, pp. 93-100.

Carberry, J. J. 1967, *Chemical and Catalytic Reaction Engineering*, 1st Edition, United States of America: McGraw-Hill.

Carmo, A. C., de Souza, L. K. C., da Costa, C. E. F., Longo, E., Zamian, J. R. & da Rocha Filho, G. N. 2009, "Production of biodiesel by esterification of palmitic acid over mesoporous aluminosilicate Al-MCM-41", *Fuel*, vol. 88, no. 3, pp. 461-468.

Çayli, G. & Küsefoğlu, S. 2008, "Increased yields in biodiesel production from used cooking oils by a two-step process: Comparison with one step process by using TGA", *Fuel Processing Technology*, vol. 89, no. 2, pp. 118-122.

Chai, F., Cao, F., Zhai, F. Y., Chen, Y., Wang, X. H. & Su, Z. M. 2007, "Transesterification of vegetable oil to biodiesel using a heteropolyacid solid catalyst", *Advanced Synthesis & Catalysis*, vol. 349, no. 7, pp. 1057-1065.

Chen, X. R., Ju, Y. H. & Mou, C. Y. 2007, "Direct synthesis of mesoporous sulfated silica-zirconia catalysts with high catalytic activity for biodiesel via esterification", *Journal of Physical Chemistry C*, vol. 111, no. 50, pp. 18731-18737.

Chen, Y., Xiao, B., Chang, J., Fu, Y. Lv, P. & Wang, X. 2009, "Synthesis of biodiesel from waste cooking oil using immobilized lipase in fixed bed reactor", *Energy Conversion & Management*, vol. 50, no. 3, pp. 668-673.

Chhetri, A. B., Watts, K. C. & Islam, M. R. 2008, "Waste cooking oil as an alternate feedstock for biodiesel production", *Energies*, vol. 1, no. 1, pp. 3-18.

Chisti, Y. 2007, "Biodiesel from microalgae", *Biotechnology Advances,* vol. 25, no. 3, pp. 294-306.

Chu, W., Yang, X., Ye, X. & Wu, Y. 1996, "Vapor phase esterification catalyzed by immobilized dodecatungstosilicic acid (SiW_{12}) on activated carbon", *Applied Catalysis A: General*, vol. 145, no. 1-2, pp. 125-140.

Colucci, J. A., Borrero, E. E. & Alape, F. 2005, "Biodiesel from an alkaline transesterification reaction of soybean oil using ultrasonic mixing", *Journal of the American Oil Chemists' Society*, vol. 82, no. 7, pp. 525-530.

Concellón, A., Vázquez, P., Blanco, M. & Cáceres, C. 1998, "Molybdophosphoric acid adsorption on titania from ethanol–water solutions", *Journal of Colloid and Interface Science*, vol. 204, no. 2, pp. 256-267.

Cooke, B. S., Abrams, S. & Bertram, B. 2003, "*Purification of biodiesel with adsorbent materials*, US Patent 0509959P.

Corma, A., Martínez, A. & Martínez, C. 1996, "Acidic Cs^+, $NH4^+$, and K^+ salts of 12-tungstophosphoric acid as solid catalysts for isobutane/2-butene alkylation", *Journal of Catalysis*, vol. 164, no. 2, pp. 422-432.

Cruz-Hernandez, C. & Distillates, F. 2009, "Recent advances in fast gas-chromatography: Application to the separation of fatty acid methyl ester", *Journal of Liquid Chromatography & Related Technologies,* vol. 32, no. 11-12, pp. 1672–1688.

Cvengros, J. & Povazanec, F. 1996, "Production and treatment of rapeseed oil methyl esters as alternative fuels for diesel engines", *Bioresources Technology*, vol. 55, pp. 145-152.

Das, T. K., Chandwadkar, A. J. & Sivasanker, S. 1996, "Studies on the synthesis, characterization and catalytic properties of the large pore titanosilicate ETS-10", *Journal of Molecular Catalysis*, vol. 107, pp. 199-205.

David, F., Sandra, P. & Vickers, A. K. 2005, "Column selection for the analysis of fatty acid methyl esters", *Agilent Technologies*, 5989-3760EN, pp 1-12.

Davis, J. P., Geller, D., Faircloth, W. H. & Sanders, T. H. 2009, "Comparisons of biodiesel produced from unrefined oils of different peanut cultivars", *Journal of the American Oil Chemists' Society*, vol. 86, no. 4, pp. 353-361.

Demirbas, A. 2006, "Biodiesel production via non-catalytic SCF method and biodiesel fuel characteristics", *Energy Conversion & Management*, vol. 47, no. 15-16, pp. 2271-2282.

Demirbas, A. 2007, "Importance of biodiesel as transportation fuel", *Energy Policy***,** vol. 35, no. 9, pp. 4661-4670.

Demirbas, A. 2009, "Potential Resources of Non-edible Oils for Biodiesel", *Energy Sources, Part B: Economics, Planning, & Policy*, vol. 4, no. 3, pp. 310-314.

Demirbas, M. F. & Balat, M. 2006, "Recent advances on the production and utilization trends of bio-fuels: A global perspective", *Energy Conversion & Management*, vol. 47, no. 15-16, pp. 2371-2381.

Di Cosimo, J. I., Díez, V. K., Xu, M., Iglesia, E. & Apesteguía, C. R. 1998, "Structure and surface and catalytic properties of Mg-Al basic oxides", *Journal of Catalysis*, vol. 178, no. 2, pp. 499-510.

Di Serio, M., Tesser, R., Pengmei, L. & Santacesaria, E. 2008, "Heterogeneous catalysts for biodiesel production", *Energy & Fuels*, vol. 22, no. 1, pp. 207-217.

Dias, J. M., Alvim-Ferraz, M. C. M. & Almeida, M. F. 2008, "Comparison of the performance of different homogeneous alkali catalysts during transesterification of waste and virgin oils and evaluation of biodiesel quality", *Fuel*, vol. 87, no. 17-18, pp. 3572-3578.

Díez, V. K., C. R. Apesteguía, C. R. & Di Cosimo, J. I. 2003, "Effect of the chemical composition on the catalytic performance of Mg_yAlO_x catalysts for alcohol elimination reactions", *Journal of Catalysis*, vol. 215, no. 2, pp. 220-233.

Dmytryshyn, S. L., Dalai, A. K., Chaudhari, S. T., Mishra, H. K. & Reaney, M. J. 2004, "Synthesis and characterization of vegetable oil derived esters: evaluation for their diesel additive properties", *Bioresource Technology*, vol. 92, no. 1, pp. 55-64.

Dorado, M. P., Ballesteros, E., Arnal, J. M., Gomez, J. & Lopez Gimenez, F. J. 2003, "Testing waste olive oil methyl ester as a fuel in a diesel engine", *Energy & Fuels*, vol. 17, no. 6, pp. 1560-1565.

dos Reis, S. C. M., Lachter, E. R., Nascimento, R. S. V., Rodrigues Jr., J. A. & Reid, M. G. 2005, "Transesterification of Brazilian vegetable oils with methanol over ion-exchange resins", *Journal of the American Oil Chemists' Society*, vol. 82, no. 9, pp. 661-665.

Dote, Y., Sawayama, S., Inoue, S., Minowa, T. & Yokoyama, S. 1994, "Recovery of liquid fuel from hydrocarbon-rich microalgae by thermochemical liquefaction", *Fuel*, vol. 73, no. 12, pp. 1855-1857.

Dubé, M. A., Tremblay, A. Y. & Liu, J. 2007, "Biodiesel production using a membrane reactor", *Bioresource Technology*, vol. 98, no. 3, pp. 639-647.

Ellis, N., Guan, F., Chen, T. & Poon, C. 2008, "Monitoring biodiesel production (transesterification) using in situ viscometer", *Chemical Engineering Journal*, vol. 138, no. 1-3, pp. 200-206.

El-Mashad, H. M., Zhang, R. & Avena-Bustillos, R. J. 2008, "A two-step process for biodiesel production from salmon oil", *Biosystems Engineering*, vol. 99, no. 2, pp. 220-227.

Encinar, J. M., González, J. F. & Rodríguez-Reinares, A. 2007, "Ethanolysis of used frying oil. Biodiesel preparation and characterization", *Fuel Processing Technology*, vol. 88, no. 5, pp. 513-522.

Endalew, A. K., Kiros, Y. & Zanzi, R. 2011, "Inorganic heterogeneous catalysts for biodiesel production from vegetable oils", *Biomass & Bioenergy*, vol. 35, no. 9, pp. 3787-3809.

EN 1S0 12966-2. 2011, "*Animal and vegetable fats and oils- gas chromatography of fatty acid methyl esters: Part 2: Preparation of methyl esters of fatty acids*", pp. 1-28.

EU Regulation 2568/91. 1991, *Official Journal EU*, document L248 5/9/1991.

Europan Biodiesel Board. 2012, *The EU biodiesel industry: production by country* [Online]. Available at: http://www.ebb-eu.org/stats.php [Accessed: 28 May 2012].

European Commision. 2010, *EU energy and transport in figures statistical pocketbook 2010* [Online]. Available at: http://ec.europa.eu/energy/publications /doc/2010_energy_transport_figures.pdf [Accessed: 27 May 2012].

European Commision. 2011a, *Consumption of energy* [Online]. Available at: http://epp.eurostat.ec.europa.eu/statistics_explained/index.php/Consumption_of_energy [Accessed: 27 May 2012].

European Commision. 2011b, *Biofuels in the Europan Union: A vision for 2030 and beyond* [Online]. Available at: ftp://ftp.cordis.europa.eu/pub/fp7/energy/docs/ biofuels_ vision_2030_ en.pdf [Accessed: 27 May 2012].

Essayem, N. 2001, "In situ FTIR studies of the protonic sites of $H_3PW_{12}O_{40}$ and its acidic cesium salts $M_xH_{3-x}PW_{12}O_{40}$", *Journal of Catalysis*, vol. 197, no. 2, pp. 273-280.

Faccini, C. S, Cunha, M. E. D., Moraes, M. S. A, Krause, L. C., Manique, M. C., Rodrigues, M. R. A., Benvenutti, E. V. & Caramão, E. B. 2011, "Dry washing in biodiesel purification: a comparative study of adsorbents". *Journal of the Brazilian Chemical Society*, vol. 22, no. 3, pp. 558-563.

Falco, M. G., Córdoba, C. D., Capeletti, M. R. & Sedran, U. 2010, "Basic ion exchange resins as heterogeneous catalysts for biodiesel synthesis", *Advanced Materials Research*, vol. 132, pp. 220-227.

Felizardo, P., Correia, M. J. N., Raposo, I., Mendes, J. F., Berkemeier, R. & Bordado, J. M. 2006, "Production of biodiesel from waste frying oils", *Waste Management*, vol. 26, no. 5, pp. 487-494.

Feng, Y., He, B., Cao, Y., Li, J., Liu, M., Yan, F. & Liang, X. 2010, "Biodiesel production using cation-exchange resin as heterogeneous catalyst", *Bioresource Technology*, vol. 101, no. 5, pp. 1518-1521.

Fishel, C. T. & Davis, R. J. 1994, "Characterization of Mg-Al mixed oxides by temperature-programmed reaction of 2-propanol", *Langmuir*, vol. 10, no. 1, pp. 159-65.

Foglia, T. A. Nelson, L. A. & Marmer, W. N. 1998, "Production of biodiesel, lubricants and fuel and lubricant additives", US Patent 5,713, 965.

Formo, M. W. 1954, "Ester reactions of fatty materials", *Journal of the American Oil Chemists' Society*, vol. 31, no. 11, pp. 548-559.

Freedman, B., Butterfield, R. & Pryde, E. H. 1986, "Transesterification kinetics of soybean oil", *Journal of the American Oil Chemists' Society*, vol. 63, no. 10, pp. 1375-1380.

Freedman, B., Pryde, E. H. & Mounts, T. L. 1984, "Variables affecting the yields of fatty esters from transesterified vegetable oils", *Journal of the American Oil Chemists' Society*, 61, no. 10, pp.1638–1643.

Fröhlich, A. & Rice, B. 2009, "Sources of methyl ester yield reduction in methanolysis of recycled vegetable oil", *Journal of the American Oil Chemists' Society*, vol. 86, no. 3, pp. 269-275.

Fu, B. S., Gao, L. J., Niu, L, Wei, R. P. & Xiao, G. M. 2009, "Biodiesel from waste cooking oil via heterogeneous superacid catalyst SO_4^{2-}/ZrO_2", *Energy & Fuels*, vol. 23, no. 1, pp. 569-572.

Fukuda, H., Kondo, A. & Noda, H. 2001, "Biodiesel fuel production by transesterification of oils", *Journal of Bioscience & Bioengineering*, vol. 92, no. 5, pp. 405-416.

Furuta, S., Matsuhashi, H. & Arata, K. 2004, "Biodiesel fuel production with solid superacid catalysis in fixed bed reactor under atmospheric pressure", *Catalysis Communications,* vol. 5, no. 12, pp. 721-723.

Gan, M., Pan, D., Ma, L., Yue, E. & Hong, J. 2009, "The kinetics of the esterification of free fatty acids in waste cooking oil using $Fe_2(SO_4)_3$/C catalyst", *Chinese Journal of Chemical Engineering*, vol. 17, no. 1, pp. 83-87.

Gangadwala, J., Mankar, S. & Mahajani, S. 2003, "Esterification of acetic acid with butanol in the presence of ion exchange resin as catalyststst", *Industrial & Engineering Chemistry Research*, vol. 42, no. 10, pp. 2146-2155.

Gao, L., Xu, B., Xiao, G. & Lv, J. 2008, "Transesterification of palm oil with methanol to biodiesel over a KF/hydrotalcite solid catalyst", *Energy & Fuels*, vol. 22, no. 5, pp. 3531-3535.

Garcia, C. M., Teixeira, S., Marciniuk, L. L. & Schuchardt, U. 2008, "Transesterification of soybean oil catalyzed by sulfated zirconia", *Bioresource Technology*, vol. 99, no. 14, pp. 6608-6613.

Garofalo, R. 2011, *Global biodiesel session: The EU biodiesel industry in changing times* [Online]. Available at: http://www.sarienergy.org/PageFiles/What_We_Do/activities/worldbiofuelsmarkets/Presentations/GlobalBiodieselRoundtable/Raffaello_Garofalo.pdf [Accessed: 26 May 2012].

Gaudino, M. C., Valentin, R., Brunel, D., Fajula, .F, Quignard, F. & Riondel, A. 2005, "Titanium-based solid catalysts for transesterification of methyl-methacrylate by 1-butanol: the homogeneous catalysis contribution", *Applied Catalysis A: General*, vol. 280, no. 2, pp. 157-164.

Georgogianni, K. G., Katsoulidis, A. P., Pomonis, P. J. & Kontominas, M. G. 2009, "Transesterification of soybean frying oil to biodiesel using heterogeneous catalysts", *Fuel Processing Technology*, vol. 90, no. 5, pp. 671-676.

Ghadge, S. V. & Raheman, H. 2006, "Process optimization for biodiesel production from mahua (Madhuca indica) oil using response surface methodology", *Bioresource Technology*, vol. 97, no. 3, pp. 379-384.

Ghadge, S. V. & Raheman, H. 2005, "Biodiesel production from mahua (Madhuca indica) oil having high free fatty acids", *Biomass & Bioenergy*, vol. 28, no. 6, pp. 601-605.

Ginzburg, B. Z. 1993, "Liquid fuel (oil) from halophilic algae: A renewable source of non-polluting energy", *Renewable Energy*, vol. 3, no. 2-3, pp. 249-252.

Giri, B. Y., Rao, K. N., Devi, B. L. A. P., Lingaiah, N., Suryanarayana, I., Prasad, R. B. N. & Prasad, P. S. S. 2005, "Esterification of palmitic acid on the ammonium salt of 12-tungstophosphoric acid: The influence of partial proton exchange on the activity of the catalyst", *Catalysis Communications*, vol. 6, no. 12, pp. 788-792.

Glisic, S. & Skala, D. 2009, "Design and optimization of purification procedure for biodiesel washing", *Chemical Industry & Chemical Engineering Quarterly*, vol. 15, no. 3, pp. 159-168.

Goff, M. J., Bauer, N. S., Lopes, S., Sutterlin, W. R. & Suppes, G. J. 2004, "Acid-catalyzed alcoholysis of soybean oil", *Journal of the American Oil Chemists' Society*, vol. 81, no. 4, pp. 415-420.

Gomes, M. C. S., Pereira, N. C. & Barros, S. T. D. D. 2010, "Separation of biodiesel and glycerol using ceramic membranes", *Journal of Membrane Science*, vol. 352, no. 1-2, pp. 271-276.

Granados, M. L., Poves, M. D. Z., Alonso, D. M., Mariscal, R., Galisteo, F. C., Moreno-Tost, R., Santamaría, J. & Fierro, J. L. G. 2007, "Biodiesel from sunflower oil by using activated calcium oxide", *Applied Catalysis B: Environmental*, vol. 73, no. 3-4, pp. 317-326.

Grob, R. L. & Barry, E. F. 2004, *Modern practice of gas chromatography*, 4th Edition, New Jersey: John Wiley & Sons, Inc.

Grob, S., & Hasse, H. 2006, "Reaction kinetics of the homogeneously catalysed esterification of 1-butanol with acetic acid in a wide range of initial compositions", *Industrial & Engineering Chemistry Research,* vol. 45, no. 6, pp. 1869-1874.

Gryglewicz, S. 1999, "Rapeseed oil methyl esters preparation using heterogeneous catalysts", *Bioresource Technology*, vol. 70, no. 3, pp. 249-253.

Guerreiro, L., Pereira, P. M., Fonseca, I. M., Martin-Aranda, R. M., Ramos, A. M., Dias, J. M. L., Oliveira, R. & Vital, J. 2010, "PVA embedded hydrotalcite membranes as basic catalysts for biodiesel synthesis by soybean oil methanolysis", *Catalysis Today*, vol. 156, no. 3-4, pp. 191-197.

Gui, M., Lee, K. T. & Bhatia, S. 2008, "Feasibility of edible oil vs. non-edible oil vs. waste edible oil as biodiesel feedstock", *Energy*, vol. 33, no. 11, pp. 1646-1653.

Haas, M. J., McAloon, A. J., Yee, W. C. & Foglia, T. A. 2006. "A process model to estimate biodiesel production costs", *Bioresource Technology*, vol. 97, no. 4, pp. 671-678.

Haigh, K. F., Saha, B., Vladisavljević, G. T. & Reynolds, J. C. 2012. Kinetics of the pre-treatment of used cooking oil using Novozyme 435 for biodiesel production, *20th International Congress of Chemical and Process Engineering CHISA 2012,* Prague, 25-29 August, 2012, Procedia Engineering: Elesvier, pp. 1-8.

Hamad, B., Lopes de Souza, R. O., Sapaly, G., Carneiro Rocha, M. G., Pries de Oliveira, P. G., Gonzalez, W. A., Andrade Sales, E. & Essayem, N. 2008, "Transesterification of rapeseed oil with ethanol over heterogeneous heteropolyacids", *Catalysis Communications*, vol. 10, no. 1, pp. 92-97.

Hanh, H. D., Dong, N. T., Okitsu, K., Maeda, Y. & Nishimura, R. 2007, "Effects of molar ratio, catalyst concentration and temperature on transesterification of triolein with ethanol under ultrasonic irradiation", *Journal of the Japan Petroleum Institute*, vol. 50, no. 4, pp. 195–199.

Hanh, H. D., Dong, N. T., Okitsu, K., Nishimura, R. & Maeda, Y. 2009, "Biodiesel production through transesterification of triolein with various alcohols in an ultrasonic field", *Renewable Energy*, vol. 34, no. 3, pp.766-768.

Harmer, M. A., Farneth, W. E. & Sun, Q. 1998, "Towards the sulfuric acid of solids", *Advanced Materials*, vol. 10, no. 15, pp. 1255-1257.

Harwood, H. J. 1984, "Oleochemicals as a fuel: Mechanical and economic feasibility", *Journal of the American Oil Chemists' Society*, vol. 61, no. 2, pp. 315-324.

Hattori, H. 1995, "Heterogeneous basic catalysis", *Chemical Reviews*, vol. 95, no. 3, pp. 537-58.

Hawash, S., Kamal, N., Zaher, F., Kenawi, O. & Diwani, G.E. 2009, "Biodiesel fuel from Jatropha oil via non-catalytic supercritical methanol transesterification", *Fuel*, vol. 88, no. 3, pp. 579-582.

Helfferich, F. 1962, *Ion exchange*, 1st Edition, United States of America: McGraw-Hill.

Hoekman, S. K., Broch, A., Robbins, C., Ceniceros, E. & Natarajan, M. 2012, "Review of biodiesel composition, properties, and specifications", *Renewable & Sustainable Energy Reviews*, vol. 16, no. 1, pp. 143-169.

Hsu, A-F., Jones, K. C., Foglia, T. A. & Marmer, W. N. 2004, "Continuous production of ethyl esters of grease using an immobilized lipase", *Journal of the American Oil Chemists' Society*, vol. 81, no. 8, pp. 749-752.

Hu, Q., Sommerfeld, M., Jarvis, E., Ghirardi, M., Posewitz, M., Seibert, M. & Darzins, A. 2008, "Microalgal triacylglycerols as feedstocks for biofuel production: perspectives and advances", *The Plant Journal*, vol. 54, no. 4, pp. 621-639.

Izumi, Y. & Urabe, K. 1981, "Catalysis of heteropoly acids entrapped in activated carbon", *Chemistry Letters*, no. 5, pp. 663-666.

Izumi, Y., Ono, M., Kitagawa, M., Yoshida, M. & Urabe, K. 1995, "Silica-included heteropoly compounds as solid acid catalysts", *Microporous Materials*, vol. 5, no. 4, pp. 255-262.

Jackson M. A. & King, J. W. 1996, "Methanolysis of seed oils in flowing supercritical carbon dioxide", *Journal of the American Oil Chemists' Society*, vol. 73, no. 3, pp. 353-356.

Jena, P. C., Raheman, H., Prasanna Kumar, G. V. & Machavaram, R. 2010, "Biodiesel production from mixture of mahua and simarouba oils with high free fatty acids", *Biomass & Bioenergy*, vol. 34, no. 8, pp. 1108-1116.

Jeong, G-T. & Park, D-H. 2006, "Batch (one- and two-stage) production of biodiesel fuel from rapeseed oil", *Applied Biochemistry & Biotechnology*, vol. 131, no. 1-3, pp. 668-679.

Jitputti, J., Kitiyanan, B., Rangsunvigit, P., Bunyakiat, K., Attanatho, L. & Jenvanitpanjakul, P. 2006, "Transesterification of crude palm kernel oil and crude coconut oil by different solid catalysts", *Chemical Engineering Journal*, vol. 116, no. 1, pp. 61-66.

Johnston, M. & Holloway, T. 2008, "A global comparison of national biodiesel production potentials", *Environmental Science & Technology*, vol. 41, no. 23, pp. 7967-7973.

Jothiramalingam, R. & Wang, M. K. 2009, "Review of recent developments in solid acid, base, and enzyme catalysts (heterogeneous) for biodiesel production via transesterification", *Industrial & Engineering Chemistry Research*, vol. 48, no. 13, pp. 6162-6172.

Kalam, M. A. & Masjuki, H. H. 2002, "Biodiesel from palm oil-an analysis of its properties and potential", *Biomass & Bioenergy*, vol. 23, no. 6, pp. 471-479.

Kang, Y. M. & Kim, H. S. 2001, "Emulsified transesterification of soybean oil into biodiesel", *Journal of Korean Oil Chemists' Society*, vol. 18, no. 4, pp. 298-305.

Kapil, A., Wilson, K., Lee, A. F. & Sadhukhan, J. 2011, "Kinetic modeling studies of heterogeneously catalyzed biodiesel synthesis reactions", *Industrial & Engineering Chemistry Research*, vol. 50, no. 9, pp. 4818-4830.

Karaosmanoğlu, F., Cigizoglu, K. B., Tuter, M. and Ertekin, S. 1996, "Investigation of refining steps of biodiesel production", *Energy Fuel*, vol. **10,** pp. 890-895.

Kawashima, A., Matsubara, K. & Honda, K. 2008, "Development of heterogeneous base catalysts for biodiesel production", *Bioresource Technology*, vol. 99, no. 9, pp. 3439-3443.

Kaya, C., Hamamci, C., Baysal, A., Akba, O., Erdogan, S. & Saydut, A. 2009, "Methyl ester of peanut (Arachis hypogea L.) seed oil as a potential feedstock for biodiesel production", *Renewable Energy*, vol. 34, no. 5, pp. 1257-1260.

Keggin, J. F. 1934, "The structure and formula of 12-phosphotungstic acid", *Proceedings of the Royal Society of London*, vol. 144, no. 851, pp. 75-100.

Keyes, D. B. 1932, "Esterification processes and equipment", *Industrial & Engineering Chemistry*, vol. 24, no. 10, pp. 1096-1103.

Kim, H., Kang, B., Kim, M., Park, Y.M., Kim, D., Lee, J. & Lee, K. 2004, "Transesterification of vegetable oil to biodiesel using heterogeneous base catalyst", *Catalysis Today*, vol. 93, no. 5, pp. 315-320.

Kirbaslar, S. I., Terzioglu, H. Z. & Dramur, U. 2001, "Catalytic esterification of methyl alcohol with acetic acid", *Chinese Journal of Chemical Engineering*, vol. 9, no. 1, pp. 90-96.

Kiss, A. A., Dimian, A. C. & Rothenberg, G. 2006, "Solid acid catalysts for biodiesel production – towards sustainable energy", *Advanced Synthesis & Catalysis*, vol. 348, no. 1-2, pp. 75-81.

Klepáčová, K., Mravec, D. & Bajus, M. 2005, "tert-Butylation of glycerol catalysed by ion-exchange resins", *Applied Catalysis A: General*, vol. 294, no. 2, pp. 141-147.

Knothe, G. 2005, "Dependence of biodiesel fuel properties on the structure of fatty acid alkyl esters", *Fuel Processing Technology,* vol. 86, no. 10, pp. 1059-1070.

Kouzu, M., Nakagaito, A. & Hidaka, J-S. 2011, "Pre-esterification of FFA in plant oil transesterified into biodiesel with the help of solid acid catalysis of sulfonated cation-exchange resin", *Applied Catalysis A: General*, vol. 405, no. 1-2, pp. 36-44.

Kozhevnikov, I. V. 1998, "Catalysis by heteropoly acids and multicomponent polyoxometalates in liquid-phase reactions.", *Chemical Reviews*, vol. 2665, no. 96, pp. 171-198.

Kozhevnikov, I. V., Sinnema, A., Jansen, R. J. J., Pamin, K. & Vanbekkum, H. 1995, "New acid catalyst comprising heteropoly acid on a mesoporous molecular-sieve MCM-41", *Catalysis Letters*, vol. 30, no. 1-4, pp. 241-52.

Kulkarni, M. G. & Dalai, A. K. 2006, "Waste cooking oil - an economical source for biodiesel: a review", *Industrial & Engineering Chemistry Research*, vol. 45, no. 9, pp. 2901.

Kulkarni, M. G., Gopinath, R., Meher, L. C. & Dalai, A. K. 2006, "Solid acid catalyzed biodiesel production by simultaneous esterification and transesterification", *Green Chemistry*, vol. 8, no. 12, pp. 1056-1062.

Kusdiana, D. & Saka, S. 2001, "Kinetics of transesterification in rapeseed oil to biodiesel fuel as treated in supercritical methanol", *Fuel*, vol. 80, no. 5, pp. 693-698.

Lam, M. K., Lee, K. T. & Mohamed, A. R. 2009, "Sulfated tin oxide as solid superacid catalyst for transesterification of waste cooking oil: An optimization study". *Applied Catalysis B: Environmental*, vol. 93, no. 1-2, pp. 134-139.

Lang, X., Dalai, A. K., Bakhshi, N. N., Reaney, M. J. & Hertz, P. B. 2001, "Preparation and characterization of bio-diesels from various bio-oils", *Bioresource Technology*, vol. 80, no. 1, pp. 53-62.

Leclercq, E., Finiels, A. & Moreau, C. 2001, "Transesterification of rapeseed oil in the presence of basic zeolites and related solid catalysts", *Journal of the American Oil Chemists Society*, vol. 78, no. 11, pp. 1161-1165.

Lee, D. W., Park, Y. M. & Lee, K. Y. 2009, "Heterogeneous base catalysts for transesterification in biodiesel synthesis", *Catalysis Surveys from Asia*, vol. 13, no. 2, pp. 63-77.

Lerkkasemsan, N., Abdoulmoumine, N., Achenie, L. & Agblevor, F. 2011, "Mechanistic Modeling of Palmitic Acid Esterification via Heterogeneous Catalysis", *Industrial & Engineering Chemistry Research*, vol. 50, no. 3, pp. 1177-1186.

Leung, D. Y. C & Gou, Y. 2006, "Transesterification of neat and used frying oil: Optimization for biodiesel production", *Fuel Process Technology*, vol. 87, no. 10, pp.883-890.

Leung, D. Y. C., Wu, X. & Leung, M. K. H. 2010, "A review on biodiesel production using catalyzed transesterification", *Applied Energy*, vol. 87, no. 4, pp. 1083-1095.

Li, E. & Rudolph, V. 2008, "Transesterification of vegetable oil to biodiesel over MgO-functionalized mesoporous catalysts", *Energy & Fuels*, vol. 22, no. 1, pp. 145-149.

Li, Y., Bao, G. & Wang, H. 2008, "Determination of 11 fatty acids and fatty acids methyl esters in biodiesel using ultra performance liquid chromatography", *Chinese Journal of Chromatography*, vol. 26, no. 4, pp. 494-498.

Li, J., Fu, Y. J., Qu, X. J., Wang, W., Luo, M., Zhao, C-J. & Zu, Y-G. 2012, "Biodiesel production from yellow horn (Xanthoceras sorbifolia Bunge.) seed oil using ion exchange resin as heterogeneous catalyst", *Bioresource Technology*, vol. 108, pp. 112-118.

Lin, L., Rhee, K. C. & Koseoglu, S. S. 1997, "Bench-scale membrane degumming of crude vegetable oil: Process optimization", *Journal of Membrane Science*, vol. 134, no. 1, pp. 101-108.

Lin, L., Cunshan, Z., Vittayapadung, .S, Xiangqian, S. & Mingdong, D. 2011, "Opportunities and challenges for biodiesel fuel", *Applied Energy*, vol. 88, no. 4, pp. 1020-1031.

Lingfeng, C., Guomin, X., Bo, X. & Guangyuan, T. 2007, "Transesterification of cottonseed oil to biodiesel by using heterogeneous solid basic catalysts", *Energy & Fuels*, vol. 21, no. 6, pp. 3740-3743.

Liu, Y., Lotero, E. & Goodwin Jr., J. G. 2006, "A comparison of the esterification of acetic acid with menthanol using heterogeneous versus homogeneous acid catalysis", *Journal of Catalysis*, vol. 242, no. 2, pp. 278-286.

Liu, Y., Lotero, E., Goodwin Jr., J. G. & Mo., X. 2007, "Transesterification of poultry fat with methanol using Mg–Al hydrotalcite derived catalysts", *Applied Catalysis A: General*, vol. 331, pp. 138-148.

Liu, X., He, H., Wang, Y., Zhu, S. & Piao, X. 2008, "Transesterification of soybean oil to biodiesel using CaO as a solid base catalyst", *Fuel*, vol. 87, no. 2, pp. 216-221.

Liu, Y., Wang, L. & Yan, Y. 2009, "Biodiesel synthesis combining pre-esterification with alkali catalyzed process from rapeseed oil deodorizer distillate", *Fuel Processing Technology*, vol. 90, no. 7-8, pp. 857-862.

Liu, X., Ye, M., Pu, B. & Tang, Z. 2012, "Risk management for jatropha curcas based biodiesel industry of Panzhihua Prefecture in Southwest China", *Renewable & Sustainable Energy Reviews*, vol. 16, no. 3, pp. 1721-1734.

Longlong, M. A., Pengmei, L. U., Lianhua, L. I., Wen, L. U. O. & Xiaoying, K. October 2008, "Biodiesel production form different feedstocks in pilot scale system", *Journal of Oil Palm Research*, pp. 16-21.

López, D. E., Goodwin, J., James G., Bruce, D. A. & Lotero, E. 2005, "Transesterification of triacetin with methanol on solid acid and base catalysts", *Applied Catalysis A: General*, vol. 295, no. 2, pp. 97-105.

López, D. E., Goodwin Jr., J. G. & Bruce, D. A. 2007, "Transesterification of triacetin with methanol on Nafion® acid resins", *Journal of Catalysis*, vol. 245, no. 2, pp. 381-391.

López, D. E., Goodwin Jr., J. G., Bruce, D. A. & Furuta, S. 2008, "Esterification and transesterification using modified-zirconia catalysts", *Applied Catalysis A: General*, vol. 339, no. 1, pp. 76-83.

Lotero, E., Liu, Y. J., Lopez, D. E., Suwannakaran, K., Bruce, D. A. and Goodwin, J. G. 2005, "Synthesis of biodiesel via acid catalysis", *Industrial & Engineering Chemistry Research*, vol. 44, no. 14, pp. 5353-5363.

Lou, W., Zong, M. & Duan, Z. 2008, "Efficient production of biodiesel from high free fatty acid-containing waste oils using various carbohydrate-derived solid acid catalysts", *Bioresource Technology*, vol. 99, no. 18, pp. 8752-8758.

Ma, F., Clements, L. D. & Hanna, M. A. 1998, "Biodiesel fuel from animal fat. ancillary studies on transesterification of beef tallow", *Society*, vol. 5885, no. 98, pp. 3768-3771.

Ma, F. & Hanna, M.A. 1999, "Biodiesel production: a review", *Bioresource Technology*, vol. 70, no. 1, pp. 1-15.

Mabaleha, M. B., Mitei, Y. C. & Yeboah, S. O. 2007, "A comparative study of the properties of selected melon seed oils as potential candidates for development into commercial edible vegetable oils", *Journal of the American Oil Chemists' Society*, vol. 84, no. 1, pp. 31-36.

Macala, G. S., Robertson, A. W., Johnson, C. L., Day, Z. B., Lewis, R. S., White, M. G., Iretskii, A. V. & Ford, P. C. 2008, "Transesterification catalysts from iron doped hydrotalcite-like precursors: Solid bases for biodiesel production", *Catalysis Letters*, vol. 122, no. 3-4, pp. 205-209.

Macedo, C. C. S., Abreu, F. R., Tavares, A. P., Alves, M. B., Zara, L. F., Rubim, J. C. & Suarez, P. A. Z. 2006, "New heterogeneous metal-oxides based catalyst for vegetable oil trans-esterification", *Journal of the Brazilian Chemical Society*, vol. 17, no. 7, pp. 1291-1296.

Marris, E. 2006, "Sugarcane and ethanol drink the best and drive the test", *Nature*, vol. 444, pp. 670-672.

Mazzotti, M., Neri, B., Gelosa, D., Kruglov, A. & Morbidelli, M. 1997, "Kinetics of Liquid- Phase Esterification Catalyzed by Acidic Resins", *Industrial & Engineering Chemistry Research*, vol. 36, pp. 3-10.

Meher, L. C., Vidya Sagar, D. & Naik, S. N. 2006a, "Technical aspects of biodiesel production by transesterification—a review", *Renewable & Sustainable Energy Reviews*, vol. 10, no. 3, pp. 248-268.

Meher, L. C., Dharmagadda, V. S. S., Naik & S. N. 2006b, "Optimization of alkali-catalyzed transesterification of *Pongamia pinnata* for production of biodiesel", *Bioresource Technology*, vol. 97, no. 12, pp. 1392-1397.

Melero, J. A., Iglesias, J. & Morales, G. 2009, "Heterogeneous acid catalysts for biodiesel production: current status and future challenges", *Green Chemistry*, vol. 11, no. 9, pp. 1285-1308.

Miao, X. & Wu, Q. 2006, "Biodiesel production from heterotrophic microalgal oil", *Bioresource Technology*, vol. 97, no. 6, pp. 841-846.

Milne, T. A., Evans, R. J. & Nagle, N. 1990, "Catalytic conversion of microalgae and vegetable oils to premium gasoline, with shape-selective zeolites", *Biomass*, vol. 21, no. 3, pp. 219-232.

Minowa, T., Yokoyama, S. Y., Kishimoto, M. & Okakurat, T. 1995, "Oil production from algal cells of Dunaliella Tertiolecta by direct thermochemical liquefaction", *Fuel*, vol. 74, no. 12, pp. 1735-1738.

Mittelbach, M. & Remschmidt, C. 2004, "*Biodiesel – The comprehensive handbook*", 1st edition, Austria:Boersedruck Ges.m.b.H.

Mizuno, N. & Misono, M. 1998, "Heterogeneous Catalysis", *Chemical reviews*, vol. 98, no. 1, pp. 199-218.

Moffat, J. B. & Kasztelan, S. 1988, "The Oxidation of methane on heteropolyoxometalates II. Nature and stability of the supported species", *Journal of Catalysis*, vol. 109, no. 1, pp. 206-211.

Mootabadi, H., Salamatinia, B., Bhatia, S. & Abdullah, A. Z. 2010, "Ultrasonic-assisted biodiesel production process from palm oil using alkaline earth metal oxides as the heterogeneous catalysts", *Fuel*, vol. 89, no. 8, pp. 1818-1825.

Muniyappa, P. R., Brammer, S. C. and Noureddini, H. 1996, "Improved conversion of plant oils and animals fats into biodiesel and co-product", *Bioresource Technology*, vol. 56, no. 1, pp. 19-24.

Murugesan, A., Umarani, C., Chinnusamy, T. R., Krishnan, M., Subramanian, R. & Neduzchezhain, N. 2009, "Production and analysis of bio-diesel from non-edible oils—A review", *Renewable & Sustainable Energy Reviews*, vol. 13, no. 4, pp. 825-834.

Nagel, N. & Lemke, P. 1990, "Production of methyl fuel from microalgae", *Applied Biochemical Biotechnology*, vol. 24, no. 5, pp. 355-361.

Naik, M., Meher, L. C., Naik, S. N. & Das, L. M. 2008, "Production of biodiesel from high free fatty acid Karanja (Pongamia pinnata) oil", *Biomass & Bioenergy*, vol. 32, no. 4, pp. 354-357.

Nakato, T., Kimura, M., Nakata, S. & Okuhara, T. 1998, "Changes of surface properties and water-tolerant catalytic activity of solid acid $Cs_{2.5}H_{0.5}PW_{12}O_{40}$ in water", *Langmuir*, vol. 14, no. 2, pp. 319-325.

Narasimharao, K., Brown, D. R., Lee, A. F., Newman, A. D., Siril, P. F., Tavener, S. J. & Wilson, K. 2007, "Structure–activity relations in Cs-doped heteropolyacid catalysts for biodiesel production", *Journal of Catalysis*, vol. 248, no. 2, pp. 226-234.

Nas, B. & Berktay, A. 2007, "Energy Potential of Biodiesel Generated from Waste Cooking Oil: An Environmental Approach", *Energy Sources, Part B: Economics, Planning, and Policy*, vol. 2, no. 1, pp. 63-71.

Nelson, L. A., Foglia, T. A., Marmer, W. N. 1996, "Lipase-catalyzed production of biodiesel", *Journal of the American Oil Chemists' Society*, vol. 73, no. 9, pp. 1191–1195.

Ngo, H. L., Zafiropoulos, N. A., Foglia, T. A., Samulski, E. T. & Lin, W. 2008, "Efficient two-step synthesis of biodiesel from greases", *Energy & Fuels*, vol. 22, no. 1, pp. 626-634.

Nie, K., Xie, F., Wang, F. & Tan, T. 2006, "Lipase catalyzed methanolysis to produce biodiesel: Optimization of the biodiesel production", *Journal of Molecular Catalysis B: Enzymatic*, vol. 43, no. 1-4, pp. 142-147.

Nowinska, K. & Kaleta, W. 2000, "Synthesis of Bisphenol-A over heteropoly compounds encapsulated into mesoporous molecular sieves", *Applied Catalysis A: General,* vol. 203, no. 1, pp. 91-100.

Okuhara, T. & Nakato, T. 1998, "Catalysis by porous heteropoly compounds", *Catalysis Surveys from Japan*, vol. 2, no. 1, pp. 31-44.

Okuhara, T. 2002, "Water-tolerant solid acid catalysts", *Chemical Reviews*, vol. 102, no. 10, pp. 3641-3665.

Okuhara, T. 2003, "Microporous heteropoly compounds and their shape selective catalysis", *Applied Catalysis A: General*, vol. 256, no. 1-2, pp. 213-224.

Oliveira, C. F., Dezaneti, L. M., Garcia, F. A. C., de Macedo, J. L., Dias, J. A., Dias, S. C. L. & Alvim, K. S. P. 2010, "Esterification of oleic acid with ethanol by 12-tungstophosphoric acid supported on zirconia", *Applied Catalysis A: General*, vol. 372, no. 2, pp. 153-161.

Özbay, N., Oktar, N. & Tapan, N. A. 2008, "Esterification of free fatty acids in waste cooking oils (WCO): Role of ion-exchange resins", *Fuel*, vol. 87, no. 10-11, pp. 1789-1798.

Park, J-Y., Kim, D-K, Wang, Z-M., Lee, J-P., Park, S-C. & Lee, J-S. 2008, "Production of biodiesel from soapstock using an ion-exchange resin catalyst", *Korean Journal of Chemical Engineering*, vol. 25, no. 6, pp. 1350-1354.

Park, J. Y.; Kim, D. G.; Lee, J. S. 2010, "Esterification of free fatty acids using water-tolerable Amberlyst as a heterogeneous catalyst", *Bioresource Technology,* vol. 101, no. 1, pp. S62-S65.

Pasias, S., Barakos, N., Alexopoulos, C. & Papayannakos, N. 2006, "Heterogeneously catalyzed esterification of FFAs in vegetable oils", *Chemical Engineering & Technology*, vol. 29, no. 11, pp. 1365-1371.

Patel, D. & Saha, B. 2007, "Heterogeneous kinetics and residue curve map (RCM) determination for synthesis of n-hexyl acetate using ion-exchange resins as catalysts", *Industrial & Engineering Chemistry Research*, vol. 46, no. 10, pp. 3157-3169.

Paze´, C., Bordiga, S. & Zecchina, A. 2000, "H_2O Interaction with Solid $H_3PW_{12}O_{40}$: An IR Study.", *Langmuir*, vol. 16, no. 21, pp. 8139-8144.

Peng, B., Shu, Q., Wang, J., Wang, G., Wang, D. & Han, M. 2008, "Biodiesel production from waste oil feedstocks by solid acid catalysis", *Process Safety & Environmental Protection*, vol. 86, no. 6, pp. 441-447.

Pesaresi, L., Brown, D. R., Lee, A. F., Montero, J. M., Williams, H. & Wilson, K. 2009, "Cs-doped $H_4SiW_{12}O_{40}$ catalysts for biodiesel applications", *Applied Catalysis A: General*, vol. 360, no. 1, pp. 50-58.

Philippou, A., Rocha, J., Anderson, M. W. 1999, "The strong basicity of the microporous titanosilicate ETS-10", *Catalysis Letters*, vol. 57, no. 3, pp. 151-153.

Pizzio, L. R. & Blanco, M. N. 2003, "Isoamyl acetate production catalyzed by $H_3PW_{12}O_{40}$ on their partially substituted Cs or K salts", *Applied Catalysis A: General*, vol. 255, no. 2, pp. 265-277.

Pope, M. T. 1983, "Heteropoly and Isopoly Oxometalates", *Inorganic Chemistry Concepts: Chemical Compound*, vol. 8, pp. 101.

Predojević, Z. J. 2008, "The production of biodiesel from waste frying oils: A comparison of different purification steps", *Fuel*, vol. 87, no. 17-18, pp. 3522-3528.

Qu, Y., Peng, S., Wang, S., Zhang, Z. & Wang, J. 2009, "Kinetic study of esterification of lactic acid with isobutanol and n-butanol catalyzed by ion-exchange resins", *Chinese Journal of Chemical Engineering*, vol. 17, no. 5, pp. 773-780.

Ragit, S. S., Mohapatra, S. K., Kundu, K. & Gill, P. 2011, "Optimization of neem methyl ester from transesterification process and fuel characterization as a diesel substitute", *Biomass & Bioenergy*, vol. 35, no. 3, pp. 1138-1144.

Ramadhas, A. S., Jayaraj, S. & Muraleedharan, C. 2005, "Biodiesel production from high FFA rubber seed oil", *Fuel*, vol. 84, no. 4, pp. 335-340.

Ramos, M. J., Fernández, C. M., Casas, A. Rodrìguez, L. & Pérez, Á. 2009, "Influence of fatty acid composition of raw materials on biodiesel properties", *Bioresource Technology*, 100, no. 1, pp. 261-268.

Rashid, U. & Anwar, F. 2008, "Production of biodiesel through optimized alkaline-catalyzed transesterification of rapeseed oil", *Fuel*, vol. 87, no. 3, pp. 265-273.

Russbueldt, B. M. E. & Hoelderich, W. F. 2009, "New sulfonic acid ion-exchange resins for the preesterification of different oils and fats with high content of free fatty acids", *Applied Catalysis A: General*, vol. 362, no. 1-2, pp. 47-57.

Rattanaphra, D., Harvey, A.P., Thanapimmetha, A. & Srinophakun, P. 2011, "Kinetic of myristic acid esterification with methanol in the presence of triglycerides over sulfated zirconia", *Renewable Energy*, vol. 36, no. 10, pp. 2679-2686.

Reddy, C. R. V., Oshel, R. & Verkade, J. G. 2006, "Room temperature conversion of soybean-oil and poultry fat to biodiesel catalyzed by nanocrystalline calcium oxides", *Energy & Fuels*, vol. 20, no. 3, pp. 1310-1314.

Reddy, C. R. V., Fetterly, B. M. & Verkade, J. G. 2007, "Polymer-supported a zidoproazaphosphatrane: a recyclable catalyst for the room-temperature transformation of triglycerides to biodiesel", *Energy & Fuels*, vol. 21, no. 4, pp. 2466-2472.

Rocchiccioli-Deltcheff, C., Fournier, M., Franck, R. & Thouvenot, R. 1983, "Vibrational investigations of polyoxometalates. 2. Evidence for anion-anion interactions in molybdenum (V1) and tungsten (V1) compounds related to the keggin structure", *Inorganic Chemistry*, vol. 22, no. 2, pp. 207-216.

Salamatinia, B., Mootabadi, H., Bhatia, S. & Abdullah, A. Z. 2010, "Optimization of ultrasonic-assisted heterogeneous biodiesel production from palm oil: A response surface methodology approach", *Fuel Processing Technology*, vol. 91, no. 5, pp. 441-448.

Salvi, B. L. & Panwar, N. L. 2012, "Biodiesel resources and production technologies – A review", *Renewable & Sustainable Energy Reviews*, vol. 16, no. 6, pp. 3680-3689.

Santos, J. S., Dias, J. A., Dias, S. C. L., Garcia, F. A. C., Macedo, J. L., Sousa, F. S. G. & Almeida, L. S. 2011, "Mixed salts of cesium and ammonium derivatives of 12-tungstophosphoric acid: Synthesis and structural characterization", *Applied Catalysis A: General*, vol. 394, no. 1-2, pp. 138-148.

Sanz, M. T., Murga, R. Beltrán, S. & Cabezas, J. L. "Autocatalyzed and ion-exchange-resin-catalyzed esterification kinetics of lactic acid with methanol", *Industrial & Engineering Chemistry Research,* vol. 41, no.3, pp. 512-517.

Sarin, R., Sharma, M., Sinharay, S. & Malhotra, R. K., 2007, "Jatropha-palm biodiesel blends: an optimum mix for Asia", *Fuel*, vol. 86, no.10-11, pp. 1365-1371.

Satriana & Supardan, M. D. 2008, "Kinetic study of esterification of free fatty acid in low grade crude palm oil using sulfuric acid", *Asean Journal of Chemical Engineering*, vol. 8, no. 1, pp. 1-8.

Schmitt, M. & Hasse, H. 2006, "Chemical equilibrium and reaction kinetics of heterogeneously catalysed *n*-hexyl acetate esterification", *Industrial & Engineering Chemistry Research*, vol. 45, no. 12, pp. 4123-4132.

Sharma, Y., Singh, B. & Upadhyay, S. 2008, "Advancements in development and characterization of biodiesel: A review", *Fuel*, vol. 87, no. 12, pp. 2355-2373.

Sharma, Y.C. & Singh, B. 2008, "Development of biodiesel from karanja, a tree found in rural India", *Fuel,* vol. 87, no. 8-9, pp. 1740-1742.

Sharma, Y. C., Singh, B., Korstad, J. & Roberts, O. 2010, "Advancements in solid acid catalysts for ecofriendly and economically viable synthesis of biodiesel", *Biofuels, Bioproducts & Biorefining*, vol. 5, no. 1, pp. 69-92.

Shashikant, V. G. & Hifjur, R. 2006, "Process optimization for biodiesel production from mahua (Madhuca indica) oil using response surface methodology", *Bioresource Technology*, vol. 97, pp: 379-384.

Shay, E. G. 1993, "Diesel fuel from vegetable oil; Status and opportunities", *Biomass Energy*, vol. 4, no. 4, pp. 227-242.

Shibasaki-Kitakawa, N., Honda, H., Kuribayashi, H., Toda, T., Fukumura, T. & Yonemoto, T. 2007, "Biodiesel production using anionic ion-exchange resin as heterogeneous catalyst", *Bioresource Technology*, vol. 98, no. 2, pp. 416-421.

Shibasaki-Kitakawa, N., Tsuji, T., Chida, K., Kubo, M. & Yonemoto, T. 2010, "Simple continuous production process of biodiesel fuel from oil with high content of free fatty acid using ion-exchange resin catalysts", *Energy & Fuels*, vol. 24, no. 6, pp. 3634-3638.

Shibasaki-Kitakawa, N., Tsuji, T., Kubo, M. & Yonemoto, T. 2011, "Biodiesel production from waste cooking oil using anion-exchange resin as both catalyst and adsorbent", *BioEnergy Research*, vol. 4, no. 4, pp. 287-293.

Silva, V. M. T. M. & Rodrigues, A. E. 2006, "Kinetic studies in a batch reactor using ion exchange resin catalysts for oxygenates production: Role of mass transfer mechanisms", *Chemical Engineering Science*, vol. 61, no. 2, pp. 316-331.

Silitonga, A. S., Atabani, A. E., Mahlia, T. M. I., Masjuki, H. H.,Badruddin, I. A. & Mekhilef, S. A. 2011, "A review on prospect of Jatropha curcas for biodiesel in Indonesia", *Renewable & Sustainable Energy Reviews*, vol. 15, no. 8, pp. 3733-3756.

Singare, P. U., Lokhande, R. S. & Madyal, R. S. 2011, "Thermal degradation studies of some strongly acidic ca-tion exchange resins", *Open Journal of Physical Chemistry*, vol. 1, no. 2, pp. 45-54.

Slover, H. T. & Lanza, E. 1979, "Quantitative analysis of food fatty acids by capillary gas chromatography", *Journal of the American Oil Chemists' Society,* vol. 56, no. 12, pp. 933–943.

Soriano, N., Venditti, R. & Argyropoulos, D. 2009, "Biodiesel synthesis via homogeneous Lewis acid-catalyzed transesterification", *Fuel*, vol. 88, no. 3, pp. 560-565.

Srilatha, K., Lingaiah, N., Devi, B. L. A. P., Prasad, R. B. N., Venkateswar, S. & Prasad, P. S. S. 2009, "Esterification of free fatty acids for biodiesel production over heteropoly tungstate supported on niobia catalysts", *Applied Catalysis A: General*, vol. 365, no. 1, pp. 28-33.

Srilatha, K., Lingaiah, N., Sai Prasad, P. S., Prabhavathi Devi, B. L. A. & Prasad, R. B. N. 2011, "Kinetics of the esterification of palmitic acid with methanol catalyzed by 12-tungstophosphoric acid supported on ZrO_2", *Reaction Kinetics, Mechanisms & Catalysis*, vol. 104, no. 1, pp. 211-226.

Srivastava, P. K. & Verma, M. 2008, "Methyl ester of karanja oil as an alternative renewable source energy", *Fuel*, vol. 87, no. 8-9, pp. 1673-1677.

Srivastiva, A. & Prasad, R. 2000, "Triglycerides-based diesel fuels", *Renewable & Sustainable Energy Review*, vol. 4, no. 2, pp.111-133.

Stamenković, O. S., Veličković, A. V. & Veljković, V. B. 2011, "The production of biodiesel from vegetable oils by ethanolysis: Current state and perspectives", *Fuel*, vol. 90, no. 11, pp. 3141-3155.

Stavarache, C., Vinatoru, M., Nishimura, R. & Maeda, Y. 2005, "Fatty acids methyl esters from vegetable oil by means of ultrasonic energy", *Ultrasonics Sonochemistry*, vol. 12, no. 5, pp. 367–372.

Steinigeweg, S. & Gmehling, J. 2003, "Esterification of a fatty acid by reactive distillation", *Industrial & Engineering Chemistry Research*, vol. 42, no. 15, pp. 3612-9.

Suppes, G. J., Dasari, M. A., Doskocil, E. J., Mankidy, P. J. & Goff, M. J. 2004, "Transesterification of soybean oil with zeolite and metal catalysts", *Applied Catalysis A: General*, vol. 257, no. 2, pp. 213-223.

Supple, B., Holward-Hildige, R., Gonzalez-Gomez, E. & Leahy, J. J. 2002, "The effect of steam treating waste cooking oil on the yield of methyl ester", *Journal of the American Oil Chemists' Society*, vol 79, no. 2, pp. 175-178.

Talukder, M. M. .R, Wu, J. C., Lau, S. K., Cui, L. C., Shimin, G. & Lim, A. 2009, "Comparison of Novozym 435 and Amberlyst 15 as Heterogeneous Catalyst for Production of Biodiesel from Palm Fatty Acid Distillate", *Energy & Fuels*, vol. 23, no. 1, pp. 1-4.

Tateno, T. & Sasaki T. 2004, "*Process for producing fatty acid fuels comprising fatty acids esters*", US Patent 6818026.

Taufiq-Yap, Y. H., Lee, H. V., Yunus, R. & Juan, J. C. 2011, "Transesterification of non-edible Jatropha curcas oil to biodiesel using binary Ca–Mg mixed oxide catalyst: Effect of stoichiometric composition", *Chemical Engineering Journal*, vol. 178, pp. 342-347.

Tesser, R., Di Serio, M., Guida, M., Nastasi, M. & Santacesaria, E. 2005, "Kinetics of oleic acid esterification with methanol in the presence of triglycerides", *Industrial & Engineering Chemistry Research*, vol. 44, no. 21, pp. 7978-7982.

Tesser, R., Casale, L., Verde, D., Di Serio, M. & Santacesaria, E. 2009, "Kinetics of free fatty acids esterification: Batch and loop reactor modelling", *Chemical Engineering Journal*, vol. 154, no. 1-3, pp. 25-33.

Tesser, R., Di Serio, M., Casale, L., Sannino, L., Ledda, M. & Santacesaria, E. 2010a, "Acid exchange resins deactivation in the esterification of free fatty acids", *Chemical Engineering Journal*, vol. 161, no. 1-2, pp. 212-222.

Tesser, R., Casale, L., Verde, D., Di Serio, M. & Santacesaria, E. 2010b, "Kinetics and modeling of fatty acids esterification on acid exchange resins", *Chemical Engineering Journal*, vol. 157, no. 2-3, pp. 539-550.

Tewari, D. N. 2007, "*Jatropha and bio-diesel*", New Dehli: Ocean Books Pvt. Ltd

Tomasevic, A. V. & Silver-Marinkovic, S. S. 2003, "Methanolysis of used frying oil", *Fuel Process Technology*, vol. 81, no. 1, pp. 1-6.

Traboulsi, A., Dupuy, N., Rebufa, C., Sergent, M. & Labed, V. 2012, "Investigation of gamma radiation effect on the anion exchange resin Amberlite IRA-400 in hydroxide form by Fourier transformed infrared and 13C nuclear magnetic resonance spectroscopies", *Analytica Chimica Acta*, vol. 717, pp. 110-121.

Umar, M., Patel, D. & Saha, B. 2009, "Kinetic studies of liquid phase ethyl tert-butyl ether (ETBE) synthesis using macroporous and gelular ion exchange resin catalysts", *Chemical Engineering Science*, vol. 64, no. 21, pp. 4424-4432.

Upham, P., Thornley, P., Tomei, J. & Boucher, P. 2009, "Substitutable biodiesel feedstocks for the UK: a review of sustainability issues with reference to the UK RTFO", *Journal of Cleaner Production*, vol. 17, pp. S37-S45.

US Energy Infromation Administration. 2011, *International energy outlook* [Online]. Available at: http://205.254.135.7/forecasts/ieo/pdf/0484(2011).pdf [Accessed: 26 May 2012].

Van Gerpen, J. 2005, "Biodiesel processing and production", *Fuel Processing Technology*, vol. 86, no. 10, pp. 1097-1107.

Van Rhijn, W. M., De Vos, D. E., Sels, B. F., Bossaert, W. D. & Jacobs, P. A. 1998, "Sulfonic acid functionalized ordered mesoporous materials as catalysts for condensation and esterification reactions", *Chemical Communications*, no. 3, pp. 317-318.

Vazquez, P. G., Blanco, M. N. & Caceres, C. V. 1999, "Catalysts based on supported 12-molybdophosphoric acid", *Catalysis Letters*, vol. 60, no. 4, pp. 205-215.

Veljković, V. B., Lekićević, S. H., Stamenković, O. S., Todorović, Z. B. & Lazic, M. L. 2006, "Biodiesel production from tobacco (Nicotiana tabacum L.) seed oil with a high content of free fatty acids", *Fuel*, vol. 85, no. 17-18, pp. 2671-2675.

Veljković, V. B., Stamenković, O. S., Todorović, Z. .B, Lazić, M. L. & Skala, D. U. 2009, "Kinetics of sunflower oil methanolysis catalyzed by calcium oxide", *Fuel*, vol. 88, no. 9, pp. 1554-1562.

Vicente, G., Martinez, M. and Aracil, J. 2004, "Intergrated biodiesel production: A comparison of different homogeneous catalysts systems", *Bioresource Technology*, vol. 92, no. 3, pp. 297-305.

Vicente, G., Martinez, M., Aracil, J. & Esteban, A. 2005, "Kinetics of sunflower oil methanolysis", *Industrial & Engineering Chemistry Research*, vol. 44, no. 15, pp. 5447-5454.

Vyas, A. P., Subrahmanyam, N. & Patel, P. A. 2009, "Production of biodiesel through transesterification of Jatropha oil using KNO_3/Al_2O_3 solid catalyst", *Fuel*, vol. 88, no. 4, pp. 625-628.

Wall, J., Van Gerpen, J. & Thompson, J. 2011, "Soap and glycerine removal from biodiesel using waterless processes", *Transactions of the ASABE*, vol. 54 no. 2, pp. 535-541.

Wan, T., Yu, P., Gong, S. K., Li, Q. & Luo, Y. B. 2008, "Application of KF/MgO as a heterogeneous catalyst in the production of biodiesel from rapeseed oil", *Korean Journal of Chemical Engineering*, vol. 25, no. 5, pp. 998-1003.

Wang, Y., Ou, S., Liu, P. & Zhang, Z. 2007, "Preparation of biodiesel from waste cooking oil via two-step catalyzed process", *Energy Conversion & Management*, vol. 48, no. 1, pp. 184-188.

Watkins, S. R., Lee, F. A. & Wilson, K. 2004, "Li-CaO catalyzed tri-glyceride transesterification for biodiesel applications", *Green Chemistry*, vol. 6, no. 7, pp. 335-340.

Worapun, I., Pianthong, K. & Thaiyasuit, P. 2012, "Two-step biodiesel production from crude Jatropha curcas L. oil using ultrasonic irradiation assisted", *Journal of Oleo Science*, vol. 61, no. 4, pp. 165-172.

Xie, W. & Li, H. 2006, "Alumina-supported potassium iodide as a heterogeneous catalyst for biodiesel production from soybean oil", *Journal of Molecular Catalysis A: Chemical*, vol. 255, no. 1-2, pp. 1-9.

Xie, W., Peng, H. & Chen, L. 2006a, "Transesterification of soybean oil catalyzed by potassium loaded on alumina as a solid-base catalyst", *Applied Catalysis A: General*, vol. 300, no. 1, pp. 67-74.

Xie, W., Peng, H. & Chen, L. 2006b, "Calcined Mg–Al hydrotalcites as solid base catalysts for methanolysis of soybean oil", *Journal of Molecular Catalysis A: Chemical*, vol. 246, no. 1-2, pp. 24-32.

Xie, W. L. & Yang, Z. Q. 2007, "Ba-ZnO catalysts for soybean oil transesterification", *Catalysis Letters*, vol. 117, no. 3-4, pp. 159-65.

Xie, W. L., Yang, Z. Q. & Chun, H. 2007a, "Catalytic properties of lithium-doped ZnO catalysts used for biodiesel preparations", *Industrial & Engineering Chemistry Research*, vol. 46, pp. 7942-7949.

Xie, W., Huang, X. & Li, H. 2007b, "Soybean oil methyl esters preparation using NaX zeolites loaded with KOH as a heterogeneous catalyst", *Bioresource Technology*, vol. 98, no. 4, pp. 936-939.

Xu, L. L., Wang, Y. H., Yang, X., Yu, X. D., Guo, Y. H. & Clark, J. H. 2008, "Preparation of mesoporous polyoxometalate-tantalum pentoxide composite catalyst and its application for biodiesel production by esterification and transesterification", *Green Chemistry*, vol. 10, no. 7, pp. 746-55.

Yadav, G. D. & Nair, J. J. 1999, "Sulfated zirconia and its modified versions as promising catalyst for industrial processes", *Microporous & Mesoporpous Materials*, vol. 33, no. 1-3, pp. 1-48.

Yadav, G. D. & Kirthivasan, N. 1997, "Synthesis of bisphenol-A: comparison of efficacy of ion exchange resin catalysts vis-à-vis heteropolyacid supported on clay and kinetic modelling", *Applied Catalysis A: General*, vol. 154, no. 1-2, pp. 29-53.

Yadav, G. D. & Kulkarni, H. B. 2000, "Ion-exchange resin catalysis in the synthesis of isopropyl lactate", *Reactive & Functional Polymers*, vol. 44, no. 2, pp. 153-165.

Yadav, G. D. & Murkute, A. D. 2004, "Preparation of a novel catalyst UDCaT-5: enhancement in activity of acid-treated zirconia - effect of treatment with chlorosulfonic acid vis-à-vis sulfuric acid", *Journal of Catalysis*, vol. 224, no. 1, pp. 218-223.

Yalçinyuva, T., Deligoz, H., Boz, S. & Guerkaynak, M. A. 2008, "Kinetics and mechanism of myristic acid and isopropyl alcohol esterification reaction with homogeneous and heterogeneous catalysts", *International Journal of Chemical Kinetics*, vol. 40, no. 3, pp. 136-144.

Yan, S. L., Lu, H. F. & Liang, B. 2008, "Supported CaO catalysts used in the transesterification of rapeseed oil for the purpose of biodiesel production", *Energy & Fuels*, vol. 22, no. 1, pp. 646-51.

Yan, S., DiMaggio, C., Mohan, S., Kim, M, Salley, S. O. & Ng, K. Y. S. 2010, "Advancements in Heterogeneous Catalysis for Biodiesel Synthesis", *Topics in Catalysis*, vol. 53, no. 11-12, pp. 721-736.

Yang, W., Billy, J., Taârit, Y. B., Védrine, J. C. & Essayem, N. 2002, "$H_3PW_{12}O_{40}$ supported on Cs modified mesoporous silica : catalytic activity in n-butane isomerisation and in situ FTIR study Comparison with microporous $Cs_xH_{3-x}PW_{12}O_{40}$", *Catalysis Today*, vol. 73, pp. 153-165.

Yang, H. S., Jeong, G. T., Park, S. H., Park, J. H. & Park D. H. 2007, "Reaction condition for biodiesel production from animal fats", *Korean Journal of Biotechnology & Bioengineering*, vol. 22, no.4, pp. 228-233.

Yang, Z. & Xie, W. 2007, "Soybean oil transesterification over zinc oxide modified with alkali earth metals", *Fuel Processing Technology*, vol. 88, no. 6, pp. 631-638.

Yoosuk, B., Udomsap, P., Puttasawat, B. & Krasae, P. 2010, "Modification of calcite by hydration–dehydration method for heterogeneous biodiesel production process: The effects of water on properties and activity", *Chemical Engineering Journal*, vol. 162, no. 1, pp. 135-141.

Yu, X., Wen, Z., Lin, Y, Tu, S. T., Wang, Z & Yan, J. 2010, "Intensification of biodiesel synthesis using metal foam reactors", *Fuel*, vol. 89, no. 11, pp. 3450-3456.

Yun, L. & Ling, W. 2009, "Bio-diesel preparation from waste oil using cation exchange resin as heterogeneous catalyst", *Chemistry & Technology of Fuels & Oils*, vol. 45, no. 6, pp. 417-424.

Zeng, H., Feng, Z., Deng, X. & Li, Y. 2008, "Activation of Mg–Al hydrotalcite catalysts for transesterification of rape oil", *Fuel*, vol. 87, no. 13-14, pp. 3071-3076.

Zhang, J. & Jiang, L. 2008, "Acid-catalyzed esterification of Zanthoxylum bungeanum seed oil with high free fatty acids for biodiesel production", *Bioresource Technology*, vol. 99, no. 18, pp. 8995-8998.

Zhang, S., Zu, Y., Fu, Y., Luo, M., Zhang, D. & Efferth, T. 2010, "Rapid microwave-assisted transesterification of yellow horn oil to biodiesel using a heteropolyacid solid catalyst", *Bioresource Technology*, vol. 101, no. 3, pp. 931-936.

Zhang, X., Li, J., Chen, Y., Wang, J. H., Feng, L. L., Wang, X. H. & Cao, F. H. 2009, "Heteropolyacid nanoreactor with double acid sites as a highly efficient and reusable catalyst for the transesterification of waste cooking oil", *Energy & Fuels*, vol. 23, pp. 4640-4646.

Zhang, Y., Dubé, M. A., McLean, D. D. & Kates, M. 2003a, "Biodiesel production from waste cooking oil: 1. Process design and technological assessment", *Bioresource Technology*, vol. 89, no. 1, pp. 1-16.

Zhang, Y., Dubé, M. A., McLean, D. D. & Kates, M. 2003b, "Biodiesel production from waste cooking oil: 2. Economic assessment and sensitivity analysis", *Bioresource Technology*, vol. 90, no. 3, pp. 229-240.

Zheng, S., Kates, M., Dubé, M. A. & McLean, D. D. 2006, "Acid-catalyzed production of biodiesel from waste frying oil", *Biomass & Bioenergy*, vol. 30, no. 3, pp. 267-272.

Zhu, H., Wu, Z., Chen, Y., Zhang, P., Duan, S., Liu, X. & Mao, Z. 2006, "Preparation of biodiesel catalyzed by solid super base of calcium oxide and its refining process", *Chinese Journal of Catalysis*, vol. 27, no. 5, pp. 391-396.

Zieba, A., Matachowski, L., Lalik, E. & Drelinkiewicz, A. 2009, "Methanolysis of Castor Oil Catalysed by Solid Potassium and Cesium Salts of 12-Tungstophosphoric Acid", *Catalysis Letters*, vol. 127, no. 1-2, pp. 183-94.

Zieba, A., Matachowski, L., Gurgul, J., Bielańska, E. & Drelinkiewicz, A. 2010, "Transesterification reaction of triglycerides in the presence of Ag-doped $H_3PW_{12}O_{40}$", *Journal of Molecular Catalysis A: Chemical*, vol. 316, no. 1-2, pp. 30-44.

Zubir, M. I. & Chin, S. Y. 2010, "Kinetics of modified zirconia-catalyzed heterogeneous esterification reaction for biodiesel production", *Journal of Applied Sciences*, vol. 10, no. 21, pp. 2584-2589.

11 APPENDIX A

11.1 JOURNAL PUBLICATIONS

(1) Haigh, K. F., Abidin, S. Z., Saha, B. & Vladisavljević, G. 2012, "Pretreatment of used cooking oil for the preparation of biodiesel using heterogeneous catalysis", *Progress in Colloid and Polymer Science*, vol. 139.

(2) Abidin, S. Z., Haigh, K. F. & Saha, B. "Esterification of free fatty acids (FFAs) in used cooking oil (UCO) using ion exchange resins as catalysts: An efficient pre-treatment method for biodiesel feedstock", *Industrial and Engineering Chemistry Research*, 2012, submitted.

(3) Abidin, S. Z., Patel, D. & Saha, B. "Quantitative analysis of fatty acids composition in the used cooking oil (UCO) by gas chromatography-mass spectrometry (GC-MS)", *The Canadian Journal of Chemical Engineering*, 2012, submitted.

(4) Haigh, K. F., Abidin, S. Z., Vladisavljević, G. & Saha, B. "Comparison of Novozyme 435 and Purolite D5081 as heterogeneous catalysts for the pretreatment of used cooking oil for biodiesel production", *Fuel*, in preparation.

11.2 CONFERENCE PUBLICATIONS

(1) Abidin, S. Z., Haigh, K. F., Vladisavljević, G. & Saha, B. "Esterification of free fatty acids (FFAs) in used cooking oil (UCO) using ion exchange resins as catalysts", *8th European Congress of Chemical Engineering*, 26-29 September 2011, Berlin, Germany.

(2) Abidin, S. Z., Haigh, K. F., Vladisavljević, G. & Saha, B. "Esterification of free fatty acids using ion exchange resin as a catalyst: An efficient pre-treatment method for biodiesel production", *3rd International Congress on Green Process Engineering*, 6-8 December 2011, Kuala Lumpur, Malaysia.

(3) Abidin, S. Z., Haigh, K. F. & Saha, B. "Ion exchange resins catalysed esterification of free fatty acids (FFAs) in used cooking oil (UCO) with methanol: An efficient pre-treatment method for biodiesel production", *The International Ion Exchange Conference*, 19-21 September 2012, Cambridge, United Kingdom.